Clozapine-induced paroxysmal discharges

Michael Fisher

Thesis submitted in partial fulfilment of the requirements for the degree of Doctor of Philosophy

Newcastle University

Faculty of Medical Science

Institute of Neuroscience

February 2013

Abstract

The atypical antipsychotic clozapine is a widely prescribed and effective treatment for the positive and negative symptoms of schizophrenia, but reports of side effects are common. In one study EEG abnormalities were observed in 53% of patients treated with clozapine, and the absence or presence of EEG abnormalities correlated with the plasma clozapine concentration.

Here, epileptiform activity was present in conventional EEG recordings from a 32 year old male patient with psychiatric illness taking clozapine for 3 weeks. Brief (ca.100ms), transient epileptiform spikes occurred at a frequency of approximately 2 per h and originated primarily in parietal cortex. One month after withdrawal of clozapine, epileptiform spikes were no longer present.

An *in vitro* model was developed using the equivalent region of association cortex, namely 2° somatosensory cortex, in normal rat brain slices to probe such activity with increased spatial and temporal resolution, and to investigate mechanisms underlying its generation. Wide band *in vitro* recordings revealed that clozapine (10-20μM) induced regular, frequent very fast oscillations (VFO, > 70Hz) in this region. These VFO comprised short transient high frequency discharges and were maximal in patches along layer V. The atypical antipsychotic olanzapine, but not the classical antipsychotic haloperidol, also induced prominent VFO in this region.

Sharp electrode intracellular recordings revealed that there was almost no correlation between the somatic activity of layer V regular spiking (RS) pyramidal cells and field VFO, but layer V intrinsically bursting (IB) cells did correlate to some extent with the local field. Interestingly, IB cell spikelets were also weakly correlated with field VFO suggesting a role for axonal hyperexcitability in this cell type in the mechanism.

Clozapine-induced VFO persisted following blockade of AMPA, NMDA, and $GABA_A$ chemical synaptic receptors, and the gap junction blockers carbenoxolone and quinine also failed to significantly attenuate the power of this activity. Although octanol abolished clozapine-induced VFO, it was not clear that this effect resulted from blockade of gap junctions as this drug also blocks spikes.

In addition to VFO events, clozapine (10-20μM) also induced occasional, spontaneous transient paroxysmal discharges, similar to the EEG phenomena, in 33% (11/33 slices) of slices *in vitro*. Sharp electrode intracellular recordings revealed that clozapine-induced full paroxysmal discharges were associated with spikes, EPSPs and IPSPs in layer V RS and IB cells, suggesting that these events were mediated via chemical synaptic transmission in both of these cell types. Multi-electrode array recordings of local field potentials and units suggested that clozapine-induced paroxysmal events started superficially in association cortex, moved deeper and then propagated horizontally along these deep layers.

The onset of clozapine-induced VFO was accompanied by a significant elevation in parvalbumin immunoreactivity, particularly in layer II-IV, where there was a greater than twofold increase in the signal, and this may be relevant to the therapeutic action of the drug.

Acknowledgements

I would especially like to thank my supervisor Prof. Miles Whittington for his enthusiasm, outstanding academic guidance and direction, and all the help, support and encouragement throughout the project. His energy and focus are inspirational. Special thanks are also due to my second supervisor, Dr. Fiona LeBeau, for advice, perceptive suggestions, encouragement, and for being lovely.

I am very grateful to Dr. Ian Schofield for providing the clinical EEG data.

Thanks are also due to Prof. Ceri Davies and Prof. Roger Traub for their input, and my assessors, Dr. Mark Cunningham and Dr. Sasha Gartside, for their helpful suggestions.

I would also like to acknowledge excellent tuition in histology from Dr. Anna Simon, and in data analysis from Dr. Jennifer Simonotto.

I would like to thank the former postdocs Dr. Anita Roopun and Dr. Michelle Pierce, and also Dr. Lucy Carracedo, for all their fantastic assistance and support in the lab in the early stages. I would also like to thank the lab technician Karen for her work in supporting the lab.

I am grateful to Matt and Henrik for marvellous advice with regard to data analysis, to Gina for being a wonderful smiley presence in the lab, and to Steve for being a complete and utter legend. In addition to those above, I would like to mention Anaïs, Bernadette, Chris, Claire, Cyril, Dan, Dee, Ed, Emma, Felix, Isla, John, Kathryn, Leonie, Natalie, Sabine, Sam, Vasileios, and all the students who have passed through the postgraduate office over the years and made it such a friendly and fun place to work. I would also like to thank Harbi, Lauren, Stephan, Tom and others in the institute, and my former housemates Hamid, Agathe, Alice, Camille, Claire, Jess, Joanne, Katja, Lauren, Siobhan, Tara and Willemijn, for all their friendship over the years; and my family, for their kindness.

Contents

List of illustrations

Chapter 1

General Introduction

This thesis demonstrates an *in vitro* model of transient epileptiform discharges associated with adverse reaction to the atypical antipsychotic clozapine. By way of introduction, brain rhythms and their physiological function in the healthy condition are first considered, before schizophrenia pathology, how this may relate to mechanisms associated with dysfunctional brain rhythms, and comorbidity of schizophrenia with epilepsy. Next, antipsychotics, drugs used to treat schizophrenia, and the particular effectiveness of clozapine and possible mechanisms underlying its actions are considered. Finally, pathological EEG abnormalities associated with antipsychotics, and possible mechanisms underlying such epileptiform activity, are introduced.

1.1 Brain rhythms and cognitive function

The concept of recording electrical activity in the brain has a long history (e.g. Swartz and Goldensohn, 1998). Electroencephalography (EEG) is a non-invasive tool for detecting synchronous activity in the brain by means of recording electrical activity from the scalp. Hans Berger (1873-1941) was one of the first scientists to use this technique to record brain rhythms from humans, discovering the 'Berger rhythm' (now termed alpha activity). It is now known that rhythmic brain activity occurs continuously in particular frequency bands according to behavioural state and has been observed in cerebral cortex, subcortical structures and cerebellar cortex. Rhythmic EEG activity can be categorised according to its frequency, delta (0-3Hz), theta (4-7Hz), alpha (8-12Hz), beta (13-30Hz), gamma (30-80Hz) and very fast oscillations (VFO, > 70-80Hz).

The concept of the importance of brain rhythms, or neural oscillations, in facilitating brain function in sensory physiology has arisen in part with the finding that in the vertebrate olfactory system neural activity occurs in synchronised oscillations (Adrian, 1950;Gray and Skinner, 1988;Di Prisco and Freeman, 1985). Further evidence demonstrated that oscillatory activity occurs in sensory cortex when awake animals direct their attention to stimuli (Lopes da Silva et al., 1970;Rougeul et al., 1979;Bouyer et al., 1981;Bouyer et al., 1987;Freeman and van Dijk, 1987).

It is now thought that neural oscillations allow precise temporal correlations to be made between neural responses in different brain regions. Beta and gamma oscillations are important in the precise synchronisation of local cortical networks (Gray and Singer, 1989;Womelsdorf et al., 2007), while lower frequency oscillations may have a greater role in longer range synchronisation (von Stein, 2000).

There is considerable evidence linking oscillations to particular cognitive process including working memory, attention and consciousness. For example, gamma oscillations have a role in perception (Gray et al., 1989), synaptic plasticity (Wespatat et al., 2004), short-term memory (Tallon-Baudry and Bertrand, 1999), attention (Fries et al., 2001) and perhaps even consciousness itself (Melloni et al., 2007); beta oscillations are important in sensory gating (Hong et al., 2008), are also involved in some aspects of attention (Gross et al., 2004), and appear to play a critical role in fine motor control (Kilner et al., 2000). Some rhythms may be particularly associated with pathological conditions, such as VFO seen in patients with epilepsy. However, even in this case the rhythm also has a physiological role: VFO is implicated in memory consolidation and sensory perception (see section 1.5). This does not stop clinicians and researchers using EEG signatures to help to understand pathological states. Of particular relevance to this thesis are the changes in 'normal' EEG rhythms such as the gamma rhythm seen in schizophrenia. This is introduced below.

1.2 Schizophrenia

Schizophrenia is a disorder in which impairments occur in many of the cognitive processes associated with oscillations (Park and Holzman, 1992;Uhlhaas and Silverstein, 2005). Such impairments lead to problems in social and occupational capability in individuals with schizophrenia. Symptoms of schizophrenia can be classified as positive, negative or cognitive. Positive symptoms include hallucinations, delusions, abnormal psychomotor activity, and thought disorder. Negative symptoms describe problems such as social withdrawal, reduced motivation, an impaired ability to recognise and express emotion, and reduced speech. Cognitive symptoms relate to impairments in processes such as selective attention, working memory, episodic memory, understanding of language and executive control. In particular, research effort in schizophrenia has been directed at working memory (Barch and Smith, 2008), which is critically dependent on dorsolateral prefrontal cortex (DLPFC) circuitry in humans (Miller and Cohen, 2001). Activity in this brain region is impaired during working memory tasks in schizophrenic patients (Van Snellenberg et al., 2006;Deserno et al., 2012).

Deficits in working memory occur in schizophrenic patients regardless of medication status, and are present in early stages of the disorder (Barch and Smith, 2008) including prodromally in childhood and adolescence, years before schizophrenia is first diagnosed (Lesh et al., 2011;Davidson et al., 1999;Cosway et al., 2000). Cognitive deficits are also

independent of psychosis (Keefe and Fenton, 2007), represent the best indicator for the long-term outcome of patients (Green, 1996), and occur to a lesser extent in unaffected relatives of those with schizophrenia (Egan et al., 2001). As such, cognitive deficits are considered a critical, core aspect of the dysfunction in this illness.

1.2.1 Pathology of schizophrenia

1.2.1.1 GABAergic deficits in schizophrenia

As mentioned above, healthy cognitive function may be related to the generation of neural oscillations including synchronised gamma activity (Gray et al., 1989) across networks distributed throughout cortex. In schizophrenia cognitive deficits are linked to reduced power and synchrony of these gamma oscillations which provides clues as to underlying primary pathology (Bichot et al., 2005;Gonzalez-Burgos et al., 2010;Uhlhaas and Singer, 2010). Inhibitory GABAergic interneurons have a critical role in the mechanisms underlying normal gamma oscillations by producing rhythmic inhibitory post synaptic potentials (IPSPs) in pyramidal neurons (Traub et al., 2004;Fries et al., 2007). In particular fast spiking interneurons which contain the calcium-binding protein parvalbumin may be especially important in generating gamma rhythms (Klausberger and Somogyi, 2008;Cardin et al., 2009), and their activity has been shown to have a causal role in generating gamma rhythms in mice *in vivo* (Sohal et al., 2009).

A consistent finding in post-mortem studies has been that GAD67, one of the main enzymes that synthesise GABA, is reduced in the DLPFC of patients with schizophrenia (Bird et al., 1978;Hanada et al., 1987), and this occurs selectively in layers III-V (Akbarian et al., 1995), where gamma rhythms are most prominent (Glykos et al., 2012).

Expression of the GABA membrane transporter GAT1 is also reduced suggesting that, in addition to synthesis, re-uptake of GABA is also impaired in schizophrenia (Volk et al., 2001). Given the critical role of GABAergic interneurons in the mechanisms underlying gamma oscillations (Traub et al., 2004;Fries et al., 2007), one possibility, considered in more detail below, is that cognitive impairments in schizophrenia arise from reduced gamma synchrony resulting from impaired GABA-mediated inhibition.

For example, reduced GAT1 could alter rhythmicity of oscillations in schizophrenia. MEG data show auditory clicks at 40Hz elicit a gamma response in normal individuals,

but both beta and a lower amplitude gamma in patients with schizophrenia. A network simulation of the auditory cortex showed that increasing the decay time of IPSPs, such as might occur with reduced GAT function, produced a similar profile of neural oscillations (Vierling-Claassen et al., 2008).

Parvalbumin-containing interneurons may also be particularly affected in schizophrenia (Beasley and Reynolds, 1997;Danos et al., 1998;Hashimoto et al., 2003). More recent work to that mentioned above showed that expression of parvalbumin mRNA was significantly reduced in layers III and IV, but not in layers II, V or VI of the DLPFC (Hashimoto et al., 2003). Interestingly, it was the expression level of parvalbumin mRNA per neuron rather than number of neurons with detectable parvalbumin mRNA, that was affected. The parvalbumin mRNA expression level per neuron also correlated with reductions in the density of neurons positive for GAD67 mRNA. Thus GAD67 mRNA expression is preferentially reduced in parvalbumin-immunopositive interneurons (Hashimoto et al., 2003). Dual label *in situ* hybridisation studies confirmed that in schizophrenic tissue approximately half of the neurons positive for parvalbumin mRNA did not have detectable GAD67 mRNA. Therefore it seems that parvalbumin-containing interneurons in particular may be functionally impaired in schizophrenia.

Furthermore, expression of the $GABA_A$ receptor alpha1 subunit is particularly low in pyramidal cells that receive inhibitory inputs from parvalbumin interneurons (Glausier and Lewis, 2011). Thus reduced inhibitory drive from parvalbumin cells could be a key aspect of the pathophysiology of schizophrenia and this may have bearing on the effectiveness of antipsychotic drugs like clozapine (see below and results chapter 7).

Data from animal models of schizophrenia provide a further evidence for a link between altered parvalbumin expression and deficits in gamma. Administration of methylazoxymethanol acetate reduced expression of parvalbumin in interneurons throughout the medial prefrontal cortex and ventral subiculum in rats and resulted in impaired gamma responses (Lodge et al., 2009). Furthemore, LPA1-deficient mice, which show psychomotor-gating deficits and neurochemical changes similar to those in schizophrenia, also demonstrate reduced gamma oscillations, and decreased parvalbumin immunopositive intereuron numbers in layer II of medial entorhinal cortex (Cunningham et al., 2006).

However the mechanisms by which parvalbumin cells may become dysfunctional in schizophrenia are not yet clear. Possibilities include reductions in released GABA,

lower numbers of postsynaptic $GABA_A$ receptors, alterations in the excitatory drive on to parvalbumin neurons, or loss of neurons or inhibitory inputs. A complicating factor is that lowered parvalbumin in schizophrenia may be a compensatory change secondary to deficits in GAD67 and reduced GABA. In fact, so many seemingly contrary changes in GABA system function are seen in schizophrenia that it is hard to understand mechanistically what is 'cause' and what is 'compensation' at all. This has led to other theories linking pathology to modifications in glutamate receptor-mediated excitation.

1.2.1.2 NMDA receptor hypofunction in schizophrenia

In the glutamate hypothesis of schizophrenia it is proposed that NMDA receptor hypofunction may be important in mediating aspects of schizophrenia, especially cognitive impairment (Carlsson and Carlsson, 1990;Javitt and Zukin, 1991;Jentsch et al., 1997a;Jentsch et al., 1997b;Olney and Farber, 1995). Phencyclidine (PCP), which is a non-competitive NMDA receptor antagonist, can induce a psychotomimetic state that arguably represents a good pharmacological model of schizophrenia. PCP injections can induce schizophrenia-like symptoms such as hallucinations, delusions, and cognitive deficits in normal humans (Cosgrove and Newell, 1991;Javitt and Zukin, 1991). Furthermore, in schizophrenic individuals PCP and the non-competitive NMDA receptor antagonist ketamine aggravate pre-existing symptoms (Pearlson, 1981;Javitt and Zukin, 1991;Krystal et al., 1994;Malhotra et al., 1996).

However, one caveat is that neither drug is selective for NMDA receptors. Both ketamine and PCP have a high affinity for dopamine D_2 and serotonin 5-HT_2 receptors, and act as partial agonists at the D_2 receptor (Kapur and Seeman, 2002). Ketamine may also inhibit monoamine transporters (Nishimura et al., 1998;Nishimura and Sato, 1999), and has a high affinity for μ, κ and δ opioid receptors (Hirota et al., 1999). Furthermore, PCP is a σ receptor ligand (e.g. Quirion et al., 1981;Zukin, 1982).

Nevertheless, despite their limited selectivity, various noncompetitive NMDA receptor antagonists can also increase locomotor activity and stereotyped behaviour (Schmidt, 1994;Sturgeon et al., 1982) and induce cognitive deficits and impairments in learning and memory in mice, rats, and monkeys (Danysz et al., 1988;Alessandri et al., 1989;Boyce et al., 1991;Verma and Moghaddam, 1996;Jentsch et al., 1997a;Jentsch et al., 1997b). These findings have led to the idea that hypofunction of NMDA receptor-mediated transmission may be important in the pathophysiology of schizophrenia.

In line with this, exposure to NMDA receptor antagonists is used in animals commonly as a model of possible NMDA receptor hypofunction in schizophrenia (Mouri et al., 2007). However, as NMDA receptors are expressed in various neurons throughout the brain it is unclear which neuronal cell types would be important in pharmacological models of NMDA receptor hypofunction, and thus more recent work has investigated the effect of targeted genetic knockout of NMDA receptors in interneurons (see below; Belforte et al., 2010;Carlen et al., 2012).

It has been proposed that NMDA receptor hypofunction may be primary, either directly or indirectly, to changes in parvalbumin neurons in schizophrenia (Coyle, 2006;Lisman et al., 2008;Lewis and Gonzalez-Burgos, 2006). Parvalbumin interneurons receive excitatory inputs via NMDA receptors, especially those containing the NR2A/NR2B subtype associated with changes in glutamatergic drive (Kinney et al., 2006). NMDA antagonists that induce psychosis in healthy participants also alter inhibitory synaptic transmission (Krystal et al., 1994). Furthermore, acute ketamine reduces IPSPs in mouse prefrontal cortex (Zhang et al., 2008) and decreases gamma power and IPSP amplitude in superficial layers of mouse medial entorhinal cortex (Cunningham et al., 2006).

Interestingly, the effect of NMDA receptor antagonism may be region-specific such that it can result in increases in gamma in certain regions (Roopun et al., 2008). This may be due, in part, to the amount of NMDA drive interneurons in specific brain regions receive. For example, in most brain regions there is a limited extent of NMDA receptor input into interneurons in the adult. However, in entorhinal cortex such NMDA receptor inputs remain substantial in adulthood (Jones and Buhl, 1993). The entorhinal cortex is implicated in schizophrenia as structural magnetic resonance imaging data suggest that the entorhinal cortex may be smaller in individuals with schizophrenia and related disorders (e.g. Prasad et al., 2004), and diffusion tensor imaging data suggest that entorhinal connectivity may also be disrupted (Kalus et al., 2005).

As interactions between brain rhythms in distributed regions of cortex may be essential for healthy cognition (Fries, 2005), region-by-region alterations in rhythm generation may result in a functional disconnection as occurs in schizophrenic patients (Cole et al., 2011).

Given that NMDA receptor antagonists may produce pyramidal cell disinhibition (Homayoun and Moghaddam, 2007), one possibility is that this arises mainly from

NMDA receptor hypofunction and the resulting loss of excitatory drive at synapses onto parvalbumin interneurons. In line with the proposal that NMDA receptor hypofunction is primary to alterations in parvalbumin neurons, NMDA receptor antagonists can induce lowered parvalbumin and GAD67 in parvalbumin neurons similar to that found in post-mortem schizophrenic tissue (Cochran et al., 2002;Kinney et al., 2006;Behrens et al., 2007b). On the other hand, in a recent study sub-chronic exposure to PCP or ketamine in adult mice and rats failed to change parvalbumin expression in medial prefrontal cortex or hippocampus (Benneyworth et al., 2011).

In relation to the question of which neuronal cell types are important in the proposed NMDA receptor hypofunction in schizophrenia, genetically modified mice were developed with selective knockout of the essential NR1 subunit of NMDA receptors in a mixed population of corticolimbic GABAergic interneurons in early postnatal development (Belforte et al., 2010). These mice developed a variety of behaviours resembling human schizophrenia, including novelty-induced hyperlocomotion, mating and nest-building deficits, behaviours associated with anxiety and anhedonia, and impaired social memory and spatial working memory (Belforte et al., 2010).

More selective knockout of NMDA receptors specifically in PV interneurons in adolescent mice did not result in such a wide range of behavioural phenotypes, but did result in selective deficits in habituation, working memory and associative learning (Carlen et al., 2012). Importantly, knockout of NMDA receptors in PV neurons also resulted in disrupted regulation of gamma oscillations *in vivo* (Carlen et al., 2012).

Many of the above changes associated with cortical function in schizophrenia also may play a role in some epilepsies. In particular a failure to recruit interneurons into local circuit responses – causing disinhibition – is a known feature of kindling models of epilepsy (Sloviter, 1987). Reduced inhibition in general has been thought to represent a primary cause of epileptiform activity for decades (Schwartzkroin and Prince, 1977;Schwartzkroin and Prince, 1978;Schwartzkroin and Prince, 1980). It is therefore not surprising that clinically there is a great deal of overlap and interdependence between these two illnesses.

1.3 Comorbidity of epilepsy with schizophrenia

The general idea of links between schizophrenia and epilepsy can be traced back to work by L.M. Meduna in the 1930s who described an antagonism between seizures and psychosis following his observation that the frequency of seizures reduced in certain epileptic patients after they developed psychotic symptoms similar to those in schizophrenia. Indeed this idea was important in the theoretical rationale for the original use of electro-convulsive therapy as a treatment for schizophrenia. Since then, the hypothesis of an antagonism between seizures and psychosis has been returned to (e.g. Wolf and Trimble, 1985;Stevens, 1995).

More recent work has investigated the issue of the comorbidity of schizophrenia with epilepsy. Trimble (1996) has reviewed issues relating to comorbidity and highlighted the relationship between a number of anticonvulsant drugs, their clinical effectiveness, and the emergence of severe psychiatric symptoms including psychoses presenting very much like the positive symptoms associated with early schizophrenia. The term 'forced normalisation' is used to suggest that the balance between excitation and inhibition in the brains of epilepsy patients, in compensation for underlying pathology, serves to push the system to a point where seizures are more likely. If the seizures are treated then this compensatory imbalance is disrupted and 'alternative psychosis' is manifest. This thesis deals with an example of the converse of this situation: One where excitatory and inhibitory balance in the brain is homeostatically adjusted to compensate for an overt psychosis. The working hypothesis is that treatment of that psychosis generates epileptiform hyperexcitability *de novo*, or in patients, may uncover the compensatory hyperexcitability that was keeping the pyschosis at bay in the first place.

If the above imbalances and compensatory changes in excitation and inhibition are taking place in the brains of patients with epilepsy and/or schizophrenia, can a further understanding of the primary pathologies at work lead to a more mechanistic understanding of either disorder?

Various studies have highlighted a link between schizophrenia and temporal lobe epilepsy (TLE). There is considerable evidence for a higher prevalence of schizophrenia-like psychosis in patients with TLE compared to non-epileptic individuals (Bredkjaer et al., 1998;Sachdev, 1998;Schwartz and Marsh, 2000;Gaitatzis et al., 2004). A study with a large cohort of patients found an incidence of schizophrenia or schizophrenia-like psychosis three times greater in subjects with

epilepsy compared to non-epileptic individuals. The risk of such psychosis increased with the number of admissions to hospital for epilepsy, and interestingly, common genetic or environmental causes were suggested by the finding that a family history of epilepsy was a significant risk factor for such psychosis (Qin et al., 2005). Misdiagnosis of epilepsy as schizophrenia can occur (e.g. Prueter et al., 2002), and antiepileptic drugs can reduce psychotic symptoms in some cases (Hosak and Libiger, 2002). Both disorders are linked with an onset in late adolescence, deficits in cognition and memory, and hallucinations (Slater and Moran, 1969;Taylor, 2003).

Thus, dysfunctional activity in temporo-limbic areas may be a common feature of schizophrenia and TLE, and, more specifically, it is possible that both of these disorders reflect dysfunctional synchronous activity in local networks in temporal lobe structures.

The idea that epilepsy involves irregular and excessive synchronous activity within neuronal networks has been prevalent for some time. Extreme hypersynchrony can lead to a pathologically oscillating network which is no longer capable of meaningful information processing. For example, heightened gamma activity can occur in the EEG of epileptic patients (Hirai et al., 1999;Willoughby et al., 2003), and has even been suggested to be a prerequisite for the the development of seizures (Willoughby et al., 2003). Conversely, the cognitive and affective derangements that occur in schizophrenia have been suggested to arise from deficits in the integration or synchronisation of activity in distributed neuronal networks. The disorder is increasingly being seen as the manifestation of abnormal neuronal synchrony in cortical networks. In particular, as mentioned above, various studies show deficits in gamma rhythmogenesis in cortical networks in schizophrenic patients (e.g. Spencer et al., 2003;Spencer et al., 2004;Symond et al., 2005).

Thus, both disorders may entail dysfunction in the neuronal circuits that generate gamma activity. Although the underlying mechanism of gamma generation is complicated (see Whittington et al., 2011), it is clear that interactions within populations of GABAergic inhibitory interneurons are an essential component driving and controlling synchrony via a coherent output to principal neurones (e.g. see Traub et al., 1996;Gloveli et al., 2005;Cunningham et al., 2003). Dysfunction of GABAergic inhibition has been associated with both epilepsy and schizophrenia for some time (Keverne, 1999;Cossart et al., 2005). The latter is introduced in detail in 1.2.1.1 above but here the introduction looks for parallels in epilepsy syndromes and models.

In light of the role of interneurons in rhythmogenesis, it is unlikely that epileptogenesis results from a straightforward loss of the dampening effect of synaptic inhibition. In epilepsy, some GABAergic interneurons are affected but others appear less susceptible to the pathology. The effects of selective loss of sub-populations of hippocampal interneurons has been reviewed elsewhere (Magloczky and Freund, 2005). Studies suggesting that TLE results in selective degeneration of principal neurones in cortical layer III suggest that GABAergic interneurons may be spared (Eid et al., 1999;Kobayashi et al., 2003), especially those that contain parvalbumin (Du et al., 1993;Du et al., 1995;Eid et al., 1999). However, although Van Vliet et al. (2004) showed preservation of parvalbumin-immunopositive neurones in layer III in a rat model of TLE, this study also found that these interneurones were reduced in layer II, V and VI, and there was a reduction in calretinin-immunoreactive neurones across all layers.

Chandelier cells are powerful inhibitory interneurons that also contain parvalbumin. A loss of chandelier cells may have important consequences for cortical circuits and has been suggested to be a mechanism underling TLE (DeFelipe, 1999). Markers for their synaptic specialisations onto principal cells form one of the most robust post-mortem markers of pathology in patients with schizophrenias (see below). These neurons are also likely to be important in generating synchrony in principal cell populations. Chandelier cells are also immunoreactive for the cell adhesion molecule PSA-NCAM (Arellano et al., 2002), a marker for plastic changes. PSA-NCAM is increased in TLE patients (Mikkonen et al., 1998), so it is possible that an expansion of inhibitory connections from chandelier cells and other interneurons could increase synchrony and underlie epileptogenesis. In line with this, widespread synchronous gamma oscillations can give rise to epileptiform burst discharges in hippocampus (Traub et al., 2005b).

The full physiological and biochemical implications of chronic epileptic conditions on synaptic inhibition is not clear. Some *in vitro* studies that made use of intracellular recordings suggested that, following a monosynaptic IPSP protocol, interneurons in epileptic rat brain slices were still capable of inducing IPSPs similar to those elicited in control tissue (Bear et al., 1996;Fountain et al., 1998). However, more studies are needed to further investigate the effect of epileptic conditions on interneurons and inhibitory synaptic transmission.

In general, evidence in post mortem tissue from schizophrenia patients points to multiple pre- and postsynaptic abnormalities in interneurons which weakens their

inhibitory control over pyramidal cells – a situation which would be expected to bias brain networks towards hyperexcitability and perhaps seizures. Antipsychotic therapy is currently thought to address this imbalance of excitation and inhibition (Lewis et al., 2012). However, if this were the case then the comorbidity issues addressed above would not constitute a clinical problem and incidences of *de novo* expression of seizure-like events with antipsychotic therapy would not occur.

However, imbalance between synaptic excitation and inhibition is not the only potential candidate mechanisms for epilepsy and schizophrenia. Patterns of local network activity, manifest as frequencies over ca. 80 Hz (very fast oscillations, VFO) have long been associated with epilepsy. They were first reported in patients with frontal or temporal lobe epilepsies over 20 years ago (Allen et al., 1992;Fisher et al., 1992). They are seen in infants and adults and associated with the onset of a very wide range of seizure subtypes (Worrell et al., 2004;Khosravani et al., 2009). In fact they have been proposed as the single most effective biomarker for epileptogenic tissue in human brains (Jacobs et al., 2012). They can also be manifest in small sections of human tissue maintained *in vitro* (Roopun et al., 2010) and can be readily generated in a number of rodent *in vitro* models of seizures (e.g. Cunningham et al., 2012).

Interestingly, the animal model studies have been able to show that epileptiform VFO survives blockade of most types of inhibitory and excitatory chemical synaptic activity, suggesting a non-synaptic origin. Traub (2001) proposed a mechanism for such rhythms that involved direct communication between principal cell axons via gap junctions. A great deal of such direct connections exist in the cortex of immature brains where they are thought to guide local circuit formation (Yu et al., 2012), perhaps explaining the preponderance of VFO in seizures in infants described above. However, while the level of gap junctional connectivity between neurons reduces with age they can be seen in adult rodent brains (Dhillon and Jones, 2000;Mercer et al., 2006;Wang et al., 2010;Hamzei-Sichani et al., 2007;Hamzei-Sichani et al., 2012). In addition, neocortical epileptic foci are often associated with the presence of neuronal progenitor cells or even newly formed neurons (Liu et al., 2008). These neurons in turn express large quantities of gap junctions and may serve as hubs in aberrant local networks leading to seizure.

Evidence for high frequency oscillations associated with schizophrenia is more sparse. Sensory evoked potential studies have shown an increase in the amplitude and latency of VFO in patients, with a negative correlation between VFO power and thought disorder and delusions (Norra et al., 2004). The ketamine model of both positive and

negative symptoms of schizophrenia is associated with increased VFO in rodent nucleus accumbens (Hunt et al., 2006).

VFO also manifest as a critical component of persistent gamma rhythms (e.g. Cunningham et al., 2004). In models of these rhythms, known to be disrupted in schizophrenia and related animal models, the excitatory drive to the local network is achieved via ectopic action potential generation in axons. Percolation of this activity through neighbouring, gap junctionally connected axons provides a brief burst of VFO which is ideally situated to drive local circuit interneurons (Whittington and Traub, 2003). In neocortex, excitation of axons can, paradoxically, occur through activity of axo-axonic (chandelier) interneurons (Howard et al., 2005). It is thought the location of the inhibitory synapses in cartridges along the proximal axon of principal cells causes direct depolarisation of the axon (Szabadics et al., 2006). As chandelier cells are GABAergic, chloride extrusion mechanisms and expression of the potassium chloride cotransporter 2 (KCC2) are important in determining the polarity of the postsynaptic response. Thus the low density of KCC2 in the axonal initial segment (Szabadics et al., 2006) is thought to result in a higher concentration of intracellular Cl^- and a depolarising response to GABA at these sites on the axon. Thus the decrease in chandelier cell functional markers in schizophrenia and epilepsy (above) may serve to decrease axonal excitability and thus reduce persistent gamma rhythm generation and overall neocortical network excitability. This thesis will reconsider a possible role for axonal excitability in antipsychotic-induced seizure-like activity in later results chapters.

1.4 Antipsychotics

1.4.1 Therapeutic effectiveness of clozapine

Chloropromazine was the first drug used to treat schizophrenia in the 1950s and introduced the idea of antipsychotics that target the dopamine D_2 receptor (e.g. Creese et al., 1976). More potent typical antipsychotics became available in the years that followed as medicinal chemists developed drugs with improved affinity for the D_2 receptor. However, these drugs were associated with the debilitating extrapyramidal side effects of parkinsonian syndromes and tardive dyskinesia as a result of the blockade of dopaminergic transmission in the basal ganglia. In addition, these drugs were associated with only limited improvements in psychosocial and cognitive function (Green, 1996).

By the early 1970s some of the advantages in the use of the antipsychotic clozapine, which was termed 'atypical' as it did not cause movement disorder to same extent as previous antipsychotics, were becoming clear. Clozapine has a reduced tendency to cause extrapyramidal side effects and an unparalleled effectiveness in treating schizophrenia (Kane et al., 1988). Specifically, clozapine may be superior to other typical and atypical antipsychotics in terms of the treatment of negative symptoms, refractory positive symptoms and even certain cognitive deficits (Davis, 2006;Kane et al., 1988;Keefe et al., 1999;Kumari et al., 1999;Lee et al., 1999;Wahlbeck et al., 2000). Clozapine is also particularly effective among antipsychotics in preventing suicide and helping clinical compliance (Conley and Kelly, 2001;McEvoy et al., 2006;McGurk, 1999;Meltzer et al., 2003;Spivak et al., 2003).

On the other hand, clozapine is associated with salient side effects such as agranulocytosis, weight gain and diabetes, and, interestingly, EEG abnormalities and seizures (e.g.Kumlien and Lundberg, 2009;Juul et al., 1985;Toth and Frankenburg, 1994), and for this reason tends only to be prescribed in cases when other antipsychotics have been insufficiently effective. In relation to seizures, clozapine may sometimes, but not always (Antony et al., 2008), be contraindicated in epilepsy. EEG abnormalities and seizures associated with clozapine are considered in more detail below (section 1.4.3).

1.4.2 Mechanisms underlying the action of clozapine

In addition to antagonising dopamine D_2 receptors, clozapine has a complex receptor binding profile and acts on multiple targets (Roth et al., 2004). For example, clozapine has a high affinity for 5-HT_{2A}, 5-HT_{2C}, 5-HT_6, 5-HT_7 serotonin receptors, dopamine D_4 receptors, muscarinic M_1, M_2, M_3, M_4, and M_5 receptors, and adrenergic α_1- and α_2-receptors (Roth et al., 2004). Clozapine also acts on NMDA and $GABA_A$ receptors (see section 1.4.2.1 and 1.4.2.2 below). In view of the glutamate and dopamine hypotheses of schizophrenia and the convergence of susceptibility genes around these neurotransmitter systems, one possibility is that clozapine may exert its complex action on multiple targets to normalise both glutamatergic and dopaminergic neurotransmission (Roth et al., 2004). Focal excitation or excitation-induced depolarization inactivation of DA neurons (Chiodo and Bunney, 1983;Hand et al., 1987), may also have a role in the antipsychotic effect of clozapine and other antipsychotics.

In attempting to identify the important targets in the therapeutic effect of clozapine, it was noted that the atypical antipsychotic risperidone blocks the effects of lysergic acid diethylamide (LSD) via its action on 5-HT_{2A} receptors (Colpaert, 2003). Following systematic analysis of the pharmacology of various typical and atypical antipsychotics, it was suggested that the key pharmacological action of atypical antipsychotics was the higher affinity for 5-HT_{2A} receptors versus that for D_2 receptors (Meltzer et al., 1989;Altar et al., 1986). With this idea in mind pharmaceutical companies attempted to develop new drugs with the same effectiveness of clozapine but without its side effects. Various atypical antipsychotics, such as olanzapine and quetiapine, which met this 5-HT_{2A}/ D_2 criteria, were then introduced. While such drugs provide further useful treatment options, so far none have proved more effective than clozapine in treating schizophrenia (Leucht et al., 2003;Tuunainen et al., 2002).

In developing novel atypical antipsychotics, further attempts have been made to identify compounds that mimic clozapine's actions on dopamine and serotonin receptor subtypes. However, such attempts have had limited success, possibly because more multi-target approaches are necessary. For example, the D_4 antagonist L-745,870 (Bristow et al., 1997), and the 5-HT2A/D4 antagonist fananserin (Truffinet et al., 1999), were not effective in treating schizophrenia. Similarly, the 5-HT2A selective antagonist M100907 (de Paulis, 2001) was not as effective as haloperidol, the comparator, in treating symptoms of schizophrenia.

As well as ameliorating positive and negative symptoms of schizophrenia, atypical antipyschotics may also have a small beneficial effect on cognition (Meltzer and McGurk, 1999). One possible explanation for the cognitive-enhancing properties of atypical antipsychotics relate to their action on 5-HT2A (Williams et al., 2002), 5-HT6 (Woolley et al., 2001) receptors, or boosted dopamine transmission in the prefrontal cortex (Castner et al., 2000).

In addition to its actions on metabotropic receptors, clozapine may modulate inhibitory and excitatory synaptic transmission.

1.4.2.1 Effects of clozapine on inhibitory synaptic transmission

In cultured neurons in the ventral tegmental area (VTA), clozapine suppressed GABAergic inhibitory synaptic transmission (Michel and Trudeau, 2000). Inhibitory post-synaptic currents (IPSCs) evoked in isolated GABAergic neurons were depressed by clozapine in a concentration-dependent manner. Likewise, GABA-induced currents were depressed by clozapine in a concentration-dependent manner to a comparable extent. Furthermore, clozapine reduced the amplitude of miniature IPSCs in a similar manner to SR-95531, a specific $GABA_A$ receptor antagonist (Michel and Trudeau, 2000). Similarly, in cultured hippocampal neurons, clozapine reduced inhibitory synaptic transmission (Ohno-Shosaku et al., 2011).

Interestingly, a different study failed to find such a clear effect of clozapine on inhibitory transmission (Gemperle et al., 2003). In rat prefrontal cortex slices IPSPs were measured in layer V pyramidal cells following stimulation of layer II. There was a trend whereby clozapine concentration-dependently reduced IPSPs but this failed to reach statistical significance (Gemperle et al., 2003). Interestingly, at higher concentrations of clozapine (100-300µM) some cells fired epileptiform discharges in this study.

It is possible therefore that the clozapine-sensitivity of GABAergic synapses is higher in the VTA (Michel and Trudeau, 2000) and hippocampus (Ohno-Shosaku et al., 2011) compared to that in prefrontal cortex (Gemperle et al., 2003). The interaction of clozapine with $GABA_A$ receptors may depend on their subunit composition (Korpi et al., 1995;Squires and Saederup, 1998). Alternatively, the difference may be due to the use of brain slice preparations rather than cultured neurons.

1.4.2.2 Effects of clozapine on excitatory synaptic transmission

The effects of clozapine on excitatory synaptic transmission have also been investigated in a number of studies. Microdialysis experiments *in vivo* in freely moving rats demonstrated that clozapine, but not haloperidol, increased extracellular glutamate in the medial prefrontal cortex (Daly and Moghaddam, 1993;Yamamoto et al., 1994). In cultured hippocampal neurons clozapine depressed glutamatergic neurotransmission (Ohno-Shosaku et al., 2011). Furthemore, clozapine inhibited glutamate release in nerve terminals isolated from rat prefrontal cortex (Yang and Wang, 2005). In the CA1 region of rat hippocampal slices 50µM clozapine induced a transient depression followed by a small potentiation of extracellular field potentials (Baskys et al., 1993). However, in one

study 10-300μM clozapine had no significant effect on EPSPs in slices of rat prefrontal cortex (Gemperle et al., 2003).

In contrast, in a different study 50-100nM clozapine enhanced NMDA-evoked responses and the NMDA receptor contribution to EPSPs/EPSCs elicited by electrical stimulation in rat medial prefrontal cortex (Arvanov et al., 1997). It is possible that the concentration of clozapine used by Arvanov et al. (50-100nM) was lower than the therapeutic concentration of clozapine in cerebrospinal fluid (see section 4.4.4).

Interestingly, in this study, clozapine did not potentiate pharmacologically isolated NMDA receptor-mediated EPSCs, and the potentiating effect of clozapine on NMDA receptor-mediated neurotransmission was eliminated by the AMPA antagonist CNQX (Arvanov et al., 1997). For this reason, it was thought that the effect of clozapine did not result from its direct interaction with NMDA receptors on pyramidal neurons. Indeed it was possible that the action of clozapine on NMDA responses was secondary to its binding to other receptors. For example, it could be speculated that antagonism of dopamine and serotonin receptors by clozapine could remove the inhibitory influence of serotonin and dopamine and thus increase glutamate release (Kornhuber and Kornhuber, 1986;Maura et al., 1989;Maura et al., 1988a;Maura et al., 1988b;Peris et al., 1988).

Chronic clozapine treatment reduced MK-801 binding in the medial prefrontal cortex (Tarazi et al., 1996;McCoy and Richfield, 1996;Giardino et al., 1997) and reduced expression of the NMDA NR-2C subunit in frontal cortex (Riva et al., 1997). This reduction in expression of NMDA receptors may be a compensatory response to the enhancement of NMDA receptor-mediated transmission by clozapine (Arvanov et al., 1997).

There is also interest in the possibility that clozapine may boost NMDA receptor-mediated transmission via the glycine modulatory site. Interestingly, glycine, D-serine and sarcosine, when combined with antipsychotics such as risperidone or olanzapine, have significant beneficial effects on negative symptoms (Javitt, 2006;Tsai and Lin, 2010). In contrast, such compounds are ineffective when combined with clozapine (Evins et al., 2000;Tsai et al., 1999;Goff et al., 1996;Tsai and Lin, 2010), possibly because clozapine may already increase synaptic glycine levels.

In another study, the role of clozapine in modulating glycine transport was investigated (Javitt et al., 2005). Selective inhibitors were used to investigate processes involved in glycine transport in synaptosomes. In addition to glycine type 1 transporters, glycine transport was also mediated by System A transporters in these preparations, and,

interestingly, System A transporters were inhibited by clozapine (Javitt et al., 2005). Inhibition of glycine transporters would raise synaptic glycine, resulting in upregulated NMDA receptor-mediated transmission, provided that glycine binding sites were previously unsaturated. Thus clozapine may mediate enhanced NMDA receptor-mediated transmission via inhibition of System A-type glycine transporters (Javitt et al., 2005).

Interestingly, clozapine did facilitate long-term potentiation in the layer II-V pathway in rat prefrontal cortex slices (Gemperle et al., 2003). In line with a role in the induction of synaptic plasticity, clozapine also potentiated NMDA receptor-mediated currents in most pyramidal cells in this region (Gemperle et al., 2003).

In considering the mechanisms through which clozapine may enhance NMDA receptor-mediated currents – and contrary to ideas proposed from the studies mentioned above various binding studies have suggested that clozapine has a direct effect on the NMDA receptor complex (Lidsky et al., 1993;Lidsky et al., 1997;Banerjee et al., 1995;McCoy and Richfield, 1996;Shim et al., 1999). These effects *in vitro*, in intact brain tissue may have been masked by larger effects on pre- or post-synaptic modulation of monoamine signalling. This may explain the discrepancies between results in this research area.

Interestingly, paired-pulse experiments in cultured hippocampal neurons suggested that clozapine may also modulate synaptic transmission presynaptically, possibly via inhibition of voltage-gated Ca^{2+} and Na^{+} channels (Ohno-Shosaku et al., 2011).

An incidental and unexpected finding related to the extent to which clozapine accumulated in slices *in vitro* (Gemperle et al., 2003). Following *in vitro* experiments the concentration of clozapine in slices was determined after 2h perfusion using high-pressure liquid chromatography and mass-spectrometric detection (Gemperle et al., 2003). Unexpectedly, there was an 18-fold accumulation of clozapine in the slice compared to the perfusing medium, a level of accumulation similar to that which has been reported *in vivo* in rodents where the concentration of clozapine in brain is 16-24 times greater than that in plasma (Baldessarini et al., 1993;Weigmann et al., 1999).

1.4.2.3 Efficacy of clozapine in NMDA hypofunction models of psychosis

In addition to electrophysiological studies examining the effect of clozapine on excitatory synaptic transmission *in vitro*, there is evidence that clozapine may potentiate NMDA receptor signalling in NMDA hypofunction models of psychosis. Indeed it is possible that clozapine's actions on NMDA receptors may be important in the mechanisms that distinguish it from other atypical and typical antipsychotics.

Cognitive impairments, an important aspect of schizophrenia, occur in regular PCP abusers (Cosgrove and Newell, 1991). Furthermore, cognitive deficits as assessed in the delayed activation T-maze and object retrieval with a detour task also occur in animals under repeated exposure to PCP (Jentsch et al., 1997a;Jentsch et al., 1997b). Interestingly, such cognitive impairments induced by PCP could be mitigated by clozapine (Jentsch et al., 1997a).

Clozapine, and the selective 5-HT_{2A} receptor antagonist M100907 (Kehne et al., 1996), but not haloperidol or the D2 receptor antagonist raclopride, prevent acute PCP-induced blockade of NMDA responses in pyramidal neurons in slices from rat medial prefrontal cortex (Wang and Liang, 1998). Furthermore, in rats repeated PCP injections induced a hypersensitive response to NMDA in medial prefrontal cortex neurons, and treatment with clozapine, but not haloperidol, prevented this hyperactivity of NMDA receptors (Arvanov and Wang, 1999).

Clozapine, but not haloperidol, also reduces psychosis induced by the NMDA receptor antagonist ketamine (Lahti et al., 1995;Malhotra et al., 1997). Similarly, in monkeys clozapine improves cognitive deficits associated with subchronic PCP administration.

Using ensemble recording in freely moving rats, NMDA receptor antagonism disrupted the rate and pattern of neuronal activity in prefrontal cortex to give a state of cortical hyperactivity (Jackson et al., 2004). The increased firing rate in most neurons correlated with behavioural impairments (Jackson et al., 2004).

Similar *in vivo* ensemble unit recording in awake rats was used to investigate the effect of clozapine and haloperidol on spontaneous neuronal activity in the normal baseline state, and in the disrupted state following challenge with the NMDA receptor antagonist MK801 (Homayoun and Moghaddam, 2007). Clozapine, but not haloperidol, had a state-dependent effect on the spontaneous firing rate of prefrontal cortex cells which depended on their baseline activity. That is, clozapine increased the firing rate of

neurons with low baseline activity and reduced the firing rate of neurons with high baseline activity. Clozapine also reversed the disruptive cortical hyperactivity resulting from NMDA receptor antagonism, and this reversal was correlated with reduced behavioural impairments (Homayoun and Moghaddam, 2007). This is similar to the effect in other studies whereby clozapine reduced behavioural impairments associated with NMDA receptor antagonists in humans (Duncan et al., 1998;Malhotra et al., 1997) and animals (Bakshi et al., 1994).

In line with the possible importance of inhibition of system A-type glycine transporters in clozapine's enhancement of NMDA receptor-mediated transmission (see section 1.4.2.2 above), positive modulation of the glycine modulatory site on NMDA receptors, either directly with D-serine or by blocking glycine transporter-1, had a similar effect to that of clozapine but not haloperidol in rescuing MK-801 induced impairments in social recognition (Shimazaki et al., 2010).

1.4.3 Pathological EEG abnormalities associated with antipsychotics

In line with the idea that treatments for psychosis can raise excitability (1.4.2.2 above), it is now well established that those antipsychotic drugs most effective in treating psychosis have the potential to induce paroxysmal EEG changes and seizures. Indeed, clozapine, a particularly effective antipsychotic (Kane et al., 1988), was associated with the highest risk of generalised EEG abnormality compared to other antipsychotics (Centorrino et al., 2002). In terms of modern atypical drugs, after clozapine the risk of EEG abnormality is greatest with olanzapine and risperidone (Centorrino et al., 2002).

In one study EEG abnormalities were observed in 53% of patients treated with clozapine, and the absence or presence of EEG abnormalities correlated with the plasma clozapine concentration (Haring et al., 1994). While other studies reported an incidence of clozapine-associated EEG alterations between 16% (Naber et al., 1989) and 75% (Koukkou et al., 1979), Haring et al. (1994) was considered a good predictor of the true extent of clozapine-associated EEG alterations because of the absence of potentially confounding psychotropic or anticholinergic co-medications, the prospective design, and analysis of the effect of the drug on the premedication baseline EEG. Controversies over the dose-dependence of clozapine-related EEG abnormalities are probably explained by the variability in the clozapine plasma concentration for a given dose (Haring et al., 1990).

Clozapine-related abnormal EEG activity included slowing of activity related to sleepiness, abnormal theta, abnormal delta, and importantly, intermittent sharp transients, spike discharges, and spike-wave paroxysms (e.g. Malow et al., 1994;Welch et al., 1994;Haring et al., 1994;Freudenreich et al., 1997;Centorrino et al., 2002). Theta and delta abnormalities included generalised or frontal symmetrical theta slowing, delta slowing, and asymmetrical focal theta or delta (e.g. Haring et al., 1994;Centorrino et al., 2002). Qualitative identification of EEG abnormalities would be typically be made by qualified individuals, e.g. an experienced electroencephalographer (Haring et al., 1994) or board-certified neurologists (Centorrino et al., 2002).

In addition to the above EEG abnormalities and seizure-like transient events, clozapine has also been reported to generate more overt epileptiform events. The incidence of full-seizures following clozapine treatment is likely dose dependent and may be 1.3-2.8% (Devinsky et al., 1991;Pacia and Devinsky, 1994). It has been estimated that after 3.8 years of clozapine treatment the cumulative risk of seizures rises to 10% (Devinsky et al., 1991). The more frequent paroxysmal activity associated with clozapine versus haloperidol (Koukkou et al., 1979) may explain the higher incidence of seizures in patients treated with clozapine compared to those treated with typical neuroleptics (Lindstrom, 1988;Naber et al., 1989;Haller and Binder, 1990).

Similar to the findings in human studies, in rats intraperitoneal clozapine induced paroxysmal slow waves and spike activity in amygdala, hippocampus and cortex *in vivo* (Denney and Stevens, 1995). This clozapine treatment also produced dose-dependent myoclonic jerks when rats were partially restrained.

Olanzapine is a thienobenzodiazepine derivative with structural and pharmacological similarity to clozapine, and, like clozapine, it has a concentration-dependent association with EEG abnormalities (Amann et al., 2003;Degner et al., 2011). The risk of EEG abnormalities associated with olanzapine is fairly similar across studies; for example 35% (Amann et al., 2003), 38.5% (Centorrino et al., 2002), or 40.9% (Degner et al., 2011) of patients treated with olanzapine were affected. Olanzapine may also induce myoclonus (Camacho et al., 2005;Deshauer et al., 2000), even when only prescribed at a low dose, albeit chronically (Block Rosen et al., 2012). Reports of seizures associated with olanzapine, although present in the literature (e.g. Wyderski et al., 1999;Woolley and Smith, 2001;Bonelli, 2003), are not as common as those associated with clozapine (Komossa et al., 2010).

1.5 Possible mechanisms underlying clozapine-induced epileptiform events

Possible mechanisms underlying clozapine-induced epileptiform activity include VFO, which are associated with epilepsy (see section 1.3 and 1.5.1.3) and occur during transient epileptiform activity in humans (e.g. Jacobs et al., 2008), $GABA_A$ receptor-mediated transmission, which may be suppressed by clozapine (see section 1.4.2.1), and NMDA receptor-mediated transmission which may also be modulated by clozapine (see section 1.4.2.2).

1.5.1 Very fast oscillations (VFO)

VFO, which can also be termed 'ripples' due to their fast and transient nature, may be relevant to clozapine's action of raising excitability in brain tissue (chapter 4). It is becoming increasingly apparent that they form a fundamental component of human cortical epileptiform events (Roopun et al., 2010), particularly those manifest as spontaneous, transient discharges. An understanding of VFO may provide insights into the electrophysiology underlying both healthy physiological processes and pathological activity such as seizures. To date little is known about how VFO may be generated at the level of neurons and networks, how they may be pharmacologically manipulated, and what their role is in normal and pathological brain function. Here literature describing physiological and pathological roles for VFO and mechanisms underlying each are considered.

1.5.1.1 Physiological role of VFO

Sharp waves, large negative field excitatory postsynaptic potentials (EPSPs) lasting tens of milliseconds, were first observed in EEG recordings from rat hippocampus *in vivo*. They were observed during slow-wave (non-dreaming) sleep, eating, drinking and awake immobility (Buzsaki, 1986). Sharp waves were not observed during locomotion, which results in theta and gamma frequency oscillations. It was later observed that low-amplitude VFO, or ripples, were superimposed on the sharp waves (Buzsaki et al., 1992).

Further to the finding that sharp wave/ripples occurred in slow-wave sleep (Buzsaki et al., 1992), Wilson and McNaughton (1994) performed a study which suggests a possible physiological role for ripples in memory consolidation. Simultaneous multi-array recordings were taken from multiple rat hippocampal place cells during spatial behavioural tasks. The recordings were also taken during slow-wave sleep both before

and after the behavioural tasks. Correlations of activity occurred in which cells which fired together when the animal was present in a specific location were selectively more likely to fire together in sleep following than in sleep preceding the tasks. Oscillation recordings from multiple unit recording sites in the hippocampus confirmed that intermittent sharp wave/ripple activity occurred during sleep. The correlations were greater when ripples were present compared to the periods in between when ripples were absent (Wilson and McNaughton, 1994). Interestingly, sharp/wave ripples are initiated in CA3, and the output layers of entorhinal cortex show neuronal behaviour that correlates with sharp waves in CA1 (Chrobak and Buzsaki, 1994). As such the induced correlations during sharp waves (Wilson and McNaughton, 1994) may result from adaptations in the hippocampus which are then transmitted to the output layers of entorhinal cortex. The sharp waves in hippocampus and entorhinal cortex have a strong depolarising effect on postsynaptic targets in neocortex that may serve to transfer memory information from hippocampus to neocortex.

This demonstration, of replay of information obtained during active behaviour in sleep, is consistent with theories of memory consolidation. It would fit into a scheme in which there is an important role for synaptic plasticity in the hippocampus in the preliminary storage of event memories (e.g.Bliss and Collingridge, 1993). Encoded neural activation patterns associated with previous active behaviour are then reactivated during slow-wave sleep in a memory consolidation process in which information stored in the hippocampus is transferred to neocortex.

In addition to its role in memory consolidation in hippocampus, there is also evidence that VFO has a role in sensory perception when generated in neocortex. A brisk induced twitch of the whiskers of an anaethetised rat evokes a response in sensory neocortex upon which VFO are superimposed (Barth, 2003). The VFO are generated in cortex, triggered by inputs from the thalamus (Staba et al., 2003), and organised in cortex spatially according to intracortical pathways (Barth, 2003;Staba et al., 2005). Interestingly, multiunit somatosensory neural responses in layer IV have a 1:1 correspondence to mechanical whisker stimulations at rates up to 320Hz (Ewert et al., 2008), suggesting a role for VFO in encoding in this case.

VFO components are present in somatosensory evoked responses in piglets (Ikeda et al., 2002) and humans (Curio, 2000;Curio et al., 1994). In piglets, it has been proposed that the response may be initiated by thalamocortical axonal terminals (Ikeda et al., 2002;Ikeda et al., 2005) and cortical somata and dendrites (Okada et al., 2005).

Auditory stimuli, particularly when it is unexpected, can also evoke VFO in the anterior temporal cortex of awake human patients (Edwards et al., 2005).

1.5.1.2 Mechanisms underlying physiological VFO

VFO occur in telencephalic structures, such as hippocampus, entorhinal cortex and neocortex. Spontaneous VFO can occur in physiological conditions *in vivo*, for example superimposed on physiological sharp waves in hippocampus and deep entorhinal cortex (Buzsaki et al., 1992;Chrobak and Buzsaki, 1996;Ylinen et al., 1995b). VFO can also be superimposed on responses in the cortex evoked by sensory stimulation of a somatosensory (Jones and Barth, 1999;Jones et al., 2000;Baker et al., 2003;Curio et al., 1994;Okada et al., 2005) or auditory modality (Lakatos et al., 2005).

VFO can also be superimposed on spontaneous or evoked sharp waves *in vitro* (Maier et al., 2002;Maier et al., 2003;Nimmrich et al., 2005). Interestingly, these authors showed that sharp wave /ripples could be readily observed in mouse hippocampal slices *in vitro* (Maier et al., 2002;Maier et al., 2003;Nimmrich et al., 2005). During these sharp-wave ripples *in vitro*, unlike suggestions from *in vivo* work, many pyramidal cells are hyperpolarized (Maier et al., 2002;Behrens et al., 2007a). Unlike in mouse slices, sharp wave/ripples do not normally occur in unstimulated rat hippocampal slices *in vitro*, in which the sharp wave component is absent (Draguhn et al., 1998). It is not known why this discrepancy occurs, but it has been suggested that more circuitry may be preserved in mouse slices (Insausti, 1993) or that the mouse slice preparation is more excitable.

VFO can be superimposed on neuronal population responses. For example, *in vivo*, VFO of approximately 200Hz are superimposed on physiological sharp waves in the hippocampus (Buzsaki et al., 1992;Ylinen et al., 1995a;Klausberger et al., 2003). In investigating the cellular mechanisms and function of such oscillations, it is important to consider the relationship between the slower responses, which may result from synchronized synaptic currents, and the superimposed VFO which appear to be far too fast to be supported by conventional chemical synaptic processes.

In vitro approaches are useful in investigating mechanisms underlying oscillatory activity. Following the discovery of sharp wave/ripples *in vivo* (Buzsaki et al., 1992), spontaneous VFO were later observed without sharp waves in a seminal study in hippocampal slices *in vitro* (Draguhn et al., 1998). The VFO were confined to the pyramidal cell layer, and there were local patches of differing levels of VFO activity at

different longitudinal positions along the pyramidal cell layer (Draguhn et al., 1998). Coherent VFO activity was confined to 120µm regions *in vitro* (Draguhn et al., 1998), notably smaller than the region of coherence *in vivo*, ~5mm (Chrobak and Buzsaki, 1996).

The VFO persisted following blockade of $GABA_A$ receptors, AMPA receptors and NMDA receptors together. Furthermore, these VFO persisted when nominally calcium-free artificial cerebrospinal fluid was used to block calcium-dependent synaptic transmission. Thus, these VFO did not require conventional chemical synaptic neurotransmission at the synapse. Interestingly, in addition to blocking synaptic transmission, low Ca^{2+} medium enhances VFO (Draguhn et al., 1998). Three different gap-junction blockers, carbenoxolone, octanol and halothane, each reversibly suppressed these VFO, suggesting that electrotonic coupling at gap junctions is necessary for the generation of these VFO.

These VFO occurred more often when neuronal excitability was increased by increasing K^+, application of carbachol, application of 4-aminopyridine, or exclusion of calcium from artificial cerebrospinal fluid (Draguhn et al., 1998). NH_4Cl, increases intracellular alkalinisation (Thomas, 1984), which elevates gap junction coupling (Spray et al., 1981). Interestingly, application of NH_4Cl increased the frequency and duration of these VFO (Draguhn et al., 1998).

Overall these data provided strong evidence that spontaneous VFO in the hippocampus *in vitro* results from electrotonic coupling at gap junctions (Draguhn et al., 1998). Network modelling predicts that such coupling would occur between pyramidal cell axonal branches (Traub et al., 2012).

However, although some studies supported the importance of gap junctions in the mechanisms underlying VFO in telencephalic structures, other studies suggested alternative mechanisms. When ripples were discovered it was observed that interneurons could discharge at the frequency of the (field) ripple, whereas pyramidal cell somata did not (Buzsaki et al., 1992).

Further observations were then made about the firing of identified interneurons. A histologically verified basket cell discharged at the frequency of ripples (Ylinen et al., 1995a). Basket cells and bistratified cells discharged in phase with ripples, axoaxonic interneurons fired immediately prior to and at the onset of a ripple, but then were silent, and cholecystokinin basket cells and cholecystokinin dendrite-targeting cells only

discharged infrequently (Klausberger et al., 2003;Klausberger et al., 2004;Klausberger et al., 2005). Furthermore, phasic IPSPs, which occurred at the frequency of ripples, were observed in pyramidal cells (Ylinen et al., 1995a). Experimental alterations of the membrane potential and intracellular Cl^- were in line with the synaptic potentials being mediated by $GABA_A$ receptors (Ylinen et al., 1995a).

Taken together, the data above have led to the suggestion that networks of fast-spiking interneurons generate ripple oscillations, but other evidence suggests that alternative explanations should be considered. Firstly, VFO persist following blockage of $GABA_A$ receptors *in vitro* and *in vivo* (Maier et al., 2003;Jones and Barth, 2002). Indeed, VFO persist following complete blockage of chemical synaptic transmission, and in these conditions principal spikelets occur at the frequency of VFO (Draguhn et al., 1998). VFO induced by ejection of a concentrated K^+ solution in the dentate gyrus also occurs in Ca^{2+}-free artificial cerebrospinal fluid (Towers et al., 2002).

Secondly, the activity of the somata of pyramidal cells cannot be generalised to the activity of the whole of the pyramidal cell. Thus although there is only infrequent firing of the somata of pyramidal cells, this does not exclude the possibility that pyramidal cell axons are involved in the generation of ripples. Indeed, there is evidence of antidromic spikes during VFO (Draguhn et al., 1998;Papatheodoropoulos, 2008). Furthermore, the fact that VFO may be manifest as recurring population spikes suggests co-ordinated activity of pyramidal cells rather than interneurons. In support of this, intracellular recordings from a pyramidal cell show activity that corresponded to the field ripples (Draguhn et al., 1998). There were two types of depolarisation in the pyramidal cell that corresponded to the population spikes: action potentials that were inflected or had an initial shoulder or notch associated with being antidromic, or spikelets.

Thirdly, intracellular recordings from a putative pyramidal cell show no evidence of phasic IPSPs in sharp wave/ripples induced by application of KCl in mouse hippocampal slices when $GABA_A$ receptors are blocked (Nimmrich et al., 2005). Consistent with previous findings (Draguhn et al., 1998), ripples persist following additional blockade of ionotropic glutamate receptors, but do not occur in the presence of the gap junction blocker octanol (Nimmrich et al., 2005).

Fourthly, VFO superimposed on rat somatosensory cortex potentials evoked by whisker stimulation persist and actually occur more following topical application of the $GABA_A$ receptor antagonist bicuculline (Jones and Barth, 2002).

Interestingly, data which have led to the idea that interneurons generate ripples (Buzsaki et al., 1992;Ylinen et al., 1995a;Klausberger et al., 2003;Klausberger et al., 2004), can be re-interpreted in a model whereby pyramidal cell axons generate VFO (Traub and Bibbig, 2000). The transient nature of the oscillation can be explained in that axons and cells must reach a sufficient level of depolarisation for the ripple to occur (Traub and Bibbig, 2000).

Cerebellar VFO *in vitro* are also dependent on gap junctions as they are associated with spikelets, are suppressed by gap junction blockers, and survive in conditions in which synaptic transmission is blocked by use of low Ca^{2+} artificial cerebrospinal fluid.

Overall, different mechanisms underlying VFO may be possible according to, for example, the brain region, the experimental conditions and co-existence of other oscillatory activity.

1.5.1.3 Pathological role of VFO in seizures and epilepsy

VFO can also occur in connection with epileptogenesis *in vivo*. VFO can occur immediately prior to an interictal burst or seizure, and/or superimposed on bursts within a seizure (Akiyama et al., 2005;Akiyama et al., 2006;Asano et al., 2005;Fisher et al., 1992;Grenier et al., 2003;Jirsch et al., 2006;Kobayashi et al., 2004;Traub et al., 2005a;Urrestarazu et al., 2006;Worrell et al., 2004). For example, in anaesthetised cats in which seizures occurred spontaneously or were electrically induced, VFO were prominent during seizure onset, and it was thought that although VFO occur in the normal healthy network state, they could have a role in starting seizures when their amplitude reaches a particular threshold (Grenier et al., 2003).

Furthermore, VFO can occur without seizures or bursts in epileptogenic brain, often at frequencies greater than 250 or 300Hz, termed ‘fast ripples’. Fast ripples can be confined to volumes of approximately $1mm^3$ of tissue, and may be important in seizure pathology (Bragin et al., 1995;Bragin et al., 1999a;Bragin et al., 1999b;Bragin et al., 2002b;Bragin et al., 2002a;Bragin et al., 2003;Bragin et al., 2005;Staba et al., 2002;Staba et al., 2004).

For example, Staba et al. (2002) performed a study which supports the idea that fast ripples may be pathological events associated with seizure genesis. In patients with mesial temporal lobe epilepsy, quantitative analysis of EEG recordings in the hippocampus and entorhinal cortex during non-rapid eye movement sleep showed two

distinct groups of events corresponding to fast ripples and slow VFO. The ratio of the occurrence of fast ripples to slow VFO was significantly greater in brain regions ipsilateral to seizure onset compared to that in brain regions contralateral to seizure onset. This ratio was also higher in ipsilateral regions which had hippocampal atrophy compared to regions contralateral to seizure commencement and hippocampal atrophy.

Furthermore, during sleep and wakefulness in patients with medial temporal lobe epilepsy, the occurrence of slow VFO in epileptogenic and nonepileptogenic temporal lobe was comparable, but fast VFO were significantly associated with epileptogenic regions (Staba et al., 2004). In support of this idea, surgical removal of brain regions associated with seizure-related fast ripples in children with pharmaco-resistant neocortical epilepsy appeared to prevent further seizures (Ochi et al., 2007).

Similar results have been obtained in focal epileptic patients using implanted EEG macroelectrodes rather than microelectrodes (Jirsch et al., 2006). Fast ripples were observed when focal seizures started in the mesial temporal lobe (Jirsch et al., 2006). However, there was also evidence that slow VFO levels were elevated compared to the background level in seizures in ¾ mesial temporal patients (Jirsch et al., 2006). Microelectrode recordings from patients with mesial temporal lobe epilepsy, suggest that the cellular networks involved in the generation of fast ripples may be more localised than those involved in slow VFO (Bragin et al., 2002b).

In patients with intractable focal epilepsy, VFOs occurred more frequently and for a longer duration inside the seizure onset zone compared to outside it, and the rate of VFOs represented a more accurate method of identifying the seizure onset zone than the rate of spikes (Jacobs et al., 2008). Interestingly, fast ripples may be a good marker of the generation of focal epileptic activity as a result of their restricted electrical field compared to spikes or sharp waves (Rodin, 2005).

Correspondingly, VFO can occur in connection with epileptogenesis *in vitro*, as it does *in vivo*. VFO can occur immediately prior to an interictal burst or seizure (Pais et al., 2003;Khosravani et al., 2005), superimposed on epileptiform bursts (Schwartzkroin and Prince, 1977;Wong and Traub, 1983), or in between bursts (Traub et al., 2005a).

Application of kainate together with antagonists of $GABA_A$ and $GABA_B$ receptors in the rat auditory cortex *in vitro*, results in epileptiform bursts which contain VFO (Traub et al., 2005a). Electrical coupling between axons is important in determining epileptogenic activity in this case (Traub et al., 2005a).

While the mechanism of generation of physiological sharp wave/ripples has yet to be definitively established, the mechanism of VFO generation in epileptic tissue is perhaps even less clear. Indeed it still remains unclear whether the structure of VFO associated with interictal discharges is the same as that of physiological sharp waves. In terms of the mechanism, *in vivo* recordings in the human hippocampus demonstrate an association between field VFO and interneuron activity (Le Van et al., 2008). However, the gap junction blocker halothane suppresses VFO that occur with seizures (Grenier et al., 2003). Furthermore, similar to physiological VFO, *in vitro* data combined with modelling suggest that principal cell axons coupled by gap junctions have the major role in generating epileptiform bursts (Traub et al., 2005b).

In experiments in which kainate had been administered intrahippocampally to induce seizures in rats, inhibition appeared to be retained *in vitro* in regions of slices generating fast ripples, but antagonism of $GABA_A$ receptors increased the size of the region generating fast ripples (Bragin et al., 2002a).

Various studies using both *in vivo* and *in vitro* models of epilepsy demonstrate that carbenoxolone and other gap junction blocking agents suppress seizure discharges (Gareri et al., 2004;Gigout et al., 2006;He et al., 2009;Jahromi et al., 2002;Kohling et al., 2001;Nilsen et al., 2006;Perez-Velazquez et al., 1994;Ross et al., 2000;Szente et al., 2002). In the *in vivo* studies, drug application was either through local application to the brain, intraventricular or systemic routes. Seizure discharges induced by 4-aminopyridine are also lower in connexin36 knockout mice compared to littermate controls (Maier et al., 2002). However, the mechanism by which this occurs is unclear as the involvement of excessive GABA release in seizures induced by 4-aminopyridine raises the possibility that interneuron activity is affected in the knockout phenotype. In general, blockade of gap junctions only partially rather than fully suppressed epileptiform activity, but the effect of halothane on spontaneous seizures in the cat *in vivo* was close to complete abolition (Grenier et al., 2001;Grenier et al., 2003).

In contrast, in a model of epilepsy where the extracellular concentration of K^+ is modulated, blockade of ionotropic glutamate receptors abolished fast ripples in rat hippocampal slices (Dzhala and Staley, 2004). In this model it was thought that synchronous bursts in pyramidal cells and similar intrinsic firing patterns among local neurons were required for fast ripples, and that this synchronous activity depended on glutamatergic synaptic transmission. With regard to the high extracellular K^+ used in this study (Dzhala and Staley, 2004), there is good evidence for a link between

disrupted regulation of extracellular K^+ and epileptogenesis in human epilepsies and animal models (e.g. Frohlich et al., 2008).

Data from a lithium-pilocarpine animal model of epilepsy suggest another possible mechanism still, that ripples may reflect a pathological desynchronisation of normal ripple activity in the CA3 region of the hippocampus (Foffani et al., 2007). In this model lithium-pilocarpine is administered to rats to induce *status epilepticus*. A perfusion medium which increases excitability induced sharp wave/ripples in CA3 slices from normal rats; fast ripples were also induced in CA3 slices from epileptic rats. Fast ripples were associated with unreliable cell firing resulting from synaptically driven fluctuations in membrane potential. Reducing the fluctuations in membrane potential rescued spike-timing reliability and restored normal ripples in epileptic hippocampus. Conversely, modulation of the delayed rectifier potassium current to reduce spike timing reliability in normal hippocampus resulted in desynchronisation of ripples. Thus it was concluded that impairments in spike-timing reliability are important in the mechanism underlying fast ripples in this model.

As mentioned above, a recent study, using human epileptic tissue rather than animal models, cast light on the mechanism of VFO generation in epilepsy (Roopun et al., 2010). *In vitro*, spontaneous VFO associated with interictal discharges occur in human tissue which had been surgically removed from epileptic neocortex. Interestingly, intracellular recordings reveal VFO in compound EPSPs in fast spiking interneurons with a delayed phase compared to the field VFO. Furthermore, there was a weak recruitment of somatic pyramidal cell and interneuron spiking, and VFO power was not related to either synaptic excitation or inhibition of principal cells. VFO persist following blockade of $GABA_A$ receptors but is suppressed by the gap junction blocker carbenoxolone. Overall, the observations of Roopun et al. (2010) support the idea that VFO in epileptic cortex is generated by activity in the pyramidal cell axonal plexus rather than by interneurons.

1.5.2 The role of $GABA_A$ receptors in seizure-like activity

In light of the suppression of $GABA_A$ receptor-mediated inhibition by clozapine (Michel and Trudeau, 2000;Ohno-Shosaku et al., 2011), and clozapine's ability to cause epileptiform activity, it is interesting to consider the role of $GABA_A$ receptors in seizure-like activity.

Early studies showed that blocking $GABA_A$ receptor-mediated inhibition induces epileptiform activity in animals *in vitro* (Schwartzkroin and Prince, 1978;Schwartzkroin and Prince, 1980) and *in vivo* (Matsumoto and Marsan, 1964;Prince, 1968;Dichter and Spencer, 1969;Ayala et al., 1973). The feline generalised penicillin epilepsy model, in which penicillin, a weak $GABA_A$ antagonist, induces generalised spike-wave discharges, became well-established in epilepsy research (e.g. Avoli and Gloor, 1982b;Avoli and Gloor, 1982a).

Indeed, application of various $GABA_A$ receptor antagonists, including bicuculline, picrotoxin or penicillin to isolated hippocampal or neocortical brain slice preparations *in vitro* has been a widely used approach in epilepsy research. Such approaches demonstrated that $GABA_A$ receptor function is important in limiting neuronal network synchrony and controlling transmission in polysynaptic pathways (Miles and Wong, 1983;Miles and Wong, 1987).

Complex roles for GABAergic neurotransmission in epilepsy are emerging with the proposal that GABAergic neurotransmission may contribute to epileptiform synchrony (Avoli et al., 1993;Avoli et al., 1996a;Avoli et al., 1996b;Avoli et al., 1996c;de Curtis and Gnatkovsky, 2009). Another example of the complex relationship between $GABA_A$ receptors and epilepsy is demonstrated by the finding that inhibition may actually be strengthened in the dentate gyrus in the kindling model of temporal lobe epilepsy (Otis et al., 1994).

Nonetheless, a role for the partial inhibition of $GABA_A$ receptors continues to be highlighted in the generation of epileptiform activity. While full blockade of $GABA_A$ receptors *in vitro* induces interictal activity but not prolonged ictal discharges, partial reduction of GABAergic inhibition can generate full seizure-like activity. For example, partial disinhibition conferred by transient arterial application of the $GABA_A$ receptor antagonist bicuculline to the guinea pig isolated brain preparation induces seizures in the entorhinal-hippocampal region (Gnatkovsky et al., 2008). In line with this, a partial reduction in fast $GABA_A$ receptor-mediated inhibition has been suggested to trigger seizures in computer models of temporal lobe seizures (Wendling et al., 2002;Labyt et al., 2006).

In isolated preparations, $GABA_A$ receptor antagonism in most cases induces short-lasting interictal spikes or prolonged afterdischarges similar to those seen after high frequency stimulation. Seizure-like events themselves typically require a brain

preparation including interconnected regions, such as the hippocampal-parahippocampal slice preparation (Walther et al., 1986;Jones and Lambert, 1990a;Jones and Lambert, 1990b;Dreier and Heinemann, 1991).

Recent work has highlighted the importance of chloride homeostasis in GABA signalling in temporal lobe epilepsy (e.g. Cohen et al., 2002;Huberfeld et al., 2007;Miles et al., 2012). The level of chloride in neurons controls post-synaptic GABA signalling (Farrant and Kaila, 2007) and therefore altered chloride homeostasis can change the strength and sign of GABAergic responses.

In slices from patients with temporal lobe epilepsy, the subiculum generated spontaneous interictal discharges (Cohen et al., 2002;Huberfeld et al., 2007). Interestingly, the reversal potentials for isolated GABA-mediated synaptic events were depolarised in some subicular pyramidal cells suggesting that Cl^- homeostasis was altered.

Further evidence of altered Cl^- homeostasis in brain tissue from patients with temporal lobe epilepsy arises from *in situ* hybridisation and immunohistochemistry studies. Expression of the Na-K-2Cl cotransporter NKCCl (Delpire et al., 1994), which typically transports Cl^- into cells, seems to be increased in epileptic tissue, whereas expression of the K-Cl cotransporter KCC2 (Payne et al., 1996), which transports Cl^- out of cells, appears to be reduced (Huberfeld et al., 2007;Munoz et al., 2007;Palma et al., 2006). Interestingly, KCC2 expression appears to be selectively disrupted in those cells that discharged during interictal events (Huberfeld et al., 2007). Other work using slice and animal models of focal epilepsies has confirmed that altered Cl^- homeostasis may play a role in the generation of epileptiform activity via a reduction in the strength of GABAergic hyperpolarisation, or sometimes even via depolarising GABAergic responses (Khalilov et al., 2003;Jin et al., 2005;Pathak et al., 2007).

1.5.3 The role of NMDA receptors in seizure-like activity

As clozapine may agonise NMDA receptors (section 1.4.2.2), and it is conceivable that this is relevant to its ability to cause seizures, here the role of NMDA receptors in seizure-like activity is considered.

The use of Mg^{2+} free medium induces epileptiform activity in rat hippocampus and entorhinal cortex, which is dependent on activity of NMDA receptors (Walther et al., 1986;Mody et al., 1987;Jones and Lambert, 1990b). Similarly, low extracellular Mg^{2+}

also induces NMDA receptor-dependent ictal activity in slices from epileptic human neocortex (Avoli et al., 1991).

In another model, it has been reported that the K^+ channel blocker 4-aminopyridine (4AP) can induce epileptiform activity in rat entorhinal cortex, and the ictal discharges but not interictal discharges or slow field potentials were abolished by antagonism of NMDA receptors (Avoli et al., 1996a). Incidentally, the ability of NMDA receptor antagonists to abolish ictal activity in hippocampal-entorhinal cortical slices has only been reported in slices from adult animals. Thus NMDA receptor-mediated mechanisms in deep entorhinal cortex may be important in ictal discharges in the adult limbic system.

Further evidence of a role for NMDA receptors in epileptiform activity is that NMDA antagonists act as anticonvulsants in various *in vivo* models of epileptiform discharges. For example, in amygdala-kindled rats, which can be used to model seizures, NMDA receptor antagonists have anticonvulsant effects (Loscher and Honack, 1991). Furthermore, the NMDA receptor antagonist D-CPP-ene [3-(2-carboxy-piperazine-4-yl)-1-propenyl-1-phosphonic acid] increases the threshold for electroshock-induced seizures in mice (Zarnowski et al., 1994).

In line with a role for NMDA receptors in seizures, seizure-related neuronal damage may arise in part from NMDA receptor-mediated influx of Ca^{2+} into neurons (Meldrum and Garthwaite, 1990).

1.6 Aims and objectives

This introduction has considered neural oscillations, the pathology of schizophrenia and how it may relate to dysfunctional oscillatory activity, possible mechanisms underlying this dysfunction, and comorbidity and parallels between schizophrenia and epilepsy. Literature relating to the antipsychotic clozapine, its effectiveness, its mechanism of action and its potential to induce pathological epileptiform activity and seizures has also been reviewed. Finally, possible mechanisms such as VFO, and altered excitatory and inhibitory synaptic transmission were proposed which may be relevant to such increased neuronal excitability.

From this background the aims of this thesis are as follows:

- To present new data from patients presenting with epileptiform activity and seizure-like side-effects associated with clozapine therapy for serious psychiatric

illness in Newcastle in order to demonstrate the type of transient epileptiform activity the thesis attempts to model *in vitro*.

- To establish whether clozapine could generate similar epileptiform activity in normal brain tissue rather than the clinical situation in which clozapine is administered to patients already showing abnormal brain activity associated with psychiatric illness – i.e. is the epileptiform activity seen with clozapine a direct effect of the drug or a consequence of compensation for this abnormal activity (forced normalisation).
- To map the distribution and spatial extent of such activity in terms of its laminar distribution in the cortical column and its longitudinal distribution throughout the regions of interest to attempt to focus-in on the cell types and local circuits involved for further study.
- From above, to investigate the pharmacological properties of such activity in relation to synaptic and non-synaptic mechanisms.
- To investigate the activity of specific types of neurons in relation to such activity and to attempt to determine its cellular basis.
- Given the reduced expression of parvalbumin in post-mortem samples from individuals with schizophrenia, to investigate the effect of clozapine treatment and associated excitability on parvalbumin immunoreactivity in normal brain tissue in an attempt to relate the hyperexcitability induced by clozapine to the drug's antipsychotic efficacy.

Chapter 2

Methods

2.1 Animal provision

In vitro brain slice preparations were obtained from young adult male Wistar rats aged between 28 and 70 days and weighing approximately 150-250g. Animals were supplied by Charles River and housed in a pathogen-free environment in the University of Newcastle Comparative Biology Centre. Animals were exposed to a 12 hour light/dark cycle and were able to eat and drink freely.

2.2 Anaesthesia and animal procedures

Surgical procedures undertaken in this thesis were carried out under appropriate personal and project licenses, and conformed to regulations set out in the UK Animals (Scientific Procedures) Act, 1986.

Rats were lightly anaesthetised in a 5 litre bell jar using the volatile anaesthetic isofluorane (Abbott Laboratories Ltd., Kent, UK) at a dose sufficient to prevent the righting reflex. Rats were then given an intramuscular injection of ketamine (dose ~100mg/kg; Pfizer Ltd., Kent, UK) and xylazine (dose ~10mg/kg; Millpledge Pharmaceuticals, Retford, UK) in the gluteal region of the hind leg for deep anaesthesia and muscle relaxation. The absence of the tail-pinch, pedal withdrawal and corneal reflexes were used to establish deep anaesthesia. Once deep anaesthesia was established, the abdominal cavity was opened and the rib cage excised to provide access to the heart. After the insertion of a catheter into the left ventricle of the heart, an incision was made into the right atrium for intracardial perfusion with 60mls ice-cold, oxygenated (carbogen gas, 95% O_2, 5% CO_2) sucrose-containing artificial cerebrospinal fluid (sACSF) at a rate of approximately 0.8ml/s. The purpose of the intracardial perfusion was to preserve neurons, especially GABA-ergic interneurons, in a maximal level of healthiness (Aghajanian and Rasmussen, 1989;Kuenzi et al., 2000). The inclusion of sucrose instead of NaCl in sACSF has been proposed to preserve the vitality of neurons by the prevention of the neurotoxic entry of chloride into cells which would result in cell swelling and lysis (Aghajanian and Rasmussen, 1989).

2.3 Preparation of brain slices

An incision was made along the midline of the head and neck to expose the skull and rostral spinal column, and the spinal cord was severed. To access the brain, the skull was dissected rostrally along the sagittal suture from the exposed severed spinal column, and skull and *dura mater* were peeled away. The brain was then excised and

gently transferred to ice-cold oxygenated sACSF. Following coronal trimming of the brain to remove the cerebellum, the dorsal surface of the brain was glued promptly to the chuck of the Leica VT1000 vibratome (Leica Microsystems, Nussloch GmbH, Germany). The chuck was then fastened to the cutting chamber of the vibratome, and the cutting chamber was filled with ice-cold oxygenated sACSF.

Horizontal cortical sections were sliced in the vibratome at a thickness of 450µm, which is sufficiently thick to permit a viable intact neuronal microcircuit capable of producing oscillations, but also sufficiently thin to allow adequate oxygenation of the slice. Immediately after each slice was taken, it was gently transferred with a fine paint brush to fresh ice-cold oxygenated sACSF. Brain regions were identified with reference to maps of horizontal sections in a rat brain atlas (Paxinos and Watson, 1998). In the atlas, brain regions are defined with regard to Bregma, an anatomical landmark point at the intersection between the sagittal and coronal suture. In terms of dorsovental position in the rat brain, sections containing 2º somatosensory cortex were those between 4.1 and 6.1mm ventral from Bregma (Bregma -4.10 to -6.10mm; Paxinos and Watson, 1998); and sections containing the CA2 region of the hippocampus were taken from levels between 4.1 and 6.82mm ventral from Bregma (Bregma -4.10 to -6.82mm; Paxinos and Watson, 1998). Slices were trimmed down with a scalpel to produce sections containing 2º somatosensory cortex and sometimes adjoining regions, or, in the CA2 experiments, sections containing hippocampus and surrounding cortex.

2.4 Slice maintenance

Dissected sections were placed on lens cleaning tissue in a holding chamber containing oxygenated ACSF, and left to equilibrate for approximately 1 hour at room temperature. 3-4 slices were then transferred to an interface recording chamber, and remaining slices were left in the holding chamber for use in later experiments. In the recording chamber, slices were maintained on three layers of lens cleaning tissue at the interface between oxygenated ACSF and humidified carbogen gas (95% O_2, 5% CO_2). A peristaltic pump (Gilson S.A.S., Villera Le Bel, France) was used to circulate the ACSF through the chamber at a flow rate of approximately 1ml/min for continual perfusion of slices. Once the slices were in the recording chamber, the temperature of circulating ACSF was raised to approximately 34ºC using a flow heater (Grant Instruments Ltd., Cambridge, UK). Slices were left to equilibrate to this near-physiological temperature for 30 minutes prior to control recordings and application of the oscillogenic agent or drug.

2.5 Drugs and solutions

sACSF used in the preparation of slices consisted of: 252mM sucrose, 3mM KCl, 1.25mM NaH_2PO_4, 2mM $MgSO_4$, 2mM $CaCl_2$, 24mM $NaHCO_3$, and 10mM glucose. Normal ACSF, in which slices were maintained subsequently, lacked sucrose but instead contained 126mM NaCl and lowered concentrations of both $MgSO_4$ and $CaCl_2$. Thus normal ACSF consisted of: 126mM NaCl, 3mM KCl, 1.25mM NaH_2PO_4, 1mM $MgSO_4$, 1.2mM $CaCl_2$, 24mM $NaHCO_3$, and 10mM glucose. The concentration of Mg^{2+} (1mM) and Ca^{2+} (1.2mM) in normal ACSF, although lower than that traditionally used for cortical slice preparations (2mM Mg^{2+}, 2mM Ca^{2+}), was chosen to more closely mimic the ionic composition of cerebrospinal fluid *in situ* (Sanchez-Vives and McCormick, 2000;Yamaguchi, 1986;Zhang et al., 1990).

Drugs were stored in dry solid form in conditions which met advice from the supplier. To prepare stock solutions, drugs were dissolved in distilled water, or, if insoluble in water, in the solvent DMSO. In those cases where drugs were dissolved in DMSO, the final concentration of DMSO in ACSF perfused slices was ≤ 0.2% v/v, except in the maximal concentration (50µM) of the concentration response experiment for haloperidol and olanzapine, in which case it was 0.5% v/v. Drug stock solutions were refrigerated (4ºC) or stored in frozen aliquots (-20ºC) according to advice from the supplier. The appropriate volume of drug stock solution was transferred into the bath to achieve the correct final drug concentration in ACSF perfused slices.

Suppliers of drugs and chemicals

Drug/chemical	*Supplier*
Calcium chloride	VWR
Carbenoxolone	Sigma-Aldrich
Clozapine	Tocris
Disodium hydrogen phosphate	Sigma-Aldrich
DMSO	Sigma-Aldrich
D-AP5	Tocris
d-tubocurarine	Sigma-Aldrich
Gabazine	Tocris

Glucose	VWR
Haloperidol	Sigma-Aldrich
Magnesium sulphate	Sigma-Aldrich
NBQX	Tocris
Nicotine	Sigma-Aldrich
Octanol	Sigma-Aldrich
Olanzapine	Bosche Scientific
Potassium acetate	Sigma-Aldrich
Quinine	Sigma-Aldrich
Sodium bicarbonate	VWR
Sodium chloride	VWR
Sodium dihydrogen phosphate	VWR
Sucrose	Fisher Scientific

2.6 Recording techniques

2.6.1 Extracellular recording

Micropipettes used for recording extracellular field potentials were pulled from thin walled borosilicate glass capillary tubes with filaments (1.2mm OD x 0.94mm ID; Harvard Apparatus Ltd, Kent, UK) using a P-97 Flaming/Brown type horizontal micropipette puller (Sutter Instruments Co., Novata, CA, USA) to give a resistance in the range of approximately 2-5MΩ. Extracellular micropipettes were filled with the standard ACSF used in experiments.

After slices had been left to equilibrate to 34ºC in the recording chamber, extracellular electrodes were positioned in layer V of 2º somatosensory cortex. Accurate placement of electrodes was achieved by visualising the slice under a microscope, and Narishige manipulators permitted fine control of electrode positions. Control recordings were taken prior to application of the oscillogenic agent to determine whether subsequent oscillations were a direct result of the oscillogenic agent or related to spontaneous activity. In most experiments clozapine was chosen as the oscillogenic agent, but in certain experiments haloperidol, olanzapine, gabazine (see section 4.3.8) or d-tubocurarine (see section 4.3.9) were appropriate alternatives. Oscillogenic agents were introduced into the bath and reached slices via circulating ACSF. After application of the oscillogenic agent, slices were typically left for 1 hour before probing for activity by

adjusting electrode positions to find patches of VFO. Optimal VFO usually took 1-2.5 hours, but occasionally up to 4 hours, to develop. Following discovery of an optimal patch of VFO, oscillatory activity could be studied in various ways. Laminar and longitudinal profiles, pharmacological experiments, intracellular recordings, and multi-array recordings of units and local field potentials (LFPs) were possible. In pharmacological experiments, electrodes remained stationary for the remainder of the experiment after their optimal position was established. Pharmacological agents were bath applied and recordings used to assess their effect were taken typically after the agent had been applied for 1 hour. In experiments where the pharmacological agent had an effect on oscillatory activity, washout experiments were sometimes performed. In these experiments, the bath of circulating ACSF was replaced with a bath of comparable ACSF minus the pharmacological agent in question, and activity was left to recover.

2.6.2 Multichannel array recording

In multi-electrode array experiments, once oscillatory activity had developed its presence was first verified with the standard extracellular glass microelectrode before use of the electrode array. Silicon electrode grids (Utah arrays purchased from Cyberkinetics Inc., USA) were used for multi-electrode recordings of LFPs and units. The grids were square, 10x10 electrode arrays, with a distance of 0.4mm between electrode tips, and electrode shank length of 1.2mm. The impedances of the different electrodes varied from 230-370kΩ. Electrode arrays were epoxy cemented onto a Teflon headstage holder (Molecular Devices) and mounted onto a 3D patch manipulator (Scientifica, UK). To ensure that electrode tips were oriented in the same plane as the slice, the electrode grid was aligned from top to bottom and left to right with the upper surface of the recording chamber. The electrode grid was then positioned over the oscillating region of 2º somatosensory cortex and lowered gently onto the surface of the slice such that tissue penetration was less than 50µm.

2.6.3 Intracellular sharp electrode recording

Sharp micropipettes for intracellular recordings were pulled from standard wall borosilicate glass capillary tubes with filaments (1.2mm OD x 0.69 ID; Harvard Apparatus Ltd, Kent, UK) using the same puller to give a resistance in the range of 80-150MΩ. Sharp micropipettes were filled with 2M potassium acetate.

Sharp electrode intracellular recordings with a resting membrane potential less than -50mV and action potential amplitude greater than 50mV were deemed usable.

Electrophysiological characterisation of neurons was achieved using a 0.3nA depolarising step with a duration of 300ms, as described previously (McCormick et al., 1985). EPSPs were revealed by injection of negative DC current until the membrane potential of the cell was hyperpolarised to -70mV to mask concurrent IPSPs, and conversely, IPSPs themselves were revealed, when successful, by injection of tonic, positive current until the membrane potential of the cell was depolarised away from the chloride reversal potential to -30mV.

2.7 Data acquisition

2.7.1 Glass microelectrode recording

Signals were initially amplified by pre-amplifiers in the headstages (npi electronic GmbH, Germany). Extracellular signals were recorded in current-clamp mode, with band-pass filtering between 0.001-1kHz, and given extra amplification using an npi EXT 10-2F amplifier (npi electronic GmbH, Germany). Intracellular signals were recorded in DC mode, with low-pass filtering at 2kHz using an npi BRAMP-01R bridge amplifier (npi electronic GmbH, Germany). Humbugs (Quest Scientific Instruments Inc., North Vancouver, Canada) eradicated 50Hz mains noise from the raw signals. An Instrutech ITC-16 A/D converter (Instrutech Corp., NY, USA) was used to digitize signals at 10kHz. Recordings were visualised on-line using Axograph X 1.3.1 software (Axon instruments) for Mac OS X, and data were stored on an Apple iMac computer (Apple Computer Inc.) for off-line analysis in MATLAB software (The MathWorks Inc.).

2.7.2 Multi-electrode array recording

Utah electrode arrays were connected to a 128 channel Cerebus digitiser/amplifier via analogue pre-amplifiers. Central (Blackrock Microsystems Inc. USA) was used for online collection of data from the electrode array, which was digitized at 30kHz and subsequently exported to Neuroexplorer (Nex Technologies, Littleton, USA). Time series data from each channel was band-pass filtered between 0.1-500Hz, downsampled to 2kHz, and saved continuously. Furthermore, timestamps for units, and the digitised template for every detected spike were also saved for *post-hoc* analysis. Spikes were detected on-line during data collection, with manually specified parameters using both threshold crossing and 2-window template matching. Such manual spike sorting is illustrated in Fig. 2.1. Amplitude thresholds were set at a level below any stereotyped

noise. Unit time stamps and time series for LFPs were exported to MATLAB (The MathWorks Inc.) for analysis off-line.

2.8 Data analysis

In terms of software, MATLAB 7.10 (The MathWorks Inc., Natick, MA, USA) was used for *post-hoc* data analysis, SigmaPlot 11.0 (Systat Software Inc., Chicago, Illinois, USA) was used for statistical tests, and figures were collated in Microsoft Powerpoint (Microsoft Corp., Redmond, USA).

2.8.1 Analysis of oscillatory activity

The main parameters used to quantify extracellular recordings of VFO in LFPs were the modal frequency of VFO, the amplitude of the modal VFO, and the area power in the VFO band (70-1000Hz). Power spectra, which are a means of quantifying the various frequency components of oscillatory activity, were used to examine these properties. The standard method of calculating power spectra for gamma frequency oscillations, whereby a fast Fourier transform (FFT) algorithm is computed on the entire trace, was not applicable because of the non-stationary nature of the VFO signal. Instead, power spectra were calculated by performing FFT analysis on segments of traces where VFO were present. The MATLAB 'pwelch' function (Welch, 1967) was used for FFT analysis in a script provided by J.D. Simonotto (Roopun et al., 2010b), and VFO were detected using an amplitude threshold.

The FFT algorithm extracts the sinusoidal waveform components which make up the oscillation, and then computes the power of each of these waveforms. Data were then plotted as the sum of the voltage squared at a specific frequency, for a frequency range of 60-1000Hz. The modal frequency of VFO and the amplitude of the modal VFO corresponded to the X and Y value of the peak in the power spectra respectively. VFO band area power was quantified by summing the power values in the power spectra from 70-1000Hz. Pooled power spectra, which are plots of the average power spectra from individual experiments, were used to present data. In most cases, analysis was performed on three concatenated 60s traces, or a single 180-300s trace.

In typical experiments the amplitude threshold below which VFO troughs were detected was manually specified. Alternative amplitude threshold criteria were used in the haloperidol and olanzapine concentration response experiments for a standardised comparison. In these experiments, the control trace, which was taken before drugs were

applied, was used to calculate the amplitude threshold for all subsequent traces in the dose response. This threshold was calculated as the mean Y value minus 5 standard deviations of the Y value in the control trace.

Additional parameters were also measured to further characterise VFO. These were the burst frequency, the inter-burst interval (Fig. 2.2), the number of spikes per burst, the inter-spike interval within bursts (Fig. 2.2), the peak-to-peak spike amplitude (Fig. 2.2), and the proportion of time during the trace that VFO were present. 'Bursts' were defined as VFO which met amplitude threshold criteria, comprised more than two troughs and lasted longer than 25ms. Bursts were deemed to end when there was a period equal to or greater than 30ms in which there were no troughs below the amplitude threshold. A new burst would then be deemed to start after any subsequent troughs which met the burst criteria above. The burst concept was relevant in the following parameters: burst frequency, inter-burst interval, number of spikes per burst, and inter-spike interval within bursts.

Another method of analysing oscillatory activity is the sliding-window fast Fourier transform algorithm (known as a 'spectrogram' in MATLAB). The spectrogram represents instantaneous power spectra of short epochs of activity, and is useful for showing how oscillatory activity changes over time. Oscillatory power is illustrated in a colour array, with time and frequency on the X- and Y-axis respectively. In this thesis, 4s epochs of activity were used for spectrograms, and for the sliding window data were sampled every 50ms with an overlap of 45ms.

Cross-correlation analysis can be used to compare the degree of synchrony between signals from different positions in cortex, with a sinusoidal plot in the resulting graph indicating synchronised signals. In this thesis, cross-correlation analysis was performed in Axograph software to quantify the intra-burst synchrony and phase-lag between ~30-100ms bursts sampled from two electrodes positioned between 100 and 900µm apart along layer V of 2º somatosensory cortex. The synchrony value corresponded to the point on the Y-axis where it is intersected by the central peak, and the phase lag value corresponded to the X value of the first side peak. To quantify synchrony at a lower temporal resolution, the number of burst events which appeared coincident or synchronous in 60s traces were also counted by eye.

Cross-correlation analysis in Axograph was also used to relate intracellular recordings of spikes, EPSPs and IPSPs to concurrent field activity. The inter-spike interval in bursts of intrinsically bursting cells was analysed in MATLAB.

2.8.2 Statistical analysis

For VFO analysis, LFP data were band-pass filtered (60-1000Hz) in MATLAB using zero-phase distortion finite impulse response filters (i.e. the 'filtfilt' function in MATLAB), prior to statistical analysis. Statistical tests were performed using SigmaPlot 11.0 (Systat Software Inc., Chicago, Illinois, USA). It was firstly established whether data were normally distributed (Kolmogorov-Smirnov test) and had equal variance (parametric data), or not (non-parametric data). In the case of matched data from two samples, for example, data relating to an oscillation before and after a pharmacological manipulation, paired t-tests were used for the comparison when data were parametric, or, for non-parametric data, the Wilcoxon signed ranks test was used. For unmatched parametric data from two samples an unpaired t-test was used when data were parametric, or, for non-parametric data, the Mann-Whitney rank sum test was used. For data from three or more samples, for example, a concentration response experiment, a one-way analysis of variance (ANOVA) test was used when data were parametric; or, for non-parametric data, a Friedman one-way ANOVA on ranks test was used when data were matched, or, for unmatched data, a Kruskal-Wallis one-way ANOVA on ranks test was used.

For data where the effect of two or more independent variables was investigated, for example, the concentration response for different antipsychotics, a two-way ANOVA test was used when data were parametric, or for non-parametric data, a Friedman two-way ANOVA on ranks test was used. Following ANOVA tests, the all pairwise multiple comparison procedures test (Dunn's method) was used for *post-hoc* comparisons. Parametric data were expressed as mean ± standard error of the mean (SEM), and for these data error bars on graphs symbolised the SEM. Non-parametric data were expressed in terms of the median value and corresponding interquartile range (Q1 → Q3), and for these data error bars on graphs symbolised the interquartile range. Results were considered significant, indicating that the difference between the groups was greater than would be expected by chance, when $P < 0.05$.

2.9 Immunohistochemistry

Immunohistochemistry was performed to visualise parvalbumin-immunoreactive interneurons in 2º somatosensory cortex. Following any necessary extracellular recordings, the glass electrode was gently raised, then the slice was removed from the recording chamber and gently covered on both sides with pieces of nitrocellulose filter discs (Sartorius AG, 37075 Goettingen, Germany), which prevented the slice from deforming in the fixative. The resulting nitrocellulose sandwich was fixed in chilled 4% paraformaldehyde (PFA) dissolved in 0.1M phosphate buffer (PB). Following storage at 4ºC in the fixative for > 48 hours, the slice was transferred to 0.1M PB, with a drop of 0.05% Na-azide to prevent bacterial contamination, and refridgerated (4ºC) until batch processing. Slices were then glued to the chuck of a Leica VT1000 vibratome (Leica Microsystems, Nussloch GmbH, Germany) and re-sectioned at a thickness of 40µm in ice-cold 0.1M PB.

Following re-sectioning, sections were washed three times in 0.1M PB over 20 minutes, prior to immersion in 1% H_2O_2 (Sigma-Aldrich) for 10 minutes to diminish the endogenous peroxidase activity. Sections were then rinsed three times over 15 minutes in 0.3% Triton PBS (made up by dissolving Triton X-100, from Sigma-Aldrich, in 0.1M PB). Sections were then gently agitated for two hours in blocking solution containing 3% normal horse serum (Vector Laboratories Inc., Burlingame, CA 94010, USA) dissolved in 0.3% Triton PB. Sections were then incubated overnight at 4ºC in the 1º antibody Swant, 235 (Swant, Bellinzona, Switzerland, a monoclonal anti-parvalbumin antibody produced in mice), which was dissolved in the blocking solution at a concentration of 1:5000.

Following overnight incubation, sections were rinsed three times in 0.1M PB over 30 minutes. Sections were then incubated for two hours in biotinylated anti-mouse antibody raised in horse, dissolved in 0.1M PB at a concentration of 1:200. The 2º antibody was included in the Vectastain ABC kit (Vector Laboratories Inc., Burlingame, CA 94010, USA). Sections were then washed three times in 0.1M PB over 30 minutes, prior to gentle agitation for 2 hours with HRP-streptavidin, dissolved in 0.1M PB at a concentration of 1:200. The HRP-streptavidin solution was made up by adding two drop of solution A and two drops of solution B, each from the Vectastain ABC kit, to 5mls 0.1M PB. Sections were then washed three times in 0.1M PB over 30 minutes. The peroxidise reaction was revealed by submersing sections in a solution containing 3,3'-diaminobenzidine tetrahydrochloride (DAB) and H_2O_2, which was

made up by dissolving single DAB and H_2O_2 tablets (SigmafastTM-3,3'-diaminobenzidine tetrahydrochloride, Sigma-Aldrich) in 5ml distilled water, in the dark, as per supplier advice. Sections were left in the DAB solution for 4-15 minutes, until successful staining, visible under the microscope as brown insoluble precipitates, occurred. Following successful staining, the reaction was stopped by rinsing sections twice in 0.1M PB over 20 minutes. Sections were then mounted onto gelatin-coated glass microscope slides (Waldemar Knittel, D-38114 Braunschweig, Germany) and left to dry overnight.

Following drying, sections were dehydrated by immersing slides in increasing concentrations of ethanol (70%, 95%, and two times in 100% solutions) for 10 minutes at each concentration. Subsequently, sections were immersed for 10 minutes in succession in the nontoxic histological clearing agents histoclear I and histoclear II, solvents of the histomount™ mounting medium (Thermo Scientific), prior to mounting coverslips onto slides using histomount™. The mounting medium was then left to polymerise for 24 hours, after which sections were ready for inspection under the light microscope. Cells in the 40µm sections of 2º somatosensory cortex were deemed parvalbumin-immunopositive when strong brown labelling was present, and those cells were manually counted using a handheld click-counter (ENM, UK) in microscopic view fields at a magnification of X10. Photos were taken using an AxioCam HRc digital camera (Carl Zeiss MicroImaging GmbH, Göttingen, Germany) connected to an Olympus BX 60 upright microscope (Olympus Microscopy, Essex, UK), and controlled via AxioVision 3.1 software (Carl Zeiss MicroImaging GmbH, Göttingen, Germany) on a Windows PC.

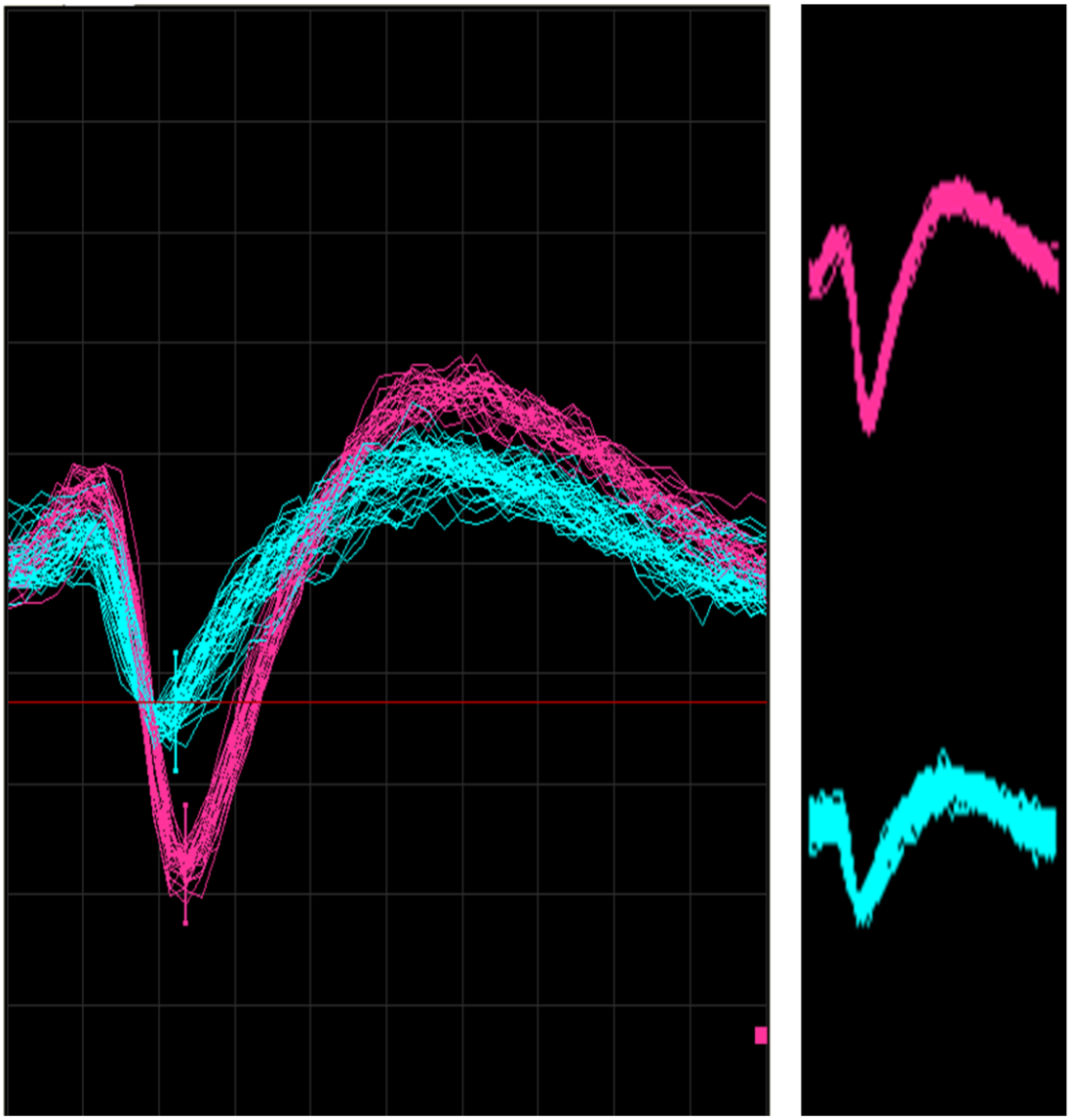

Fig. 2.1. Modified screenshot from Central (Blackrock Microsystems Inc. USA), illustrating manual spike sorting. Note the manually specified threshold (red line) and windows (see coloured markers) for the detection and classification of spike waveforms. Two distinct spike waveforms are clearly identified in this example channel.

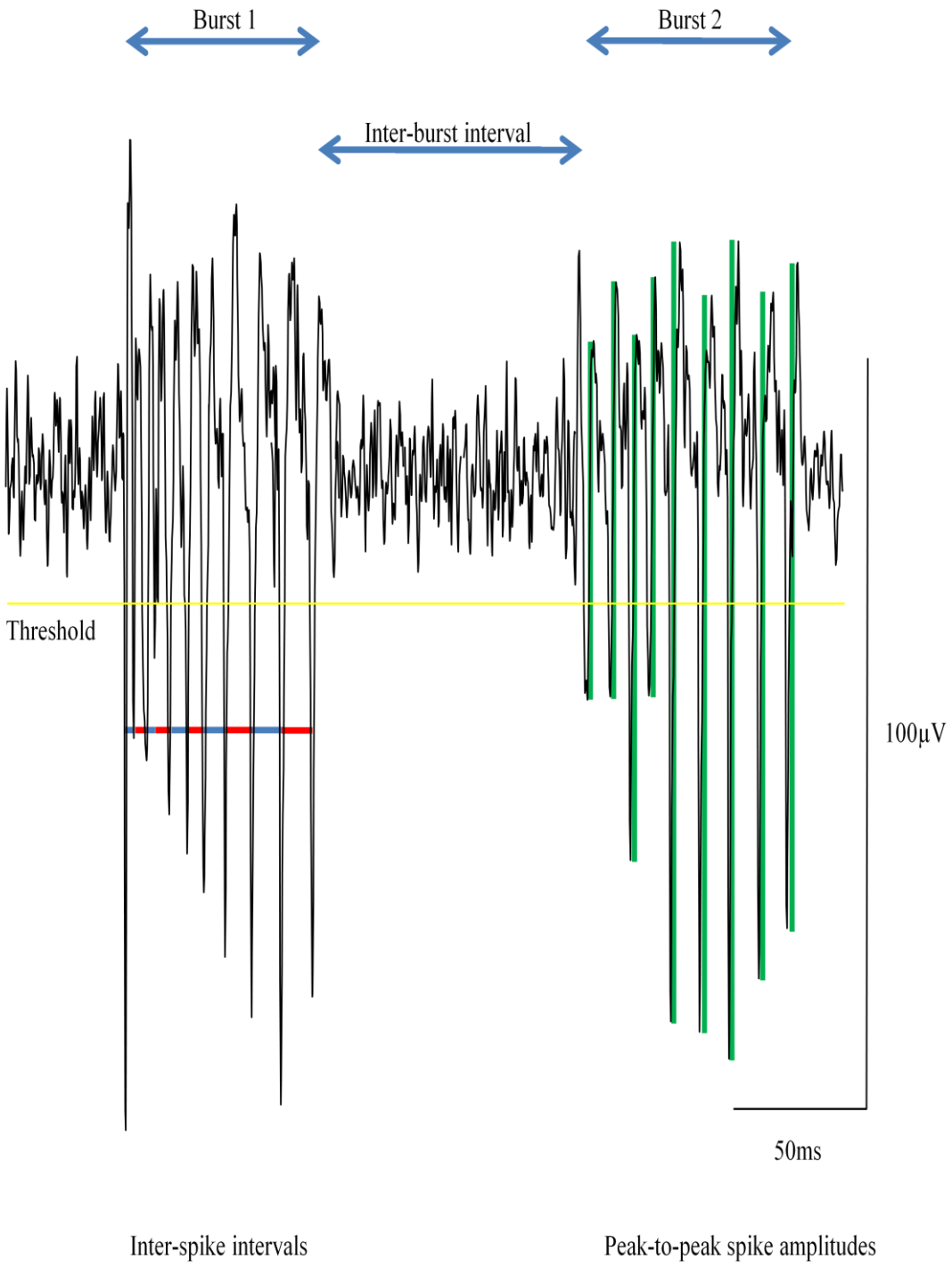

Fig. 2.2. Illustration of various additional quantitative parameters used to further characterise field very fast oscillations (VFO). Bursts of VFO were detected below a manually specified amplitude threshold (example illustrated with the yellow line). The inter-burst interval is shown with the blue arrows between the bursts. Inter-spike intervals within bursts are indicated by the alternating blue/red lines in burst 1. Peak-to-peak spike amplitudes are marked by the green lines in burst 2.

Chapter 3

Transient seizure-like events in a psychiatric patient treated with clozapine

3.1 Introduction

Aims

- To present new data from a patient presenting with seizure-like side-effects to clozapine therapy for serious psychiatric illness in Newcastle.
- To briefly discuss the consequences of these findings for shaping the *in vitro* rodent model to be used in subsequent results chapters.

3.1.1 Clozapine, paroxysmal events and seizures

As mentioned previously, many antipsychotic drugs have the potential to induce paroxysmal EEG changes and seizures. Indeed, clozapine, a particularly effective antipsychotic (Kane et al., 1988), was associated with the highest risk of EEG abnormality compared to other antipsychotics (Centorrino et al., 2002).

In one study EEG abnormalities were observed in 53% of patients treated with clozapine, and the absence or presence of EEG abnormalities correlated with the plasma clozapine concentration (Haring et al., 1994). Although reports of the incidence of clozapine-associated EEG alterations vary from 16% (Naber et al., 1989) to 75% (Koukkou et al., 1979), Haring et al. (1994) was considered a good predictor of the true extent of clozapine-associated EEG alterations because of the absence of potentially confounding psychotropic or anticholinergic co-medications, the prospective design, and analysis of the effect of the drug on the premedication baseline EEG. Clozapine-related abnormal EEG activity included slowing of activity, abnormal theta, abnormal delta, and importantly, intermittent sharp transients, spike discharges, and spike-wave paroxysms (e.g. Malow et al., 1994;Welch et al., 1994;Haring et al., 1994;Freudenreich et al., 1997;Centorrino et al., 2002). It is these events which will be introduced in this chapter and modelled *in vitro* in subsequent chapters.

Beyond the EEG abnormalities described above, clozapine can also generate full seizures. The incidence of full-seizures following clozapine treatment is likely dose dependent and may be 1.3-2.8% (Devinsky et al., 1991;Pacia and Devinsky, 1994). However, the risk of seizures has been estimated to rise to 10% after 3.8 years of treatment with clozapine (Devinsky et al., 1991). The incidence of paroxysmal activity and seizures in patients treated with clozapine is higher than that associated with typical neuroleptics.

Here EEG recordings were taken from a psychiatric patient treated with clozapine to investigate EEG abnormalities and which regions of cortex were important in generating such abnormalities. Seizure activity in this patient was also monitored and related to EEG activity.

3.2 Methods

All data was made available, anonymised, by Dr. Ian Schofield from the Neurophysiology Department of The Royal Victoria Infirmary. Basic 20-channel scalp EEG recordings were taken from a 32 year old male patient with psychiatric illness taking clozapine for 3 weeks. The patient complained of confusion and frequent (>20 per day) myoclonic jerks involving the upper limbs. The initial study was also performed with videotelemetry to allow co-registry of any EEG abnormalities with these myoclonic jerks. Following recording, clozapine was withdrawn from therapy and the patient returned for additional EEG monitoring 1 month later. The patient reported cessation of myoclonic jerks and a general improvement in confusional state 48h after withdrawal of the drug. EEG was performed on a Neuvo system sampling at 256 Hz with data output bandpassed from 0.5 – 70 Hz before analysis. Data was exported as .EDF (European Data Format) and read into Matlab using the Biosig suite of programmes (Institute of Science and Technology, Austria). Basic 2D current source density analysis was performed on these EEG recordings to localise abnormal event onset and propagation: The 'double banana' montage was used to extract voltage differentials between each channel except Fpz. The 1^{st} order differential of the voltage difference pairs was plotted to estimate dipole size and location.

3.3 Results – Transient seizure-like events in a psychiatric patient treated with clozapine

Altered EEG activity was manifest as transient epileptiform spikes occurring at ca. 2 per hour. Events were associated with intense mental activity, predominantly emerging during runs of beta (15-25 Hz) activity (Fig. 3.1B). Basic analysis of the EEG record revealed synchronised events on the majority of channels. The 'by eye' largest events were seen in the C3-P3 electrode pair (with overt phase reversal of the signal), with width 120 ± 30 ms and amplitude 110 ± 20 μV (n=5 events)). After clozapine treatment was stopped no transient epileptiform spikes were seen in the 2h of data analysed, even during overt runs of beta activity (Fig. 3.1C).

Estimates of the origin of the clozapine-associated events revealed two distinct types of activity pattern. In 3/5 events analysis of the montage data showed an origin in the left, posterior temporoparietal region (Fig. 3.2A) which propagated across the midline to the contralateral region. No projection to more anterior brain regions was observed. 2/5 events were associated with brief, upper-limb myoclonic jerks. In this case estimates of origin showed slightly more anterior and midline-oriented origin in the centroparietal region, again with a bias to the left side. These events were slightly more brief than the temporoparietal origin events and had a more overt oscillatory tail at ca. 10 Hz. Following the pattern of activity in the EEG montage, these events propagated bilaterally to the motor strip and were observed on electrode pairs including Fp1 and Fp2 (Fig. 3.2B). Invasion and activation of motor areas was very transient in both cases (30 – 80 ms) but immediately preceded the involuntary motor movements originally complained about by the patient.

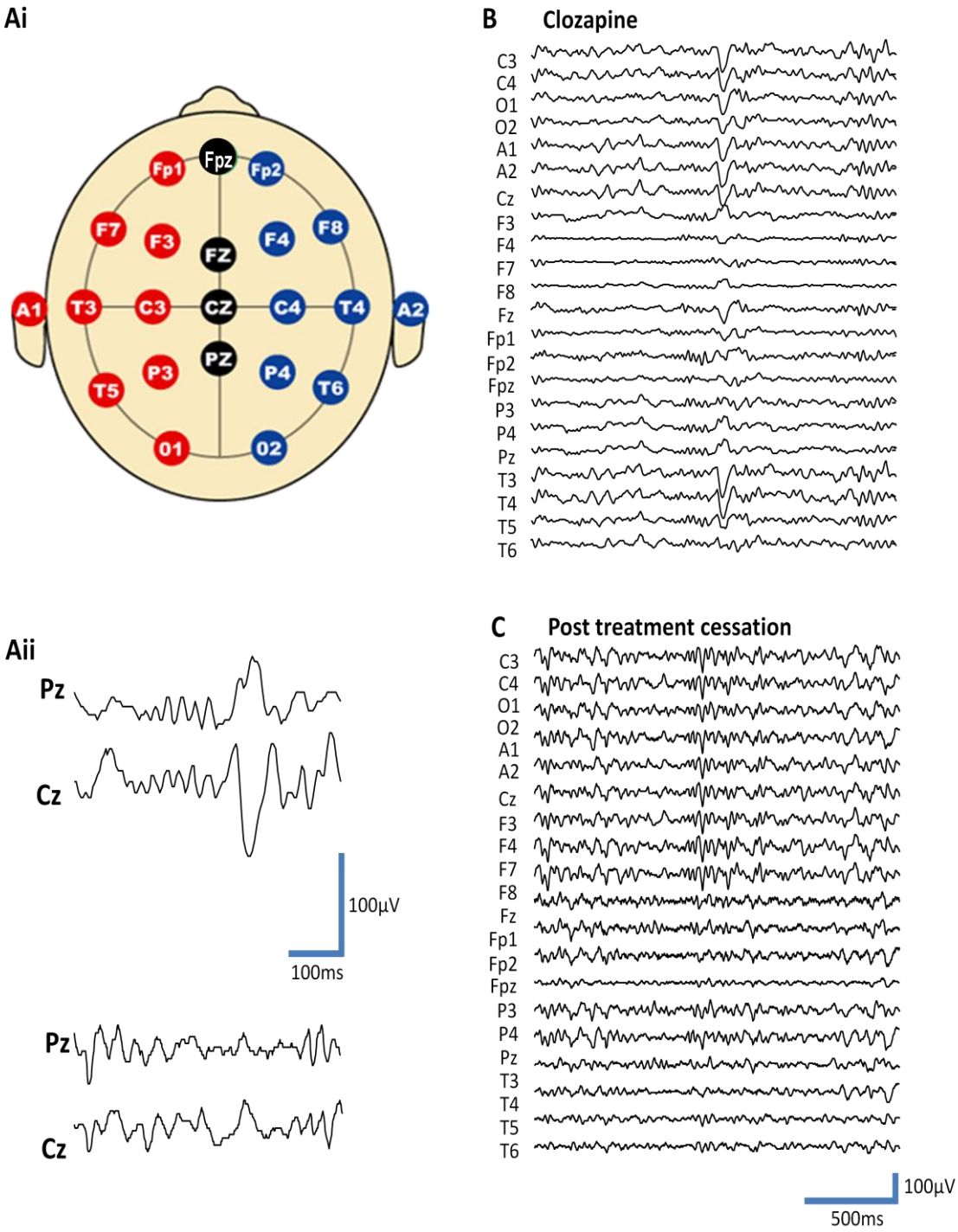

Fig. 3.1. Example of clozapine-induced transient seizure-like events in a psychiatric patient. **(***Ai***)** Cartoon illustrating the localisation of the electrodes used (the standard 10-20 system). *(Aii)* Example of the overt phase reversal between neighbouring electrodes in the double banana montage showing a transient epileptiform event arising from a background run of beta frequency activity (note the beta activity in not phase-reversed but the event is). Lower example traces show a run of beta activity in the same patient after withdrawal from clozapine treatment illustrating absence of transient epileptiform events. **(***B***)** Full, single electrode recordings of the example event shown in *Aii*. *(C)* 'Normal' EEG from the same patient following withdrawal from treatment.

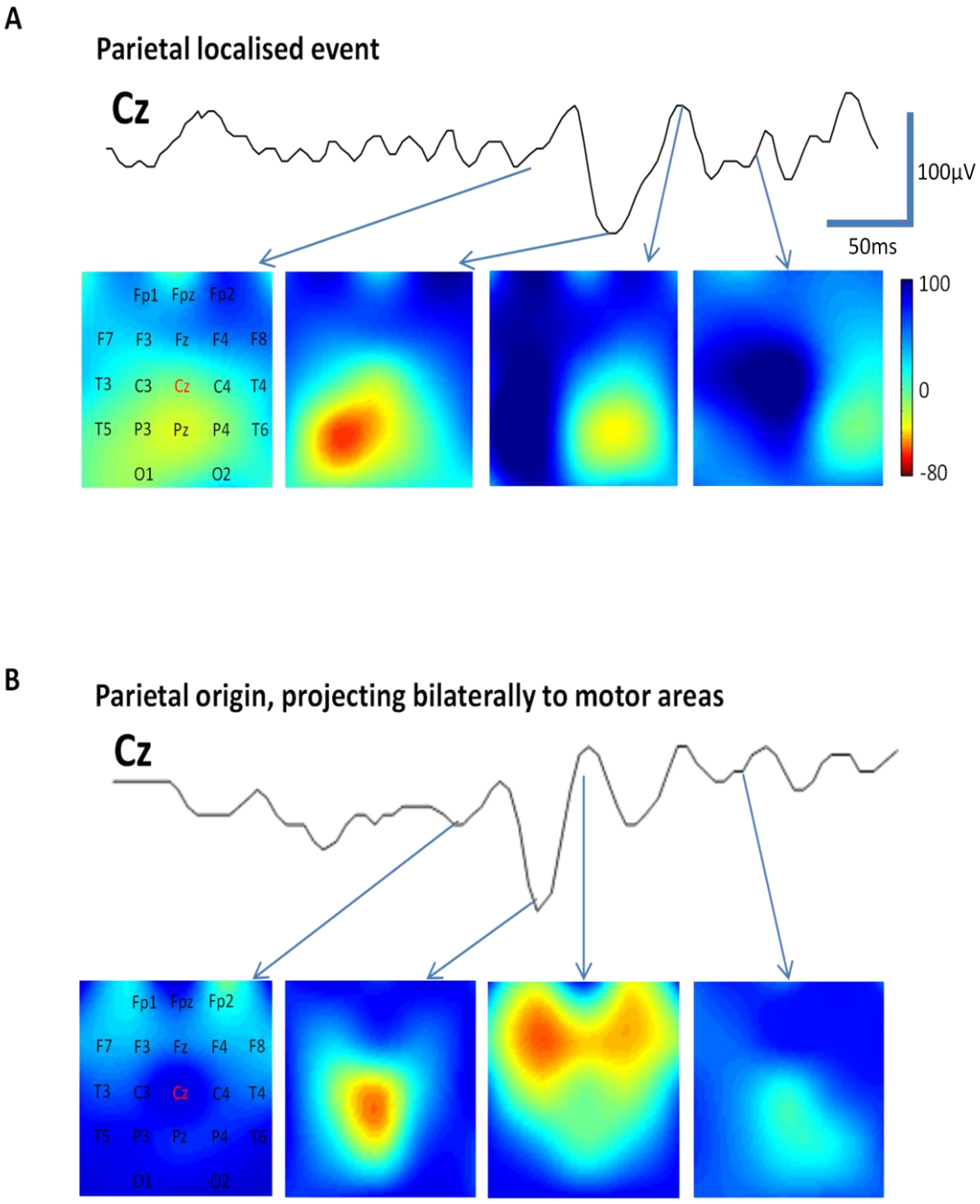

Fig. 3.2. Example of the two types of epileptiform discharge seen in the sample patient used to guide the *in vitro* model. *(A)* Example trace from electrode Cz showing a transient event arising from a run of beta activity (no motor correlate of this activity was seen). The activity maps below show the distribution of voltage changes at each of the times indicated by the arrows. Note the event starts around P3 (left temporoparietal area) before projecting to right temporoparietal area across the midline. (*B)* Example Cz trace from an event which was associated with a brief upper limb myoclonic jerk. The event main deflection is more brief but has a more overt oscillatory component. In this case the origin was more medial and projected bilaterally to the motor strip. Colour map scale in µV. Scales for colour maps and traces are the same in *A* and *B*.

3.4 Discussion

In line with the well established presence of EEG abnormalities in psychiatric patients treated with clozapine, in this thesis it was found that transient epileptiform events were present in the EEG of a patient treated with clozapine. These events equate to sharp activity and spike-wave paroxysms associated with clozapine treatment described in the literature. Furthermore, in this thesis, basic 2D current source density suggested that the transient epileptiform activity originated primarily in parietal cortex. The temporoparietal region, particularly the posterior part of this area, is associated with speech perception (Fiez et al., 1996), though interestingly the patient did not complain of any abnormality with regard to this cognitive domain. This area of the brain is involved in higher order sensory processing, and the left side (the origin of the epileptiform events here) is usually dominant. It is a multimodal area, receiving visual, auditory and somatosensory information. It is also involved in controlling hand and arm movements, which could explain the type of mycolonic jerk the patient suffered (Fogassi and Luppino, 2005).

The parietal cortex has been implicated in schizophrenia in various studies. Deficits in the connectivity and activation patterns of this brain region accompany default mode network abnormalities and reduced sensorimotor gating (Alonso-Solis et al., 2012;Hammer et al., 2013). Interestingly, reduced connectivity of the parietal cortex is also associated with schizophrenia-like psychoses relating to an underlying epilepsy (Canuet et al., 2011, see also below). It has also been implicated in the predominance of auditory (particularly voice-related) hallucinations in florid schizophrenia (Vercammen et al., 2010). Again, the left temporoparietal region appeared critical in fMRI studies, and transcranial magnetic stimulation of this area has been shown to be effective in treating some auditory hallucinations in patients with schizophrenia (Hoffman et al., 2003).

The parietal cortex is often seen to be activated in many epilepsies. However, seizures of parietal cortical origin are very rare and hard to treat. They are accompanied by a broad and disparate series of symptoms involving hypermotor activity periods, auditory hallucinations (see above), somatosensory auras, aphasia and often enuresis (Salanova, 2012). When seizures are localised to parietal cortex they are often accompanied by overt very fast oscillations (VFO or HFO, Akiyama et al., 2011). The preponderance of beta rhythms and VFO in this area has been shown to relate to the local circuit connectivity and intrinsic neuronal properties of, in particular, layer V (Roopun et al.,

2006). Roopun et al. showed that bursting behaviour in layer V intrinsically bursting neuron axons could be coupled in a network by non-chemical synaptic (gap junctional), direct axon-to-axon connections. The resulting network was very inert to conventional chemical neurotransmission and could readily generate VFO and precipitate seizure-like events.

The finding that clozapine treatment was associated with transient epileptiform events in the one patient studied here is consistent with reports in the literature of clozapine-related seizures (e.g. Juul et al., 1985). However, EEG recordings only yield some of the total information about brain rhythms and their pathology. It was therefore decided to use an *in vitro* approach to characterise the effect of clozapine on brain rhythms in more detail – using rodent slices of parietal (2º somatosensory) cortex as the substrate to examine the effects of clozapine in generating paroxysmal events and its possible relevance to the antipsychotic effects of this drug.

Chapter 4

Results – Clozapine-induced very fast oscillations *in vitro*

4.1 Introduction

Given the association of clozapine with epileptiform activity and seizures described in the previous chapter, and the limitation of scalp electrode EEG recordings in that they only yield some of the total information about brain rhythms, it was decided to use an *in vitro* approach to characterise the effect of clozapine on brain rhythms in more detail.

In particular, the *in vitro* approach allows greater spatial resolution for studying locally cortically generated rhythms and can also be used to obtain laminar information regarding such rhythms. In addition, *in vitro* recordings permit greater temporal resolution in that rhythms in the very fast band (70-1000Hz) can be studied. It is not possible to perform scalp electrode EEG recordings of very fast oscillations (VFO), which are typically highly localised and thus their signal is diminished through spatial averaging. In addition, it would be impossible to distinguish this signal from the contaminating effect of motor unit discharges. Furthermore, *in vitro* approaches are useful in studying mechanisms underlying brain rhythms as brain slices can be perfused with pharmacological agents, and intracellular recordings can readily be made from individual neurons.

Following the finding in the previous chapter that transient epileptiform events in the EEG of patients treated with clozapine originated primarily in parietal cortex, the equivalent region of association cortex was used in rat neocortical slices, namely 2° somatosensory cortex. The CA2 region of the hippocampus is also briefly considered as clozapine also induced oscillatory activity in this region.

This chapter considers VFO induced by clozapine *in vitro*, and the ability of this drug to generate full paroxysmal events themselves *in vitro* is considered in the following chapter.

Aims

Following on from the above, the aims of this chapter are as follows:

- To establish whether clozapine can generate VFO in slices of rat 2° somatosensory cortex and to characterize any such activity.
- To briefly examine whether clozapine can also generate VFO in rat hippocampal slices and to compare such activity to that in 2° somatosensory cortex.
- To investigate whether the atypical antipsychotic olanzapine and the classical antipsychotic haloperidol also induce VFO in 2° somatosensory cortex.
- To map the distribution and spatial extent of clozapine-induced VFO in 2° somatosensory cortex in terms of its laminar distribution in the cortical column and its longitudinal distribution throughout the regions of interest to attempt to focus-in on the cell types and local circuits involved for further study.
- To investigate the activity of specific types of neurons in relation to clozapine-induced VFO and to attempt to determine its cellular basis.
- To mimic oscillatory activity induced by clozapine using pharmacological agents to investigate the mechanisms underlying clozapine-induced VFO.
- To consider the possible relevance of clozapine-induced VFO to the therapeutic efficacy of clozapine.

4.1.1 Summary of the role of and possible mechanisms underlying VFO

As mentioned previously, VFO have a physiological role in memory consolidation and sensory perception, but also a pathological role in seizures. In relation to seizures, VFO can be present immediately before interictal bursts or full electrographic seizures, and/or superimposed on them, and they can also occur independently from full seizures or bursts in epileptogenic brain where they are considered a biomarker for epilepsy-related cortical pathology (Jacobs et al., 2010). Possible mechanisms underlying VFO in the literature include electrotonic coupling via gap junctions, activity of interneurons, and pathological local desynchronization of normal cortical activity.

4.1.2 Involvement of layer V in VFO

Given the laminar distribution of clozapine-induced VFO described below, it is relevant to consider the involvement of layer V in VFO. Roopun et al. (2006) describe a beta2 rhythm in layer V of neocortex that was insensitive to blockade of glutamatergic synaptic transmission, but sensitive to reductions in gap junction conductance. The

rhythm was prominent in layer V intrinsically bursting (IB) pyramidal cells, which fired bursts, spikelets and single action potentials. Similar to VFO, this activity, together with full spikes apparently generated from spikelets, was thought to be associated with antidromic activity, and the network activity was shown to result from electrotonic coupling of axons at gap junctions and not via chemical synaptic connectivity.

Similarly, VFO, thought to be gap junction dependent, were present in layer V of rat neocortex following pressure ejection of alkaline solution aimed at modelling glial cell dysfunction in epileptic foci (Cunningham et al., 2012).

Interestingly, high concentrations of clozapine (100-300μM) elicited epileptiform discharges in some layer V pyramidal cells in slices of rat prefrontal cortex (Gemperle et al., 2003). It is possible that such discharges could be relevant to clozapine-induced VFO in 2^{o} somatosensory cortex described in this chapter.

4.1.3 Pyramidal cell types in layer V of 2^{o} somatosensory cortex

Various types of excitatory and inhibitory neuron are present in layer V of neocortex. IB pyramidal cells, which fire bursts of spikes when depolarised, are prominent in layer V (Connors, 1984). Regular spiking (RS) pyramidal cells, which fire accommodating trains of single spikes when depolarised, also occur in this layer in an approximately 40:60% ratio respectively. RS cells tend to receive a generic sequence of EPSPs and IPSPs, whereas it can be challenging to experimentally detect IPSPs in IB cells (Chagnac-Amitai et al., 1990).

In addition to electrophysiological characteristics, there are also morphological differences between these two types of cell. RS cells have slim apical dendrites and axons which tend to terminate in layer II/III, but IB cells have thick apical dendrites, with prominent distal branching (tufts) that can reach layer I (Kasper et al., 1994).

Layer V IB cells can make connections with and thus receive inputs from or make outputs to cells in any other layer of the cortical column. Consistent with this, layer V may have a role in mediating outputs from the cortical column to other regions of brain (Armstrong-James et al., 1992).

4.1.4 Comparison of haloperidol, olanzapine and clozapine in relation to EEG abnormalities

In addition to examining the effect of clozapine on brain rhythms *in vitro*, the corresponding effect of the classical antipsychotic haloperidol, and that of the atypical antipsychotic olanzapine are also considered in this chapter. Therefore the similarities and differences between these antipsychotics are considered in relation to their pharmacological properties, their clinical effectiveness, and their capacity to induce EEG abnormalities, myoclonus and seizures.

Besides their classical action of dopamine D_2 receptor antagonism, antipsychotics act on many other targets and have complex receptor binding profiles (e.g. Roth et al., 2004). One of the key pharmacological features of atypical antipsychotics is thought to be the higher affinity for 5-HT_{2A} receptors compared to D_2 receptors (Meltzer et al., 1989;Altar et al., 1986). However, other pharmacological properties may be important in distinguishing atypical from classical antipsychotics. For example, agonism of NMDA receptors may be a common feature of atypical antipsychotics (Jardemark et al., 2001).

Olanzapine is a thienobenzodiazepine derivative with structural and pharmacological similarity to clozapine. Olanzapine compares favourably with the classical antipsychotic haloperidol in the treatment of schizophrenia in terms of managing psychosis, improving negative symptoms and showing a lower propensity to cause movement disorders (Fulton and Goa, 1997). Compared to clozapine, olanzapine has a less severe side effect profile, and unlike clozapine, agranulocytosis has not been attributed to olanzapine (Fulton and Goa, 1997).

Similar to clozapine, there is a concentration-dependent association between olanzapine and EEG abnormalities (Amann et al., 2003;Degner et al., 2011). Indeed, the risk of EEG abnormalites associated with clozapine and olanzapine is notably high compared to that with other antipsychotics (Centorrino et al., 2002). The risk of EEG abnormalities associated with olanzapine is fairly similar across studies; for example 35% (Amann et al., 2003), 38.5% (Centorrino et al., 2002), or 40.9% (Degner et al., 2011) of patients treated with olanzapine were affected, and this is higher than the risk associated with haloperidol, though general EEG abnormalities were seen with similar incidences between classical and atypical agents (Amann et al., 2003). Similarly,

paroxysmal activity is more frequently associated with clozapine compared to haloperidol (Koukkou et al., 1979).

As mentioned previously, clozapine may induce generalised tonic seizures, and myoclonus (Malow et al., 1994;Alldredge, 1999), for which the risk may be dose-dependent (Stevens et al., 1996;Bak et al., 1995). The incidence of seizures associated with clozapine is 1.3-2.8% (Devinsky et al., 1991;Pacia and Devinsky, 1994), which may rise to a cumulative risk of 10% after 3.8 years of treatment (Devinsky et al., 1991), and this is higher than that associated with classical antipsychotics (Lindstrom, 1988;Naber et al., 1989;Haller and Binder, 1990).

Olanzapine may also induce myoclonus (Camacho et al., 2005;Deshauer et al., 2000), even when only prescribed at a low dose, albeit chronically (Block Rosen et al., 2012). Reports of seizures associated with olanzapine, although present in the literature (e.g. Wyderski et al., 1999;Woolley and Smith, 2001;Bonelli, 2003), are not as common as those associated with clozapine (Komossa et al., 2010). However, there has been a report of a fatal status epilepticus associated with olanzapine (Wyderski et al., 1999). Further reports of seizures in patients treated with olanzapine include cases where the confounding influence of other proconvulsant drugs could not be excluded (Lee et al., 1999a;Deshauer et al., 2000;Hedges and Jeppson, 2002).

4.1.5 Effect of clozapine on $GABA_A$ receptor-mediated inhibition

Clozapine reverses the inhibitory effect of GABA on 35S-TBPS (t-butylbicyclophosphorothionate) binding (Squires and Saederup, 1991). As mentioned previously, clozapine may suppress $GABA_A$ receptor-mediated inhibition in the ventral tegmental area (Michel and Trudeau, 2000) and hippocampus (Ohno-Shosaku et al., 2011). However, the effect of clozapine on inhibitory transmission was less clear in prefrontal cortex (Gemperle et al., 2003).

Other lines of evidence support the idea that reduced GABAergic inhibition may be relevant to the therapeutic effect of clozapine. Persistent reductions in GABAergic inhibition may be involved in a range of treatments of psychosis (Squires and Saederup, 1991). For example, metrazol, which is a non-competitive GABA antagonist (Simmonds, 1980; Squires et al., 1984), is effective in the treatment of schizophrenia. In line with a possible role for $GABA_A$ receptors in schizophrenia, a group of genes associated with psychoses may encode overactive $GABA_A$ receptors (Squires and

Saederup, 1991). Together, this evidence suggests that investigation of the possible role of inhibition of $GABA_A$ receptors in relation to clozapine-induced VFO is warranted.

4.1.6 Effect of clozapine on neuronal nicotinic receptors

Similar to $GABA_A$ receptors, the effect of inhibition of neuronal nicotinic receptors may be relevant to clozapine-induced VFO. Clozapine non-competitively inhibits the function of mammalian neuronal α4β2 and α7 neuronal nicotinic receptors in human SH-EP1 cells, frog oocytes, rat brain synaptosomes and hippocampal slices (Singhal et al., 2007;Grinevich et al., 2009). However, clozapine does not appear to interact directly with the α4β2 or α7 orthosteric binding sites, as it did not displace high affinity ligands for these sites (Grinevich et al., 2009), and thus the precise mechanism through which the inhibition is mediated is unclear. The influence of clozapine's inhibition of neuronal nicotinic receptors on cognition is complex and likely depends on the subunit composition of the receptor and the brain region in question (Pocivavsek et al., 2006;Levin et al., 2009).

4.2 Methods

4.2.1 Slice preparation and maintenance

Experiments in this and the following chapters made use of rat brain slice preparations *in vitro*. Hippocampal and 2° somatosensory cortical slices were 450μm thick, and were cut in the horizontal plane from adult male Wistar rats (150-250g). Slices were prepared according to chapter 2.1-2.3 and the maintenance of slices is described in chapter 2.4. Extracellular recording techniques are described in chapter 2.6. Data acquisition, data analysis and statistical techniques are described in chapter 2.7-2.8. VFO events were induced by either clozapine, olanzapine, gabazine or d-tubocurarine according to the experiment. The area power in the VFO band (70-1000Hz) was the primary measure used to quantify extracellular recordings of VFO in LFPs.

4.2.2 Intracellular recording methods

Prior to any intracellular recordings regions of cortex generating optimal VFO were identified using an extracellular field electrode. The field electrode remained in the slice next to the intracellular electrode for the duration of the experiment to compare the intracellular activity of individual cells to the LFP. Sharp borosilicate glass microelectrodes filled with potassium acetate (2M, 80 – 150 MΩ) were used to impale cells for intracellular recordings in accordance with the details in section 2.6.3.

Electrophysiological characterisation of neurons was achieved using a 0.3nA depolarising step with a duration of 300ms, as described previously (McCormick et al., 1985). EPSPs were revealed by injection of tonic, negative DC current until the membrane potential of the cell was hyperpolarised to -70mV to mask concurrent IPSPs, and conversely, IPSPs themselves were revealed, when successful, by injection of tonic, positive current until the membrane potential of the cell was depolarised away from the chloride reversal potential to -30mV.

4.2.3 Multi-electrode array recording techniques

Following confirmation of the presence of VFO in the slice using an extracellular field electrode, multichannel recordings were performed using Utah electrode grids as described in chapter 2.7.2. Data were collected using Central software (Blackrock Microsystems inc. USA) as described in section 2.7.2 and subsequently exported to Matlab software for offline analysis.

For the colour map of the spatial distribution of activity, data were exported to MATLAB, where they were mapped with reference to electrode positions in the Utah grid provided by the supplier, interpolated and illustrated in a two dimensional 'surf' plot with a 'jet' colour map.

4.3 Results

4.3.1 Clozapine induced VFO in the CA2 region of rat hippocampus *in vitro*

Consistent with previous data (F.E.N. LeBeau and M.A. Whittington, unpublished observations), bath application of the antipsychotic clozapine (10µM) induced VFO in the CA2 region of the hippocampus *in vitro* (Fig. 4.1; n = 5 slices). Field traces revealed short, high amplitude transient high frequency discharges with variable inter-bust intervals interspersed with a near continuous presence of high frequency activity. In control conditions prior to application of clozapine, VFO were not present.

The mean VFO band (70-1000Hz) area power of clozapine-induced VFO in CA2 was $2.07 \pm 0.75\ 10^{-11} V^2$ (Fig. 4.2A). Analysis of the frequency components of VFO revealed a blur of frequencies from ~70 to ~400Hz (Fig. 4.1B) with the mean peak at 156 ± 9Hz (Fig. 4.2A). The pattern of intervals between consecutive spikes during the more overt bursts of field VFO appeared to be relatively stable, with a possible small reduction, corresponding to an increase in the instantaneous frequency, at the start of bursts (Fig. 4.2B). The pattern of amplitudes of population spikes during bursts of field VFO

appeared to be relatively stable, with a possible small increase at the start of bursts (Fig. 4.2C). Further quantitative measures of clozapine-induced VFO in CA2 are shown in Table 4.1.

In the hippocampus, VFO were localised to the CA2 pyramidal cell region. Movement of the recording electrode to record from different laminar positions suggested that VFO appeared to be confined to the pyramidal cell layer. Longitudinal movement of the recording electrode along CA3, through the CA2 pyramidal cell layer, and into CA1 suggested patches of increased or decreased activity consistent with localised activity within CA2.

4.3.2 Clozapine induced VFO in layer V of rat 2º somatosensory cortex *in vitro*

Clozapine (10-20µM) also induced VFO in layer V of rat 2º somatosensory cortex *in vitro* (Fig. 4.3). Similar to those in CA2, field VFO in 2º somatosensory cortex were present as short transient high frequency discharges with variable inter-bust intervals. Though in this neocortical region high-amplitude bursts were more overt compared to between burst activity.

The median VFO band area power of clozapine-induced VFO in somatosensory cortex was 2.63 (1.04 → 6.52) $10^{-11}V^2$ (Fig. 4.4A; n = 40 slices). Analysis of the frequency components of VFO revealed a blur of frequencies from ~70 to ~900Hz (Fig. 4.3B) with the median peak at 195 (175 → 244) Hz (Fig. 4.4A). The pattern of intervals between consecutive population spikes during bursts of field VFO appeared to be relatively stable (Fig. 4.4B). Interestingly, the pattern of amplitudes of population spikes during bursts of field VFO in somatosensory cortex (Fig. 4.4C) appeared to be different from those in CA2 (Fig. 4.2C). In somatosensory cortex, the mean spike amplitude decreased from the first to the fourth spike in the burst, before gradually increasing and stabilising. Further quantitative measures of clozapine-induced VFO in somatosensory cortex are shown in Table 4.2.

The basic properties of clozapine-induced VFO in 2º somatosensory cortex were compared with those of clozapine-induced VFO in CA2 (Fig. 4.5, cortical n = 40 slices, CA2 n = 5 slices). Interestingly, the median peak frequency of VFO in 2º somatosensory cortex was significantly greater than that of VFO in CA2 (median cortical peak frequency 195 (175 → 244) Hz, CA2 156 (137 → 176) Hz, $p < 0.05$, Mann-Whitney rank sum test, Fig. 4.5C). The higher frequency nature of VFO in 2º

somatosensory cortex compared to VFO in CA2 is evident in the pooled power spectra (Fig. 4.4A versus Fig. 4.2A), example spectrograms (Fig. 4.3B versus Fig. 4.1B), and intervals between spikes in bursts of field VFO (Fig. 4.4B versus Fig. 4.2B).

However, in quantifying VFO in 2° somatosensory cortex versus that in CA2, there was no significant difference in the median VFO band area power (median cortical VFO band area power 2.63 (1.04 → 6.52) $10^{-11}V^2$, CA2 1.67 (0.55 → 3.59) $10^{-11}V^2$, $p > 0.05$, Mann-Whitney rank sum test, Fig. 4.5A), median VFO band peak power (median cortical VFO band peak power 1.46 (0.50 → 3.73) $10^{-12}V^2$, CA2 0.80 (0.37 → 2.65) $10^{-12}V^2$, $p > 0.05$, Mann-Whitney rank sum test, Fig. 4.5B, median burst frequency (median cortical burst frequency 3.26 (1.81 → 4.18) Hz, CA2 1.61 (1.24 → 3.39) Hz, $p > 0.05$, Mann-Whitney rank sum test, Fig. 4.5D), median inter-burst interval (median cortical inter-burst interval 0.37 (0.33 → 0.63) s, CA2 0.68 (0.39 → 0.91) s, $p > 0.05$, Mann-Whitney rank sum test, Fig. 4.5E), median number of spikes per burst (median cortical number of spikes per burst 6.46 (5.38 → 9.12), CA2 4.73 (4.41 → 7.62), $p > 0.05$, Mann-Whitney rank sum test, Fig. 4.5F), median spike amplitude (median cortical spike amplitude 113 (70 → 159), CA2 97 (62 → 117) μV, $p > 0.05$, Mann-Whitney rank sum test, Fig. 4.5G), median proportion of time during the trace that VFO were present (median cortical proportion of time VFO present 17.8 (8.2 → 29.7) %, CA2 8.7 (5.9→ 30.1) %, $p > 0.05$, Mann-Whitney rank sum test, Fig. 4.5H), or median line length (median cortical line length 24.4 (18.9 → 38.3) mV/s, CA2 27.2 (12.6 → 32.1) mV/s, $p > 0.05$, Mann-Whitney rank sum test, Fig. 4.5I). The variability of clozapine-induced VFO in 2° somatosensory cortex is notable.

In this thesis it was decided to focus on VFO in 2° somatosensory cortex as they were more reliably reproducible than those in CA2 and consisted of more visually discrete events to aid analysis. Following the discovery of clozapine-induced VFO in somatosensory cortex, it was necessary to choose the appropriate clozapine concentration to use in experiments. Initially, attempts were made to induce VFO with clozapine at a concentration of 10μM, but it was later found that 20μM clozapine was associated with a higher incidence of VFO (data not shown). The mean VFO band area power of oscillatory activity associated with 5 ($n = 7$), 10 ($n = 11$), and 20μM clozapine ($n = 36$) was 1.79 ± 0.46, 2.24 ± 0.91 and 6.85 ± 1.72 $10^{-11}V^2$ respectively (Fig. 4.6). Thus, although there was only a small difference between VFO associated with 5 and 10μM clozapine, there was a clear concentration-dependent relationship between clozapine and VFO at the 10 and 20μM concentrations. As 20μM clozapine was

sufficient to induce prominent VFO routinely, it was decided not to investigate higher concentrations, which would be in danger of falling outside the therapeutically relevant concentration range in cerebrospinal fluid (see discussion section 4.4.4), and this concentration was used in subsequent experiments.

Low levels of spontaneous VFO were sometimes present in layer V of 2º somatosensory cortex. The mean VFO band area power of such activity was 0.52 ± 0.36 $10^{-11}V^2$ (n = 5). A further control was performed in which DMSO, the solvent in which antipsychotics were dissolved, was bath applied to slices for 4h. Under these conditions there was a small increase in spontaneous VFO (mean VFO band area power 0.96 ± 0.28 $10^{-11}V^2$, n = 5) but the magnitude of such activity remained substantially below (ca. 7-fold less) that associated with 20µM clozapine.

4.3.3 Concentration response for olanzapine and haloperidol on VFO in layer V of rat 2º somatosensory cortex *in vitro*

Given that clozapine induced VFO in cortex *in vitro*, it was interesting to ask whether other antipsychotics would also induce similar oscillatory activity. Specifically, it was investigated whether the atypical antipsychotic olanzapine, or the classical antipsychotic haloperidol, would induce oscillatory activity in layer V of 2º somatosensory cortex. A concentration response experiment was performed for both of these antipsychotics (Fig. 4.7). As it was unclear which of clozapine's multiple targets were important in mediating VFO, a wide range of concentrations was chosen to allow for different affinities of olanzapine or haloperidol at any shared neurotransmitter receptors.

Electrodes were positioned in layer V of 2º somatosensory cortex, and the following concentrations of antipsychotic were bath applied sequentially at 30 minute intervals: 200nM, 500nM, 2µM, 5µM, 10µM, 20µM and 50µM.

VFO were typically first observed when antipsychotics were applied at low micromolar concentrations. By the 10µM concentration point, marginal VFO were evident in 5/6 slices exposed to olanzapine, and in 6/9 slices exposed to haloperidol. At this concentration, the mean VFO band area power was 1.89 ± 1.0 $10^{-11}V^2$ in the olanzapine experiment, but only 1.35 ± 0.50 $10^{-11}V^2$ in the haloperidol experiment. By the 50µM concentration, prominent VFO were present in the olanzapine experiment, where the mean VFO band area power was 4.03 ± 2.61 $10^{-11}V^2$, whereas the effect of haloperidol remained relatively small at this concentration (mean VFO band area power 2.23 ± 0.92

$10^{-11}V^2$). Thus, similar to clozapine, olanzapine had a clear effect in inducing salient VFO, whereas haloperidol was also associated with some VFO, but only to a lesser extent.

4.3.4 Persistence of clozapine-induced VFO in layer V of rat 2º somatosensory cortex

Following application of clozapine, a delay to allow oscillatory activity to develop, and probing for an optimal patch of VFO in layer V of 2º somatosensory cortex, electrodes were left in the same position and recordings were taken at 15 minute intervals for 3 hours. Clozapine-induced VFO were persistent for 3 hours (n = 5 slices, Fig. 4.8) and did not diminish for a further hour (n = 4 slices, data not shown). There was a temporary dip in the mean area power of VFO at the 1.5 hour time point, but the overall pattern in the 3 hour time period was one of relatively stability (Fig. 4.8C). There was a small upward trend in the mean peak frequency of VFO for the first 1.5 hours prior to its stabilisation for the remainder of the experiment (Fig. 4.8D).

4.3.5 Spatiotemporal properties of clozapine-induced VFO in 2º somatosensory cortex

4.3.5.1 Patches of VFO were maximal in layer V

Glass microelectrode laminar profiles suggested that patches of clozapine-induced VFO occurred maximally tightly confined to layer Va. Utah multi-electrode array recordings are useful in investigating the spatial distribution of oscillatory activity as they allow for simultaneous acquisition of extracellular data from 96 channels over a 3.6*3.6mm grid. The VFO band area power in each of the Utah array electrodes was illustrated in a colour map which was then superimposed over an image of 2º somatosensory cortex from a rat brain atlas (Fig. 4.9, Paxinos and Watson, 1998). Utah array recordings confirmed the presence of small patches of clozapine-induced VFO, typically maximal in layer V (Fig. 4.9), but VFO could sometimes also be present in other deep and superficial layers throughout the slice.

4.3.5.2 Distribution of VFO along layer V of 2º somatosensory cortex

To further examine the spatiotemporal properties of clozapine-induced VFO, the synchrony between VFO rhythms along layer V neocortex was investigated. Following discovery of an optimal patch of clozapine-induced VFO with one glass microelectrode, a second glass microelectrode was moved distances between 100 and 900µm from the

reference electrode in a longitudinal direction along layer V of 2º somatosensory cortex. Synchrony within bursts was measured at each 200µm step by performing cross-correlation analysis on the first burst event in a 60s trace. The point in the cross-correlogram where the central peak crossed the Y axis was used as a measure of the synchrony between the two rhythms. The synchrony of the two rhythms decreased linearly as the distance between the recording electrodes increased (n = 10 slices, Fig. 4.10, 4.11). The synchronous activity of the rhythms for distances up to ~500µm, where there is still a clear central peak in the cross-correlogram, supports the idea that clozapine-induced VFO result from network activity rather than activity of only a few cells underneath the electrode. However, the synchrony of clozapine-induced VFO broke down over distances greater than ~500µm, consistent with the observation of the spatial patchiness of the rhythm.

To quantify synchrony at a lower temporal resolution, the number of VFO burst events which appeared synchronous (Fig. 4.12A) or coincident (Fig. 4.12B) in 60s traces were also counted by eye (n = 5 slices). The same pattern of synchronous activity to ~500µm was seen at the level of bursts.

In contrast, there was no clear trend in the pattern of phase lag, which corresponds to the X value of the central peak in the cross-correlogram, within bursts over the distances investigated. The mean intra-event phase lag started at 6.04 ± 1.37ms at a distance of 100µm, fell to 4.44 ± 0.66ms at 500µm, and then rose again to 7.16 ± 2.06ms at 900µm (n = 5 slices, Fig. 4.12C).

4.3.6 Intracellular activity of neurons during clozapine-induced VFO

To investigate the activity of neurons during VFO, sharp electrode intracellular recordings were taken from cell soma in cells nearby to the field potential in layer V of 2º somatosensory cortex. Intracellular recordings were taken from 35 RS cells, 7 IB cells, and 1 fast rhythmic bursting (FRB) pyramidal cell.

Much of the activity of RS and IB cells appeared to be sparse, but occasional RS and IB cells fired more frequently. Activity of cells appeared to be heterogeneous within cell types in the sense that there did not appear to be a distinctive firing pattern reliably associated with either RS or IB cells, and spike-bursts were present in an RS cell.

Intracellular activity in RS and IB cells was only relatively infrequently coincident with field VFO. Cross-correlation analysis was used to relate spike, EPSP and IPSP activity,

where present in individual cells to field VFO where any such activity coincided. There was almost no correlation between the somatic activity of layer V RS cells and field VFO (Fig. 4.13). Furthermore, there were no examples of intracellular activity in either cell type precisely phase-locked to field VFO. Somatic depolarisations with rapid kinetics, known as partial spikes or spikelets, were present in one RS cell, and putative antidromic spikes were present in 3 RS cells (Fig. 4.14). There was a high degree of variability in the amplitude of putative spikelets in the RS cell.

Interestingly, IB cell bursts (Fig. 4.15), and in particular, IB cell spikelets (Fig. 4.16) were weakly correlated with field VFO. There was considerable variability in the amplitude of the IB cell spikelets. In rare cases, IB cell bursts appeared to arise from spikelets (Fig. 4.16C), raising the possibility, but by no means unequivocally establishing, that such bursts may be antidromic.

There was also a possible relationship between the activity of an FRB cell and field VFO, whereby one FRB cell spike was in phase with field VFO (Fig. 4. 17).

4.3.7 Comparison of field VFO with IB cell bursts

If clozapine-induced VFO were to result from activity of only a small number of cells, it might possibly be conceived that clozapine-induced VFO might reflect synchronous activity of a small subpopulation of IB cells. To investigate this, the pattern of intervals between population spikes in bursts of field VFO was compared with those in concurrent recordings of bursts of spikes in IB cells (Fig. 4.18). There was a clear upward trend in the interval between consecutive spikes during IB cell bursts. The mean inter-spike interval in IB cell bursts rose from 3.7 ± 0.0ms between the first and second spike in the burst, to 7.3 ± 1.4ms between the seventh and eighth spike in the burst (n = 220 bursts in 3 cells). However, in contrast the interval between consecutive population spikes during bursts of field VFO was relatively stable. The mean interval between the first and second population spike in bursts of field VFO was 7.4 ± 0.2ms, which was a similar figure to that between the seventh and eighth spike in bursts, 7.5 ± 0.3ms (n = 887 bursts in 3 slices). This difference suggests that clozapine-induced VFO does not merely reflect synchronous activity of a small number of IB cell extracellular units.

4.3.8 Disinhibition may have a role in clozapine-induced VFO

As clozapine may suppress $GABA_A$ receptor-mediated inhibition (Michel and Trudeau, 2000;Ohno-Shosaku et al., 2011), the $GABA_A$ receptor antagonist gabazine (250nM) was bath applied to slices alone to investigate whether partial disinhibition (ca. 10% reduction in chloride conductance through $GABA_A$ receptor ionophores (Yu and Ho, 1990)) may be important in the induction of VFO by clozapine. Gabazine induced short transient high frequency discharges of VFO in layer V of 2º somatosensory cortex (Fig. 4.19). This supports the idea that disinhibition may have a role in the mechanism underlying clozapine-induced VFO. The median VFO band area power of gabazine-induced VFO was 2.30 (1.13 → 30.90) $10^{-11}V^2$ with a mean peak frequency of 226 ± 13 Hz (n = 11 slices). Further quantitative measures of gabazine-induced VFO are detailed in Fig. 4.20 and Table 4.3.

4.3.9 Inhibition of neuronal nicotinic receptors may have a role in clozapine-induced VFO

As clozapine may inhibit neuronal nicotinic receptors (Grinevich et al., 2009), slices were exposed to the broad-spectrum nicotinic receptor antagonist d-tubocurarine (d-TC; 10μM) to investigate the possible importance of this action in VFO. d-TC also induced VFO in layer V of 2º somatosensory cortex (Fig. 4.21). This supports the idea that inhibition of neuronal nicotinic receptors may have a role in the mechanism underlying clozapine-induced VFO. The median VFO band area power of d-TC-induced VFO was 2.43 (0.93 → 10.20) $10^{-11}V^2$ with a median peak frequency of 205 (195 → 234) Hz (n = 12 slices). Further quantitative measures of d-TC-induced VFO are shown in Fig. 4.22 and Table 4.4.

There was a pattern in both gabazine-induced VFO and d-TC-induced VFO whereby the mean population spike amplitude in field VFO decreased for the first approximately 15 spikes in the burst, before gradually stabilising and increasing (Fig. 4.20C, Fig. 4.22C).

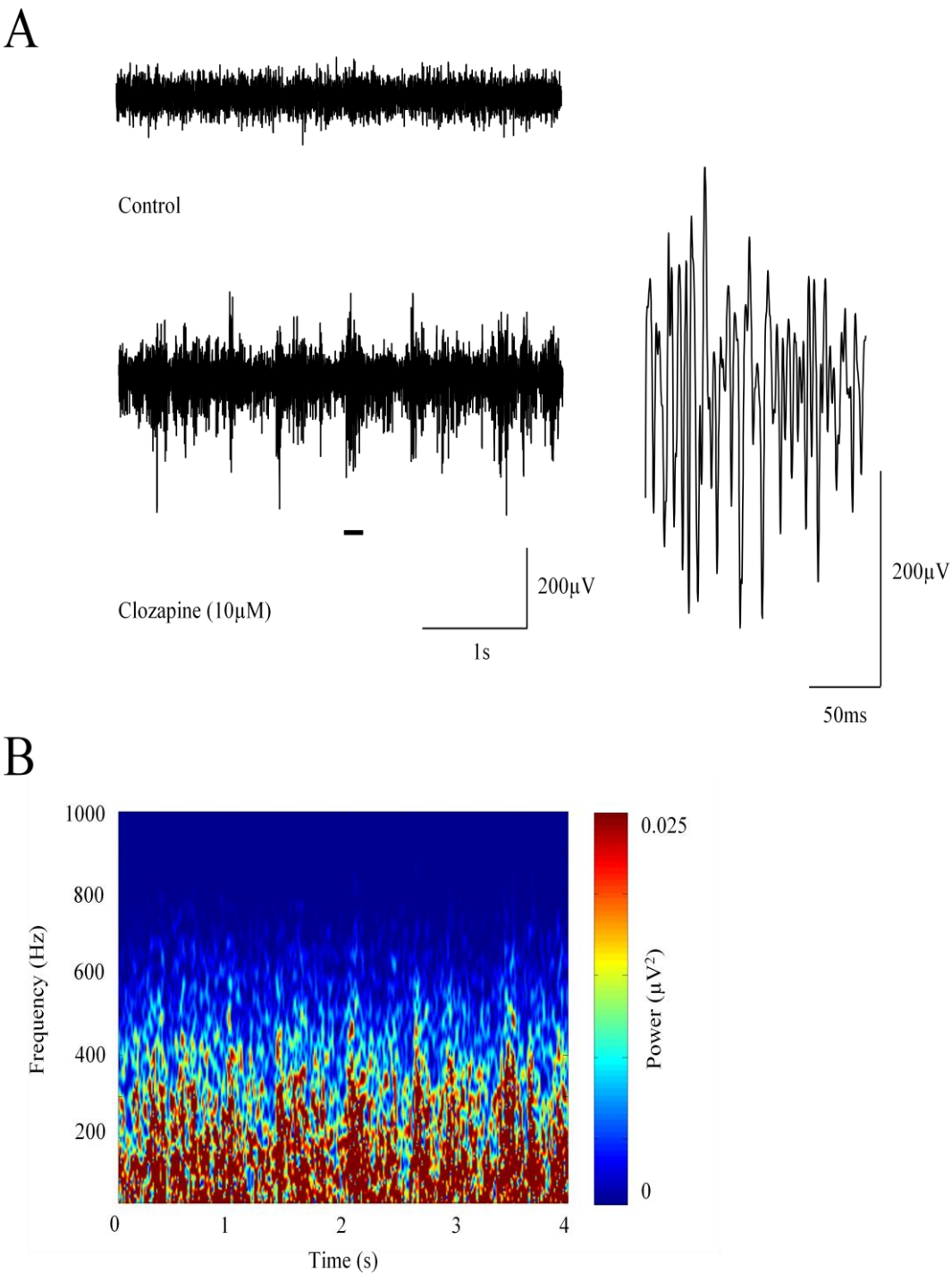

Fig. 4.1. Very fast oscillations (VFO) in the CA2 region of rat hippocampus *in vitro* following bath application of clozapine (10µM). (*A*) 60-1000Hz band-pass filtered field traces (4s duration) for control (upper left) and clozapine (10µM, lower left) conditions. A portion of the trace (150ms) corresponding to the black line is shown at higher resolution on the right. (*B*) Spectrogram illustrating high frequency (60-1000Hz) oscillatory activity for the same recording.

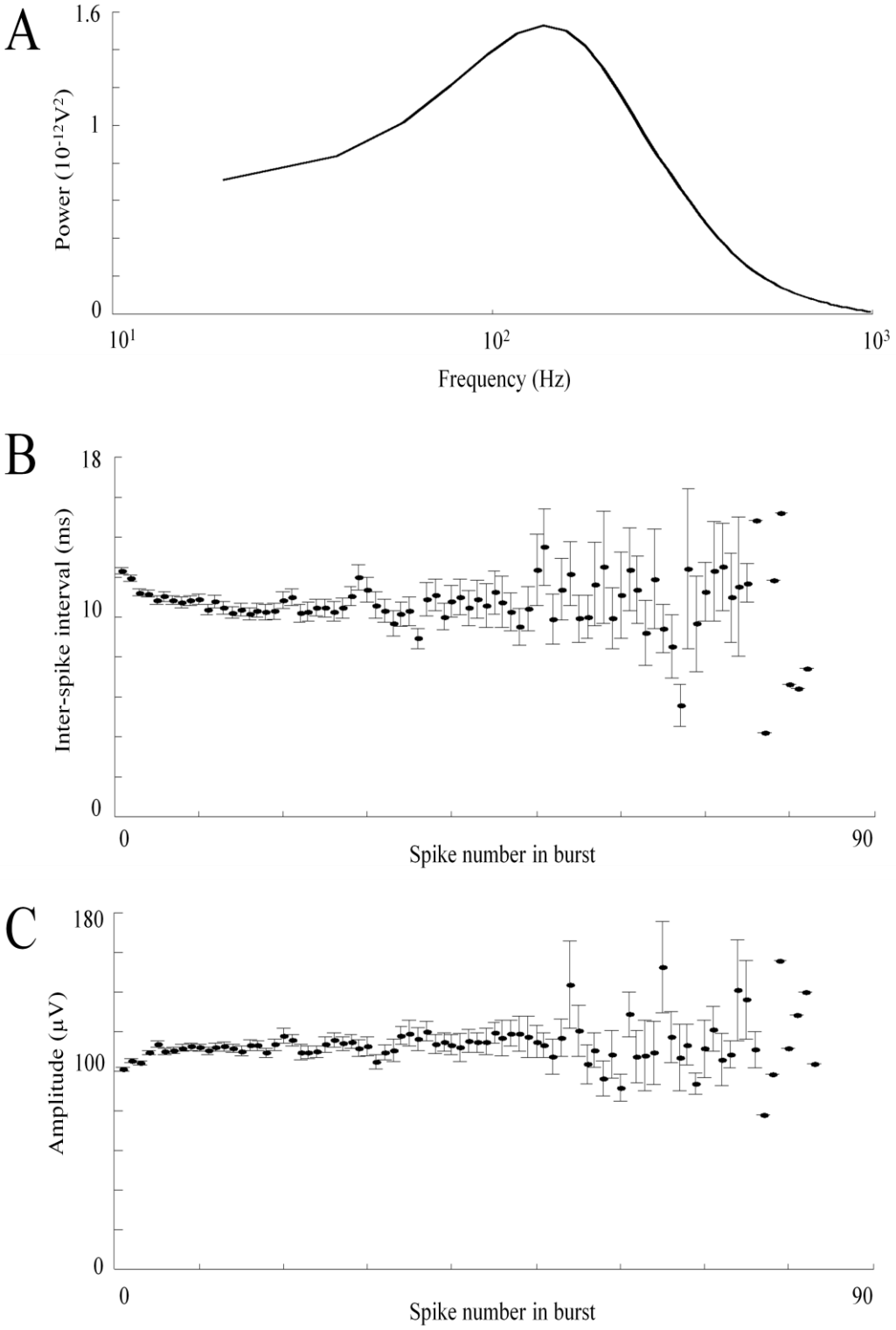

Fig. 4.2. Basic properties of clozapine-induced VFO in the CA2 region of the hippocampus (n = 5 slices). (*A*) VFO band pooled power spectra. (*B)* Intervals between consecutive population spikes during bursts of VFO (mean ± SEM). (*C)* Peak-to-peak amplitudes of population spikes during bursts of VFO (mean ± SEM). Note that the burst n numbers are lower for long bursts, corresponding to an increase in variability for the final troughs in long bursts.

Parameter	Mean ± SEM / Median (Q1 → Q3)
VFO band area power ($10^{-11}V^2$)	2.07 ± 0.75
VFO band peak power ($10^{-12}V^2$)	1.54 ± 0.70
VFO band peak frequency (Hz)	156 ± 9
Burst frequency (Hz)	2.25 ± 0.67
Inter-burst interval (s)	0.71 ± 0.18
Number of spikes per burst	4.73 (4.41 → 7.62)
Spike amplitude (μV)	91.6 ± 15.4
Proportion of time during the trace that VFO were present (%)	8.7 (5.9 → 30.1)
Line length (mV/s)	22.9 ± 4.8

Table 4.1. Quantitative measures of clozapine-induced VFO in the CA2 region of the hippocampus (n = 5 slices). Parametric data are expressed as mean ± SEM. Non-parametric data are expressed in terms of the median and interquartile range (Q1 → Q3).

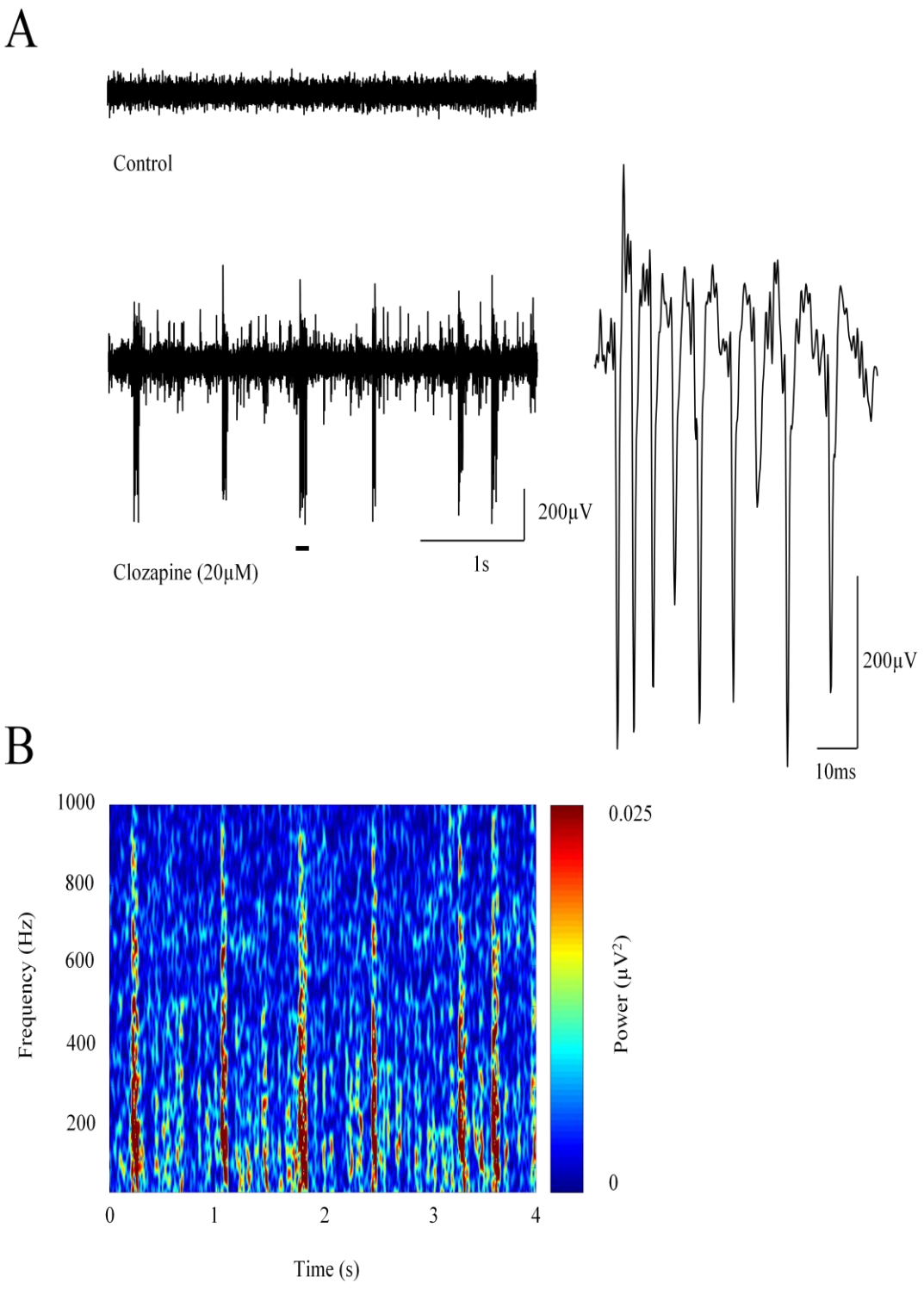

Fig. 4.3. VFO in layer V of rat 2º somatosensory cortex *in vitro* following bath application of clozapine (20µM). (*A*) 60-1000Hz band-pass filtered field traces (4s duration) for control (upper left) and clozapine (20µM, lower left) conditions. A portion of the trace (80ms) corresponding to the black line is shown at higher resolution on the right. (*B)* Spectrogram illustrating high frequency (60-1000Hz) oscillatory activity for the same recording.

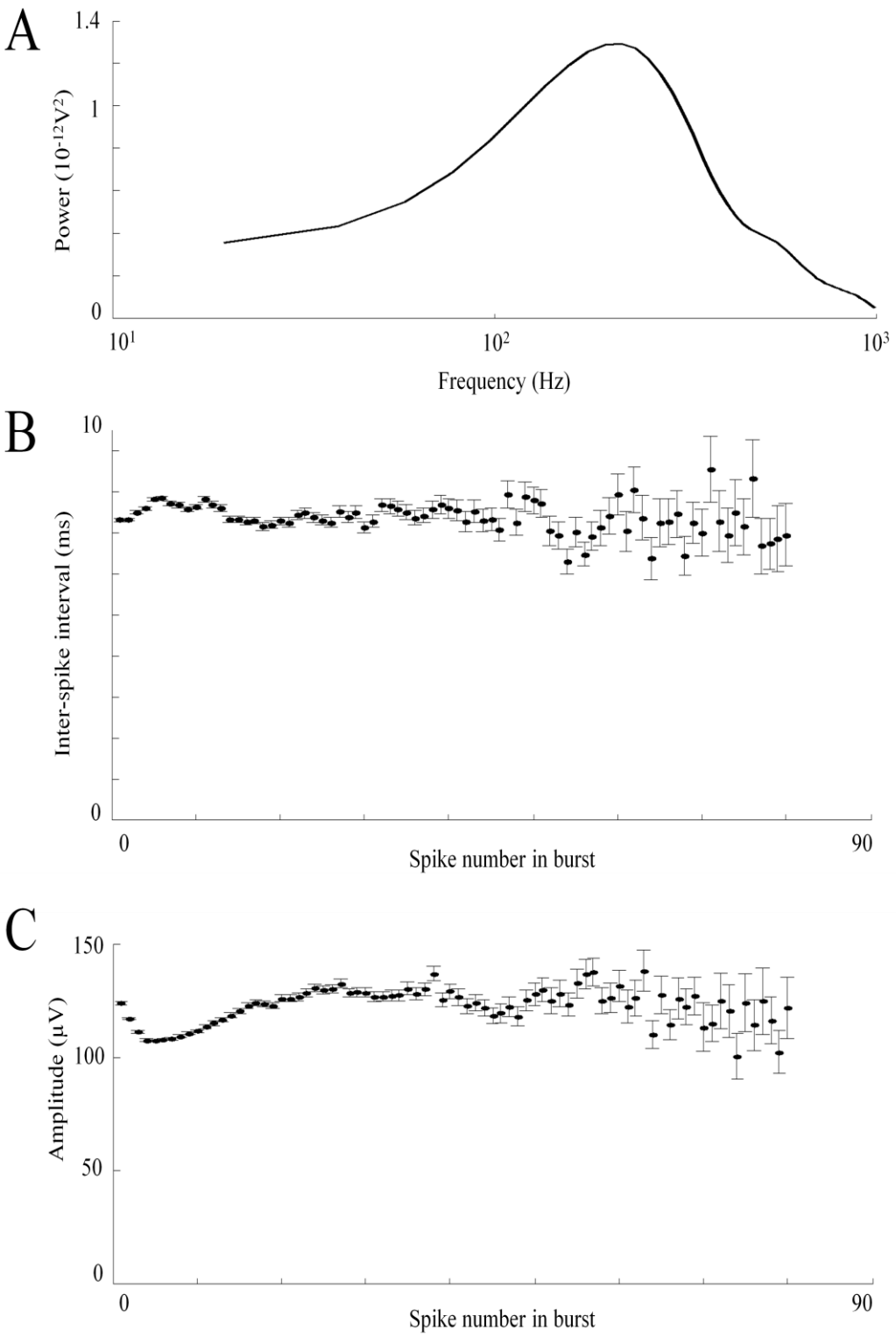

Fig. 4.4. Basic properties of clozapine-induced VFO in layer V of 2º somatosensory cortex (n = 40 slices). (*A*) VFO band pooled power spectra. (*B)* Intervals between consecutive population spikes during bursts of VFO (mean ± SEM). (*C)* Peak-to-peak amplitudes of population spikes during bursts of VFO (mean ± SEM).

Parameter	Mean ± SEM / Median (Q1 → Q3)
VFO band area power ($10^{-11}V^2$)	2.63 (1.04 → 6.52)
VFO band peak power ($10^{-12}V^2$)	1.46 (0.50 → 3.73)
VFO band peak frequency (Hz)	195 (175 → 244)
Burst frequency (Hz)	3.26 (1.81 → 4.18)
Inter-burst interval (s)	0.37 (0.33 → 0.63)
Number of spikes per burst	6.46 (5.38 → 9.12)
Spike amplitude (μV)	113 (70 → 159)
Proportion of time during the trace that VFO were present (%)	17.8 (8.2 → 29.7)
Line length (mV/s)	24.4 (18.9 → 38.3)

Table 4.2. Quantitative measures of clozapine-induced VFO in layer V of 2º somatosensory cortex (n = 40 slices). Parametric data are expressed as mean ± SEM. Non-parametric data are expressed in terms of the median and interquartile range (Q1 → Q3).

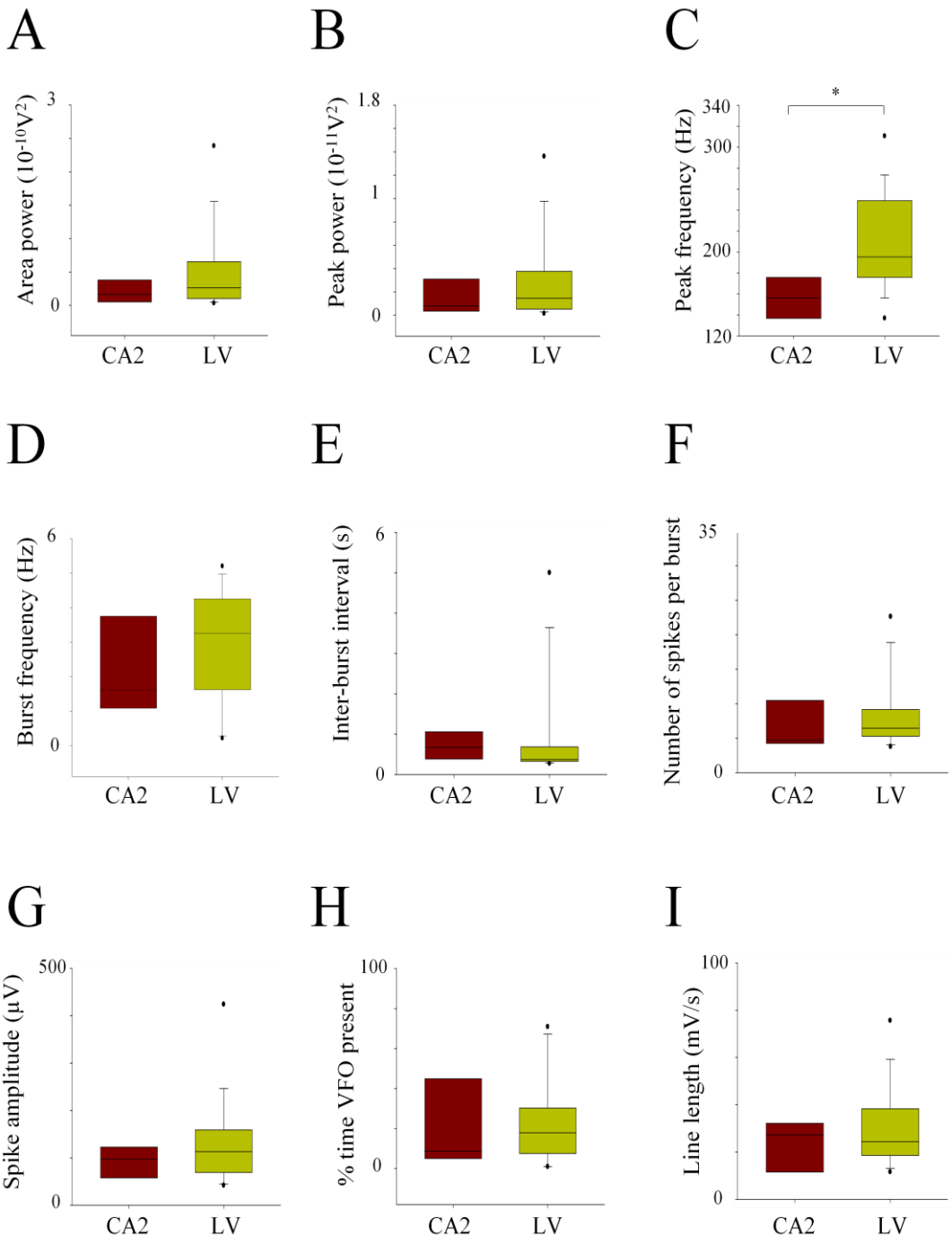

Fig. 4.5. Comparison of the basic properties of clozapine-induced VFO in the CA2 region of the hippocampus (10µM, n = 5 slices) with those of clozapine-induced VFO in layer V of 2º somatosensory cortex (10-20µM; n = 40 slices). VFO band area power (*A*), peak power (*B*), and peak frequency (*C*). Burst frequency (*D*), inter-burst interval (*E*), number of spikes per burst (*F*), spike amplitude (*G*), proportion of time during the trace that VFO were present (*H*), and line length (*I*). In the box plots, the line within the box represents the median, while the lower and upper boundaries represent the 25th (Q1) and 75th (Q3) percentile respectively. Where applicable, error bars represent the 10th and 90th percentile, and the black circles represent the 5th and 95th percentile. * denotes a significant difference ($p < 0.05$).

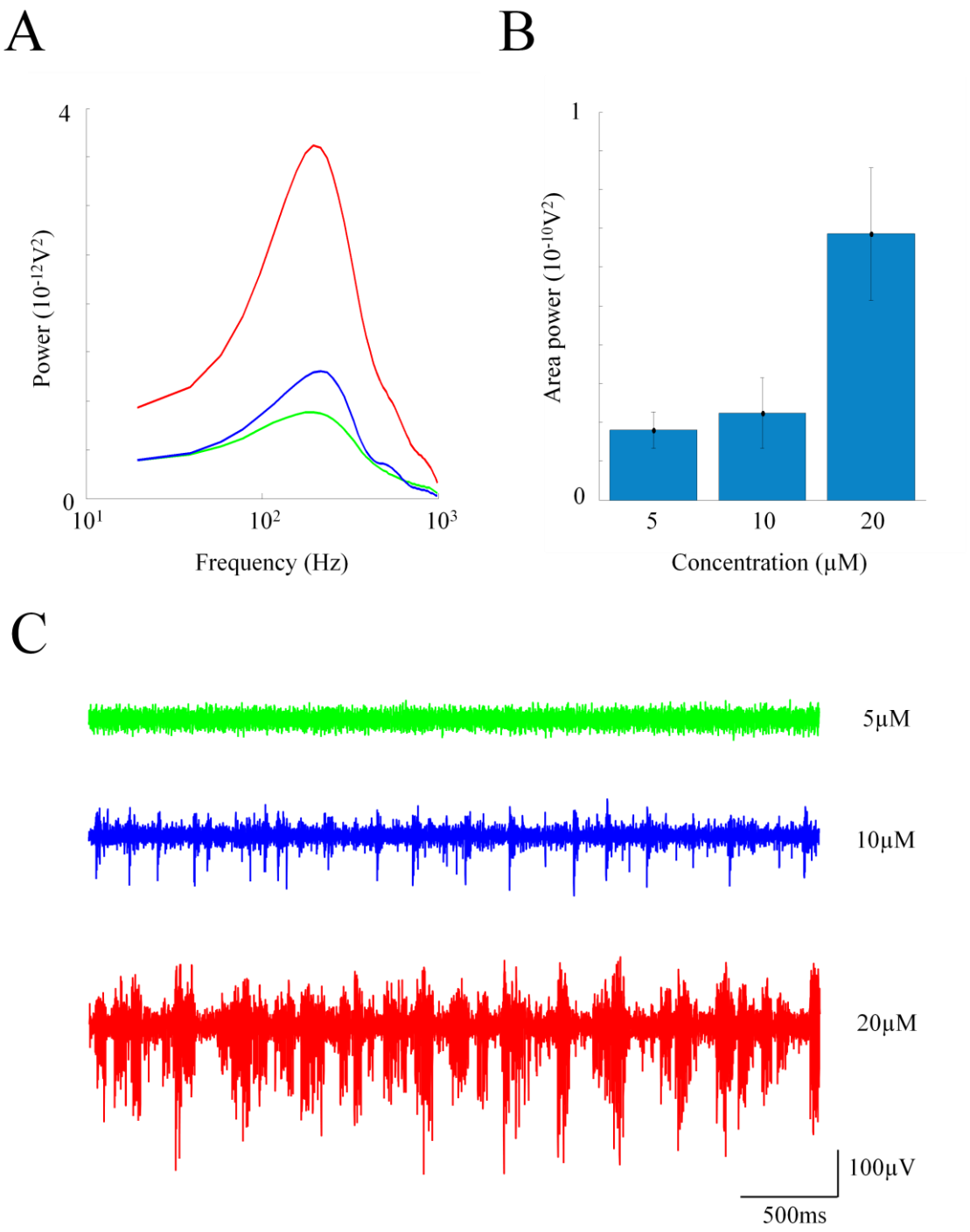

Fig. 4.6. Concentration response for clozapine on VFO in layer V of 2° somatosensory cortex. (*C*) Example field traces (60-1000Hz band-pass filtered) and (*A*) VFO band pooled power spectra for 5µM (green, n = 7 slices), 10µM (blue, n = 11 slices), and 20µM (n = 36 red slices) concentrations. (*B*) Bar chart showing area power (mean ± SEM) for each concentration.

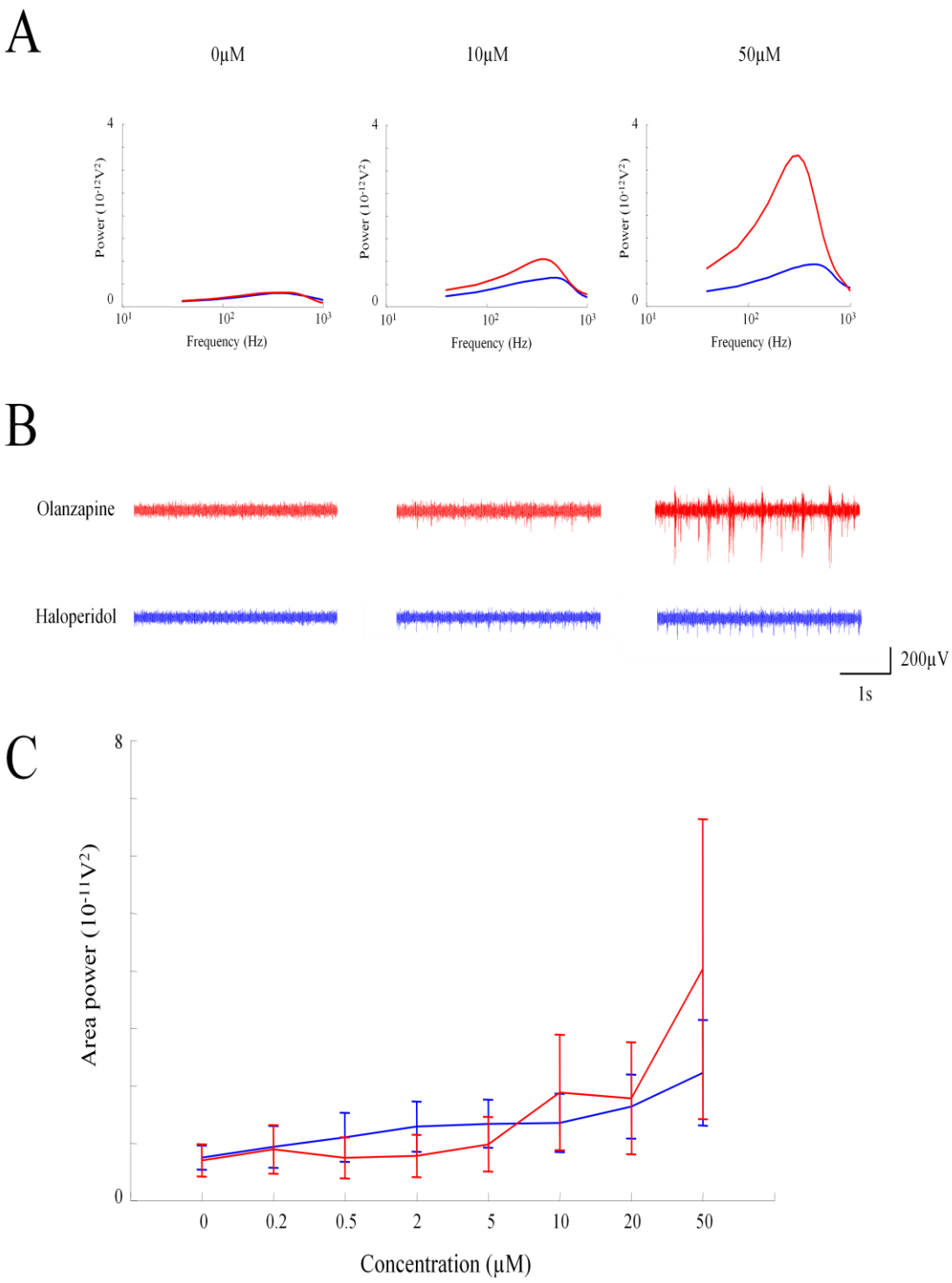

Fig. 4.7. Concentration response for olanzapine (red, n = 6 slices) and haloperidol (blue, n = 9 slices) on VFO in layer V of 2º somatosensory cortex. (*C*) Graph showing area power (mean ± SEM) of VFO following bath application of 0, 0.2, 0.5, 2, 5, 10, 20, and 50µM concentrations of olanzapine (red) or haloperidol (blue). (*B*) Example field traces (60-1000Hz band-pass filtered)and (*A*) VFO band pooled power spectra for 0, 10 and 50µM concentration conditions (olanzapine, red; haloperidol, blue).

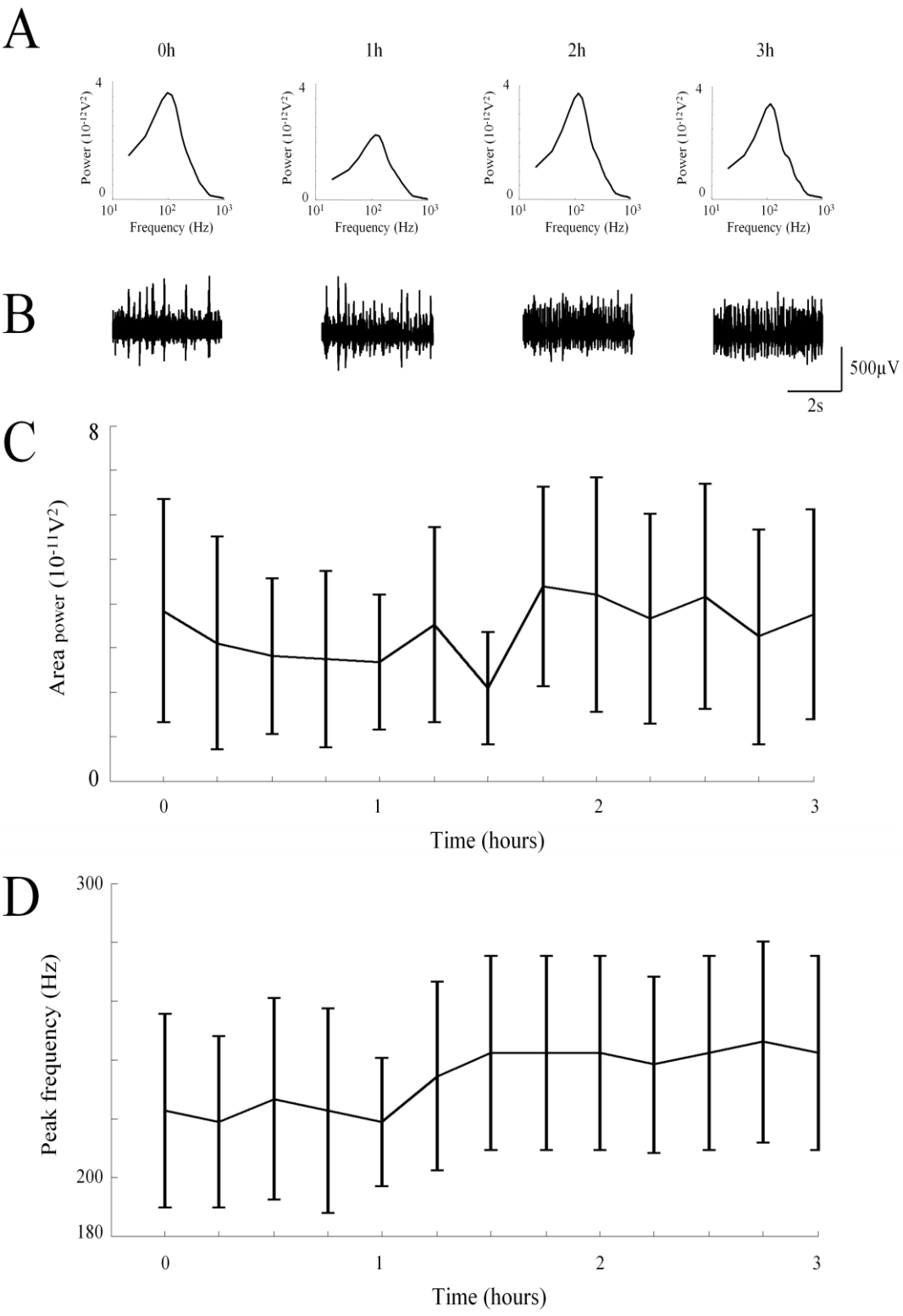

Fig. 4.8. Persistence of clozapine-induced VFO in layer V of 2º somatosensory cortex (n = 5 slices). (*C*) Area power (mean ± SEM) and (*D*) peak frequency (mean ± SEM) of VFO at 15 minute time intervals for 3 hours. (*A*) VFO band pooled power spectra and (*B*) example field traces for 0, 1, 2 and 3h timepoints.

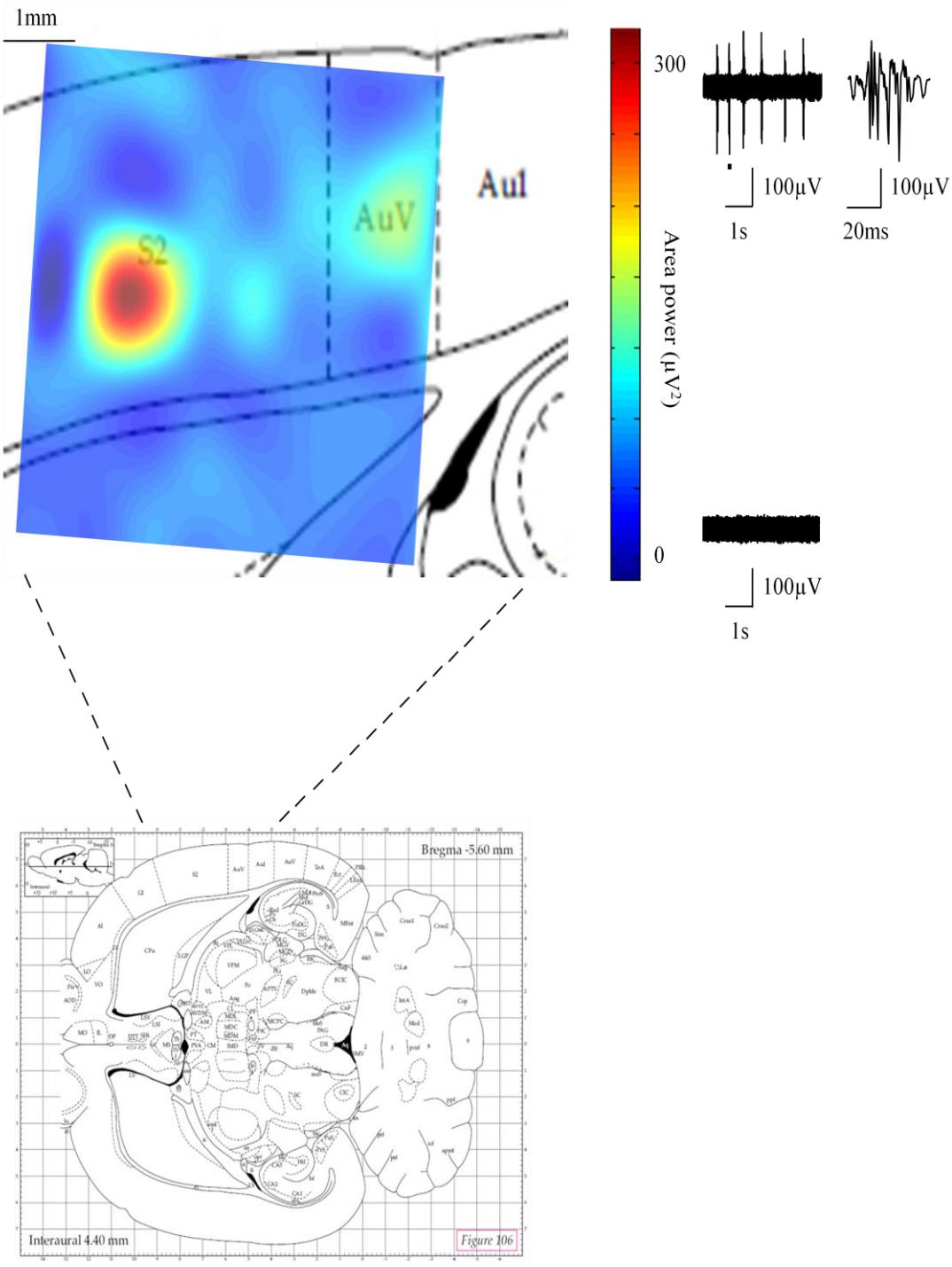

Fig. 4.9. Visual representation of the spatial distribution of clozapine-induced VFO in 2° somatosensory cortex. In the activity map, the colour corresponds to the VFO band area power, as shown in the colourbar scale on the right. Example 60-1000Hz band-pass filtered field traces with the highest (upper) and lowest (lower) VFO band area power values are shown on the right. Data were derived from an example recording with the 3.6*3.6mm 96 electrode Utah array. S2: secondary somatosensory cortex; AuV: secondary auditory cortex, ventral area; Au1: primary auditory cortex. Rat brain atlas modified from Paxinos and Watson (1998).

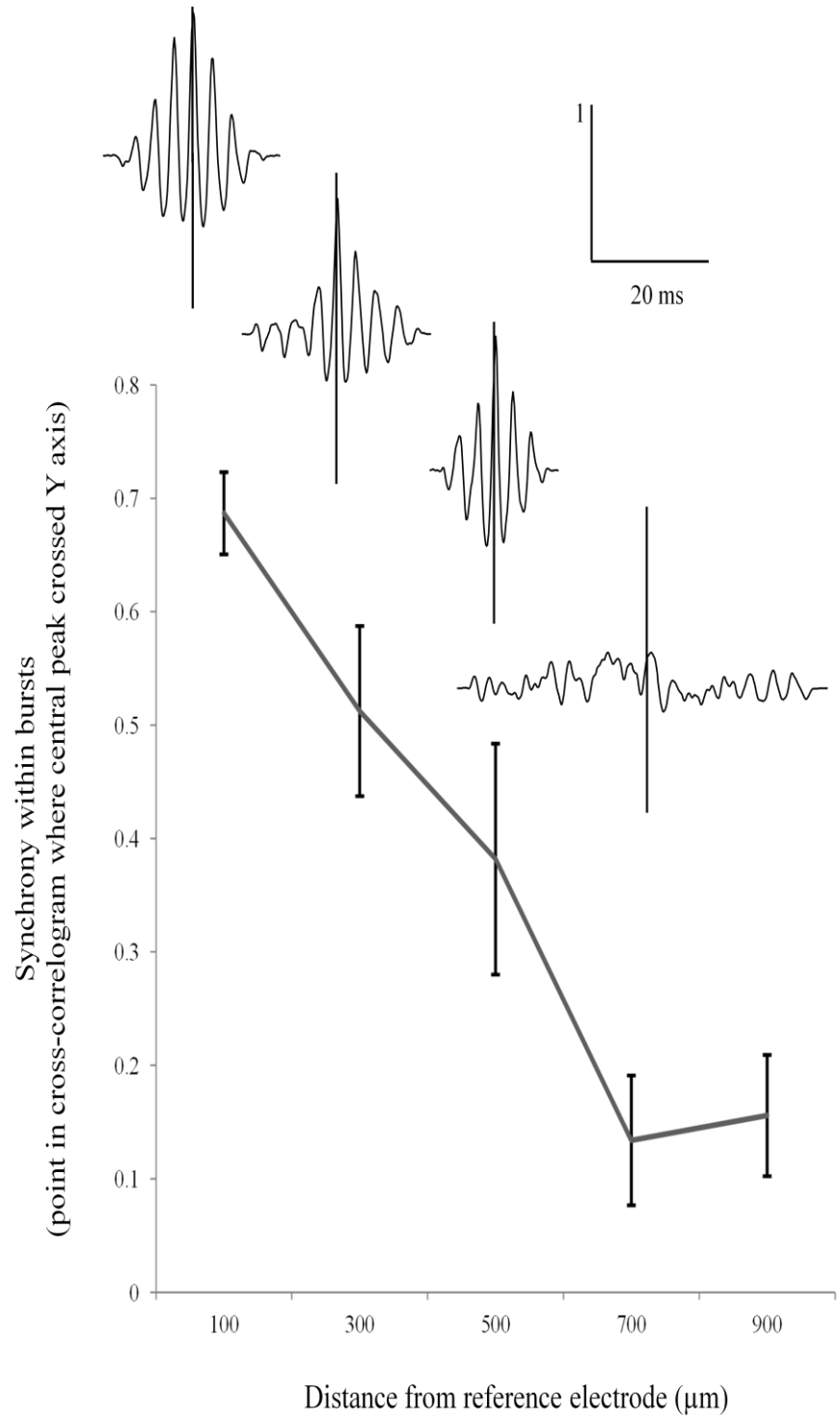

Fig. 4.10. Distribution of VFO along layer V of 2º somatosensory cortex. Example cross-correlograms and pooled data (n = 10 slices) for synchrony within bursts of VFO in field rhythms from two electrodes at distances from 100 to 900µm apart along layer V of 2º somatosensory cortex (mean ± SEM). The synchronous activity of VFO over distance is consistent with a mechanism involving activity of a local network of cells.

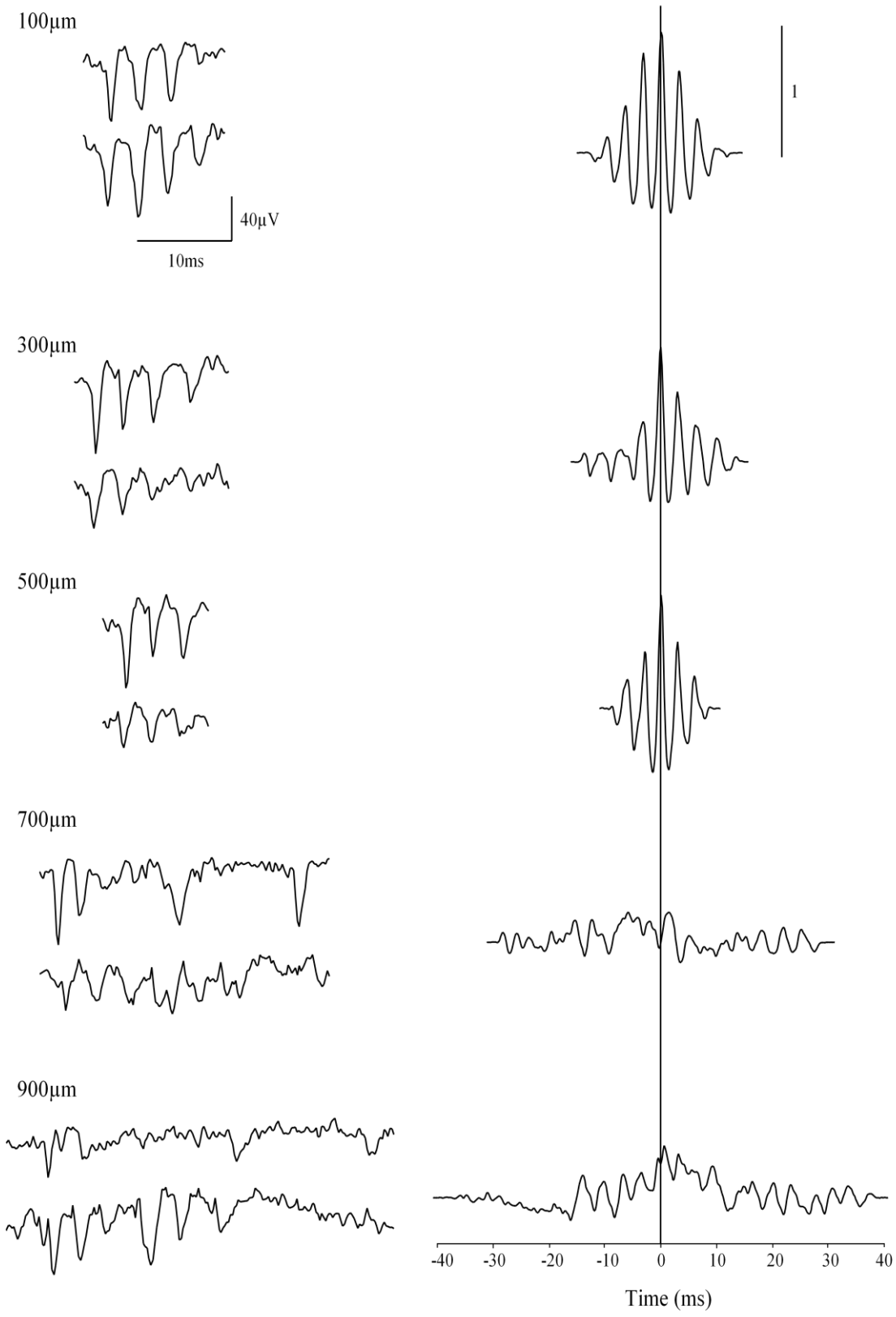

Fig. 4.11. Example traces to illustrate synchrony within bursts of VFO in field rhythms from two electrodes at various distances apart along layer V of 2º somatosensory cortex. Paired traces (left), together with the corresponding cross-correlogram (right), for paired recordings 100, 300, 500, 700 and 900µm apart.

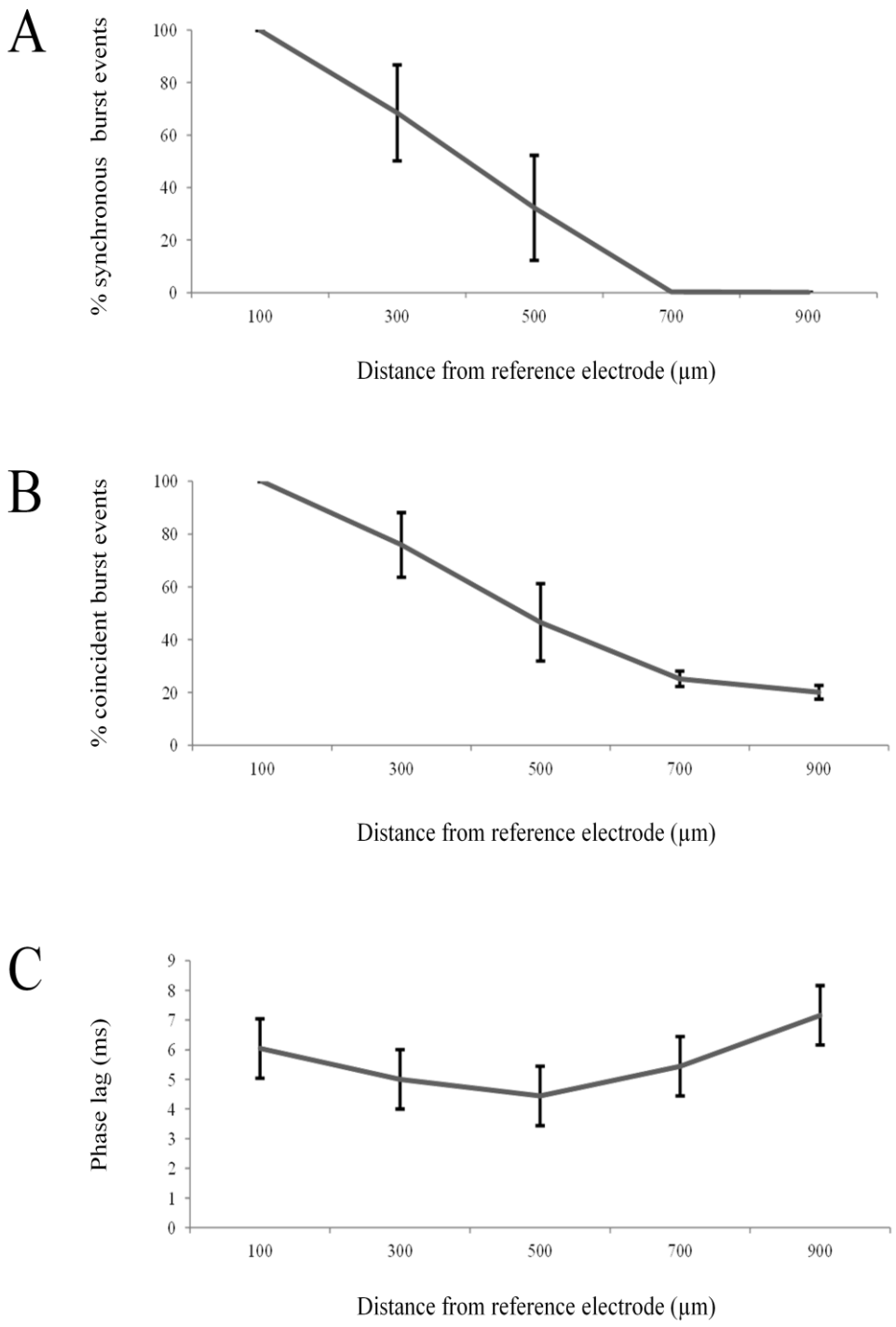

Fig. 4.12. Burst synchrony and intra-event phase lag in field rhythms from two electrodes at distances from 100 to 900µm apart along layer V of 2º somatosensory cortex (n = 5 slices). (*A*) Proportion of synchronous burst events counted by eye (mean ± SEM). (*B*) Proportion of coincident burst events counted by eye (mean ± SEM). (*C*) Intra-event phase lag (mean ± SEM).

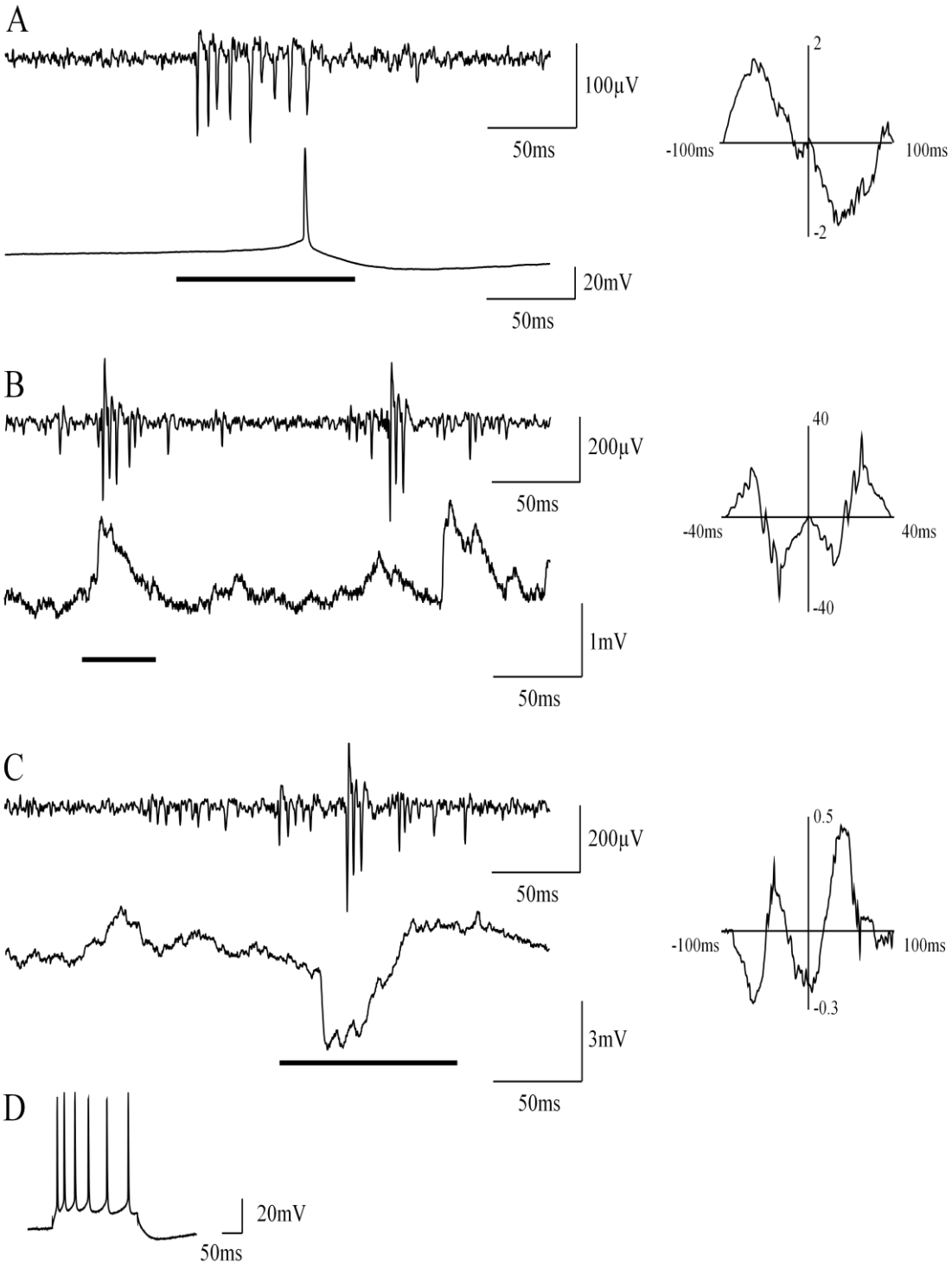

Fig. 4.13. Activity of regular spiking (RS) pyramidal cells in layer V of 2^0 somatosensory cortex during clozapine-induced VFO: examples of occasional instances where intracellular activity coincides with field VFO. Intracellular recordings of an RS cell firing at a resting membrane potential of -55mV (*A*), EPSPs while a cell was held at -70mV (*B*), and IPSPs while a cell was held at -30mV (*C*). In each case 60-1000Hz band-pass filtered field traces (300ms duration) are shown on the upper section of the panel and concurrent intracellular traces are shown on the lower section of the panel. Corresponding cross-correlations of field and intracellular activity are shown on the right. The black line marks the section of the trace used in the cross-correlation. (*D*) Electrophysiological characterisation of RS cells.

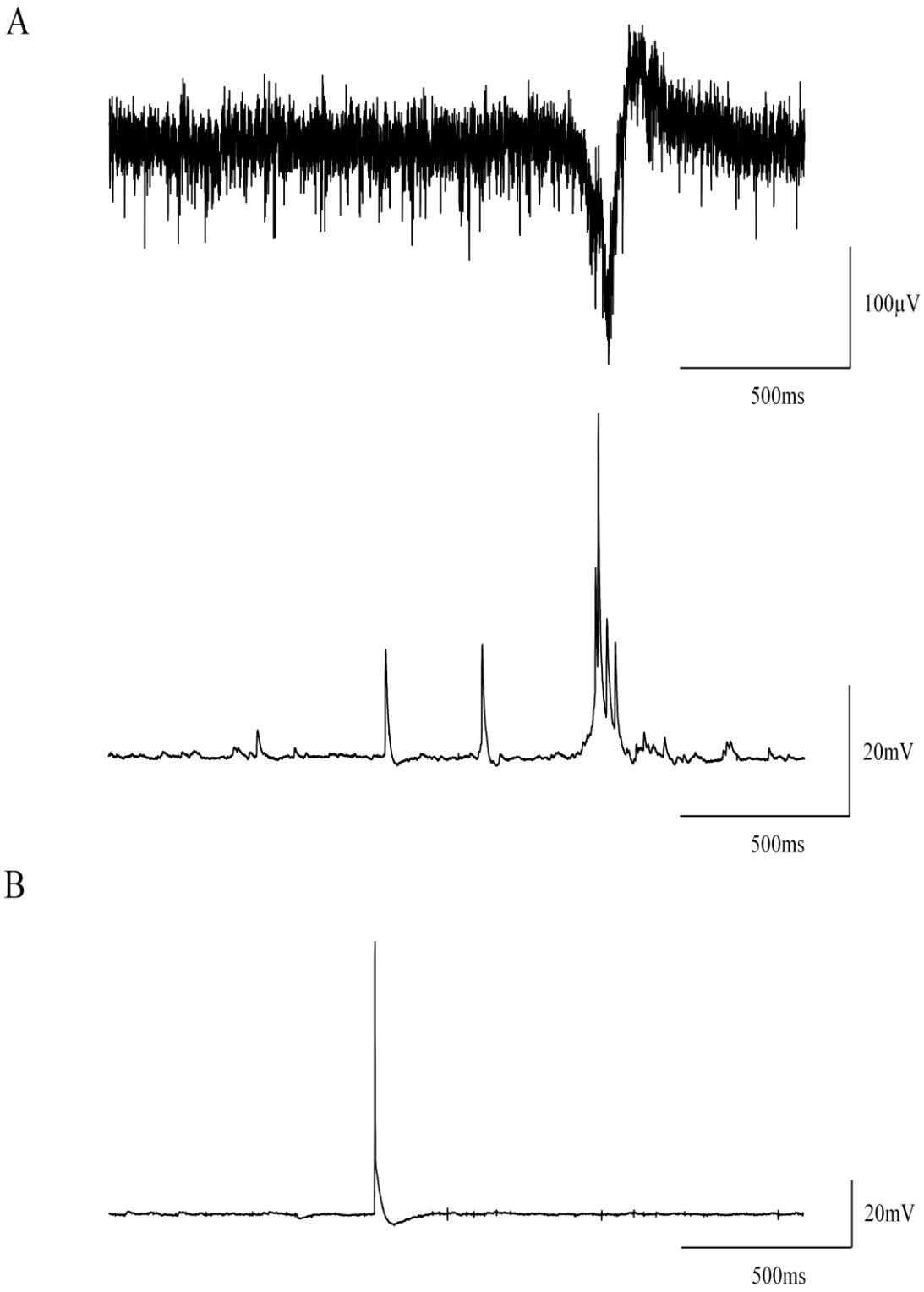

Fig. 4.14 (*A*) Intracellular recording of putative spikelets during clozapine-induced VFO in an RS cell at resting membrane potential (-67mV). The raw unfiltered field trace is shown in the upper section, and the intracellular trace in the lower section. In addition to a full action potential, spikelets are present in the burst of intracellular activity, which was associated with epileptiform activity in the field. (*B*) Intracellular recording of a putative antidromic spike in an RS cell depolarised to -70mV. Note the absence of an EPSP in the vertical rising phase of the action potential.

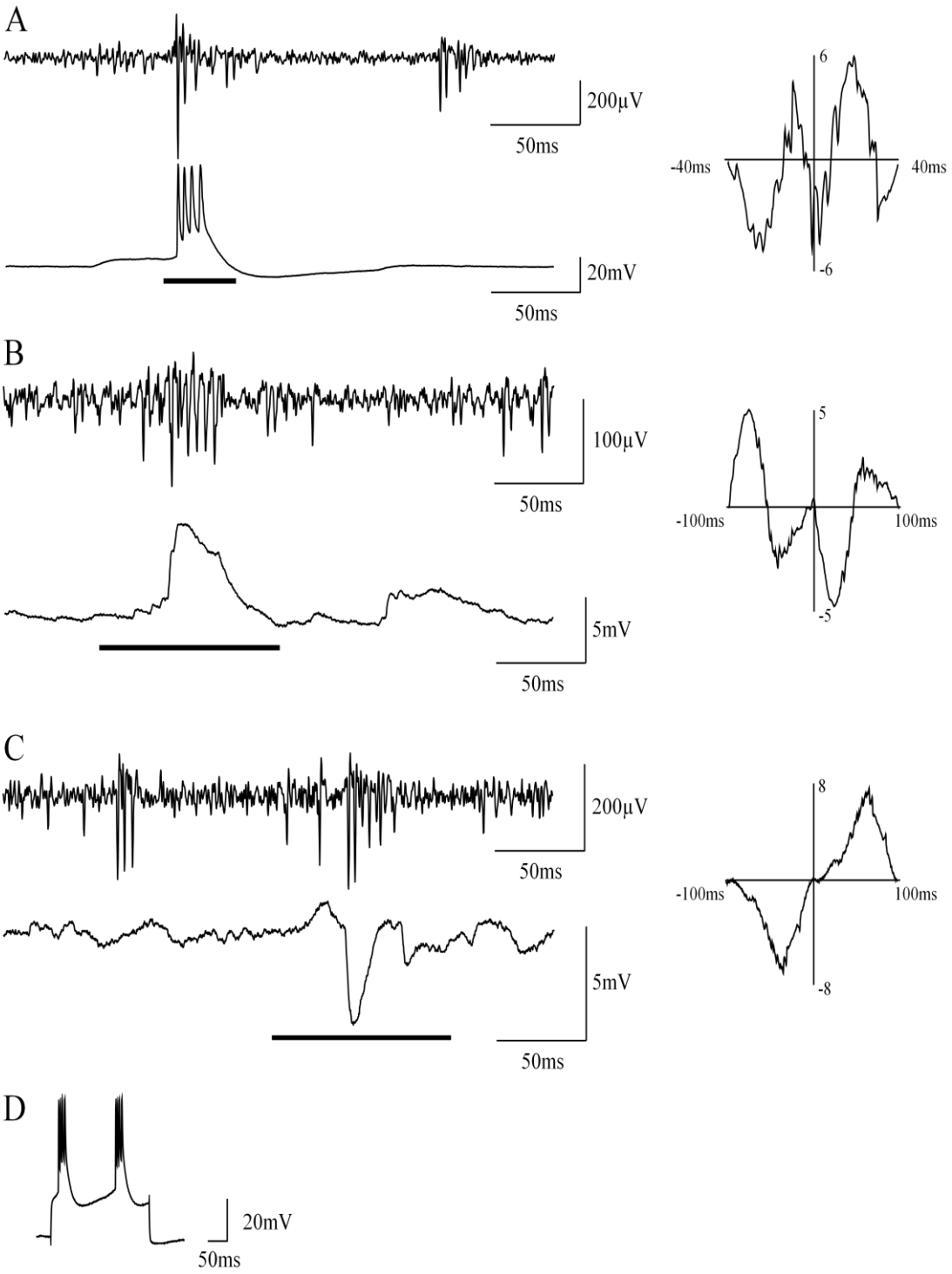

Fig. 4.15. Activity of intrinsically bursting (IB) pyramidal cells in layer V of 2^0 somatosensory cortex during clozapine-induced VFO: examples of occasional instances where intracellular activity coincides with field VFO. Intracellular recordings of an IB cell firing at a resting membrane potential of -60mV (*A*), EPSPs while a cell was held at -70mV (*B*), and IPSPs while a cell was held at -30mV (*C*). In each case 60-1000Hz band-pass filtered field traces (300ms duration) are shown on the upper section of the panel and concurrent intracellular traces are shown on the lower section of the panel. Corresponding cross-correlations of field and intracellular activity are shown on the right. The black line marks the section of the trace used in the cross-correlation. (*D*) Electrophysiological characterisation of IB cells.

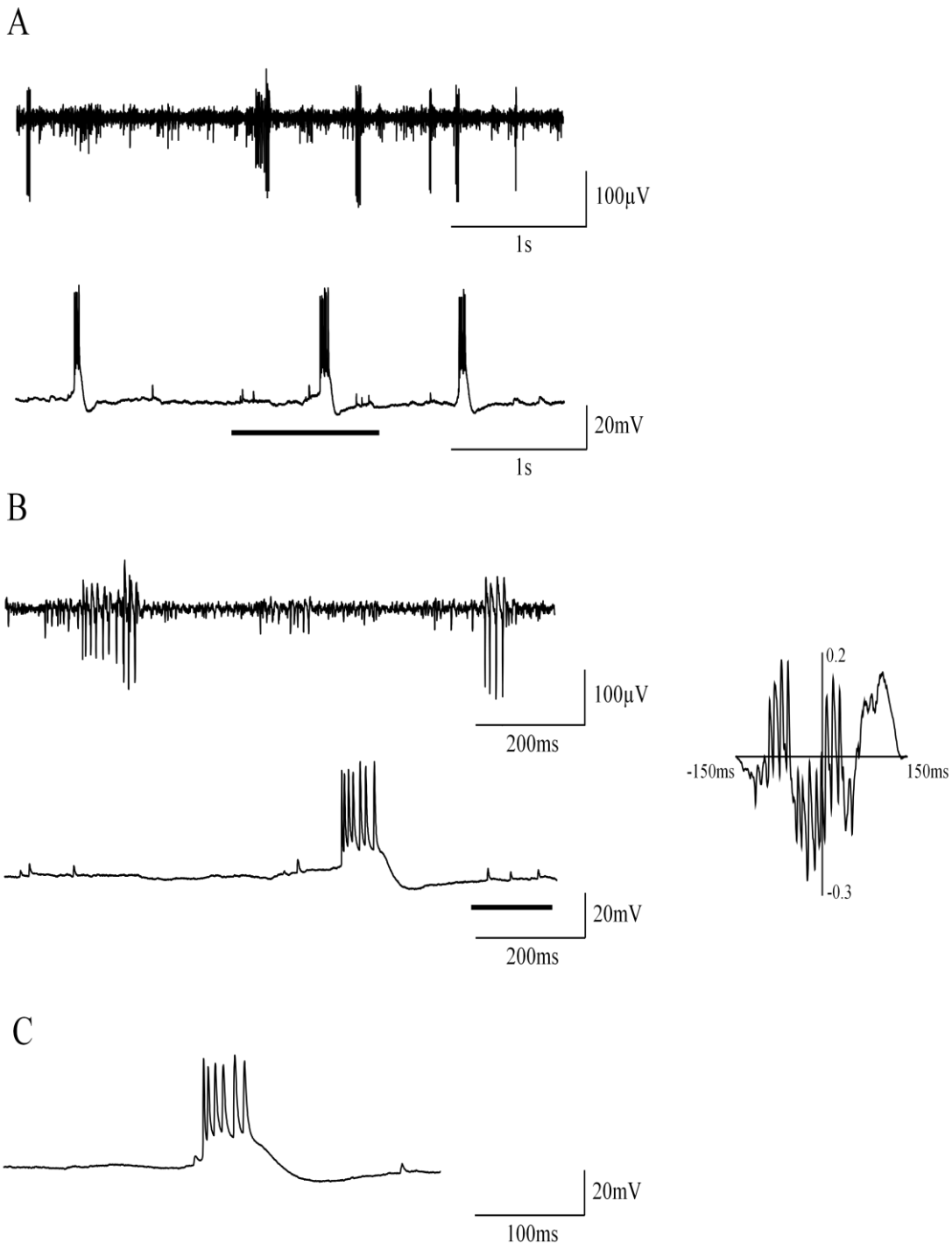

Fig. 4.16. (*A*) Intracellular recording of spikelets in a putative IB cell at resting membrane potential (4s duration trace). I was assisted with intracellular recordings for the data in this figure by M.A. Whittington. (*B)* Magnified portion of the same trace (1s duration) corresponding to the section marked by the black line in the first trace. A cross-correlation between spikelets and field VFO is shown on the right. The black line marks the section of the trace used in the cross-correlation. In each case 60-1000Hz band-pass filtered field traces are shown on the upper section of the panel and concurrent intracellular traces are shown on the lower section of the panel. (*C*) Example of an IB cell burst which appeared to arise from a spikelet.

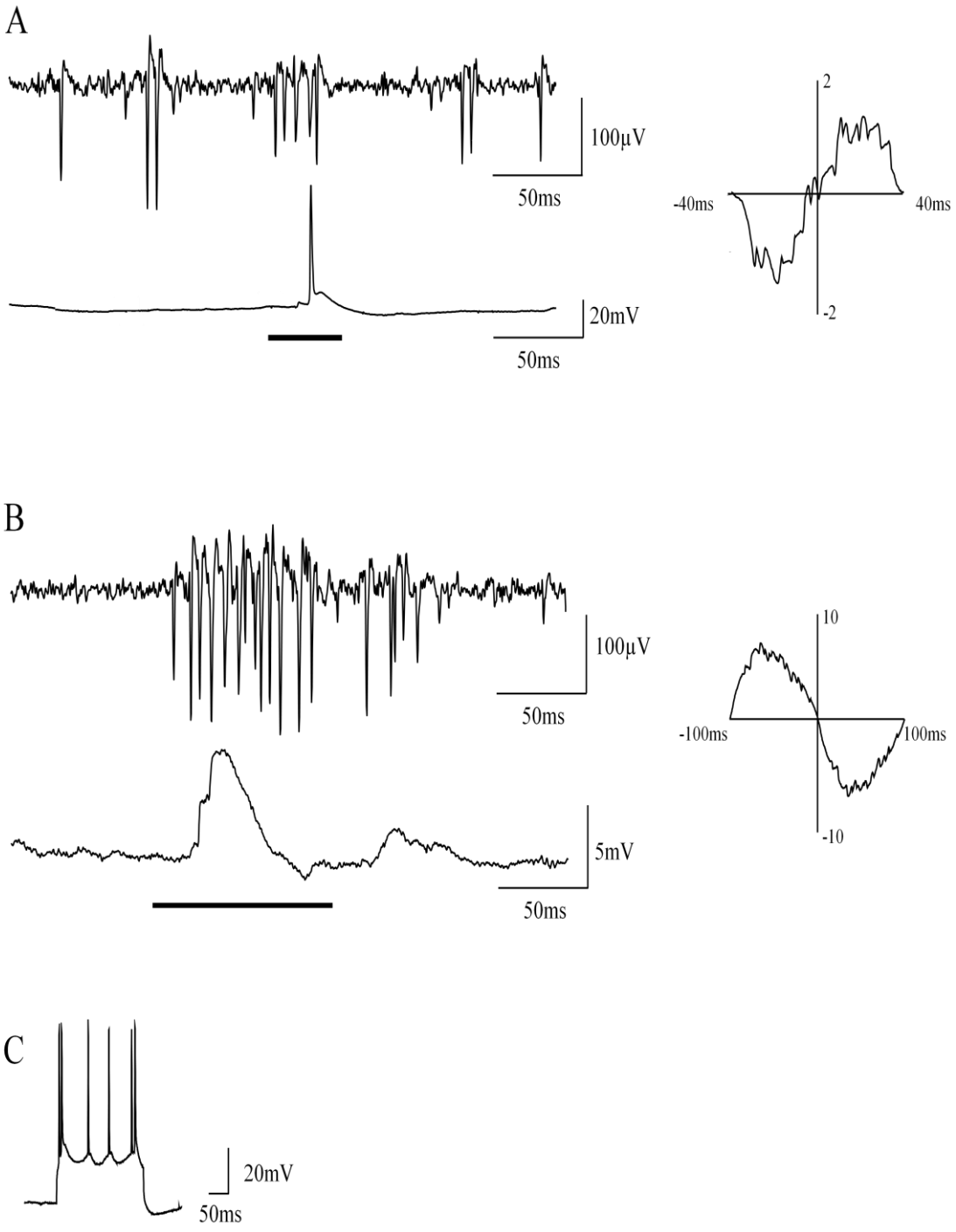

Fig. 4.17. Activity of a fast rhythmic bursting (FRB) pyramidal cell in layer V of 2^0 somatosensory cortex during clozapine-induced VFO: examples of occasional instances where intracellular activity coincides with field VFO. Intracellular recording of an FRB cell firing at resting membrane potential (-63mV) in phase with field VFO (*A*), and EPSPs while the cell was held at -70mV (*B*). In each case 60-1000Hz band-pass filtered field traces (300ms duration) are shown on the upper section of the panel and concurrent intracellular traces are shown on the lower section of the panel. Corresponding cross-correlations of field and intracellular activity are shown on the right. The black line marks the section of the trace used in the cross-correlation. (*C*) Electrophysiological characterisation of the FRB cell.

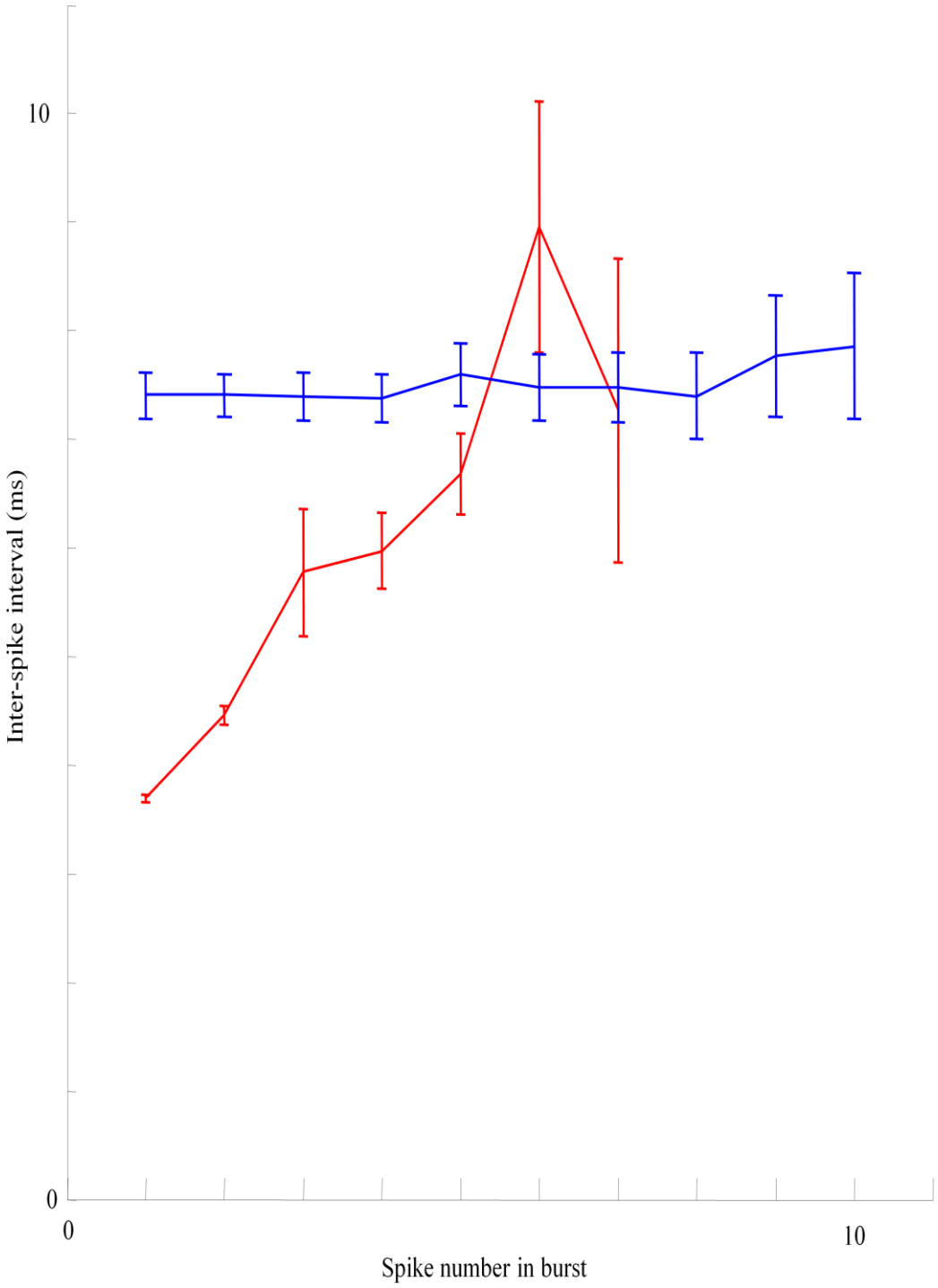

Fig. 4.18. Intervals between consecutive spikes during bursts of spikes in intracellular recordings from IB cells (red, mean ± SEM , n = 220 bursts in 3 cells) as compared to intervals between consecutive troughs in concurrent recordings of bursts of field VFO (blue, mean ± SEM , n = 887 bursts in 3 slices). The inter-spike interval increased during IB cell bursts. However, the interval between troughs was relatively stable during events in field VFO.

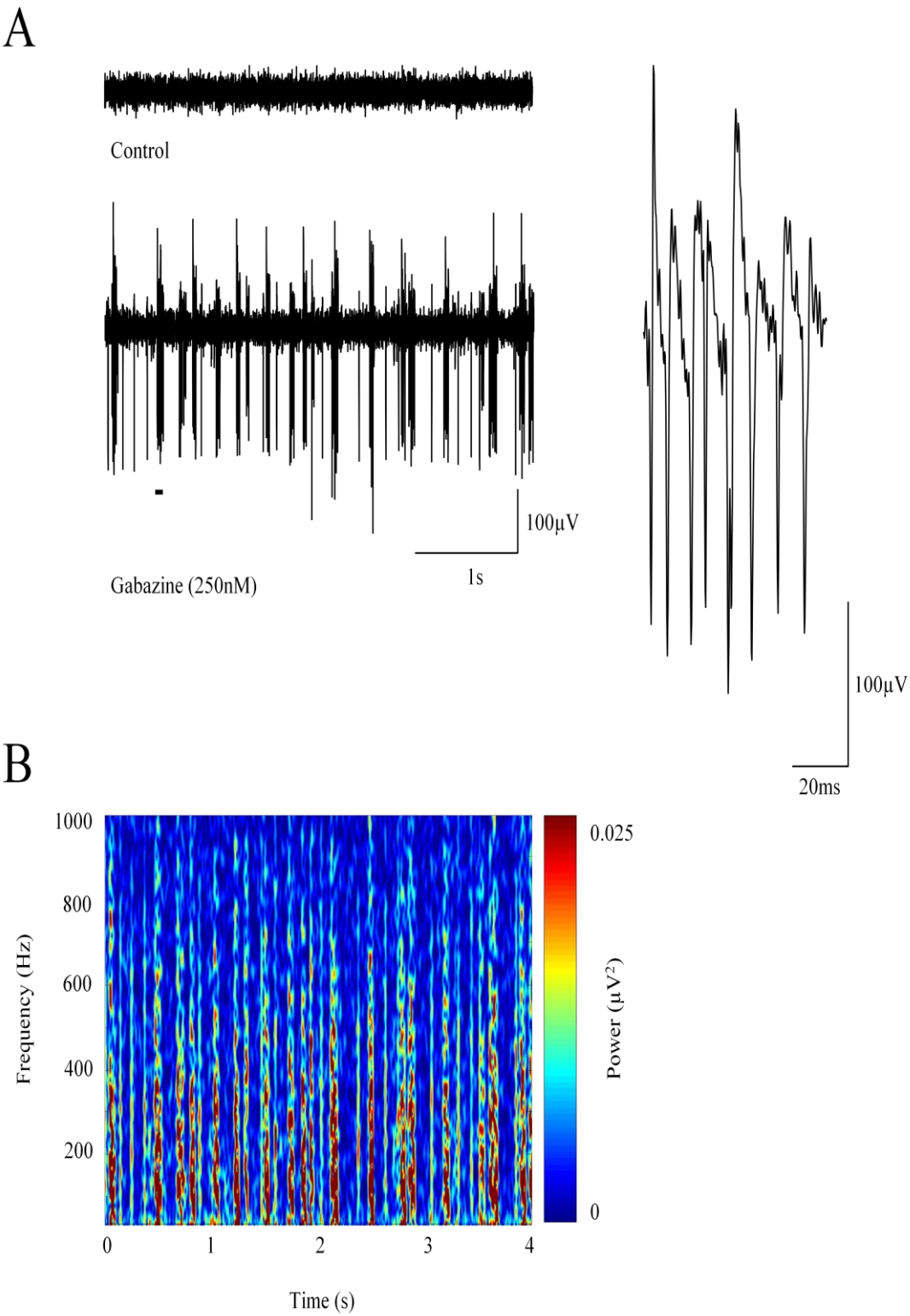

Fig. 4.19. VFO in layer V of rat 2º somatosensory cortex *in vitro* following bath application of gabazine (250nM). (*A*) 60-1000Hz band-pass filtered field traces (4s duration) for control (upper left) and gabazine (lower left) conditions. A portion of the trace (65ms) corresponding to the black line is shown at higher resolution on the right. (*B)* Spectrogram illustrating high frequency (60-1000Hz) oscillatory activity for the same recording.

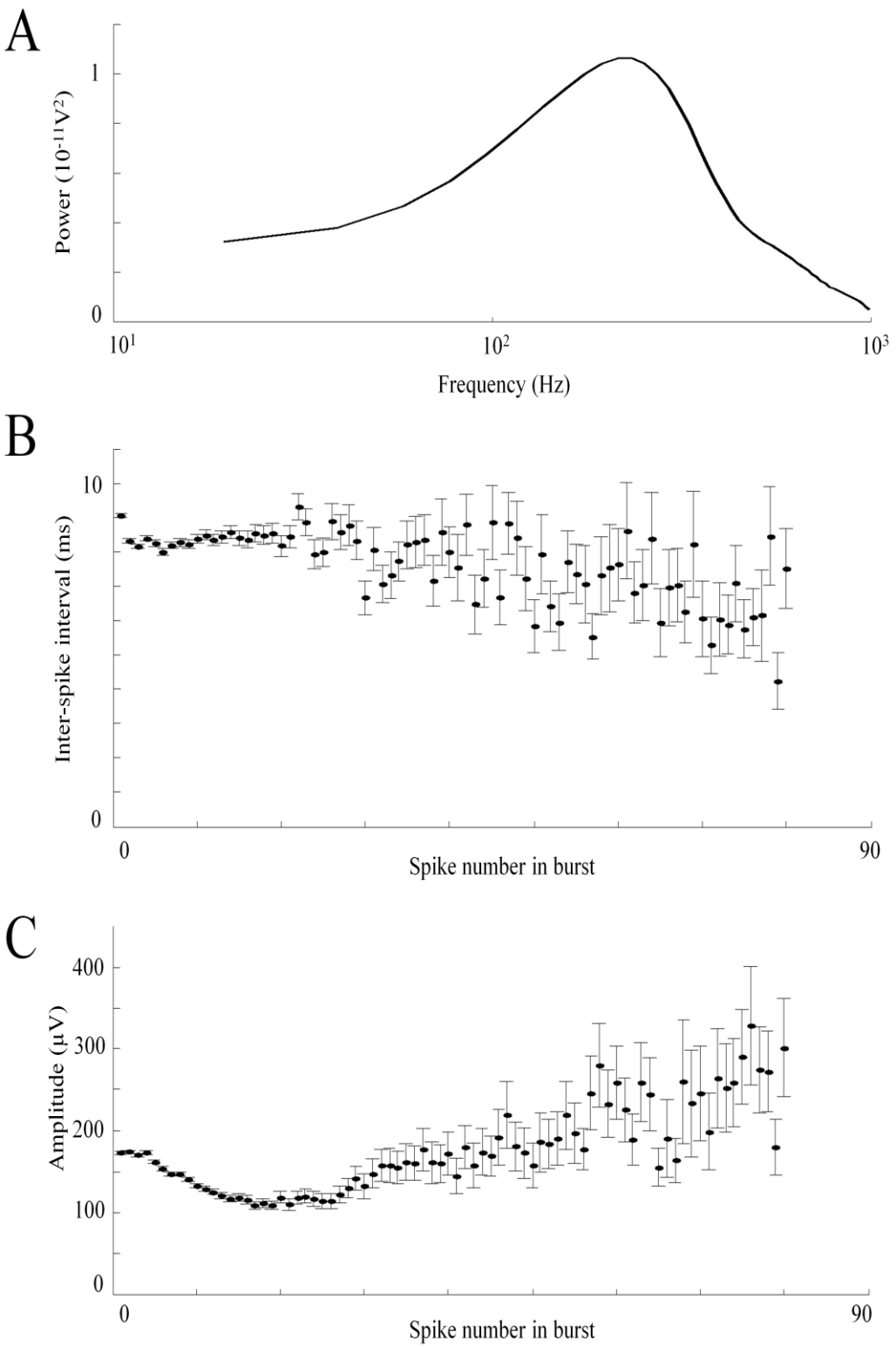

Fig. 4.20. Basic properties of gabazine-induced VFO in layer V of 2º somatosensory cortex (n = 11 slices). (*A*) VFO band pooled power spectra. (*B*) Intervals between consecutive population spikes during bursts of VFO (mean ± SEM). (*C*) Peak-to-peak amplitudes of population spikes during bursts of VFO (mean ± SEM).

Parameter	Mean ± SEM / Median (Q1 → Q3)
VFO band area power ($10^{-11}V^2$)	2.30 (1.13 → 30.90)
VFO band peak power ($10^{-12}V^2$)	1.18 (0.51 → 15.35)
VFO band peak frequency (Hz)	226 ± 13
Burst frequency (Hz)	3.74 ± 0.59
Inter-burst interval (s)	0.30 (0.27 → 2.49)
Number of spikes per burst	9.09 (6.13 → 10.36)
Spike amplitude (μV)	200 ± 51
Proportion of time during the trace that VFO were present (%)	38.2 ± 8.2
Line length (mV/s)	28.3 (20.5 → 103.0)

Table 4.3. Quantitative measures of gabazine-induced VFO in layer V of 2º somatosensory cortex (n = 11 slices). Parametric data are expressed as mean ± SEM. Non-parametric data are expressed in terms of the median and interquartile range (Q1 → Q3).

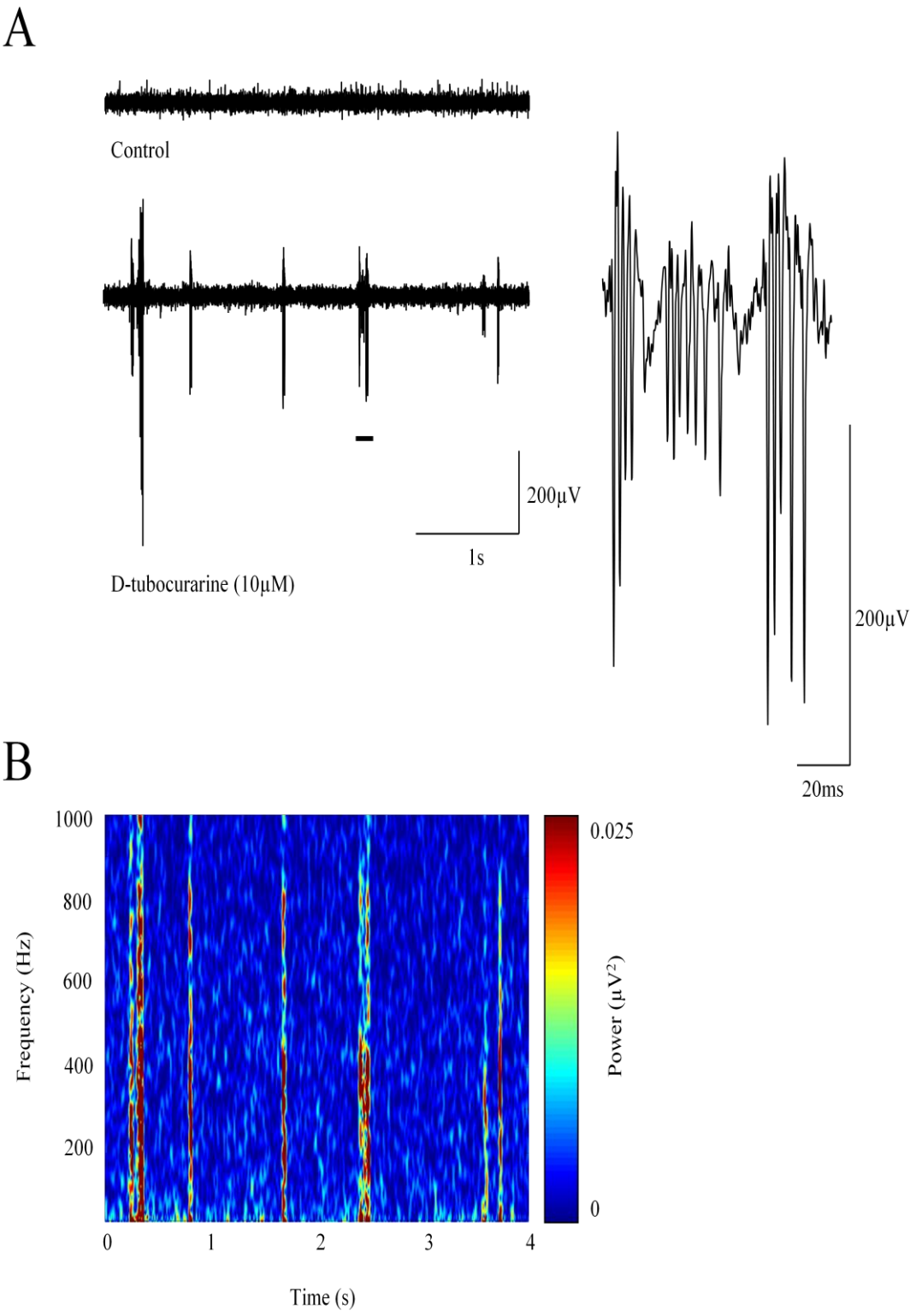

Fig. 4.21. VFO in layer V of rat 2º somatosensory cortex *in vitro* following bath application of d-tubocurarine (10µM). (*A*) 60-1000Hz band-pass filtered field traces (4s duration) for control (upper left) and d-tubocurarine (lower left) conditions. A portion of the trace (96ms) corresponding to the black line is shown at higher resolution on the right. (*B)* Spectrogram illustrating high frequency (60-1000Hz) oscillatory activity for the same recording.

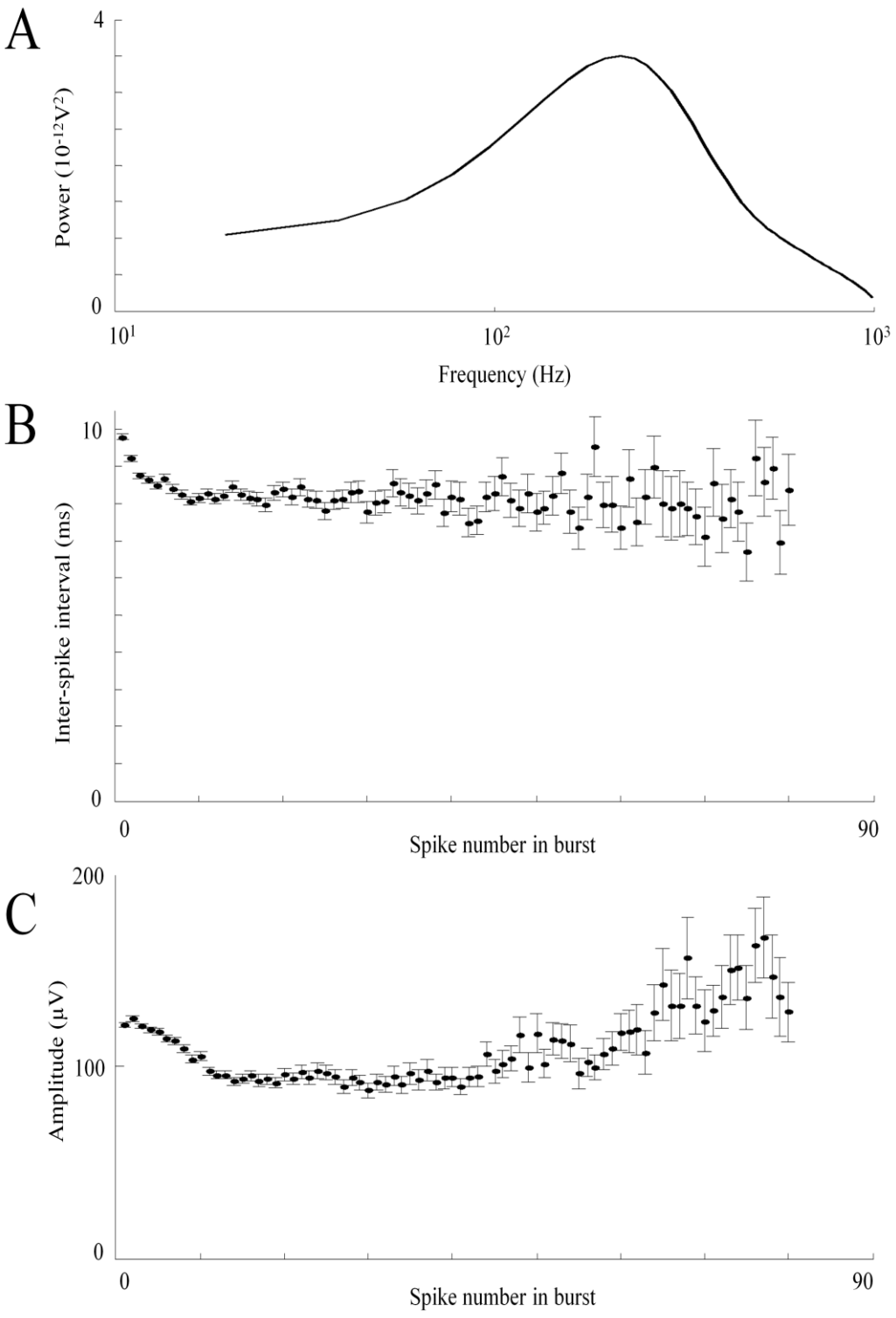

Fig. 4.22. Basic properties of d-tubocurarine-induced VFO in layer V of 2º somatosensory cortex (n = 12 slices). (*A*) VFO band pooled power spectra. (*B)* Intervals between consecutive population spikes during bursts of VFO (mean ± SEM). (*C)* Peak-to-peak amplitudes of population spikes during bursts of VFO (mean ± SEM).

Parameter	Mean ± SEM / Median (Q1 → Q3)
VFO band area power ($10^{-11}V^2$)	2.43 (0.93 → 10.20)
VFO band peak power ($10^{-12}V^2$)	1.22 (0.39 → 5.82)
VFO band peak frequency (Hz)	205 (195 → 234)
Burst frequency (Hz)	3.35 ± 0.52
Inter-burst interval (s)	0.38 (0.31 → 0.72)
Number of spikes per burst	8.15 (5.54 → 13.23)
Spike amplitude (μV)	138 ± 30
Proportion of time during the trace that VFO were present (%)	33.1 ± 7.8
Line length (mV/s)	38.6 ± 7.8

Table 4.4. Quantitative measures of d-tubocurarine-induced VFO in layer V of 2º somatosensory cortex (n = 12 slices). Parametric data are expressed as mean ± SEM. Non-parametric data are expressed in terms of the median and interquartile range (Q1 → Q3).

4.4 Discussion

Currently, clozapine-related abnormal EEG activity is known to include slowing of activity, abnormal theta, abnormal delta, intermittent sharp transients, spike discharges and spike-wave paroxysms (e.g. Malow et al., 1994;Welch et al., 1994;Haring et al., 1994;Denney and Stevens, 1995;Freudenreich et al., 1997;Centorrino et al., 2002). The presence of clozapine-induced VFO in wide band recordings *in vitro* in this thesis furthers the understanding of the effect of clozapine on brain rhythms. Such high frequency activity would not be revealed in scalp EEG recordings in the clinic in the previous chapter as a result of the filter settings (0.5 – 70 Hz), which are typical for clinical EEG. Furthermore, it would not possible to perform scalp electrode EEG recordings of such VFO as it would be impossible to distinguish them from the contaminating effect of motor unit discharges.

Further to the clinical EEG finding in the previous chapter that transient clozapine-related epileptiform activity originated primarily in parietal cortex, the presence of VFO in the isolated microcircuitry of the *in vitro* slice preparation in the functionally equivalent region of brain in the rat, 2º somatosensory cortex, is in line with the particular sensitivity of this region of cortex in the generation of clozapine-related hyperexcitability. This may be at least partially due to the prominence of gap-junctionally connected IB cells in layer V of this region. This particular local circuit has been shown to generate high frequency bursts previously (see introduction to this chapter), a property not shared by adjacent primary sensory areas (see Roopun et al., 2010a). Indeed, intracellular studies here showed the closest correlations between IB cell intracellular activity and the field VFO.

Furthermore, the presence of clozapine-induced VFO, generated *de novo* in normal brain tissue, in this chapter supports the idea that clozapine-related hyperexcitability is a direct effect of the drug rather than a consequence of compensation for abnormal activity in patients with psychiatric illness.

Clozapine-induced VFO may represent an early biomarker of clozapine-related hyperexcitability, possibly present before more severe epileptiform activity. As such, it is possible that technological developments which would permit detection of such high frequency clozapine-related activity non-invasively in the clinic (e.g. with MEG rather than EEG recordings) may be useful in the early identification of individuals at risk of more severe clozapine-related EEG abnormalities.

The apparent concentration-dependence of clozapine-induced VFO in this thesis is consistent with the finding that plasma clozapine concentrations are correlated with EEG abnormalities in a clinical study (Haring et al., 1994).

The spatial extent of coherent clozapine-induced VFO activity in this thesis was restricted to ~500µm, which is greater than the spatial extent of coherent VFO associated with spontaneous VFO in the hippocampus *in vitro* (Draguhn et al., 1998), but smaller than the region of coherence *in vivo*, ~5mm (Chrobak and Buzsaki, 1996). The spatial confinement of VFO to relatively small patches in this thesis is consistent with the finding that pathological VFO can be restricted to volumes of approximately $1mm^3$ of tissue in an animal model of epilepsy (Bragin et al., 2002a).

4.4.1 Effectiveness of haloperidol and olanzapine in inducing VFO

The finding that, similar to clozapine, olanzapine induced prominent VFO, is in line with EEG alterations associated with olanzapine in the literature (Centorrino et al., 2002;Amann et al., 2003;Degner et al., 2011). Furthermore, this, together with the low extent to which haloperidol induced VFO, is consistent with the relative risk of EEG abnormalities associated with these drugs in the clinic (Centorrino et al., 2002). Receptor targets that clozapine shares with olanzapine but not haloperidol may thus be important in mediating the induction of VFO by these antipsychotics. For example, clozapine, but not haloperidol, may enhance NMDA receptor-mediated transmission (Arvanov et al., 1997;Arvanov and Wang, 1999). Similarly, olanzapine may also facilitate NMDA receptor-mediated transmission (Jardemark et al., 2001). Clozapine may suppress $GABA_A$ receptor-mediated activity (Michel and Trudeau, 2000), but there is no evidence that haloperidol shares this property. In contrast, both clozapine and haloperidol have been reported to inhibit nicotinic neuronal receptors (Grinevich et al., 2009).

The relative absence of VFO associated with haloperidol compared to clozapine is also consistent with the lower incidence of paroxysmal activity associated with haloperidol versus clozapine (Koukkou et al., 1979), and the lower incidence of seizures associated with classical antipsychotics versus that of clozapine (Lindstrom, 1988;Naber et al., 1989;Haller and Binder, 1990).

4.4.2 Mechanisms underlying clozapine-induced VFO

Given the general finding of weak correlations between intracellular activity and field VFO, and the very low extent of intracellular activity precisely phase-locked to field VFO, the presence of relatively strong correlations between IB cell spikelets and field VFO suggests the involvement of axonal hyperexcitability in this cell type in the mechanism underlying clozapine-induced VFO.

The presence of spikelets in neuronal subtypes which contribute to the generation of the rhythm may also be a characteristic feature of gap-junction-mediated VFO (Draguhn et al., 1998;Schmitz et al., 2001). An action potential in a pre-junctional neuron can generate a response which is either above or below the threshold required to generate an action potential in the post-junctional neuron, depending on the effectiveness of the coupling at the gap junction. It is thought that spikelets might occur following subthreshold potential changes in postjunctional neurons. Thus, in addition to implicating axonal hyperexcitability in the mechanism, the presence of IB cell spikelets raises the possibility that activity is spread through the axonal plexus via electrotonic coupling at gap junctions. This possibility will be further considered in relation to the pharmacology of clozapine-induced oscillatory activity in chapter 6.

It is also possible that pathological desynchronisation of activity, similar to that involved in the CA3 region of the hippocampus in a lithium-pilocarpine animal model of epilepsy (Foffani et al., 2007), may also have a role in the mechanism underlying clozapine-induced VFO. The general finding of weak correlations between intracellular activity and field VFO, and the very low extent of intracellular activity precisely phase-locked to field VFO appears consistent with such a mechanism. However, in this thesis the substrate for VFO generation was a normal, quiescent slice. Thus there was no existing activity to 'desynchronise' in this reduced preparation. Thus the ability to generate VFO *de novo*, strongly suggests that local desynchronisation of on-going activity may not play a role in this aspect of clozapine's effects.

A role for disinhibition in the mechanism underlying clozapine-induced VFO is supported by the finding that the $GABA_A$ receptor antagonist gabazine induced VFO in layer V of 2º somatosensory cortex. The finding that d-TC also induced VFO raises the possibility that inhibition of neuronal nicotinic receptors may also be important in clozapine-induced VFO. As d-TC inhibits GABA function (Lebeda et al., 1982), it is possible that the induction of VFO by d-TC in this thesis may also be mediated via

$GABA_A$ receptors. Furthermore, the correlation between the emergence of fast ripples and the extent of neuronal loss in epileptic rats (Foffani et al., 2007) raises the possibility that the neurotoxic effect of d-TC (Dasheiff, 1985) may be relevant to its mechanism of action. As stated in the introduction to this section, clozapine has effects on both these receptor systems, whereas there is no evidence for haloperidol, at least acutely, affecting GABAergic systems directly.

The higher frequency nature of clozapine-induced VFO in 2º somatosensory cortex compared to that in CA2 raises the possibility that the mechanisms underlying cortical VFO may be different from those in CA2. There is no evidence for IB cells in this hippocampal region, but gap junctions between neurons are prominent (Mercer et al., 2007).

4.4.3 Possible physiological role of clozapine-induced VFO

In addition to their involvement in epileptic seizures (e.g. Fisher et al., 1992), VFO are associated *in vivo* with memory consolidation (Wilson and McNaughton, 1994) and sensory perception (Jones and Barth, 1999;Ikeda et al., 2002;Curio, 2000;Curio et al., 1994;Edwards et al., 2005). Thus, in addition to aiding the understanding of the mechanisms by which EEG abnormalities and seizures occur as a side effect of clozapine, it seems possible to speculate that to a certain extent the excitability associated with clozapine-induced VFO might also be relevant to the mechanisms by which clozapine exerts its therapeutic effect. Given the well-established and widespread memory deficits that occur in schizophrenia (e.g.Heinrichs and Zakzanis, 1998), and the proposed role of ripples in memory consolidation (Wilson and McNaughton, 1994), a further speculation is that clozapine might exert its therapeutic effect in part by reducing cognitive deficits via enhanced VFO.

4.4.4 Therapeutic concentration of clozapine in cerebrospinal fluid

In general, in rats and humans, at therapeutic doses, concentrations of antipsychotics in brain are often substantially higher than corresponding plasma concentrations (Cohen et al., 1992;Tsuneizumi et al., 1992;Baldessarini et al., 1993;Squires and Saederup, 1997;Weigmann et al., 1999;Kornhuber et al., 1999). This presumably occurs as a result of high penetration of the blood-brain barrier, lipophilicity, and high affinity for cerebral compartments such as lipids and membranes.

The clozapine concentration used in this thesis (10-20µM) was similar to that in other studies (Michel and Trudeau, 2000;Gemperle et al., 2003;Ohno-Shosaku et al., 2011). However, the possibility cannot be excluded that this clozapine concentration may be slightly higher than the therapeutic concentration in cerebrospinal fluid. The concentration of 20µM clozapine was necessary to regularly reproduce VFO on a day-to-day basis. Michel and Trudeau (2000) estimate that the therapeutic brain concentration of clozapine may reach 8-27µM. Clozapine concentrations used in this thesis (10-20µM) were within this range. The estimate is based on: (a) therapeutic plasma clozapine concentrations of 200-450ng/ml (Olesen, 1998); and (b) the observation that in rodents the concentration of clozapine (as measured with sophisticated chromatography techniques) accumulates in brain to a level 16-24 times greater than that in plasma (Baldessarini et al., 1993;Weigmann et al., 1999). However, they note that the cerebrospinal fluid clozapine concentration may be lower than that in the brain as a whole. A further complicating factor is that clozapine may also accumulate in slice preparations *in vitro* (Gemperle et al., 2003).

4.4.5 Future work

Given the possible role of interneurons in the mechanism underlying hippocampal VFO *in vivo* (Buzsaki et al., 1992;Ylinen et al., 1995a;Klausberger et al., 2003;Klausberger et al., 2004;Klausberger et al., 2005) it would be interesting to examine the role of interneurons in clozapine-induced VFO in cortex *in vitro*.

Furthermore, combining biocytin fills with intracellular electrophysiology would be useful in morphological characterisation of cells and investigation of dye-coupling. In addition to examining the extent of gap-junctional coupling, dye-coupling experiments may be helpful in determining the neuronal compartment(s) in which any coupling occurs.

Given the possible differences between cell types and microcircuitry in rat compared to human cortex, it would be interesting to investigate mechanisms underlying clozapine-induced VFO in human tissue *in vitro*.

Injection of rats with clozapine may represent a more realistic model of the oral administration of clozapine in the clinic compared to the acute application of clozapine to slices used in experiments in this thesis.

In light of the possible role of disinhibition in the mechanism underlying clozapine-induced VFO in this thesis, it is interesting that clozapine may suppress $GABA_A$ receptor-mediated inhibition in the ventral tegmental area (Michel and Trudeau, 2000) and hippocampus (Ohno-Shosaku et al., 2011). To determine whether or not clozapine attenuates IPSPs in 2° somatosensory cortex under experimental conditions used in this thesis, stimulation experiments could be performed to compare control intracellular IPSPs with those following application of clozapine.

4.4.6 Summary

In summary, *in vitro* clozapine induced patches of VFO in CA2, and, importantly, in 2° somatosensory cortex, where they were of a higher frequency and maximal in layer V. Axonal hyperexcitability, possibly spread through the axonal plexus, may underlie cortical clozapine-induced VFO, and a role for inhibition of $GABA_A$ receptors and/or inhibition of neuronal nicotinic receptors may also be implicated in the mechanism. The atypical antipsychotic olanzapine, but not the classical antipsychotic haloperidol, also induced prominent VFO. The different dynamics of inter-spike intervals in bursts of IB cells compared to those in bursts of field VFO suggests that clozapine-induced VFO does not result merely from synchronous bursts of a few IB cells.

Following characterisation of clozapine-induced VFO *in vitro* in this chapter, to further investigate clozapine-related epileptiform activity the next step was to investigate clozapine-induced paroxysmal discharges *in vitro*.

Chapter 5

Results – Clozapine-induced paroxysmal discharges *in vitro*

5.1 Introduction

Following the demonstration and basic characterisation of transient seizure-like events in a psychiatric patient treated with clozapine in chapter 3, and the characterisation of clozapine-induced VFO in rat brain slices of 2° somatosensory *in vitro* in chapter 4, this chapter considers clozapine-induced full paroxysmal events themselves in this region of cortex *in vitro*.

Aims

The aims of this chapter are as follows:

- To establish whether clozapine can generate full paroxysmal events, resembling those seen in patient EEG data, in slices of rat 2° somatosensory cortex.
- To map the distribution and spatial extent of clozapine-induced paroxysmal events in 2° somatosensory cortex in terms of their laminar distribution in the cortical column and longitudinal distribution throughout the regions of interest to attempt to focus-in on the cell types and local circuits involved for further study.
- Similarly, to examine the spatiotemporal progression of paroxysmal events in terms of LFPs, spike rates, spike synchrony, and spike-spike correlations, and to examine spike-field correlations.
- To investigate the activity of specific types of neurons in relation to clozapine-induced paroxysmal discharges and to attempt to determine their cellular basis.
- To compare paroxysmal events induced by gabazine with those induced by clozapine to investigate the possible role of partial disinhibition in relation to clozapine-induced paroxysmal events.

5.1.1 Clozapine-induced paroxysmal events *in vitro*

Clozapine-related abnormal EEG activity is known to include slowing of background activity, abnormal theta, abnormal delta, intermittent sharp transients and spike-wave paroxysms (Malow et al., 1994;Welch et al., 1994;Haring et al., 1994;Denney and Stevens, 1995;Freudenreich et al., 1997). Possible mechanisms underlying clozapine-induced epileptiform activity include VFO (chapter 4), NMDA receptor agonism (see section 1.4.2.2-1.4.2.3), and suppression of $GABA_A$ receptors (see below and section 1.4.2.1). Here, it was decided to investigate clozapine-induced paroxysmal events in rat brain slices to take advantage of the benefits of the *in vitro* approach in relation to the

study of cellular and molecular mechanisms (described in section 4.1). The pyramidal neuronal cell types investigated in layer V of 2º somatosensory cortex in this chapter are introduced in section 4.1.3.

5.1.2 Partial inhibition of $GABA_A$ receptors and epileptiform activity

In light of the suppression of $GABA_A$ receptor-mediated inhibition by clozapine (Michel and Trudeau, 2000;Ohno-Shosaku et al., 2011), and the finding in this thesis that, similar to clozapine, the $GABA_A$ receptor antagonist gabazine induced VFO in layer V of 2º somatosensory cortex (section 4.3.8), investigation of the possible role of $GABA_A$ receptor inhibition in relation to clozapine-induced paroxysmal events is warranted.

The relevance of GABA to seizures was initially recognised when children fed with a formula which contained insufficient vitamin B6 (pyridoxine) developed seizures (Molony and Parmelee, 1954;Coursin, 1954). As the coenzyme for glutamic acid decarboxylase (GAD), the enzyme responsible for the synthesis of GABA, pyridoxine is required for normal GABAergic neurotransmission.

Further evidence of the importance of GABA in seizures was provided when it was discovered that GABA could prevent seizures, and, conversely, drugs which hampered GABA neurotransmission could trigger convulsions (Hawkins and Sarett, 1957;Benassi and Bertolotti, 1962). Furthermore, more recently, genetic studies have identified mutations in $GABA_A$ receptors in individuals with childhood absence and febrile seizures (Wallace et al., 2001;Kananura et al., 2002).

Early studies showed that blocking $GABA_A$ receptor-mediated inhibition induces epileptiform activity in animals *in vitro* (Schwartzkroin and Prince, 1978;Schwartzkroin and Prince, 1980) and *in vivo* (Matsumoto and Marsan, 1964;Prince, 1968;Dichter and Spencer, 1969;Ayala et al., 1973). The feline generalised penicillin epilepsy model, in which penicillin, a weak $GABA_A$ antagonist, induces generalised spike-wave discharges, became well-established in epilepsy research (e.g. Avoli and Gloor, 1982b;Avoli and Gloor, 1982a).

Indeed, application of various $GABA_A$ receptor antagonists, including bicuculline, picrotoxin or penicillin to isolated hippocampal or neocortical brain slice preparations *in vitro* has been a widely used approach in epilepsy research. Such approaches demonstrated that $GABA_A$ receptor function is important in limiting neuronal network

synchrony and controlling transmission in polysynaptic pathways (Miles and Wong, 1983;Miles and Wong, 1987).

In line with the idea that failure of $GABA_A$ receptor-mediated inhibition was a requirement for generation of epileptiform discharges, reductions in the number of GABAergic symmetric synapses onto pyramidal cells were observed in monkeys with cortical focal epilepsy (Ribak et al., 1982).

However, the classical view that deficient GABA receptor signalling is a necessary requirement for the occurrence of seizures has been questioned by findings that GABAergic inhibitory mechanisms can be preserved in animal models of epilepsy (Davenport et al., 1990;Esclapez et al., 1997;Prince and Jacobs, 1998;Cossart et al., 2001;Cossart et al., 2005) and in epileptic human tissue (Isokawa-Akesson et al., 1989;Babb et al., 1989;Avoli and Olivier, 1989). Certain subtypes of interneurons are preserved in animal models of epilepsy and human epileptic tissue (Babb et al., 1989;Davenport et al., 1990;Esclapez et al., 1997) whereas other subtypes may be reduced in limbic structures (de Guzman et al., 2006;de Guzman et al., 2008).

Indeed, more complex roles for GABAergic neurotransmission in epilepsy are emerging with the proposal that GABAergic neurotransmission may contribute to epileptiform synchrony (Avoli et al., 1993;Avoli et al., 1996a;Avoli et al., 1996b;Avoli et al., 1996c;de Curtis and Gnatkovsky, 2009). Another example of the complex relationship between $GABA_A$ receptors and epilepsy is demonstrated by the finding that inhibition may actually be strengthened in the dentate gyrus in the kindling model of temporal lobe epilepsy (Otis et al., 1994).

Nonetheless, a role for the partial inhibition of $GABA_A$ receptors continues to be highlighted in the generation of epileptiform activity. While full blockade of $GABA_A$ receptors *in vitro* induces interictal activity but not prolonged ictal discharges, partial reduction of GABAergic inhibition can generate full seizure-like activity. For example, partial disinhibition conferred by transient arterial application of the $GABA_A$ receptor antagonist bicuculline to the guinea pig isolated brain preparation induces seizures in the entorhinal-hippocampal region (Gnatkovsky et al., 2008). In line with this, a partial reduction in fast $GABA_A$ receptor-mediated inhibition has been suggested to trigger seizures in computer models of temporal lobe seizures (Wendling et al., 2002;Labyt et al., 2006).

In isolated preparations, $GABA_A$ receptor antagonism in most cases induces short-lasting interictal spikes or prolonged afterdischarges similar to those seen after high frequency stimulation. Robust and frequent seizure-like events themselves typically require a brain preparation including interconnected regions, such as the hippocampal-parahippocampal slice preparation (Walther et al., 1986;Jones and Lambert, 1990a;Jones and Lambert, 1990b;Dreier and Heinemann, 1991).

Prolonged epileptiform discharges can also be induced by other experimental manipulations that alter $GABA_A$ inhibition, such as application of the K^+ channel blocker 4-aminopyridine (4AP), increased concentrations of K^+, use of Mg^{2+} free artificial cerebrospinal fluid, or high frequency electrical stimulation (Jefferys, 1990;Avoli et al., 1990;Avoli et al., 2002;de Curtis and Gnatkovsky, 2009;Fujiwara-Tsukamoto et al., 2004;Fujiwara-Tsukamoto et al., 2006;Fujiwara-Tsukamoto et al., 2007).

In terms of laminar effect, it is interesting that during interictal-like discharges induced in rat entorhinal cortex by blockade of $GABA_A$ receptors, activity in layer IV/V preceded that in layer II (Jones and Lambert, 1990a). Furthermore, following application of 4AP and glutamatergic antagonists to entorhinal cortex, the largest increases in extracellular K^+ occur in deep layers (Avoli et al., 1996a), where ictal activity may be initiated (Jones and Lambert, 1990a;Avoli et al., 1996a). Similarly, there was a reduction of inhibition in layer V of entorhinal cortex in brain slices from rats treated with pilocarpine (de Guzman et al., 2008).

5.2 Methods

5.2.1 Slice preparation and maintenance

Experiments in this chapter made use of rat brain slice preparations *in vitro*. Slices were 450μm thick sections of 2° somatosensory cortex cut in the horizontal plane from adult male Wistar rats (150-250g). Slices were prepared according to section 2.1-2.3 and the maintenance of slices is described in section 2.4. Extracellular recording techniques are described in section 2.6.1, and data acquisition is described in section 2.7-2.8. Paroxysmal events were induced by either clozapine or gabazine according to the experiment.

5.2.2 Intracellular recording methods

Prior to any intracellular recordings, regions of cortex generating paroxysmal events were identified using an extracellular field electrode. The field electrode remained in the slice next to the intracellular electrode for the duration of the experiment to compare the intracellular activity of individual cells to the LFP. Sharp borosilicate glass microelectrodes filled with potassium acetate (2M, 80 – 150 MΩ) were used to impale cells for intracellular recordings in accordance with the details in section 2.6.3. Electrophysiological characterisation of neurons was achieved using a 0.3nA depolarising step with a duration of 300ms, as described previously (McCormick et al., 1985). EPSPs were revealed by injection of tonic, negative DC current until the membrane potential of the cell was hyperpolarised to -70mV to mask concurrent IPSPs, and conversely, IPSPs themselves were revealed, when successful, by injection of tonic, positive current until the membrane potential of the cell was depolarised away from the chloride reversal potential to -30mV.

5.2.3 Multi-electrode array recording techniques

Following confirmation of the presence of paroxysmal events in the slice using an extracellular field electrode, multichannel recordings were performed using Utah electrode grids as described in section 2.7.2. Data were collected using Central software (Blackrock Microsystems inc. USA) as described in section 2.7.2 and subsequently exported to Matlab software for offline analysis.

5.2.4 Data analysis

Paroxysmal discharges were quantified in terms of their amplitude, frequency and width. In general these discharges were defined as distinct from VFO as they had large-amplitude, lower frequency components. For the multi-electrode array data, spike synchrony (time distance to the nearest spike between pairs of units), spike-spike correlations, and spike-field correlations were quantified in Neuroexplorer and exported to MATLAB for thresholding and spatial mapping with reference to electrode positions in the Utah grid provided by the supplier.

For spike-spike correlations, cross-correlations were performed between each pair of units and connectivity was quantified by measuring the point on the resulting cross-correlogram where the central peak crossed the Y-axis. Similarly, for spike-field correlations, cross-correlations were performed between unit spike rate histograms and

LFPs for each unit and LFP combination, and the correlation was quantified by measuring the point on the resulting cross-correlogram where the central peak crossed the Y-axis.

For colour maps, which were used to illustrate the progression of LFPs and spike rates, data were exported to MATLAB, where they were mapped with reference to electrode positions in the Utah grid provided by the supplier, interpolated and illustrated in two dimensional 'surf' plots with 'jet' colour maps.

5.3 Results

5.3.1 Clozapine induced transient paroxysmal discharges in layer V of rat 2º somatosensory cortex *in vitro*

In addition to VFO, clozapine (10-20µM) sometimes (33% incidence, 11/33 slices) also induced spontaneous, regularly occurring, transient paroxysmal discharges in layer V of rat 2º somatosensory cortex *in vitro*, typically present as high amplitude negative-going events with lower frequency components than VFO alone (Fig. 5.1). The mean amplitude of clozapine-induced paroxysmal discharges was 193.9 ± 10.8 µV, the mean frequency of such events was 3.24 ± 0.88 events per minute (n = 112 events in 11 slices), and their mean width was 401 ± 8 ms. VFO were typically present, before, during and after paroxysmal events in layer V (Fig. 5.1A). For comparison, the median amplitude of clozapine-induced VFO was 113 (70 → 159) µV and their median burst frequency was 3.26 (1.81 → 4.18) Hz (section 4.3.2).

To investigate whether there was any difference in VFO occurring in traces where paroxysmal discharges were present compared to that occurring in traces where paroxysmal discharges were absent, various VFO parameters were quantified and compared in relation to this condition (Table 5.1). No statistically significant differences were found in VFO parameters in relation to the presence (n = 11 slices) or absence (n = 22 slices) of paroxysmal discharges ($p > 0.05$ in each case, Mann-Whitney rank sum test or t-test as appropriate, Table 5.1).

With the same filter settings as used in clinical EEG recordings (0.5 – 70 Hz, see chapter 3), clozapine-induced paroxysmal events in rat brain slices *in vitro* had a remarkably similar appearance to transient epileptiform spikes in EEG recordings from a psychiatric patient treated with clozapine (chapter 3, Fig. 5.1 vs Fig. 3.1).

5.3.2 Intracellular activity of neurons during clozapine-induced paroxysmal discharges

To investigate the activity of neurons during clozapine-induced paroxysmal events, sharp electrode intracellular recordings were taken from cell somata in cells nearby to the field potential in layer V of 2º somatosensory cortex. Of the 35 RS cells from which intracellular recordings were taken, clozapine-induced paroxysmal discharges were present in the corresponding field in 9 cases. These paroxysmal events were also present in the field corresponding to intracellular recordings for 2 putative IB cells.

RS cells fired, sometimes in bursts of spikes, and in other cases in spike singletons, during these paroxysmal events, and the events were clearly associated with large, compound EPSPs and IPSPs in this cell type (Fig. 5.2). In many cases, RS cells were otherwise very quiescent and somatic activity in this cell type was often only observed during the paroxysmal events.

Bursting activity occurred in a putative IB cell during clozapine-induced paroxysmal discharges, and similarly to RS cells, the events were associated with large, compound EPSPs and IPSPs in this cell type (Fig. 5.3).

5.3.3 Spatiotemporal properties of clozapine-induced paroxysmal discharges in 2º somatosensory cortex

Utah multi-electrode array recordings are useful in investigating the spatial distribution of oscillatory activity as they allow for simultaneous acquisition of extracellular data from 96 channels over a 3.64*3.64mm grid. The mean amplitude of clozapine-induced paroxysmal events recorded in each of the Utah array electrodes was illustrated in a colour map which was then superimposed over an image of 2º somatosensory cortex from a rat brain atlas (Fig. 5.4, Paxinos and Watson, 1998). Clozapine-induced paroxysmal events were more widely distributed compared to clozapine-induced VFO (cf. Fig. 4.9), and in this example occurred in a consistent laminar manner longitudinally along layers IV and V, where they were maximal, with layer VI and superficial layers I-III being relatively spared.

5.3.3.1 Spatiotemporal progression of LFPs during clozapine-induced paroxysmal discharges

To further investigate the spatiotemporal properties of clozapine-induced paroxysmal discharges, the spatial progression of LFPs associated with these events was examined at 50ms intervals over a 450ms time series and illustrated in a colour map for each time point. Two examples of the spatial progression of LFPs from different slices are illustrated (Fig. 5.5 and Fig. 5.6). In one example it is revealed that the event started superficially, moved deeper, and then appeared to propagate longitudinally along deeper layers (Fig. 5.5). In the second example, activity appeared first at the edge of the array in deep layers, followed again by a clear longitudinal propagation of activity along deep layers of the slice (Fig. 5.6).

5.3.3.2 Spatiotemporal progression of unit activity during clozapine-induced paroxysmal discharges

Extracellular unit recordings confirmed the intracellular findings of bursts of spikes or single spikes during paroxysmal events, and that in terms of somatic spiking most cells were otherwise very quiescent except during such events. Fig. 5.7 clearly illustrates the close association between bursts of spikes in multiple (n = 82) extracellular units and a concurrent clozapine-induced paroxysmal discharge. The mean spike rate during clozapine-induced paroxysmal discharges was 5.74 ± 0.35 spikes per second (n = 232 units in 4 discharges in 2 slices).

To further investigate the spatiotemporal properties of clozapine-induced paroxysmal discharges, the spatial progression of unit activity associated with these events was examined in 50ms windows at 50ms intervals over a 500ms time series and illustrated in a colour map for each time point. Two examples of the spatial progression of unit spike rates from events in different slices are illustrated (Fig. 5.8 and Fig. 5.9), together with pooled data from 4 discharges in 2 slices (Fig. 5.10).

The first and second examples correspond to the same discharges as those used for the first and second examples in the LFP progression figures (Fig. 5.5 and Fig. 5.6). Similarly, the time windows correspond such that time points for LFP windows are centred on the corresponding unit activity window.

In the first example, unit activity started superficially, and moved deeper with a hint of longitudinal propagation (Fig. 5.8). The spatial progression of unit activity

corresponded well to that of LFPs (Fig. 5.8 vs Fig. 5.5). In the second example, there was a hint of a superficial origin of unit activity, and, similarly to the LFP (Fig. 5.6), a clear longitudinal propagation of unit activity along deeper layers (Fig. 5.9). The pooled data also supported a superficial origin and deep propagation of unit activity (Fig. 5.10).

5.3.3.3 Spatiotemporal progression of unit synchrony during clozapine-induced paroxysmal discharges

To further investigate the spatiotemporal properties of clozapine-induced paroxysmal discharges, the spatial progression of unit synchrony associated with these events was examined in 50ms windows at 50ms intervals over a 500ms time series and illustrated in a synchrony map for each time point. Here synchrony was measured in terms of the time distance to the nearest spike between pairs of units.

Two examples of the spatial progression of unit synchrony from events in different slices are illustrated. The first example is shown with a synchrony threshold of mean plus 3 standard deviations of the synchrony in the most synchronous time window ('high' threshold, Fig. 5.11) and also with a synchrony threshold of mean plus 1 standard deviation of the synchrony in the most synchronous time window ('low' threshold, Fig. 5.12). As the unit activity was relatively sparse in the second example, no thresholding was used in this example (Fig. 5.13). The time windows correspond to those for unit activity in the previous figures. Units between which there was high synchrony often corresponded to those associated with high spike rates in the previous figures.

The high degree of synchrony between superficial units at the start of the event in the first example, which is clearer in the low threshold illustration (Fig. 5.12), was consistent with a superficial origin of the event, and the synchrony between superficial and deep layers as the event continued was consistent with the propagation of the event from superficial to deep layers (Fig. 5.11, 5.12).

In the second example (Fig. 5.13), there was some evidence of synchrony between superficial and deep layers at the start of the event, and clear evidence of longitudinal synchrony along deep layers as the event propagated along these layers.

5.3.3.4 Spatiotemporal progression of spike-spike correlations during clozapine-induced paroxysmal discharges

To further investigate the spatiotemporal properties of clozapine-induced paroxysmal discharges, the spatial progression of spike-spike correlations associated with these events was examined in 200ms overlapping windows at 100ms intervals over a 500ms time series and illustrated in a connectivity map for each time point (Fig. 5.14). Cross-correlations were performed between each pair of units and connectivity was quantified by measuring the point on the resulting cross-correlogram where the central peak crossed the Y-axis.

Connectivity maps for spike-spike correlations resembled to some extent those for synchrony in terms of time distance to the nearest spike in the corresponding example, especially at the start of the time series (Fig. 5.14 vs Fig. 5.12).

The high degree of connectivity between superficial units at the start of the event was consistent with a superficial origin of the event, and the connectivity between superficial and deep layers as the event continued was consistent with the propagation of the event from superficial to deep layers (Fig. 5.14). In the middle of the time series there was a high degree of connectivity between units in superficial and deep layers throughout the slice. There was also some evidence of longitudinal connectivity along deep layers towards the end of the event, consistent with possible propagation along these layers in this example.

Connectivity maps were also generated for a 1s time window to cover entire events in two events from two different slices (Fig. 5.15, 5.16). In the first example, connectivity was evident between units in superficial and deep layers throughout the slice (Fig. 5.15). In the second example (Fig. 5.16), which resembled the corresponding maps for synchrony in terms of time distance to the nearest spike (Fig. 5.13), there was some evidence of connectivity between superficial and deep layers, and clear evidence of longitudinal connectivity along deep layers.

5.3.3.5 Spike-field correlations during clozapine-induced paroxysmal discharges

To further investigate the spatiotemporal properties of clozapine-induced paroxysmal discharges, maps of spike-field correlations were generated for a 1s time window to cover entire events in two example events from two different slices (Fig. 5.17, 5.18). Cross-correlations were performed between unit spike rate histograms and LFPs for

each unit and LFP combination, and synchrony was quantified by measuring the point on the resulting cross-correlogram where the central peak crossed the Y-axis.

In the first example (Fig. 5.17), there was some evidence of longitudinal spike-field correlations along superficial layers, and also of correlations between superficial units and deep LFPs. In the second example (Fig. 5.18), there was some evidence of longitudinal spike-field correlations along middle layers, and also of spike-field correlations between middle and superficial layers, and between middle and deep layers. In particular, there were correlations between units in middle layers and superficial LFPs, and between units in middle layers and deep LFPs (Fig. 5.18).

5.3.4 Gabazine induced transient paroxysmal discharges in layer V of rat 2º somatosensory cortex *in vitro*

In light of the finding in this thesis that, similar to clozapine, the $GABA_A$ receptor antagonist gabazine induced VFO in layer V of 2º somatosensory cortex (section 4.3.8), it was interesting to investigate whether gabazine would also induce transient paroxysmal events similar to those associated with clozapine. Gabazine (250nM) induced spontaneous and regular large, transient paroxysmal discharges in layer V of rat 2º somatosensory cortex *in vitro*, typically present as high amplitude negative-going events (Fig. 5.19). However, paroxysmal events induced by gabazine were larger, and had a different and more regular shape, compared to those induced by clozapine.

The mean amplitude of gabazine-induced paroxysmal discharges was 777 ± 237 µV, the mean frequency of such events was 1.53 ± 0.28 events per minute, and their mean width was 343 ± 77 ms (n = 8 slices). VFO were typically present before and during gabazine-induced paroxysmal events in layer V (Fig. 5.19A).

5.3.5 Spatiotemporal properties of gabazine-induced paroxysmal discharges in 2º somatosensory cortex

Utah multi-electrode array recordings were used to investigate the spatial distribution of gabazine-induced paroxysmal discharges. The mean amplitude of events recorded in each of the Utah array electrodes was illustrated in a colour map which was then superimposed over an image of 2º somatosensory cortex from a rat brain atlas (Fig. 5.20, Paxinos and Watson, 1998). Similar to clozapine-induced paroxysmal events, gabazine-induced paroxysmal events occurred in a laminar manner longitudinally along

layers IV and V, where they were maximal, with layer VI and superficial layers I-III being relatively spared.

5.3.5.1 Spatiotemporal progression of LFPs during gabazine-induced paroxysmal discharges

To further investigate the spatiotemporal properties of gabazine-induced paroxysmal discharges, the spatial progression of LFPs associated with these events was examined at 50ms intervals over a 450ms time series and illustrated in a colour map for each time point. The event spread horizontally along deep layers (Fig. 5.21), and more superficial layers were recruited around the middle of the event (~200-250ms).

5.3.5.2 Spatiotemporal progression of unit activity during gabazine-induced paroxysmal discharges

Similar to clozapine-induced discharges, extracellular unit recordings revealed bursts of spikes or single spikes during gabazine-induced paroxysmal events. Fig. 5.22 clearly illustrates the close association between bursts of spikes in multiple (n = 100) extracellular units and a concurrent gabazine-induced paroxysmal discharge. The mean spike rate during gabazine-induced paroxysmal discharges was 7.91 ± 0.69 spikes per second (n = 376 units in 4 discharges in 4 slices), which was greater than that during clozapine-induced discharges (5.74 ± 0.35 spikes per second, n = 232 units in 4 discharges in 2 slices). Likewise, although spiking activity outside events was again relatively sparse, there was more such activity associated with gabazine compared to clozapine.

To further investigate the spatiotemporal properties of gabazine-induced paroxysmal discharges, the spatial progression of unit activity associated with these events was examined in 50ms windows at 50ms intervals over a 500ms time series and illustrated in a colour map for each time point. An example of the spatial progression of unit spike rates is illustrated (Fig. 5.23), together with pooled data from 4 discharges in 4 slices (Fig. 5.24).

Unit activity spread horizontally along deep layers (Fig. 5.23, 5.24), and more superficial layers were recruited around the middle of the event (~200-250ms). The spatial progression of unit activity corresponded well to that of LFPs (Fig. 5.23 vs Fig. 5.21).

5.3.5.3 Spatiotemporal progression of unit synchrony during gabazine-induced paroxysmal discharges

To further investigate the spatiotemporal properties of gabazine-induced paroxysmal discharges, the spatial progression of unit synchrony associated with these events was examined in 50ms windows at 50ms intervals over a 500ms time series and illustrated in a synchrony map for each time point. Here synchrony was measured in terms of the time distance to the nearest spike between pairs of units.

An example of the spatial progression of unit synchrony in a gabazine-induced paroxysmal discharge is shown with a synchrony threshold of mean plus 3 standard deviations of the synchrony in the most synchronous time window ('high' threshold, Fig. 5.25), and also with a synchrony threshold of mean plus 1 standard deviation of the synchrony in the most synchronous time window ('low' threshold, Fig. 5.26).

The high degree of synchrony between superficial units at the start of the event was consistent with a superficial origin, and the synchrony between superficial and deep layers as the event continued was consistent with the propagation of the event from superficial to deep layers (Fig. 5.25, 5.26). There was also clear evidence of longitudinal synchrony along deep layers as the event propagated along these layers. Units between which there was high synchrony often corresponded to those associated with high spike rates.

5.3.5.4 Spike-spike correlations during gabazine-induced paroxysmal discharges

To further investigate the spatiotemporal properties of gabazine-induced paroxysmal discharges, spike-spike correlations were mapped out over a 1s time window to cover the entire event (Fig. 5.27). Cross-correlations were performed between each pair of units and connectivity was quantified by measuring the point on the resulting cross-correlogram where the central peak crossed the Y-axis. Although connectivity was evident between units in superficial and deep layers throughout the slice, there was good evidence of longitudinal connectivity along deep layers (Fig. 5.27).

5.3.5.5 Spike-field correlations during gabazine-induced paroxysmal discharges

To further investigate the spatiotemporal properties of gabazine-induced paroxysmal discharges, spike-field correlations were mapped out over a 1s time window to cover the entire event (Fig. 5.28). Cross-correlations were performed between unit spike rate histograms and LFPs for each unit and LFP combination, and synchrony was quantified

by measuring the point on the resulting cross-correlogram where the central peak crossed the Y-axis.

There was evidence of spike-field correlations in superficial and deep layers throughout the slice (Fig. 5.28). In particular though, there were longitudinal spike-field correlations along deep layers of the slice, and correlations between superficial units and deeper LFPs.

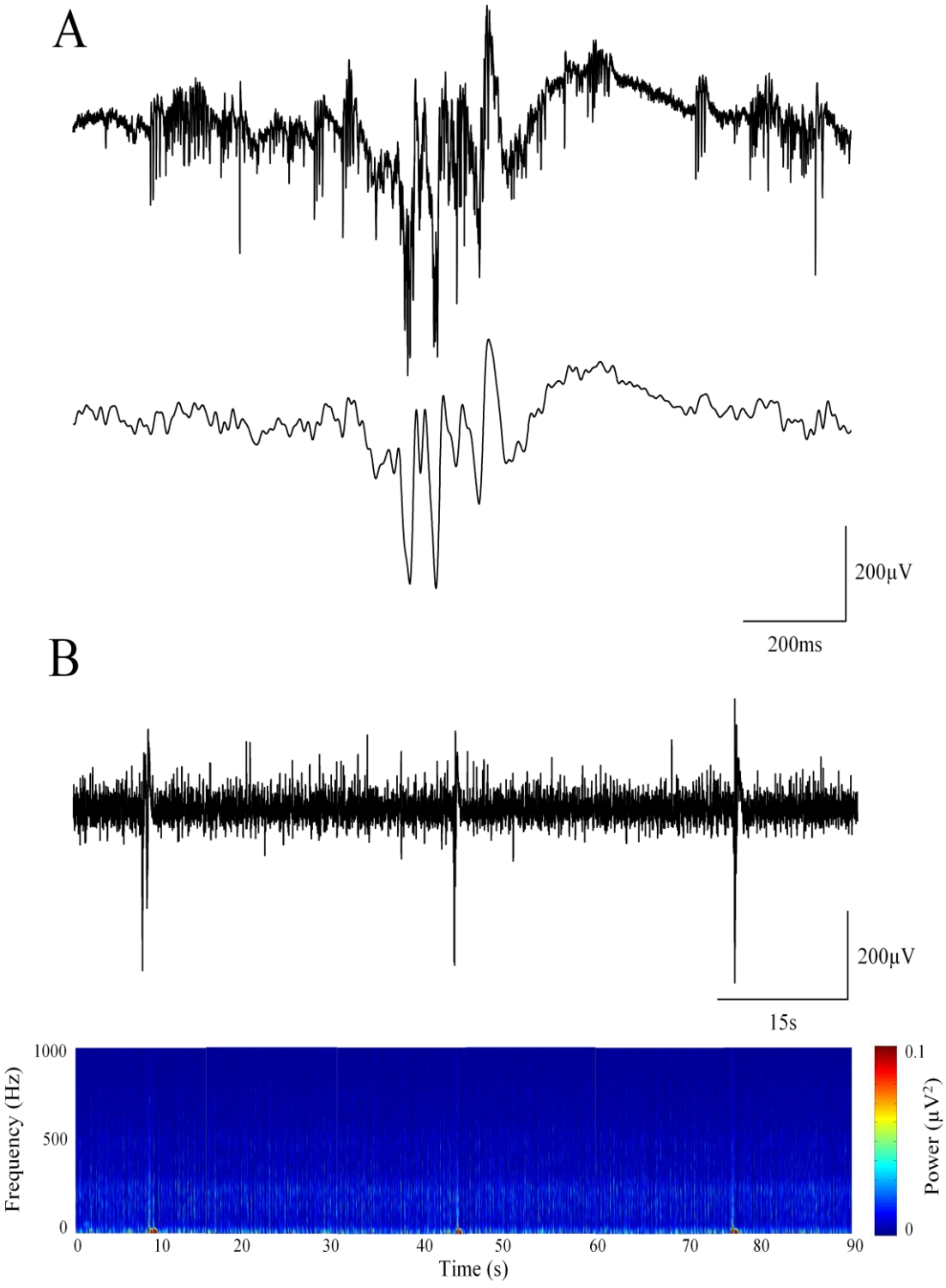

Fig. 5.1. Clozapine (20µM) induced paroxysmal discharges in layer V of rat 2° somatosensory cortex *in vitro*. (*A*) Raw unfiltered field trace (1.5s duration, upper), and the same trace with a 0.5-70Hz band-pass filter (lower). VFO occurred before, during and after the paroxysmal event. (*B*) 0.5-70Hz band-pass filtered field trace (90s duration, upper) showing 3 paroxysmal discharges at lower temporal resolution; and spectrogram (lower) for the same recording illustrating low frequency power during paroxysms, together with near continuous high frequency activity.

VFO parameter (Mean ± SEM / Median (Q1 → Q3))	VFO that occur when paroxysmal discharges are present	VFO that occur when paroxysmal discharges are absent
VFO band area power ($10^{-11}V^2$)	7.45 (5.93 → 16.20)	8.17 (3.80 → 29.50)
VFO band peak power ($10^{-13}V^2$)	6.72 (4.00 → 18.20)	6.07 (2.93 → 22.49)
VFO band peak frequency (Hz)	178 (152 → 240)	181 (171 → 239)
Burst frequency (Hz)	4.25 (1.68 → 4.63)	3.41 (2.18 → 4.46)
Inter-burst interval (s)	0.37 (0.33 → 0.81)	0.37 (0.30 → 0.51)
Number of spikes per burst	9.05 (6.00 → 15.43)	6.65 (5.54 → 8.30)
Proportion of time during the trace that VFO were present (%)	34.4 ± 7.2	23.7 ± 4.4
Line length (mV/s)	16.8 (13.6 → 22.6)	16.9 (13.3 → 26.5)

Table 5.1. VFO parameters in relation to the presence (n = 11 slices) or absence (n = 22 slices) of paroxysmal discharges. Parametric data are expressed as mean ± SEM. Non-parametric data are expressed in terms of the median and interquartile range (Q1 → Q3).

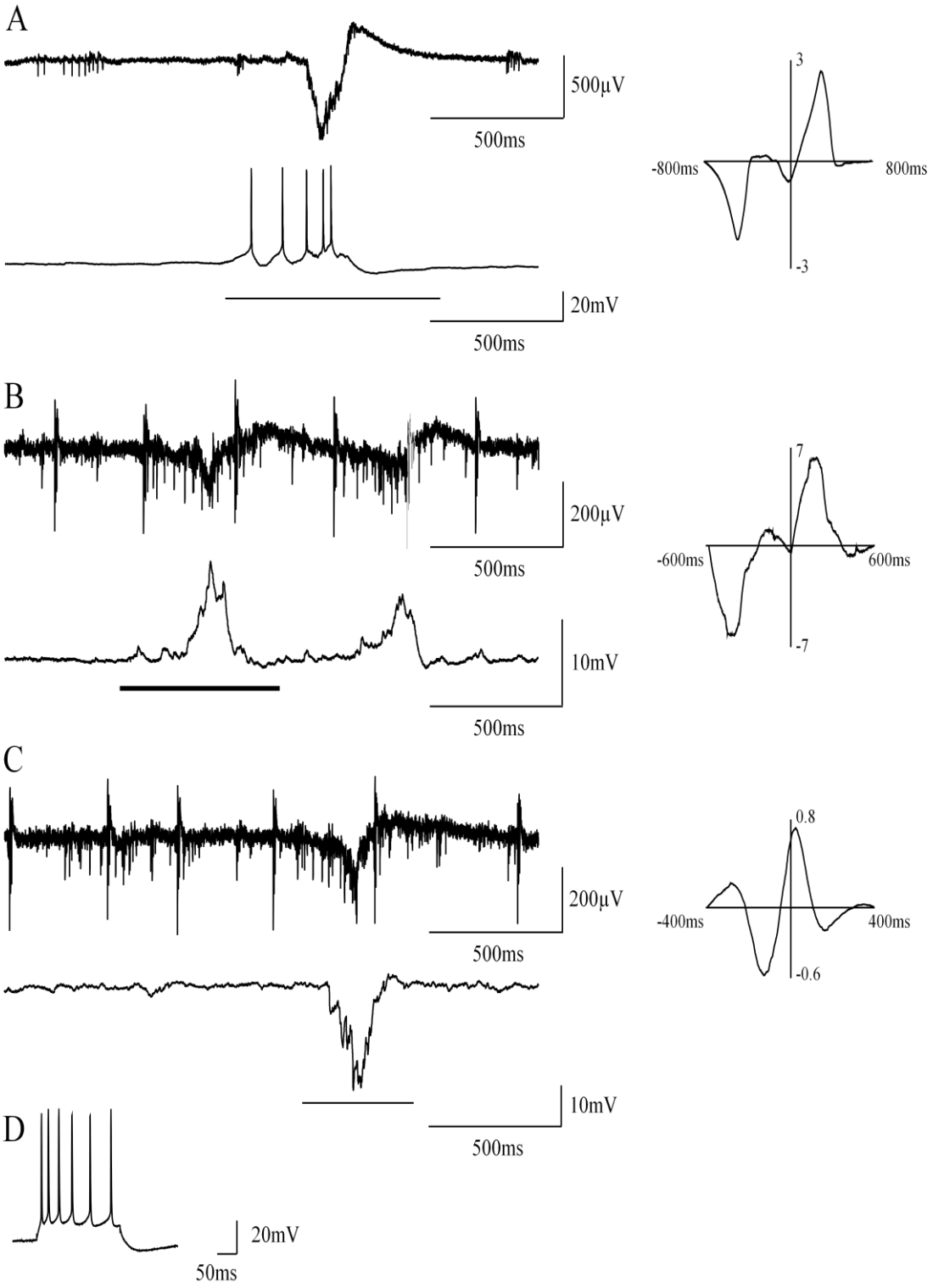

Fig. 5.2. Activity of RS cells in layer V of 2^0 somatosensory cortex during paroxysmal discharges. Intracellular recordings of an RS cell firing at a resting membrane potential of -56mV (*A*), EPSPs while a cell was held at -70mV (*B*), and IPSPs while a cell was held at -30mV (*C*). In each case raw unfiltered field traces (2s duration) are shown on the upper section of the panel and concurrent intracellular traces are shown on the lower section of the panel. Corresponding cross-correlations of field and intracellular activity are shown on the right. The black line marks the section of the trace used in the cross-correlation. (*D*) Electrophysiological characterisation of RS cells.

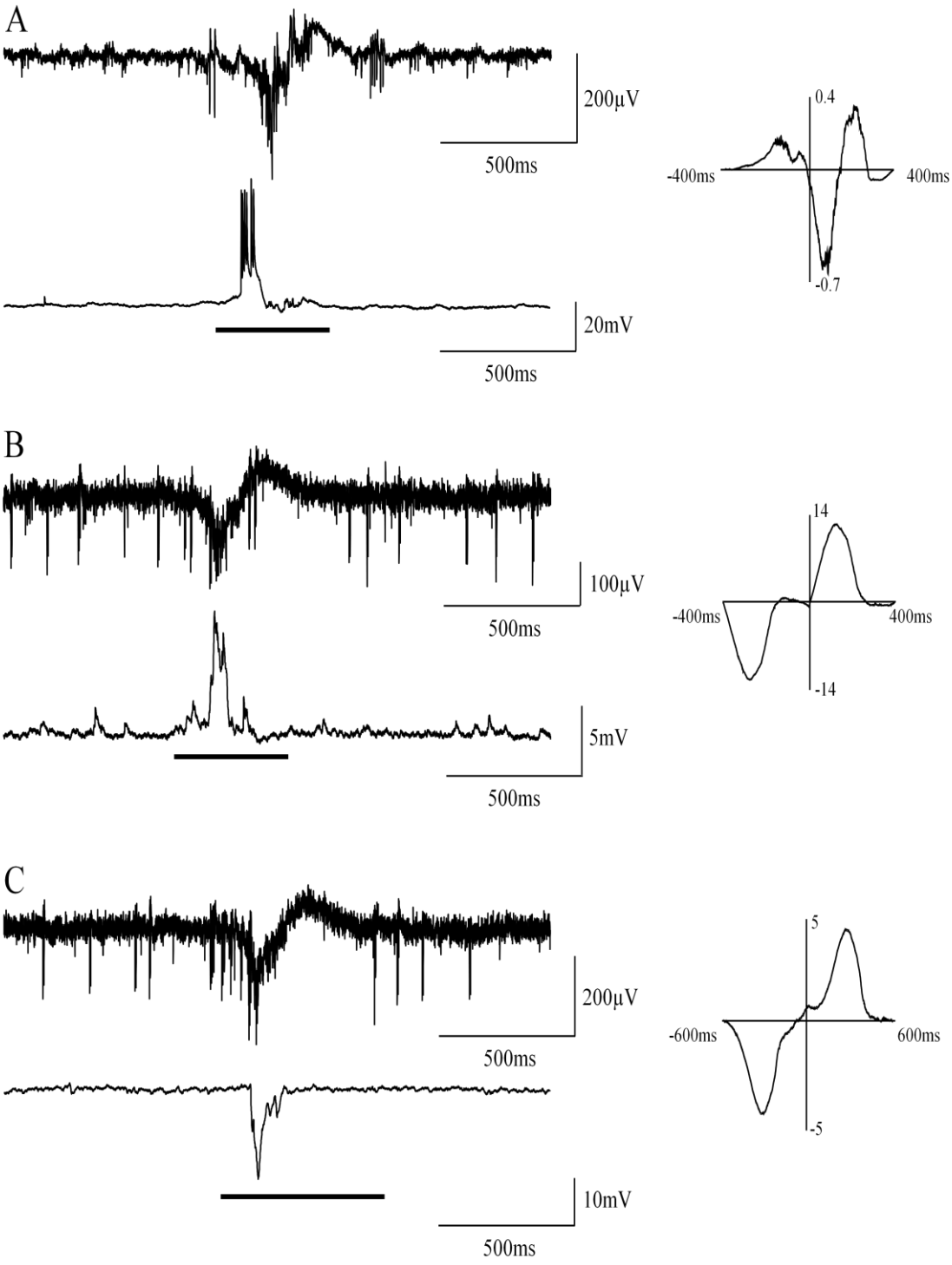

Fig. 5.3. Activity of putative IB cells in layer V of 2^0 somatosensory cortex during paroxysmal discharges. Intracellular recordings of a putative IB cell firing at resting membrane potential (*A*), EPSPs while a cell was held at -70mV (*B*), and IPSPs while a cell was held at -30mV (*C*). In each case raw unfiltered field traces (2s duration) are shown on the upper section of the panel and concurrent intracellular traces are shown on the lower section of the panel. Corresponding cross-correlations of field and intracellular activity are shown on the right. The black line marks the section of the trace used in the cross-correlation.

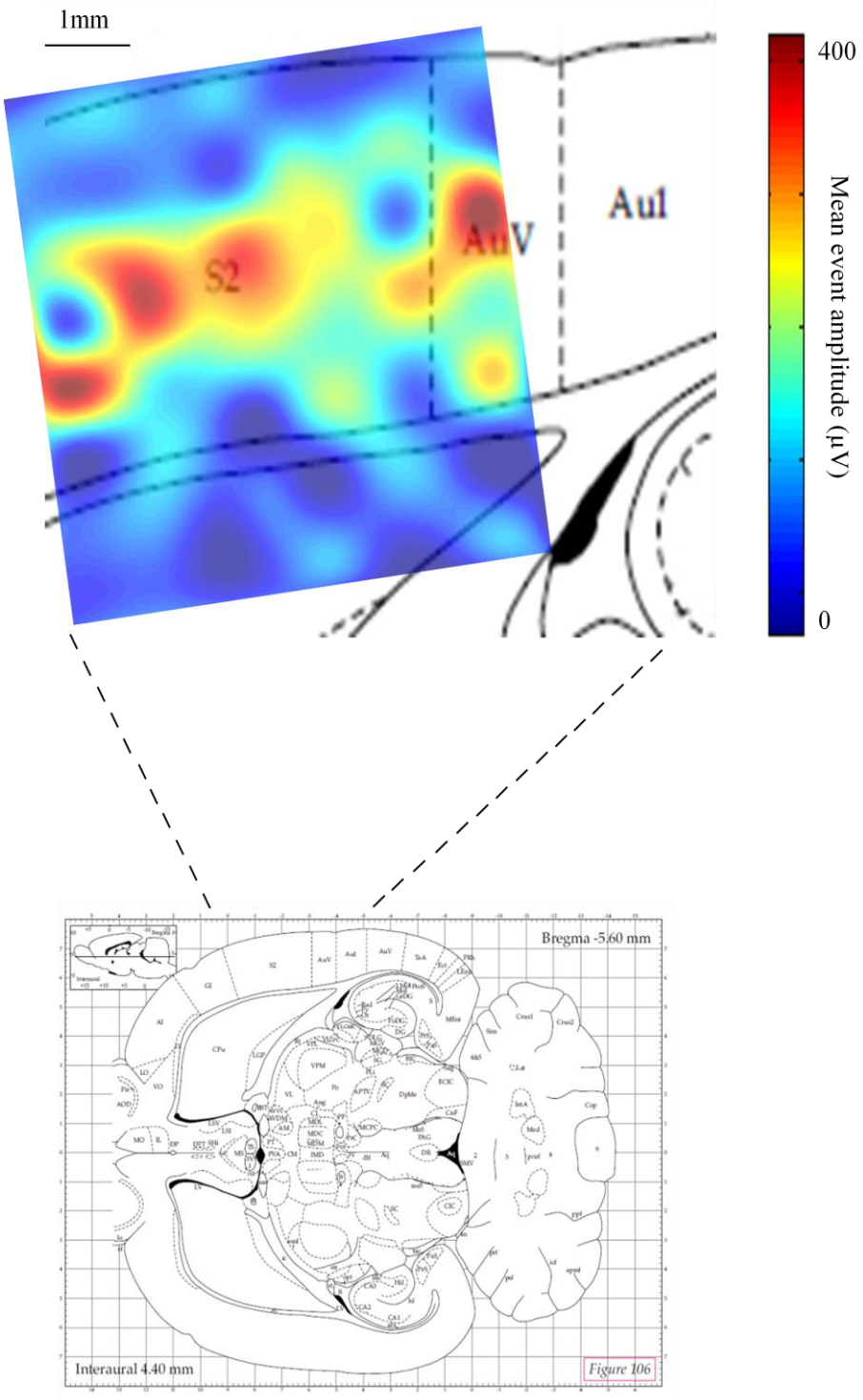

Fig. 5.4. Visual representation of the spatial distribution of clozapine-induced paroxysmal discharges in 2º somatosensory cortex. In the activity map, the colour corresponds to the mean paroxysmal discharge amplitude, as shown in the colourbar scale on the right. Data were derived from an example recording with the 3.6*3.6mm 96 electrode Utah array. S2: secondary somatosensory cortex; AuV: secondary auditory cortex, ventral area; Au1: primary auditory cortex. Rat brain atlas modified from Paxinos and Watson (1998).

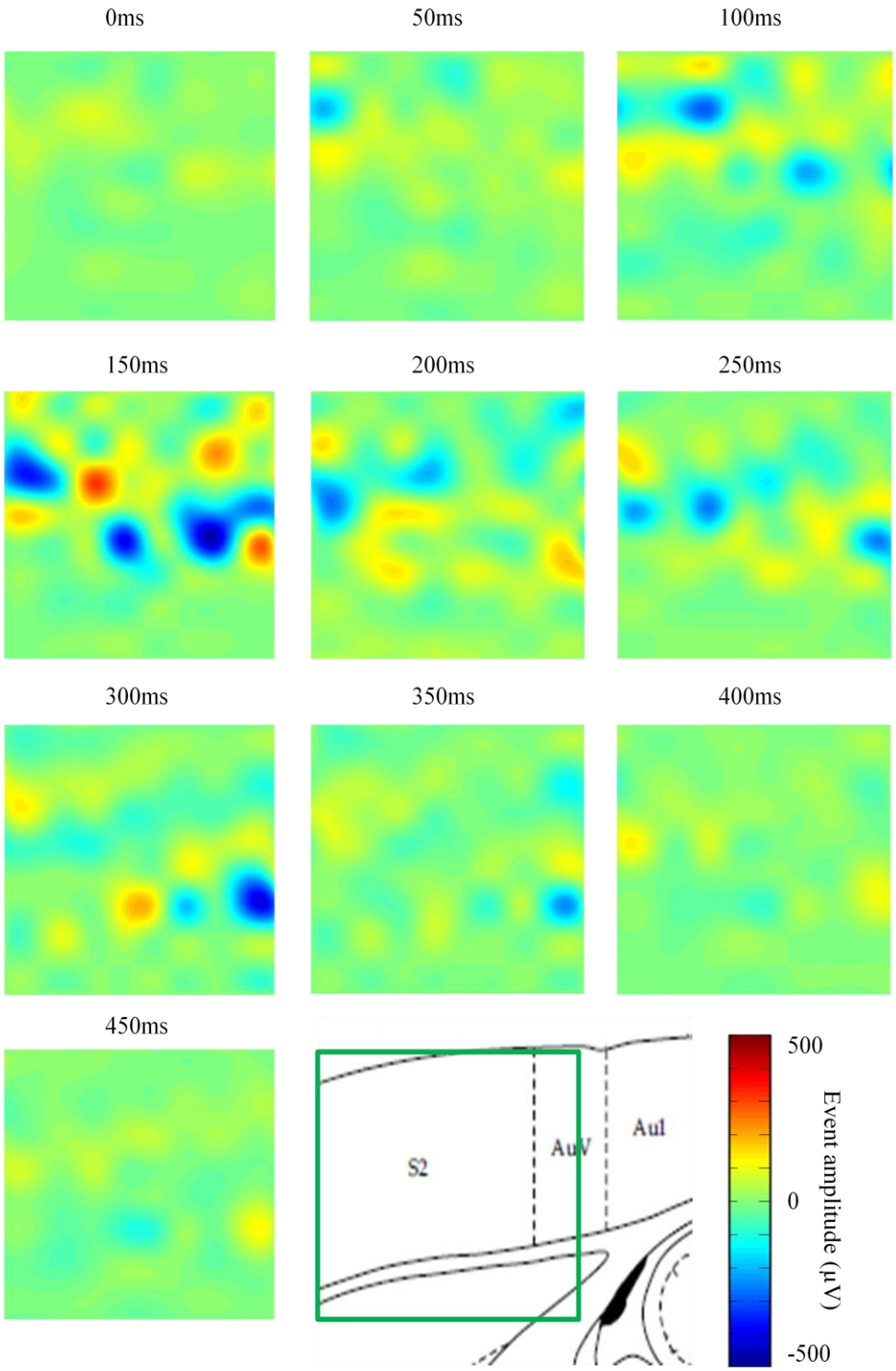

Fig. 5.5. Illustration of the progression of local field potentials (LFPs) associated with a clozapine-induced paroxysmal discharge over a 450ms time series (example 1). Activity maps were generated every 50ms from the start (top left) to end (bottom left) of the time series, as labelled. In the activity maps the colour corresponds to the amplitude of the paroxysmal discharge at that time point in the series, as shown in the colourbar scale at the bottom right. Data were derived from an example recording with the 3.6*3.6mm 96 electrode Utah array. The array was oriented as shown (green square) in 2^{o} somatosensory cortex, with the top corresponding to superficial layers and the bottom to deep layers.

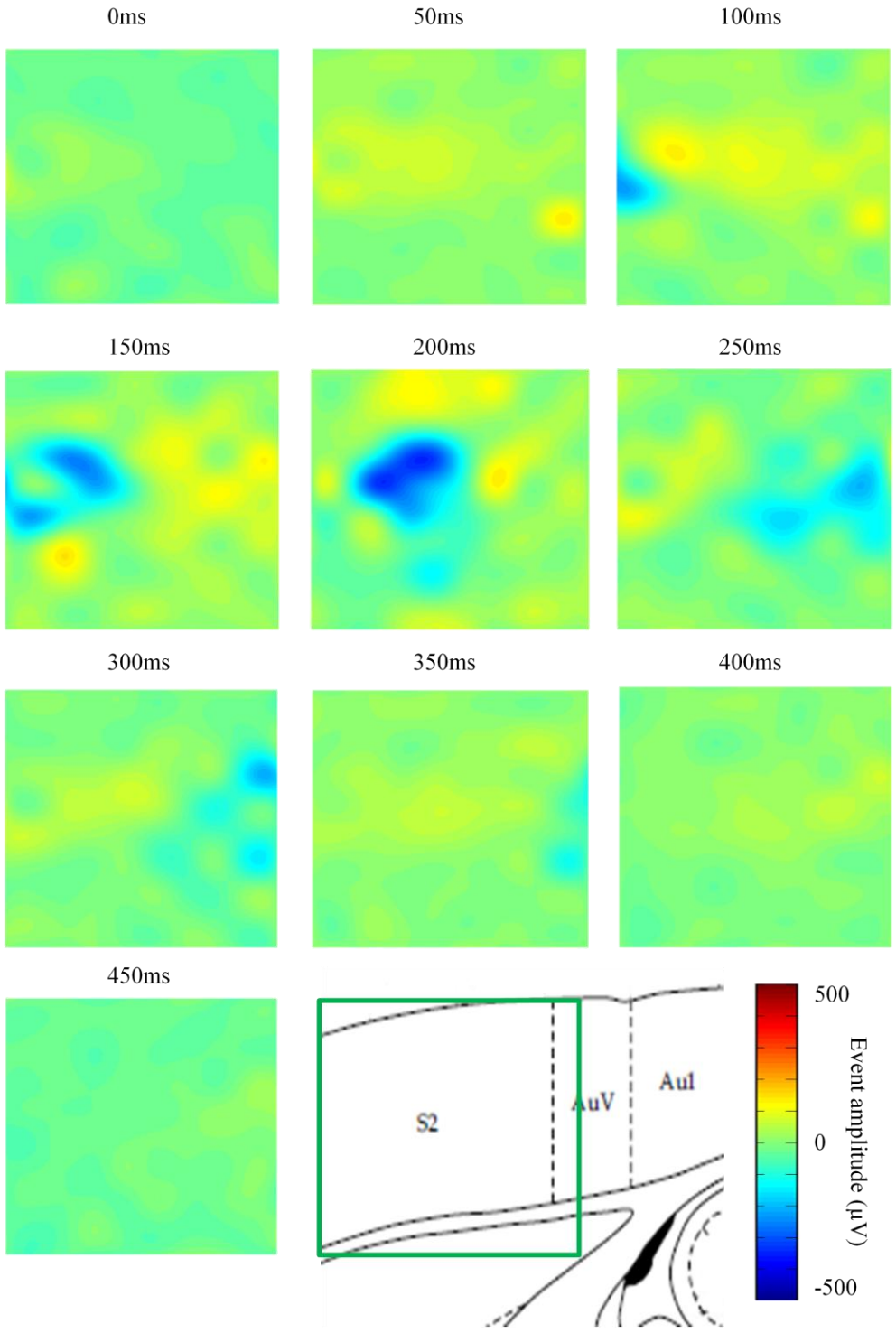

Fig. 5.6. Illustration of the progression of LFPs associated with a clozapine-induced paroxysmal discharge over a 450ms time series (example 2). Activity maps were generated every 50ms from the start (top left) to end (bottom left) of the time series, as labelled. In the activity maps the colour corresponds to the amplitude of the paroxysmal discharge at that time point in the series, as shown in the colourbar scale at the bottom right. Data were derived from an example recording with the 3.6*3.6mm 96 electrode Utah array. The array was oriented as shown (green square) in 2^{o} somatosensory cortex, with the top corresponding to superficial layers and the bottom to deep layers.

Fig. 5.7. Spike timing of multiple extracellular units during a clozapine-induced paroxysmal discharge. A concurrent recording of an LFP is shown at the top, and each row of rasters below represents spike timings for an individual unit. 82 units are shown over a 500ms time series. Data were derived from an example recording with the 96 electrode Utah array. The data illustrate the close association between bursts of spikes in multiple units and a clozapine-induced paroxysmal discharge.

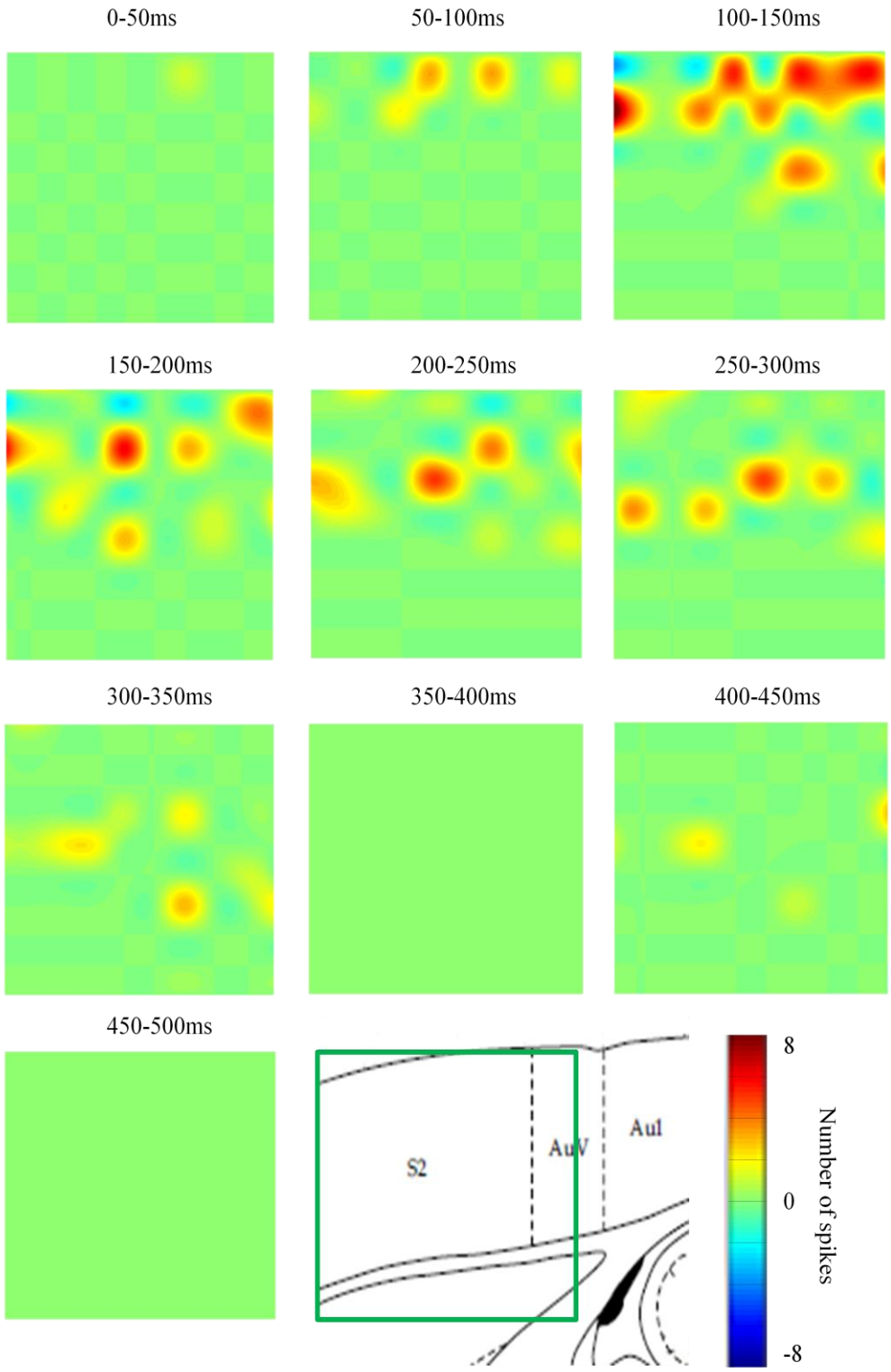

Fig. 5.8. The spatiotemporal progression of unit activity during a clozapine-induced paroxysmal discharge (example 1). Activity maps were generated for 50ms windows from the start (top left) to end (bottom left) of the 500ms time series, as labelled. In the activity maps the colour corresponds to the number of times the unit fires in the time window, as shown in the colourbar scale at the bottom right. Data were derived from an example recording with the 3.6*3.6mm 96 electrode Utah array. The array was oriented as shown (green square) in 2^{o} somatosensory cortex, with the top corresponding to superficial layers and the bottom to deep layers.

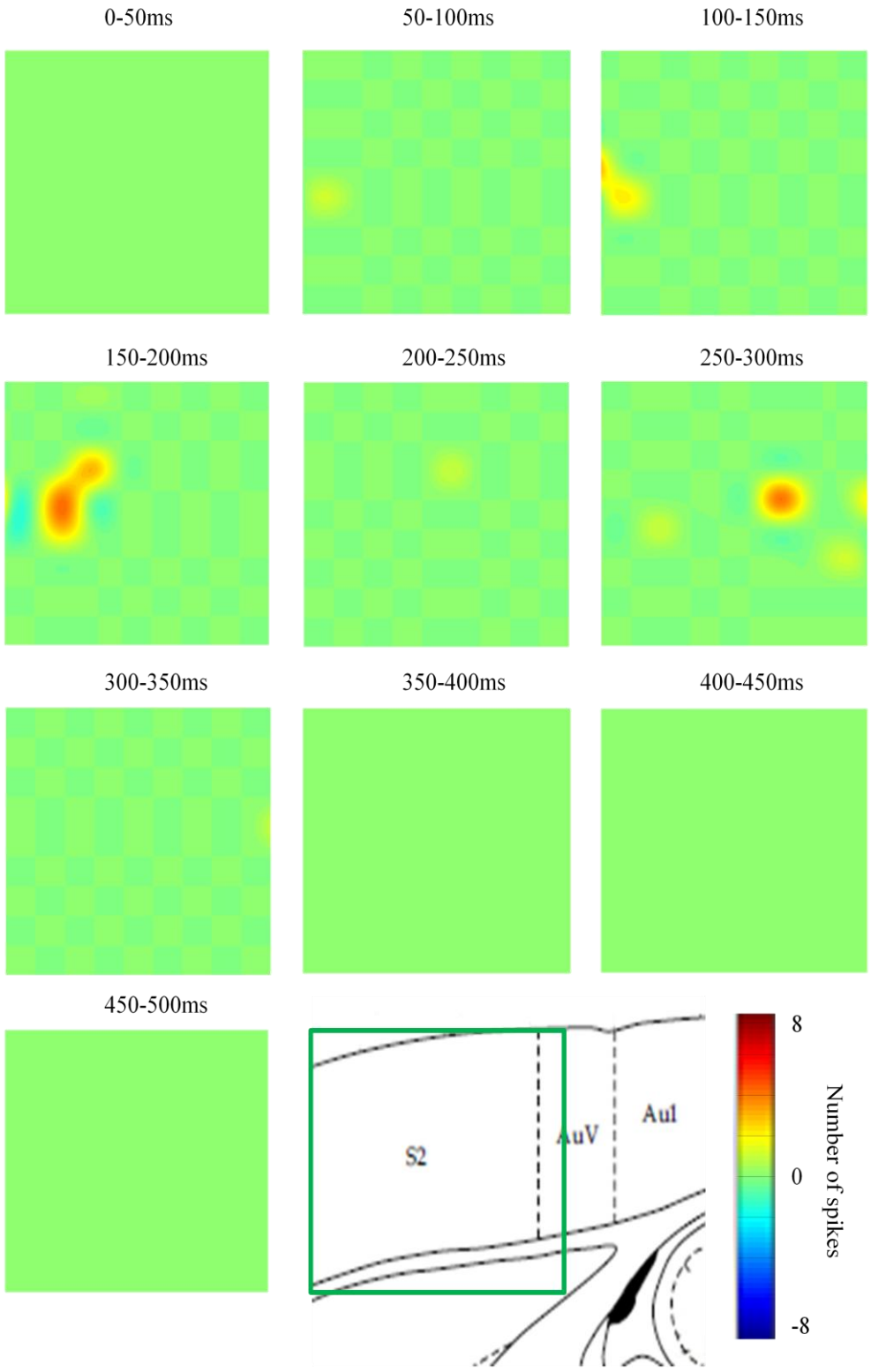

Fig. 5.9. The spatiotemporal progression of unit activity during a clozapine-induced paroxysmal discharge (example 2). Activity maps were generated for 50ms windows from the start (top left) to end (bottom left) of the 500ms time series, as labelled. In the activity maps the colour corresponds to the number of times the unit fires in the time window, as shown in the colourbar scale at the bottom right. Data were derived from an example recording with the 3.6*3.6mm 96 electrode Utah array. The array was oriented as shown (green square) in 2^{o} somatosensory cortex, with the top corresponding to superficial layers and the bottom to deep layers.

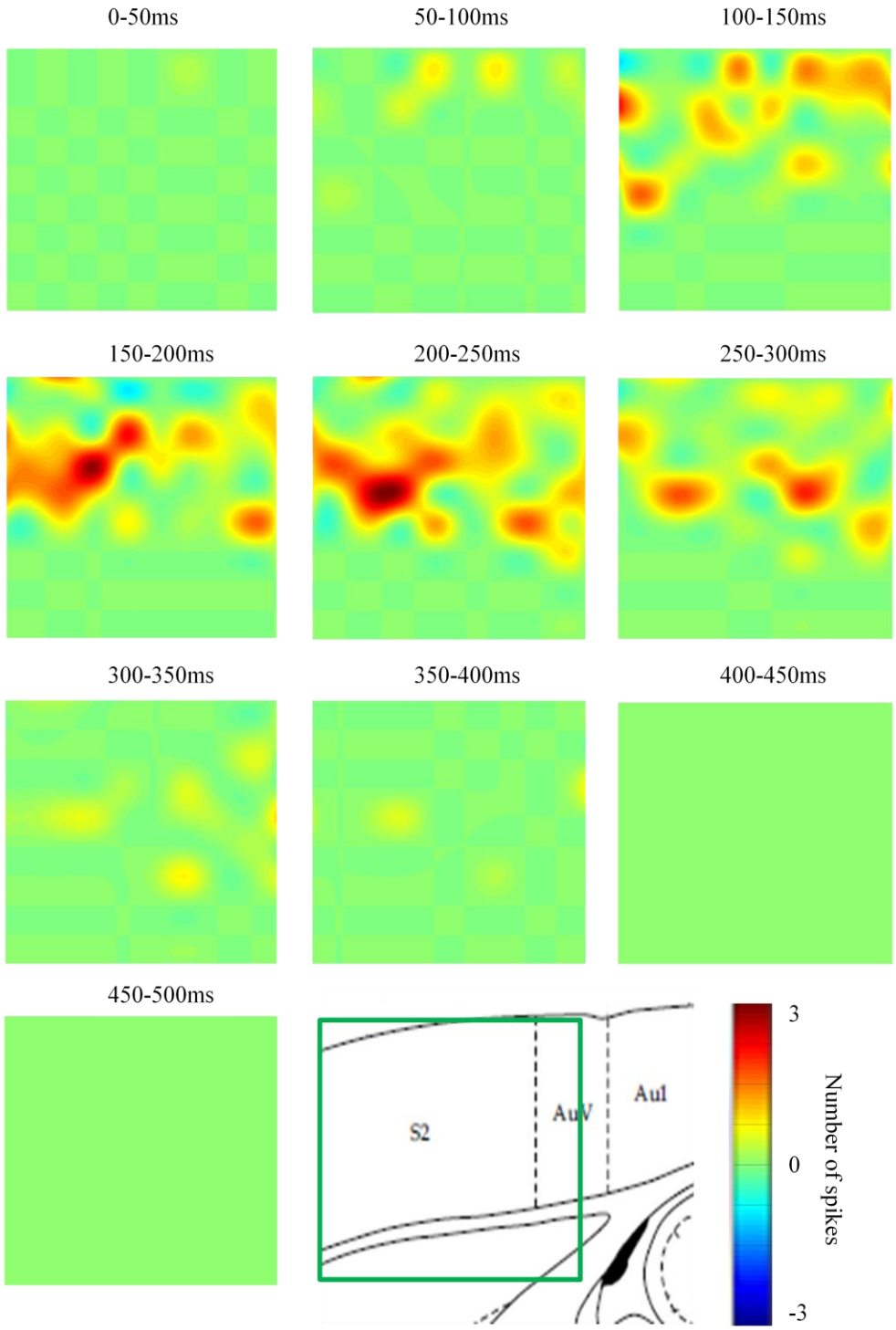

Fig. 5.10. The spatiotemporal progression of unit activity during clozapine-induced paroxysmal discharges (pooled data, n = 4 discharges in 2 slices). Activity maps were generated for 50ms windows from the start (top left) to end (bottom left) of the 500ms time series, as labelled. In the activity maps the colour corresponds to the number of times the unit fires in the time window, as shown in the colourbar scale at the bottom right. Data were derived from an example recording with the 3.6*3.6mm 96 electrode Utah array. The array was oriented as shown (green square) in 2º somatosensory cortex, with the top corresponding to superficial layers and the bottom to deep layers.

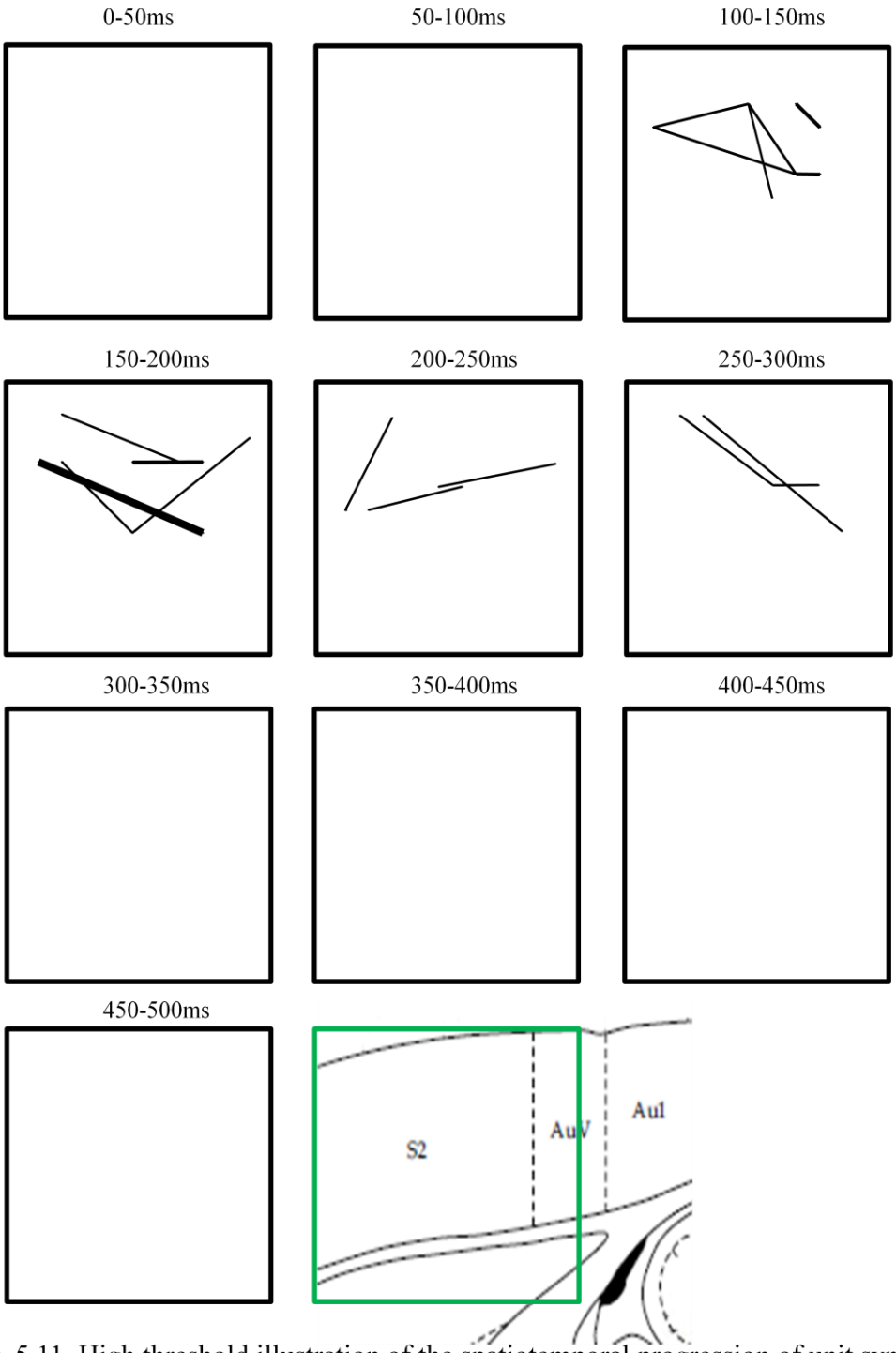

Fig. 5.11. High threshold illustration of the spatiotemporal progression of unit synchrony during a clozapine-induced paroxysmal discharge (example 1). Synchrony maps were generated for 50ms windows at 50ms intervals from the start (top left) to end (bottom left) of the 500ms time series, as labelled. In the synchrony maps the width of the line represents the inverse of the time distance to the nearest spike between pairs of units recorded from different electrodes in the 96 electrode Utah array. A high threshold is used in this example in the sense that only synchrony values greater than the mean plus 3 standard deviations of the synchrony in the most synchronous window are shown. The thickness of the dots represents the number of distinct units recorded in the channel. The array was oriented as shown (green square) in 2^{o} somatosensory cortex, with the top corresponding to superficial layers and the bottom to deep layers.

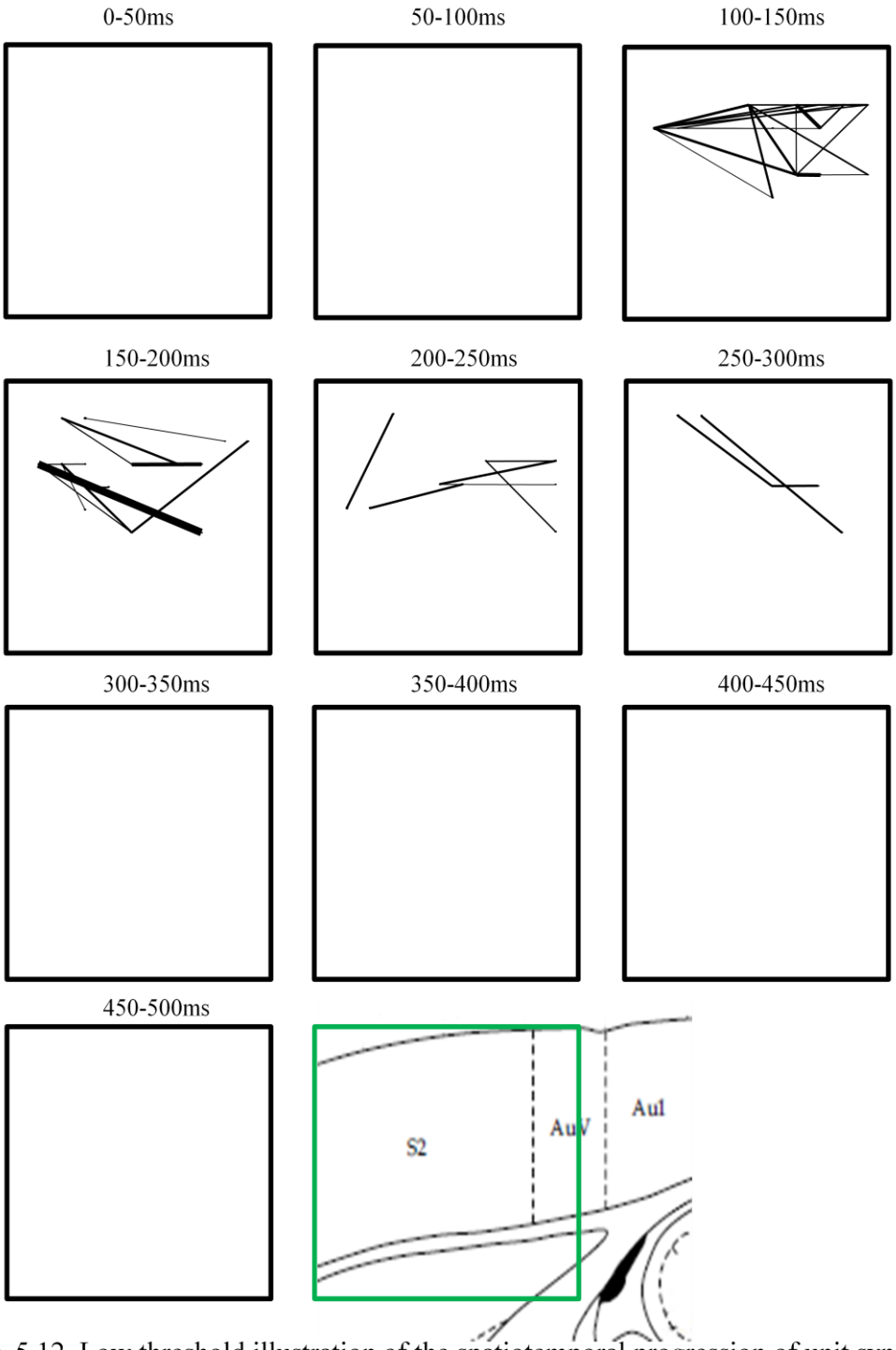

Fig. 5.12. Low threshold illustration of the spatiotemporal progression of unit synchrony during a clozapine-induced paroxysmal discharge (example 1). Synchrony maps were generated for 50ms windows at 50ms intervals from the start (top left) to end (bottom left) of the 500ms time series, as labelled. In the synchrony maps the width of the line represents the inverse of the time distance to the nearest spike between pairs of units recorded from different electrodes in the 96 electrode Utah array. A low threshold is used in this example in the sense that only synchrony values greater than the mean plus 1 standard deviation of the synchrony in the most synchronous window are shown. The thickness of the dots represents the number of distinct units recorded in the channel. The array was oriented as shown (green square) in 2^{o} somatosensory cortex, with the top corresponding to superficial layers and the bottom to deep layers.

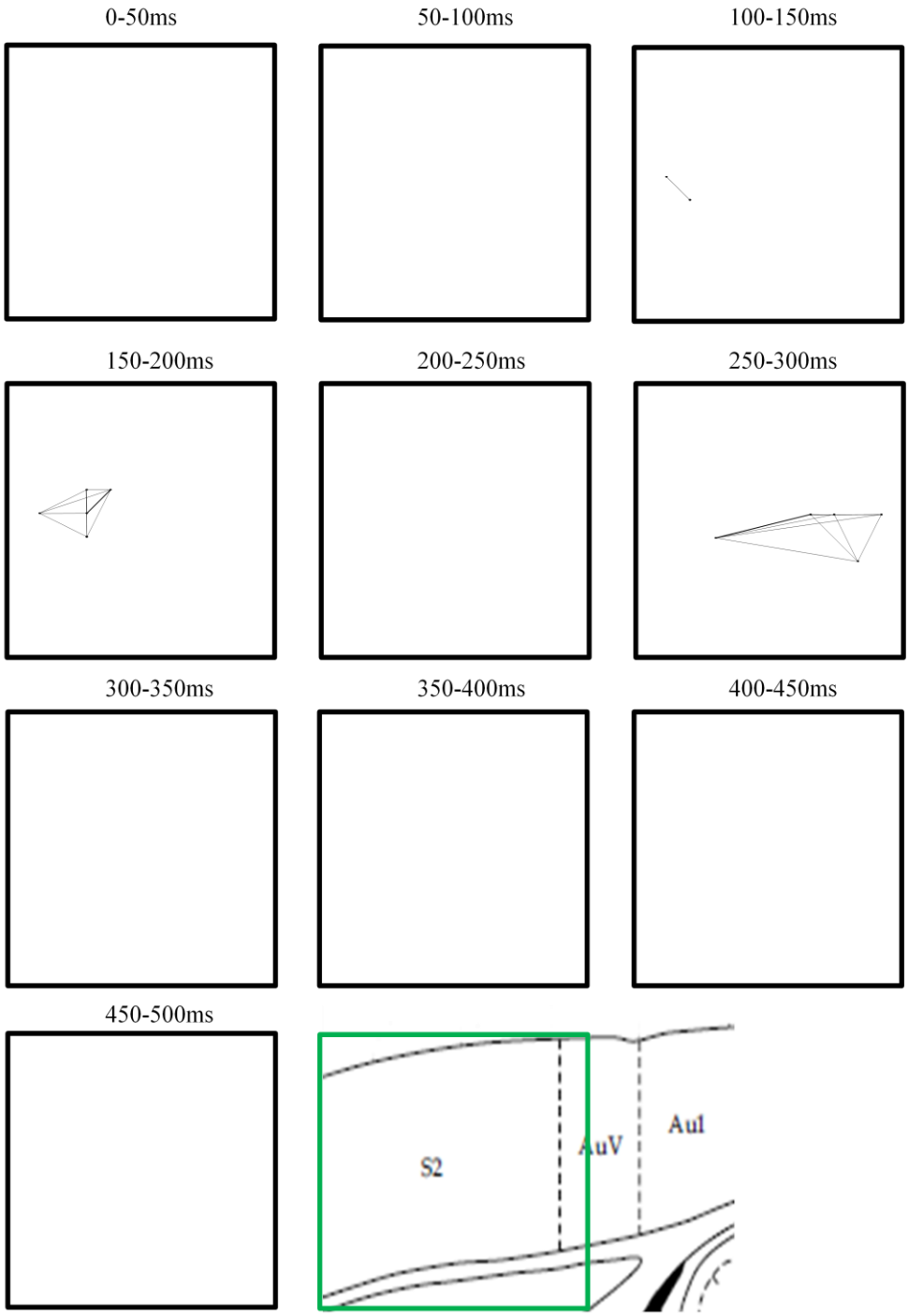

Fig. 5.13. Illustration of the spatiotemporal progression of unit synchrony during a clozapine-induced paroxysmal discharge (example 2). Synchrony maps were generated for 50ms windows at 50ms intervals from the start (top left) to end (bottom left) of the 500ms time series, as labelled. In the synchrony maps the width of the line represents the inverse of the time distance to the nearest spike between pairs of units recorded from different electrodes in the 96 electrode Utah array. As the unit activity was relatively sparse in this example, all synchrony values are shown without any thresholding. The thickness of the dots represents the number of distinct units recorded in the channel. The array was oriented as shown (green square) in 2º somatosensory cortex, with the top corresponding to superficial layers and the bottom to deep layers.

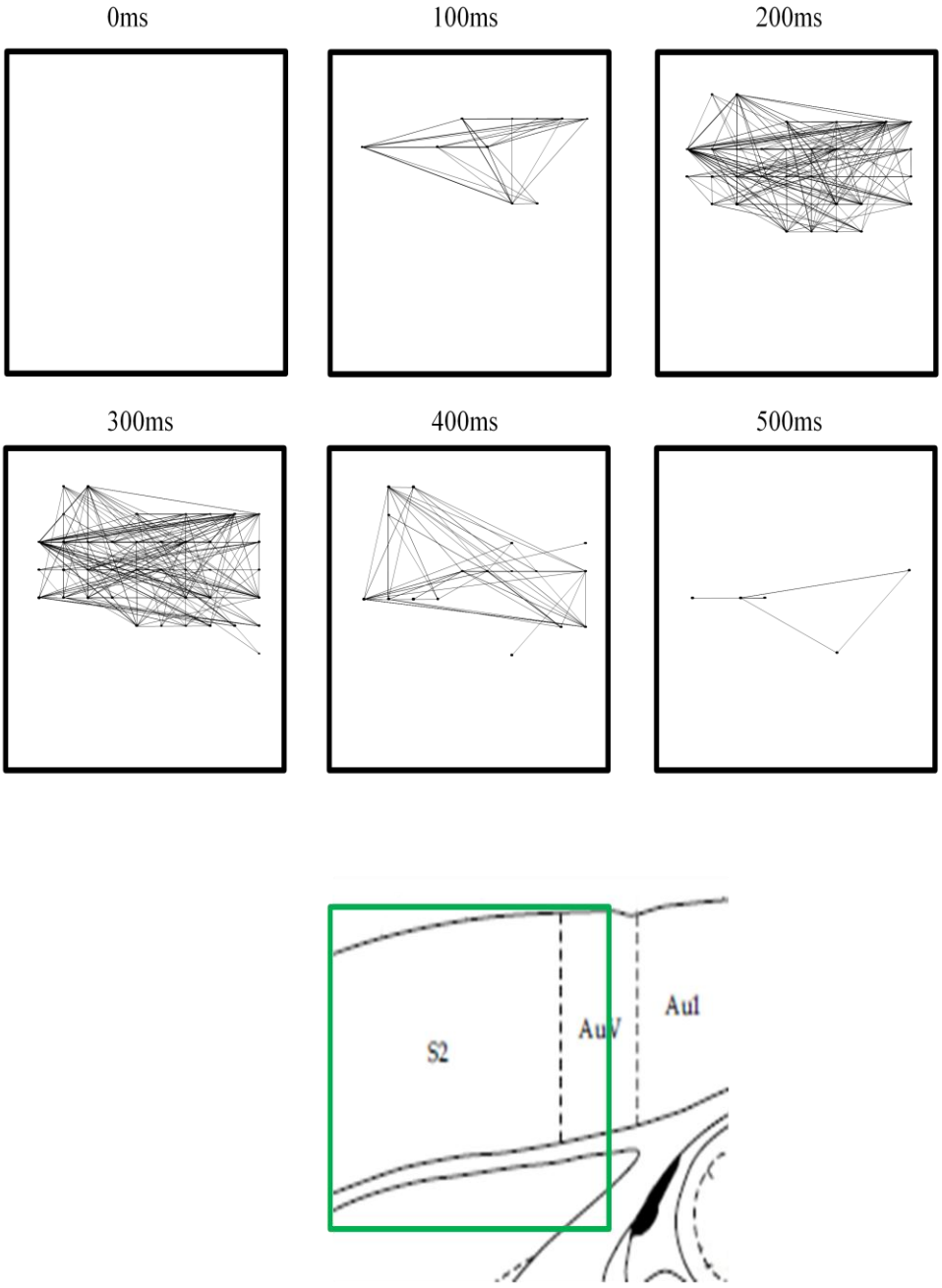

Fig. 5.14. The spatiotemporal progression of spike-spike correlations during a clozapine-induced paroxysmal discharge. Cross-correlations were performed between each pair of units from different electrodes in the 96 electrode Utah array. In the connectivity maps the width of the line represents the synchrony as measured on the cross-correlogram where the central peak crossed the Y axis. Only synchrony values greater than the mean plus 3 standard deviations of the synchrony in the most synchronous window are shown. Connectivity maps were generated for 200ms windows at 100ms intervals from the start (top left) to end (bottom right) of the 500ms time series. The thickness of the dots represents the number of distinct units recorded in the channel. The array was oriented as shown (green square) in 2^{o} somatosensory cortex, with the top corresponding to superficial layers and the bottom to deep layers.

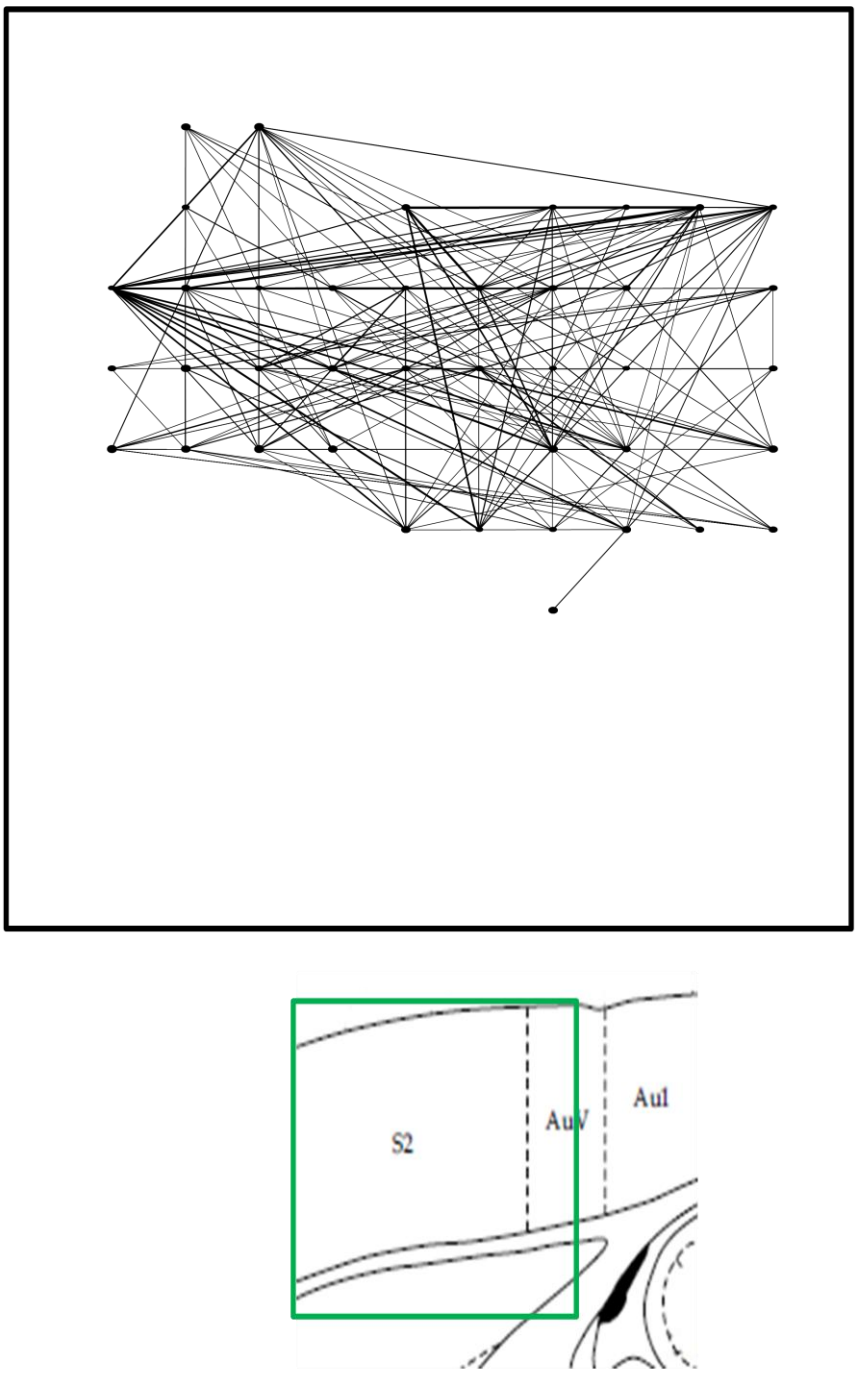

Fig. 5.15. Spike-spike correlations throughout a clozapine-induced paroxysmal discharge (example 1). Cross-correlations were performed between each pair of units from different electrodes in the 96 electrode Utah array. In the connectivity map the width of the line represents the synchrony as measured on the cross-correlogram where the central peak crossed the Y axis. Only synchrony values greater than the mean plus 3 standard deviations are shown. The connectivity map was generated for a 1s time window centred on the paroxysmal discharge. The thickness of the dots represents the number of distinct units recorded in the channel. The array was oriented as shown (green square) in 2^{o} somatosensory cortex, with the top corresponding to superficial layers and the bottom to deep layers.

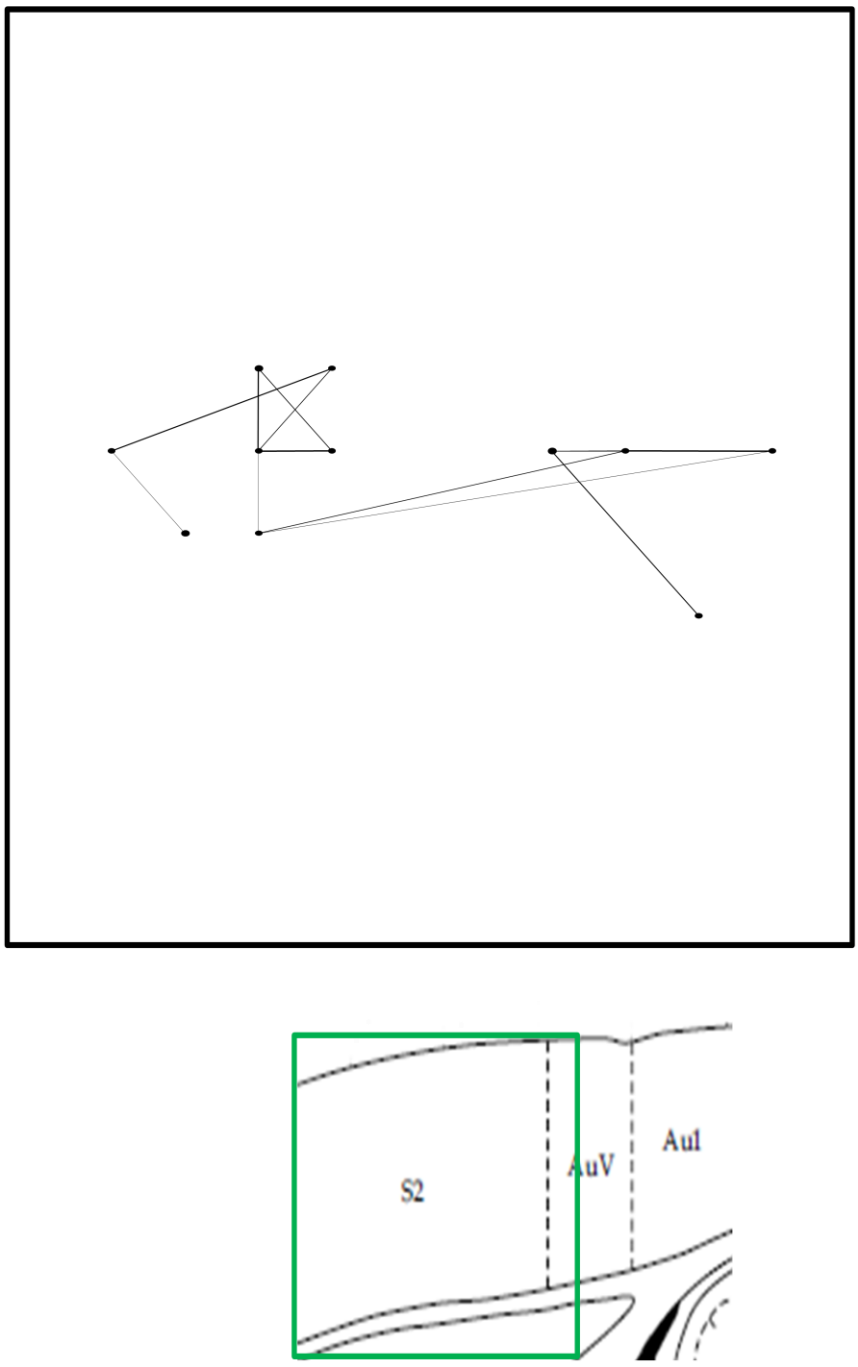

Fig. 5.16. Spike-spike correlations throughout a clozapine-induced paroxysmal discharge (example 2). Cross-correlations were performed between each pair of units from different electrodes in the 96 electrode Utah array. In the connectivity map the width of the line represents the synchrony as measured on the cross-correlogram where the central peak crossed the Y axis. Only synchrony values greater than the mean plus 3 standard deviations are shown. The connectivity map was generated for a 1s time window centred on the paroxysmal discharge. The thickness of the dots represents the number of distinct units recorded in the channel. The array was oriented as shown (green square) in 2^{o} somatosensory cortex, with the top corresponding to superficial layers and the bottom to deep layers.

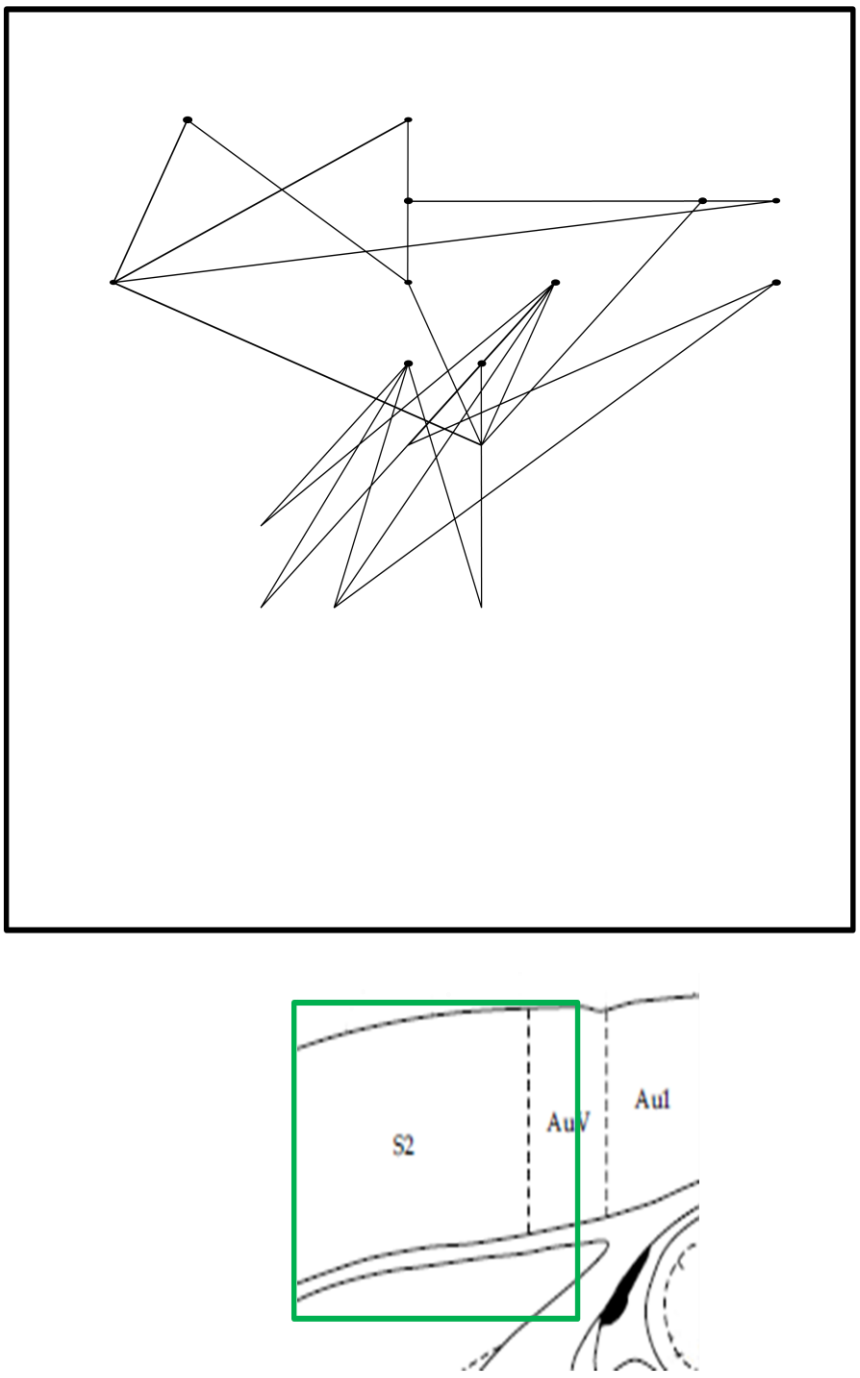

Fig. 5.17. Spike-field correlations throughout a clozapine-induced paroxysmal discharge (example 1). Cross-correlations were performed between unit spike rate histograms and LFPs for each unit and LFP combination in different electrodes in the 96 electrode Utah array. In the correlation map the width of the line represents the synchrony as measured on the cross-correlogram where the central peak crossed the Y axis. Only synchrony values greater than the mean plus 3 standard deviations are shown. The connectivity map was generated for a 1s time window centred on the paroxysmal discharge. The thickness of the dots represents the number of distinct units recorded in the channel. The array was oriented as shown (green square) in 2^{o} somatosensory cortex, with the top corresponding to superficial layers and the bottom to deep layers.

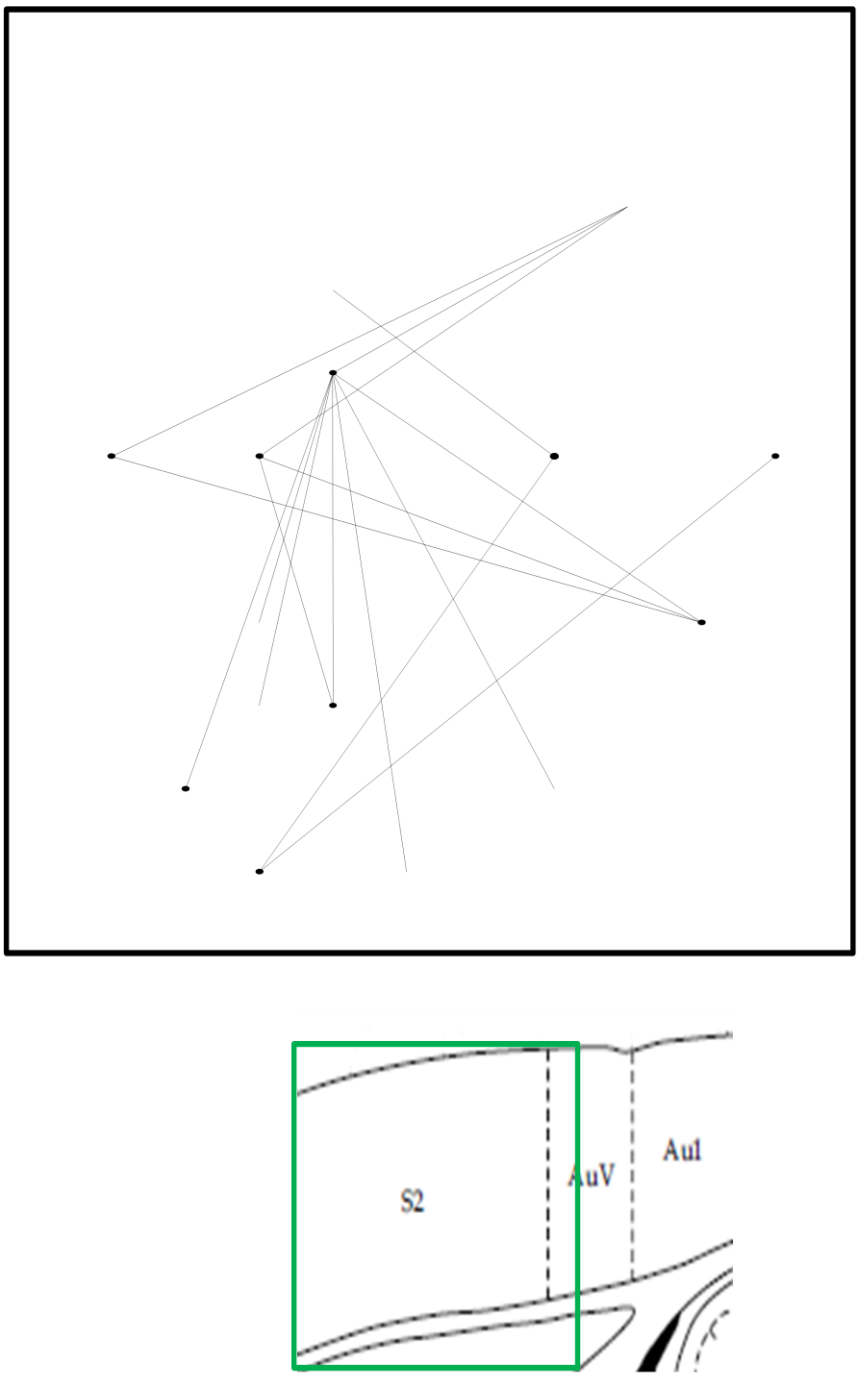

Fig. 5.18. Spike-field correlations throughout a clozapine-induced paroxysmal discharge (example 2). Cross-correlations were performed between unit spike rate histograms and LFPs for each unit and LFP combination in different electrodes in the 96 electrode Utah array. In the correlation map the width of the line represents the synchrony as measured on the cross-correlogram where the central peak crossed the Y axis. Only synchrony values greater than the mean plus 3 standard deviations are shown. The connectivity map was generated for a 1s time window centred on the paroxysmal discharge. The thickness of the dots represents the number of distinct units recorded in the channel. The array was oriented as shown (green square) in 2^{o} somatosensory cortex, with the top corresponding to superficial layers and the bottom to deep layers.

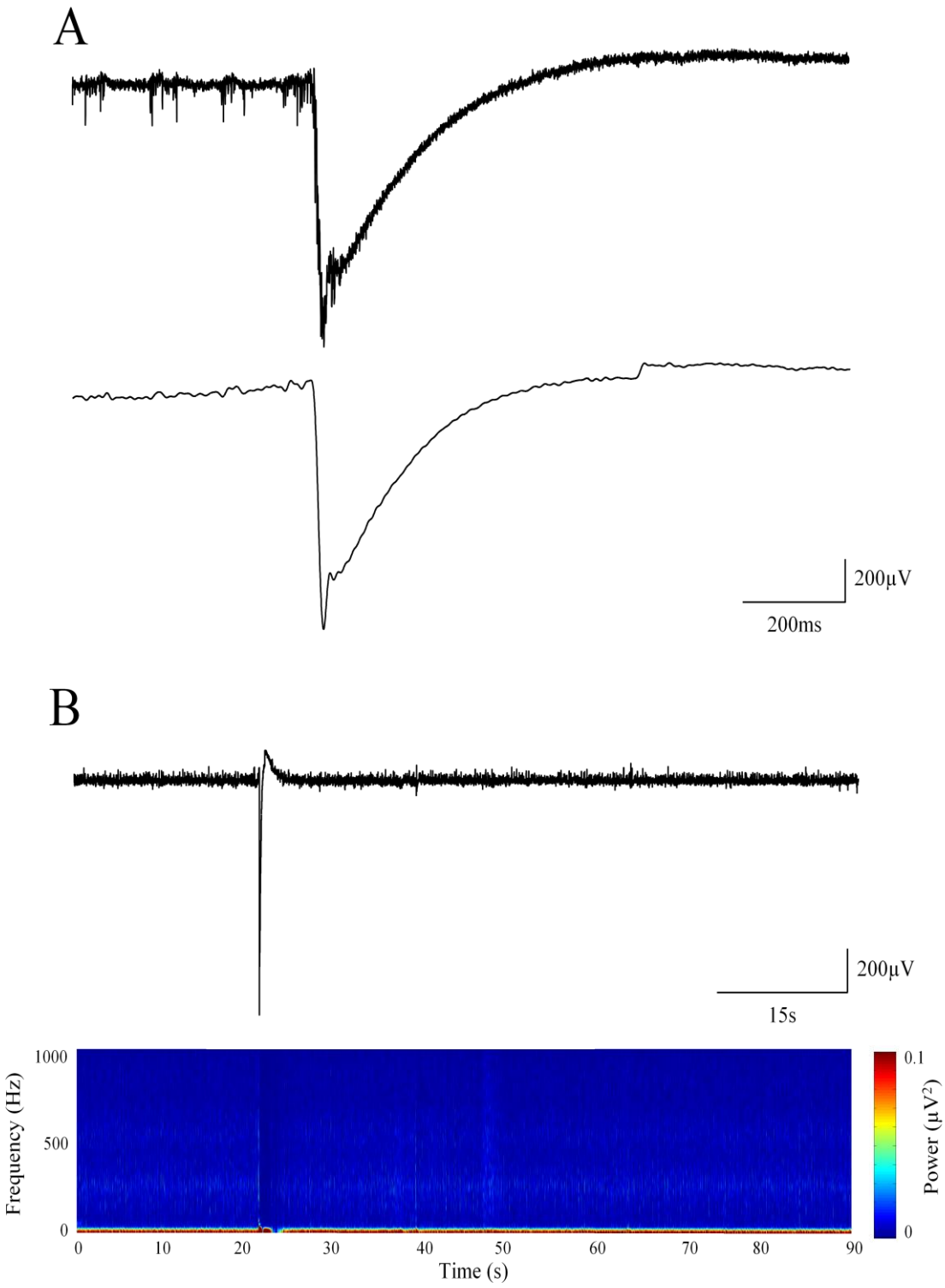

Fig. 5.19. Example of large paroxysmal discharges induced by gabazine (250 nM) in layer V of rat 2° somatosensory cortex *in vitro*. (*A*) Raw unfiltered field trace (1.5s duration, upper), and the same trace with a 0.5-70Hz band-pass filter (lower). VFO occurred before and during the paroxysmal event. (*B*) 0.5-70Hz band-pass filtered field trace (90s duration, upper) showing the paroxysmal discharge at lower temporal resolution; and spectrogram (lower) for the same recording illustrating low frequency power during the paroxysm, together with near continuous high frequency activity.

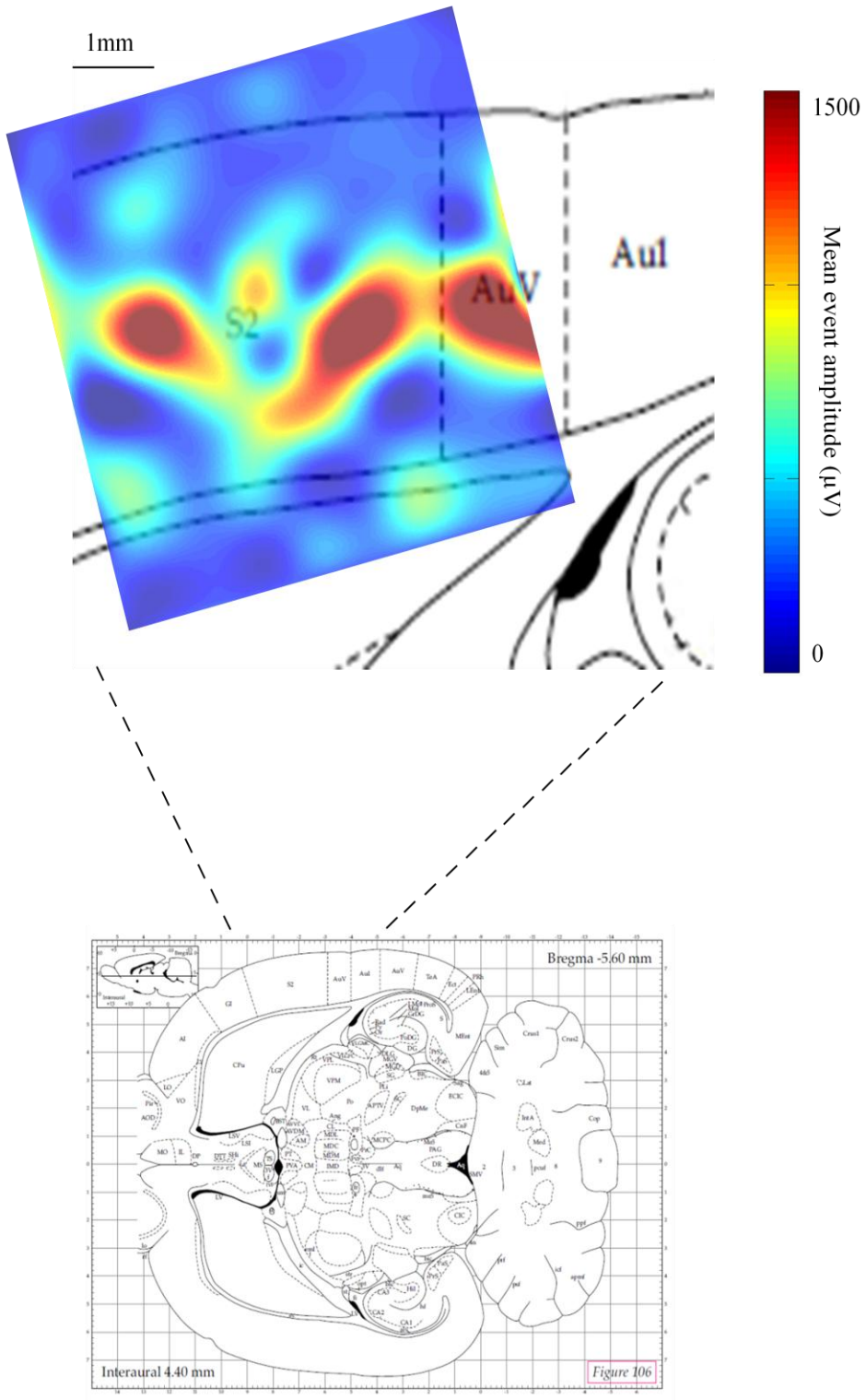

Fig. 5.20. Visual representation of the spatial distribution of gabazine-induced paroxysmal discharges in 2º somatosensory cortex. In the activity map, the colour corresponds to the mean paroxysmal discharge amplitude, as shown in the colourbar scale on the right. Data were derived from an example recording with the 3.6*3.6mm 96 electrode Utah array. S2: secondary somatosensory cortex; AuV: secondary auditory cortex, ventral area; Au1: primary auditory cortex. Rat brain atlas modified from Paxinos and Watson (1998).

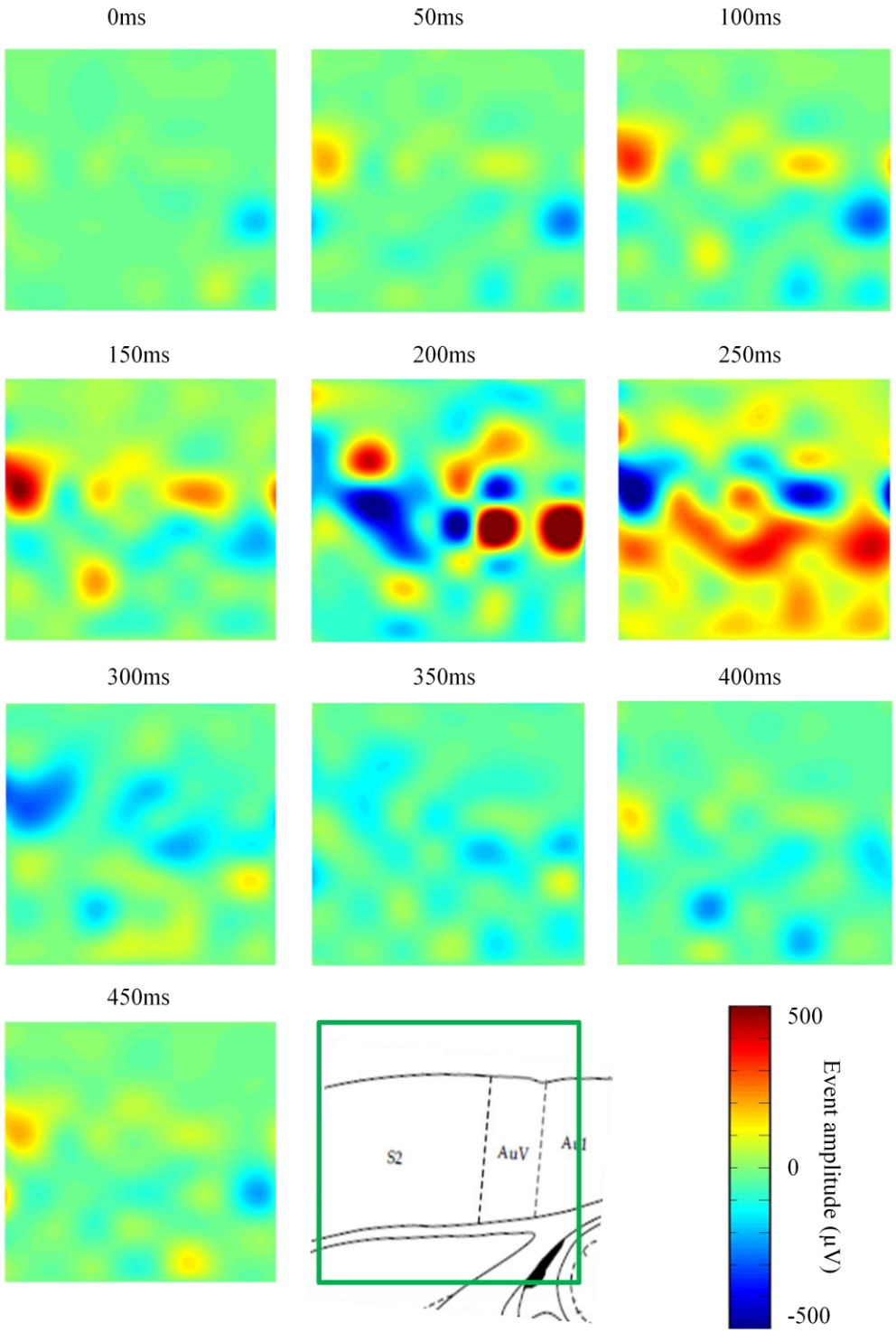

Fig. 5.21. Illustration of the progression of LFPs associated with a gabazine-induced paroxysmal discharge over a 450ms time series. Activity maps were generated every 50ms from the start (top left) to end (bottom left) of the time series, as labelled. In the activity maps the colour corresponds to the amplitude of the paroxysmal discharge at that time point in the series, as shown in the colourbar scale at the bottom right. Data were derived from an example recording with the 3.6*3.6mm 96 electrode Utah array. The array was oriented as shown (green square) in 2° somatosensory cortex, with the top corresponding to superficial layers and the bottom to deep layers.

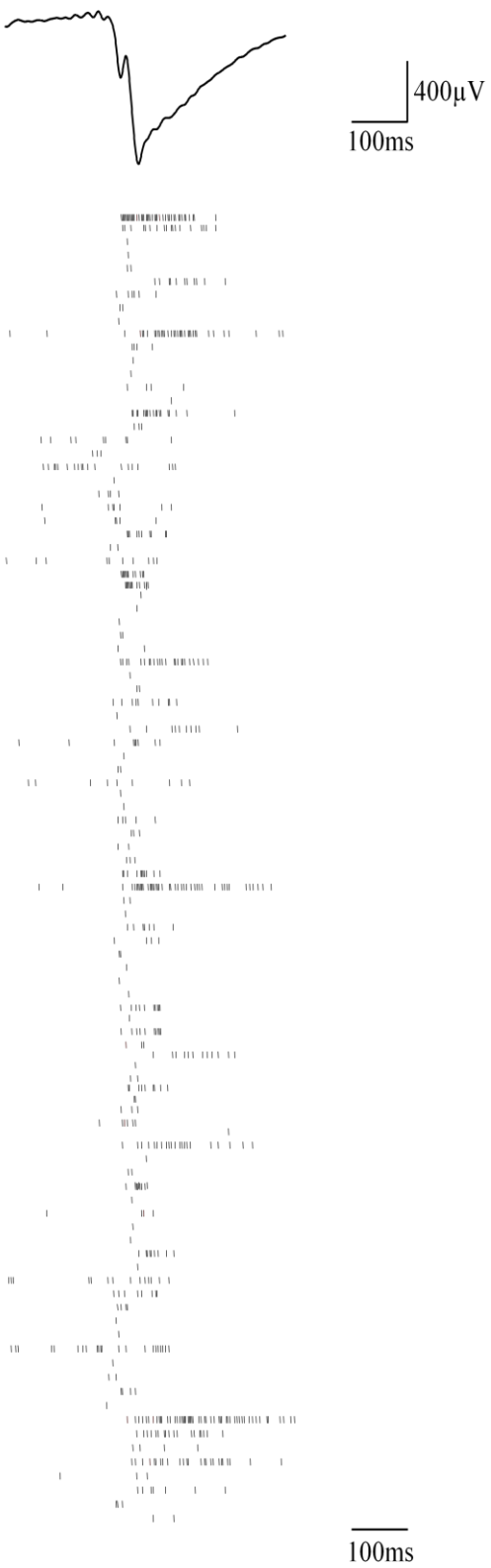

Fig. 5.22. Spike timing of multiple extracellular units during a gabazine-induced paroxysmal discharge. A concurrent recording of an LFP is shown at the top, and each row of rasters below represents spike timings for an individual unit. 100 units are shown over a 500ms time series. Data were derived from an example recording with the 96 electrode Utah array. The data illustrate the close association between bursts of spikes in multiple units and a gabazine-induced paroxysmal discharge.

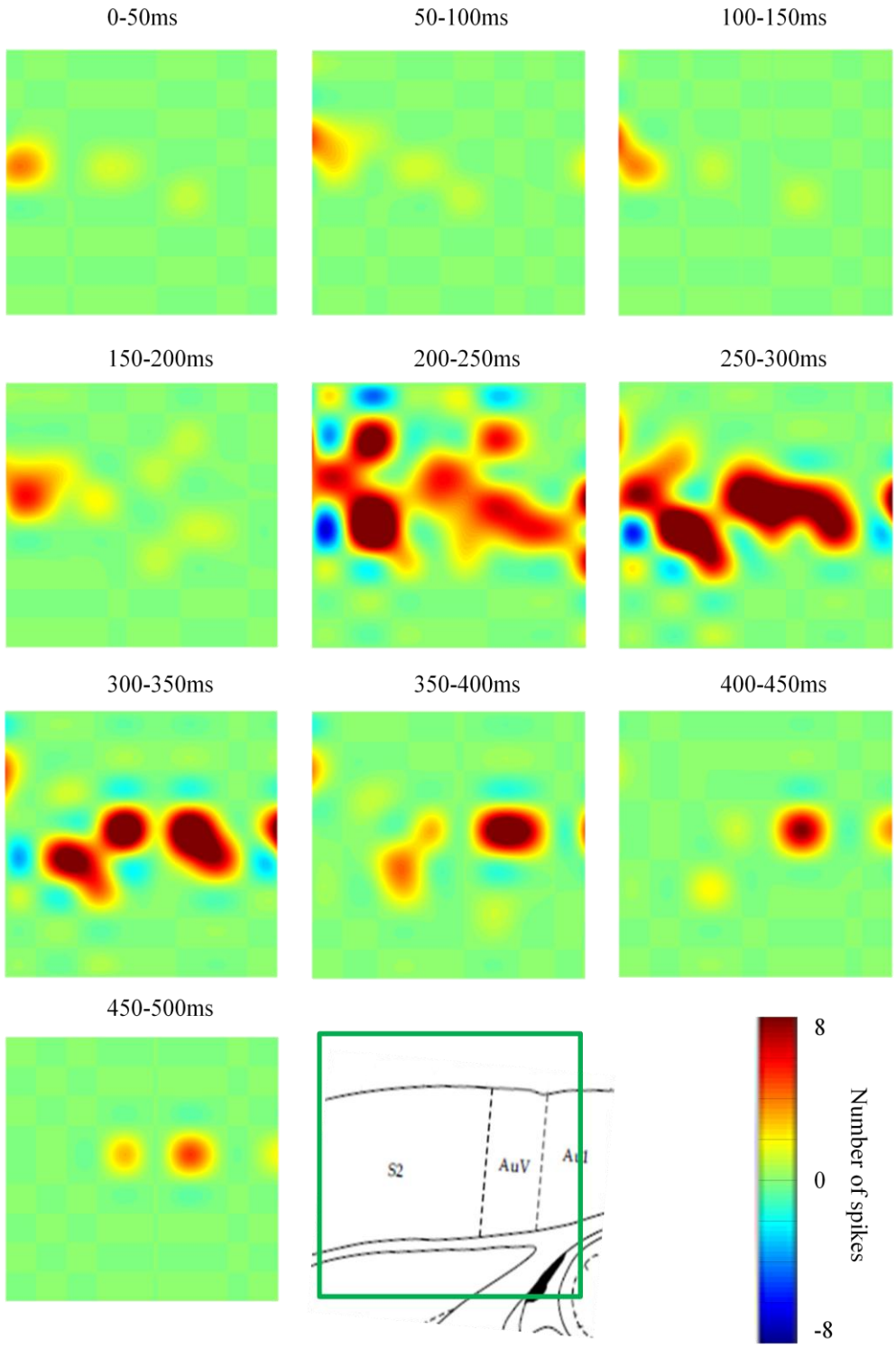

Fig. 5.23. The spatiotemporal progression of unit activity during a gabazine-induced paroxysmal discharge. Activity maps were generated for 50ms windows from the start (top left) to end (bottom left) of the 500ms time series, as labelled. In the activity maps the colour corresponds to the number of times the unit fires in the time window, as shown in the colourbar scale at the bottom right. Data were derived from an example recording with the 3.6*3.6mm 96 electrode Utah array. The array was oriented as shown (green square) in 2^0 somatosensory cortex, with the top corresponding to superficial layers and the bottom to deep layers.

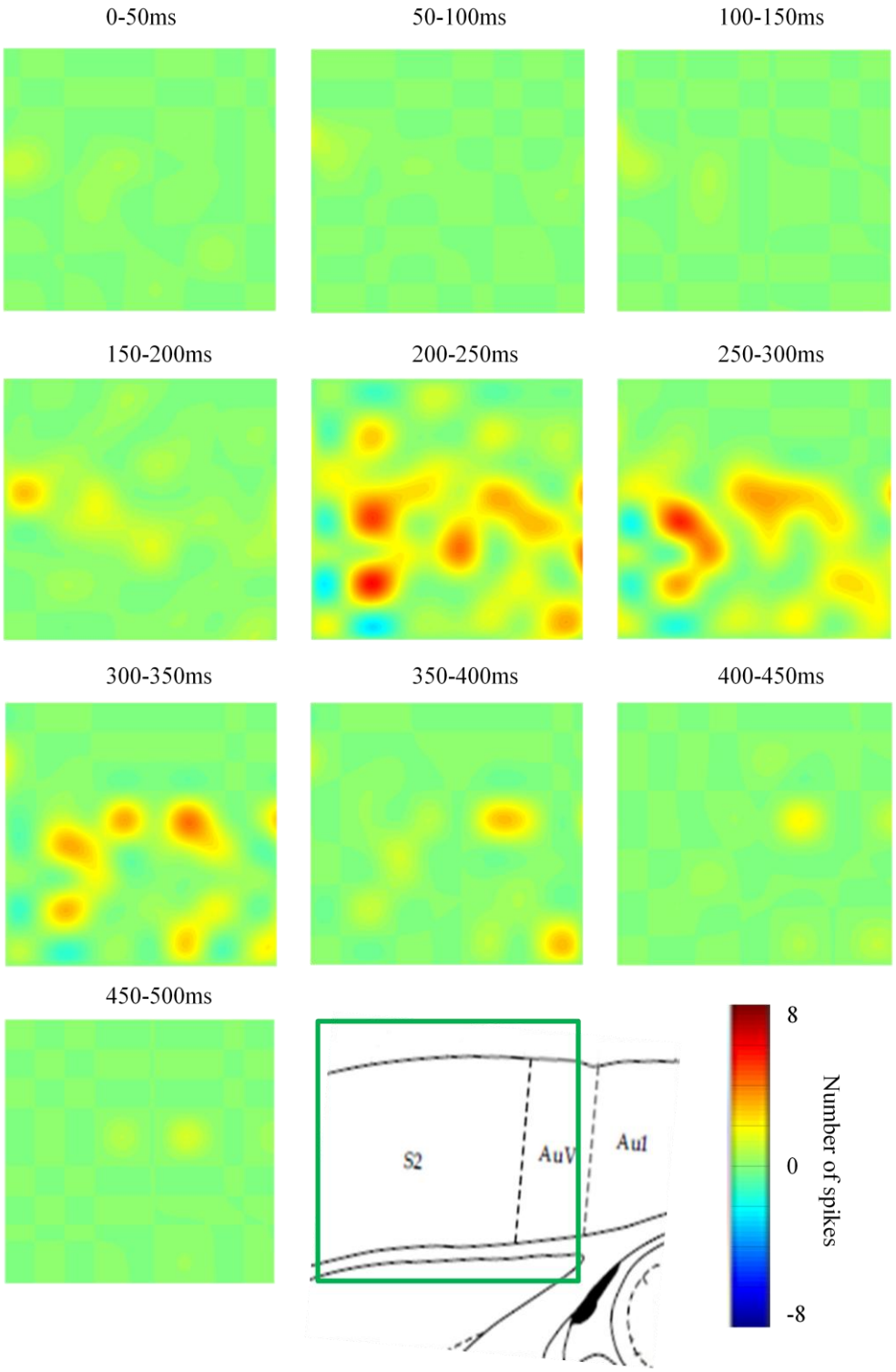

Fig. 5.24. The spatiotemporal progression of unit activity during gabazine-induced paroxysmal discharges (pooled data, n = 4 discharges in 4 slices). Activity maps were generated for 50ms windows from the start (top left) to end (bottom left) of the 500ms time series, as labelled. In the activity maps the colour corresponds to the number of times the unit fires in the time window, as shown in the colourbar scale at the bottom right. Data were derived from an example recording with the 3.6*3.6mm 96 electrode Utah array. The array was oriented as shown (green square) in 2^{o} somatosensory cortex, with the top corresponding to superficial layers and the bottom to deep layers.

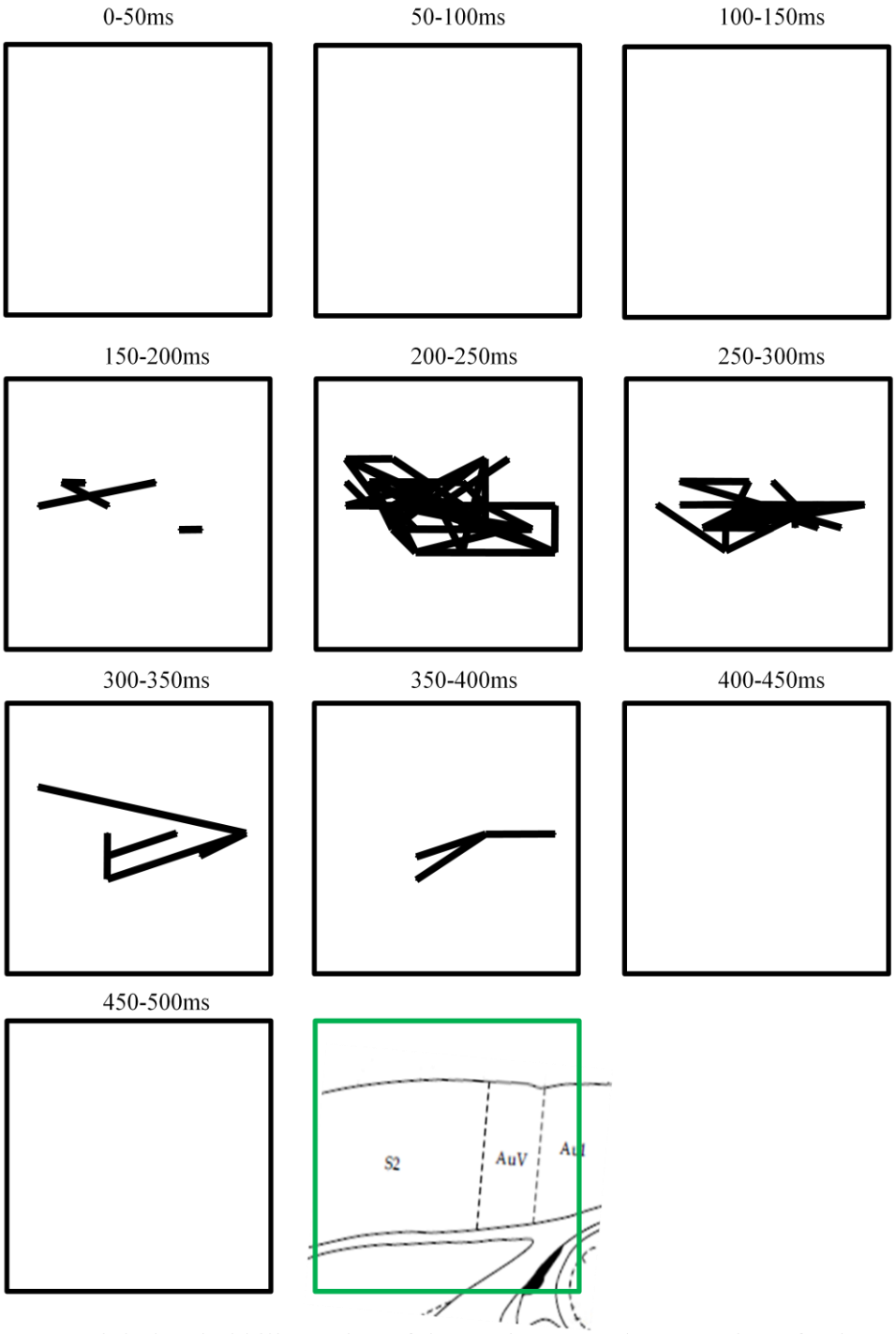

Fig. 5.25. High threshold illustration of the spatiotemporal progression of unit synchrony during a gabazine-induced paroxysmal discharge. Synchrony maps were generated for 50ms windows at 50ms intervals from the start (top left) to end (bottom left) of the 500ms time series, as labelled. In the synchrony maps the width of the line represents the inverse of the time distance to the nearest spike between pairs of units recorded from different electrodes in the 96 electrode Utah array. A high threshold is used in this example in the sense that only synchrony values greater than the mean plus 3 standard deviations of the synchrony in the most synchronous window are shown. The thickness of the dots represents the number of distinct units recorded in the channel. The array was oriented as shown (green square) in 2^{o} somatosensory cortex, with the top corresponding to superficial layers and the bottom to deep layers.

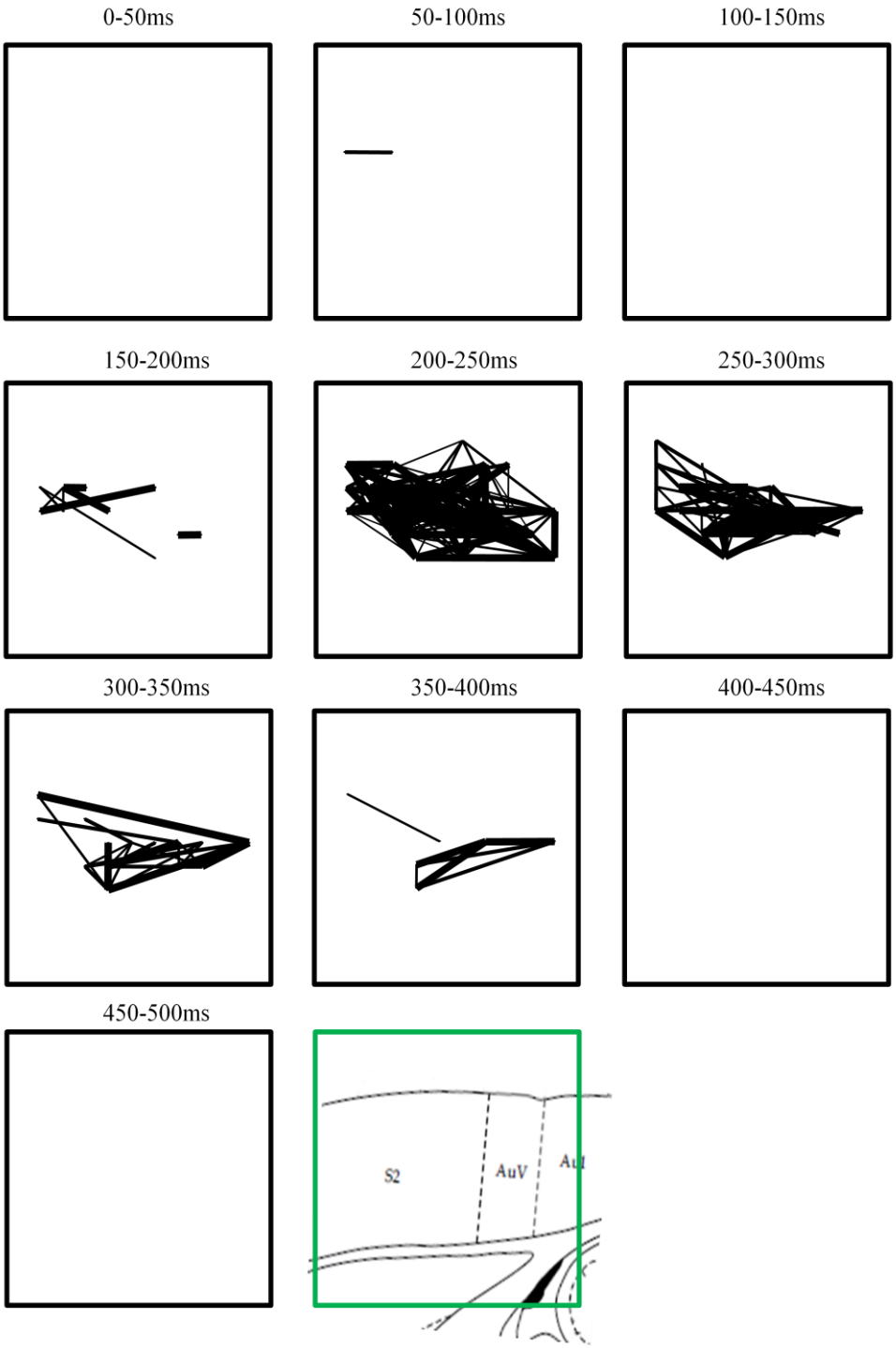

Fig. 5.26. Low threshold illustration of the spatiotemporal progression of unit synchrony during a gabazine-induced paroxysmal discharge. Synchrony maps were generated for 50ms windows at 50ms intervals from the start (top left) to end (bottom left) of the 500ms time series, as labelled. In the synchrony maps the width of the line represents the inverse of the time distance to the nearest spike between pairs of units recorded from different electrodes in the 96 electrode Utah array. A low threshold is used in this example in the sense that only synchrony values greater than the mean plus 1 standard deviation of the synchrony in the most synchronous window are shown. The thickness of the dots represents the number of distinct units recorded in the channel. The array was oriented as shown (green square) in 2^{o} somatosensory cortex, with the top corresponding to superficial layers and the bottom to deep layers.

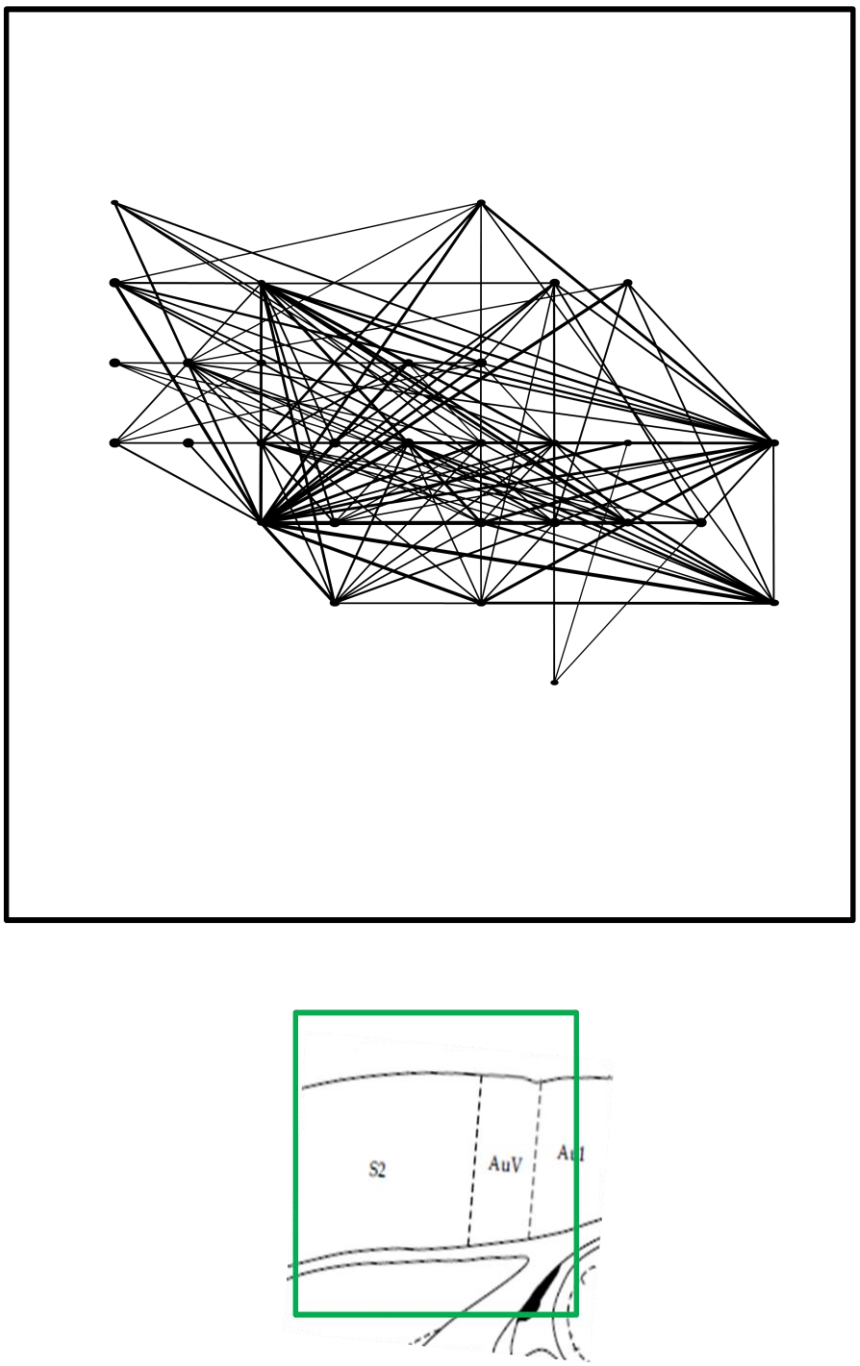

Fig. 5.27. Spike-spike correlations throughout a gabazine-induced paroxysmal discharge. Cross-correlations were performed between each pair of units from different electrodes in the 96 electrode Utah array. In the connectivity map the width of the line represents the synchrony as measured on the cross-correlogram where the central peak crossed the Y axis. Only synchrony values greater than the mean plus 3 standard deviations are shown. The connectivity map was generated for a 1s time window centred on the paroxysmal discharge. The thickness of the dots represents the number of distinct units recorded in the channel. The array was oriented as shown (green square) in 2^{o} somatosensory cortex, with the top corresponding to superficial layers and the bottom to deep layers.

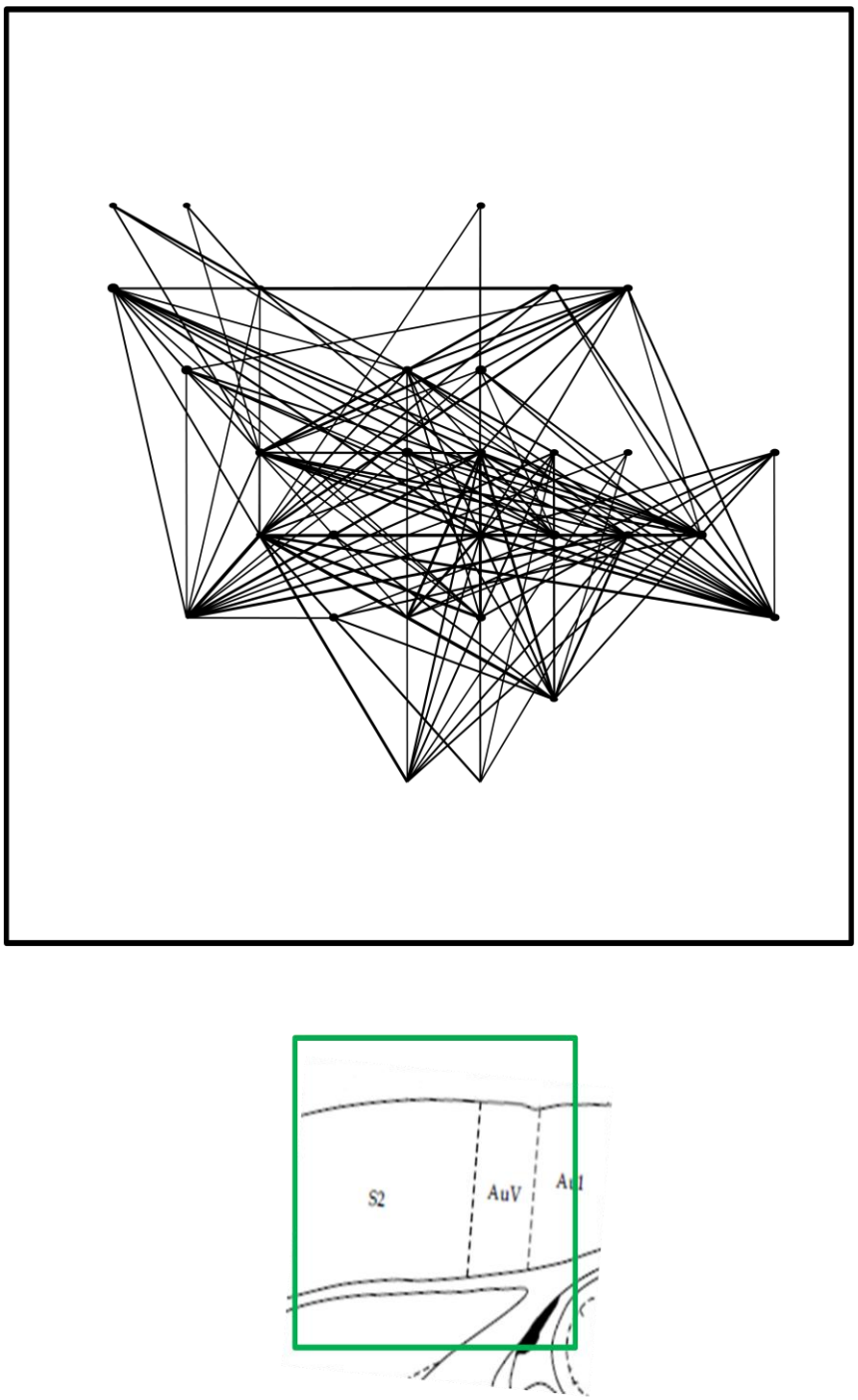

Fig. 5.28. Spike-field correlations throughout a gabazine-induced paroxysmal discharge. Cross-correlations were performed between unit spike rate histograms and LFPs for each unit and LFP combination in different electrodes in the 96 electrode Utah array. In the correlation map the width of the line represents the synchrony as measured on the cross-correlogram where the central peak crossed the Y axis. Only synchrony values greater than the mean plus 3 standard deviations are shown. The connectivity map was generated for a 1s time window centred on the paroxysmal discharge. The thickness of the dots represents the number of distinct units recorded in the channel. The array was oriented as shown (green square) in 2^{o} somatosensory cortex, with the top corresponding to superficial layers and the bottom to deep layers.

5.4 Discussion

Clozapine-related abnormal EEG activity is known to include slowing of activity, abnormal theta, abnormal delta, intermittent sharp transients, spike discharges and spike-wave paroxysms (e.g. Malow et al., 1994;Welch et al., 1994;Haring et al., 1994;Denney and Stevens, 1995;Freudenreich et al., 1997;Centorrino et al., 2002). In addition to the VFO events described in the previous chapter, clozapine also induced full paroxysmal discharges in 33% of rat brain slices *in vitro*. Clozapine-induced paroxysmal discharges in normal rat brain slices *in vitro* had a remarkably similar appearance to transient epileptiform spikes in EEG recordings from a psychiatric patient treated with clozapine (chapter 3).

Unlike VFO events, which were only weakly correlated with somatic intracellular activity, clozapine-induced paroxysmal discharges were clearly associated with spikes, EPSPs and IPSPs in layer V RS and IB cells. The association of compound EPSPs and IPSPs in layer V RS and IB cells with clozapine-induced paroxysmal events suggests that these events were mediated via network activity involving chemical synaptic transmission in both of these cell types. This is in line with the finding that paroxysmal events were more widely distributed spatially compared to the patches of clozapine-induced VFO, and idea that clozapine-induced full paroxysmal events represent a level of network hyperexcitability greater than that associated with clozapine-induced VFO alone.

Although units showed activity in superficial layers, a limitation in the approach taken was that intracellular recordings were not performed on cells in superficial layers. The deep EPSP/IPSP correlations with the field were relatively weak suggesting that activity may have been generated in superficial layers and projected deeper to layer V.

The presence of clozapine-induced full paroxysmal events in 2^{o} somatosensory cortex in the isolated microcircuitry of the *in vitro* slice preparation is further evidence for the particular sensitivity of this region of cortex in the generation of clozapine-related hyperexcitability. Furthermore, the presence of clozapine-induced paroxysmal events, generated *de novo* in normal brain tissue, further supports the idea that clozapine-related hyperexcitability is a direct effect of the drug rather than a consequence of compensation for abnormal activity in patients with psychiatric illness.

Taken together, spatiotemporal progression data for LFPs, spike rates, spike synchrony, and spike-spike correlations, and spike-field correlation data, suggested that clozapine-

induced paroxysmal events started superficially, moved deeper and then propagated along deep layers. It is possible that the absence of superficial activity in some examples may be explained in that the Utah electrode array grid may not have been positioned longitudinally in such as way that the relevant region of cortex was covered. In terms of spike-field correlations, correlations between superficial units and deeper LFPs were notable during paroxysmal events.

Interestingly, corresponding data suggested that gabazine-induced paroxysmal events also propagated along deep layers and there was some evidence of superficial recruitment. Similarities to some extent in the spatiotemporal progression of events lend some support to the idea that disinhibition may have a role in the mechanism underlying clozapine-induced paroxysmal discharges. However, gabazine-induced paroxysmal events in layer V had a different and more regular shape compared to those induced by clozapine, suggesting that partial disinhibition may not be sufficient in itself to precisely mimic clozapine-related hyperexcitability. Furthermore, intracells showed clear, large compound IPSPs, suggesting that clozapine may not have had a particularly detrimental effect on inhibition. Indeed, unit activity associated with gabazine was far more pronounced compared to that associated with clozapine suggesting that inhibition may be relatively spared.

The importance of deep layers in the propagation of paroxysmal discharges in this thesis is in line with the reduced inhibition in layer V of entorhinal cortex in brain slices from rats treated with pilocarpine (de Guzman et al., 2008). The longitudinal propagation of paroxysmal events along deep layers also further supported the idea that layer V is important in clozapine-related hyperexcitability. The superficial origin of paroxysmal discharges raises the question of the nature of any connection between the axonal hyperexcitability that may be related to clozapine-induced VFO in layer V and the superficial initiation of paroxysmal events. Furthermore, it is not known whether axonal spikes would show up in unit recordings. That is the VFO may be 'hidden' from Utah recordings, and this may explain why unit recording data implicate superficial layers, whereas deep layers appear important with respect to field and intracellular glass microelectrode data.

Following characterisation of clozapine-induced paroxysmal events *in vitro* in this chapter, and the lack of a direct correlation with purely $GABA_A$ dysfunction-mediated paroxysms, the next step was to investigate the pharmacology of clozapine-induced oscillatory activity further in the search for an underlying mechanism.

Chapter 6

Results – Pharmacology of clozapine-induced VFO and paroxysmal discharges

6.1 Introduction

Following the characterisation of clozapine-induced VFO (chapter 4) and clozapine-induced full paroxysmal events (chapter 5) in 2° somatosensory cortex, and also the lack of a direct correlation between clozapine-induced paroxysmal events and purely $GABA_A$ dysfunction-mediated paroxysms, this chapter further considers the pharmacology of clozapine-induced VFO and paroxysmal events in an attempt to identify an underlying mechanism.

Aims

The aims of this chapter are as follows:

- To investigate the effect of antagonism of ionotropic glutamate receptors on clozapine-induced VFO and paroxysmal discharges.
- To further investigate the effect of partial disinhibition on clozapine-induced VFO and paroxysmal discharges, and also, conversely, to investigate the effect of clozapine on VFO mediated by partial disinhibition.
- To investigate the effect of reducing gap junction conductance on clozapine-induced VFO and paroxysmal discharges.
- To investigate the effect of reducing gap junction conductance on synchrony of clozapine-induced VFO.
- To investigate the effect of agonism of nicotinic cholinergic receptors on clozapine-induced VFO, and also to investigate the effect of clozapine on VFO mediated by antagonism of nicotinic cholinergic receptors.

6.1.1 Mechanisms underlying clozapine-induced epileptiform activity

Possible mechanisms underlying clozapine-induced epileptiform activity include NMDA receptor agonism (see section 1.4.2.2-1.4.2.3, and below), suppression of $GABA_A$ receptors (section 1.4.2.1 and chapter 5), antagonism of neuronal nicotinic receptors (section 4.1.6 and 4.3.9), activity of fast-spiking interneurons (see section 1.5.1.2 and below), and electrotonic coupling of neurons through gap junctions (see section 1.5.1.2, 1.5.1.3 and 4.3.6, and below). With the lack of a direct correlation between clozapine-induced paroxysmal events and purely $GABA_A$ dysfunction-mediated paroxysms in the previous chapter, further investigation of the pharmacology of clozapine-induced epileptiform activity was warranted. Here, an advantage of the *in vitro* approach, the ability to readily perfuse brain slices with pharmacological agents,

irrespective of any deleterious effects at the whole organism level, was utilised to further investigate mechanisms underlying clozapine-induced VFO and paroxysmal discharges.

6.1.2 Evidence of a role for fast-spiking interneurons in the generation of VFO

When ripples were discovered it was observed that interneurons could discharge at the frequency of the field ripple, whereas individual pyramidal cell somata could not (Buzsaki et al., 1992).

Further observations were then made about the firing of identified interneurons. A histologically verified basket cell discharged at the frequency of ripples (Ylinen et al., 1995a). Basket cells and bistratified cells discharged in phase with ripples, axo-axonic interneurons fired immediately prior to and at the onset of a ripple, but then were silent, and cholecystokinin immunopositive basket cells and dendrite-targeting cells only discharged infrequently (Klausberger et al., 2003;Klausberger et al., 2004;Klausberger et al., 2005). Furthermore, phasic IPSPs, which occurred at the frequency of ripples, were observed in pyramidal cells (Ylinen et al., 1995a). Experimental alterations of the membrane potential and intracellular Cl^- were in line with the synaptic potentials being mediated by $GABA_A$ receptors (Ylinen et al., 1995a).

More recently, *in vivo* recordings in the human hippocampus demonstrated an association between field VFO and interneuron activity (Le Van et al., 2008).

Taken together, the data above have led to the suggestion that networks of fast-spiking interneurons generate ripple oscillations, but other evidence suggests that alternative explanations are possible.

6.1.3 Evidence of a role for NMDA receptors in the generation of epileptiform activity

As mentioned previously, clozapine may act on NMDA receptors (section 1.4.2.2). In this section evidence of a role for NMDA receptors in the generation of epileptiform activity is considered.

The use of Mg^{2+} free medium induces epileptiform activity in rat hippocampus and entorhinal cortex, which is dependent on activity of NMDA receptors (Walther et al., 1986;Mody et al., 1987;Jones and Lambert, 1990b). Similarly, low extracellular Mg^{2+}

also induces NMDA receptor-dependent ictal activity in slices from epileptic human neocortex (Avoli et al., 1991).

In another model, it has been reported that the K^+ channel blocker 4-aminopyridine (4AP) can induce epileptiform activity in rat entorhinal cortex, and the ictal discharges but not interictal discharges or slow field potentials were abolished by antagonism of NMDA receptors (Avoli et al., 1996a).

In a model of epilepsy where the extracellular K^+ concentration is modulated, blockade of AMPA and NMDA ionotropic glutamate receptors abolishes fast ripples in rat hippocampal slices (Dzhala and Staley, 2004). In this model it was thought that synchronous bursts in pyramidal cells and similar intrinsic firing patterns among local neurons were required for fast ripples, and that this synchronous activity depended on fast glutamatergic synaptic transmission.

6.1.4 Pharmacological evidence of a role for both NMDA receptors and gap junctions in the generation of epileptiform activity

In some cases both NMDA receptors and gap junctions are implicated in the generation of epileptiform activity.

In neocortical slices surgically removed from patients with focal cortical dysplasia, spontaneous events, comprising fast negative transients or fast transients superimposed on a slower negative shift, occur *in vitro* (Gigout et al., 2006). These events are reversibly abolished by either antagonism of NMDA receptors or reduced gap junction conductance, suggesting a role for both chemical synaptic transmission and electrotonic coupling of neurons through gap junctions in the mechanism.

Furthermore, in these slices application of the K^+ channel blocker 4-aminopyridine (4AP) induces ictal-like activity mediated by both NMDA receptor conductances (Avoli et al., 1999) and gap junctions (Gigout et al., 2006).

6.1.5 Pharmacological evidence of a role for gap junctions in the generation of VFO and epileptiform activity

Here evidence that suggests that VFO may not be mediated through conventional chemical synaptic transmission, but is instead dependent solely on electrotonic coupling of neurons through gap junctions, is considered.

Firstly, the idea of a role for interneurons in the generation of VFO is challenged by findings that VFO persist following blockage of $GABA_A$ receptors *in vitro* and *in vivo* (Maier et al., 2003;Jones and Barth, 2002;Roopun et al., 2010b). For example, VFO superimposed on rat somatosensory cortex potentials evoked by whisker stimulation persist and actually occur more following topical application of the $GABA_A$ receptor antagonist bicuculline (Jones and Barth, 2002). Furthermore, there is no evidence of phasic IPSPs in intracellular recordings from a putative pyramidal cell during sharp wave/ripples induced by application of higher than normal concentrations of KCl in mouse hippocampal slices when $GABA_A$ receptors are blocked (Nimmrich et al., 2005).

Secondly, hippocampal VFO *in vitro* persist following blockade of $GABA_A$, AMPA and NMDA receptors together (Draguhn et al., 1998;Nimmrich et al., 2005). Furthermore, VFO persist when nominally calcium-free artificial cerebrospinal fluid is used to block calcium-dependent synaptic transmission (Draguhn et al., 1998). VFO induced by ejection of a concentrated K^+ solution in the dentate gyrus also occurs in Ca^{2+}-free artificial cerebrospinal fluid (Towers et al., 2002). Thus, these VFO do not require conventional chemical synaptic neurotransmission at the synapse.

Thirdly, drugs that reduce gap junction conductance can block VFO. For example, the gap junction blockers carbenoxolone, octanol and halothane each reversibly suppress spontaneous hippocampal VFO *in vitro* (Draguhn et al., 1998). Another example is that five different gap junction blockers, with diverging effects on intrinsic membrane conductances, each reduced cerebellar VFO *in vitro* (Middleton et al., 2008).

Further evidence of a role for gap junctions in epileptiform activity is that various studies using both *in vivo* and *in vitro* models of epilepsy demonstrate that carbenoxolone and other gap junction blocking agents suppress seizure discharges (Gareri et al., 2004;Gigout et al., 2006;He et al., 2009;Jahromi et al., 2002;Kohling et al., 2001;Nilsen et al., 2006;Perez-Velazquez et al., 1994;Ross et al., 2000;Szente et al., 2002).

In one example, spontanous VFO associated with interictal discharges occur in small sections of human tissue surgically removed from epileptic neocortex and maintained *in vitro* (Roopun et al., 2010b). Partial disinhibition markedly attenuates the slow component of interictal discharges but does not affect VFO. Thus, synaptic inhibition influences the slow envelope of the interictal discharge but is not required for the generation of VFO itself. In contrast, the gap junction blocker carbenoxolone reversibly abolishes both the slow interictal envelope and VFO.

In a model of glial cell dysfunction in epileptic foci, pressure ejection of alkaline solution in layer V of rat frontal neocortex *in vitro* results in runs of fast oscillations, termed 'glissandi', where the frequency accelerates from ~30-40 to > 120Hz over a few seconds (Cunningham et al., 2012). These glissandi persist following blockade of AMPA, NMDA, and $GABA_{A\ \&\ B}$ receptors, suggesting that chemical synaptic transmission is not required but that instead there may be a role for some form of nonchemical intercellular transmission- namely the interaction between gap junction-mediated coupling and intrinsic membrane properties afforded by m-current.

The alkanization of layer V also generates ictal events, which, in contrast, are abolished by the chemical synaptic blockers (Cunningham et al., 2012).

There is further evidence of non-synaptic electrical signalling between neurons in a study in which mossy fibre activation evokes spikelets in pyramidal cells in the CA3 region of the hippocampus (Vivar et al., 2012). The spikelets occur in the presence of glutamate, $GABA_A$ and acetylcholine M_1 antagonists but are attenuated by the gap junction blocker carbenoxolone, suggesting that mossy fibres can communicate with pyramidal cells via electrical signalling.

6.2 Methods

Experiments in this chapter made use of rat brain slice preparations *in vitro*. Slices were 450µm thick sections of 2° somatosensory cortex cut in the horizontal plane from adult male Wistar rats (150-250g). Slices were prepared according to section 2.1-2.3 and the maintenance of slices is described in section 2.4. Extracellular recording techniques are described in section 2.6.1. Data acquisition, data analysis and statistical techniques are described in section 2.7-2.8.

VFO events were induced by either clozapine, gabazine or d-tubocurarine according to the experiment. The area power in the VFO band (70-1000Hz) was the primary measure used to quantify extracellular recordings of VFO in LFPs.

Paroxysmal discharges were induced by clozapine and were quantified in terms of their amplitude and frequency. In general these discharges were defined as distinct from VFO as they had large-amplitude, lower frequency components.

Pharmacological compounds were bath applied to slices for at least 1 hour to ensure sufficient time for any effect to take place, except in the case of octanol where VFO were sometimes abolished in shorter timescales.

6.3 Results

In a continued search for underlying mechanisms, the effect of pharmacological agents on clozapine-induced VFO in layer V of 2º somatosensory cortex *in vitro* was investigated.

6.3.1 The role of fast glutamatergic synaptic transmission in clozapine-induced VFO

Bath application of NBQX (20µM), which antagonises the AMPA/kainate subtypes of glutamate receptor, had no significant effect on the median VFO band area power of clozapine-induced fast activity (median control VFO band area power 8.84 (1.45 → 35.60) $10^{-11}V^2$, with NBQX 5.10 (1.64 → 42.70) $10^{-11}V^2$, $p > 0.05$, $n = 5$, Wilcoxon signed-rank test, Fig. 6.1). NBQX also had no significant effect on the mean peak frequency of clozapine-induced VFO (mean control peak frequency 186 ± 21 Hz, NBQX 194 ± 22 Hz, $p > 0.05$, $n = 5$, paired t-test, Fig. 6.1).

D-AP5 (50µM), which antagonises the NMDA subtype of glutamate receptor, also had no significant effect on the mean VFO band area power of clozapine-induced fast activity (mean control VFO band area power 2.03 ± 0.72 $10^{-10}V^2$, D-AP5 1.76 ± 0.64 $10^{-10}V^2$, $p > 0.05$, $n = 5$, paired t-test, Fig. 6.2). D-AP5 also had no significant effect on the mean peak frequency of clozapine-induced VFO (mean control peak frequency 227 ± 30 Hz, D-AP5 214 ± 27, $p > 0.05$, $n = 5$, paired t-test, Fig. 6.2).

6.3.2 The role of GABAergic fast synaptic transmission in clozapine-induced VFO

The $GABA_A$ receptor antagonist gabazine (500nM) was associated with a non-significant increase in the mean VFO band area power of clozapine-induced fast activity (mean control VFO band area power 8.34 ± 3.42 $10^{-11}V^2$, gabazine 1.17 ± 0.48 $10^{-10}V^2$, $p > 0.05$, n = 5, paired t-test, Fig. 6.3). Gabazine was also associated with a non-significant decrease in the median peak frequency of clozapine-induced VFO (median control peak frequency 156 (147 → 182) Hz, gabazine 120 (116 → 152) Hz, $p > 0.05$, n = 5, Wilcoxon signed-rank test, Fig. 6.3).

To further investigate a possible role for $GABA_A$ receptors in clozapine-induced VFO, and in light of the finding that gabazine (250nM) induced VFO in layer V of 2º somatosensory cortex (section 4.3.8), it was interesting to consider the converse situation, namely the effect of clozapine on gabazine-induced VFO. Clozapine was associated with a non-significant reduction in the mean VFO band area power of gabazine-induced fast activity (mean control gabazine-induced VFO band area power 1.66 ± 1.05 $10^{-10}V^2$, clozapine 8.80 ± 3.73 $10^{-11}V^2$, $p > 0.05$, n = 5, paired t-test, Fig. 6.4). Clozapine was also associated with a non-significant decrease in the median peak frequency of gabazine-induced VFO (median control gabazine-induced peak frequency 225 (206 → 255) Hz, clozapine 186 (147 → 211) Hz, $p > 0.05$, n = 5, Wilcoxon signed-rank test, Fig. 6.4).

6.3.3 The role of gap junctions in clozapine-induced VFO

6.3.3.1 The effect of the gap junction blocker carbenoxolone on clozapine-induced VFO

Unexpectedly, the gap junction blocker carbenoxolone (200µM) had no significant effect on the mean VFO band area power of clozapine-induced fast activity (mean control VFO band area power 1.42 ± 0.58 $10^{-10}V^2$, carbenoxolone 1.62 ± 0.87 $10^{-10}V^2$, $p > 0.05$, n = 5, paired t-test, Fig. 6.5). Higher concentrations of carbenoxolone (400µM, n = 4; 800µM, n = 3) also failed to abolish clozapine-induced VFO (data not shown). Carbenoxolone (200µM) had no significant effect on the mean peak frequency of clozapine-induced VFO (mean control peak frequency 202 ± 15 Hz, carbenoxolone 194 ± 12 Hz, $p > 0.05$, n = 5, paired t-test, Fig. 6.5).

The effect of carbenoxolone (100µM) on synchrony between clozapine-induced VFO rhythms along layer V of 2º somatosensory cortex was also investigated (Fig. 6.6).

Following discovery of an optimal patch of clozapine-induced VFO with one glass microelectrode, a second glass microelectrode was moved distances between 100 and 900µm from the reference electrode in a longitudinal direction along layer V of 2º somatosensory cortex. Synchrony within bursts was measured at each 200µm step by performing cross-correlation analysis on the first burst event in a 60s trace. The point in the cross-correlogram where the central peak crossed the Y axis was used as a measure of the synchrony between the two rhythms. Following application of carbenoxolone (100µM), synchrony measurements were repeated and it was found that synchrony was slightly reduced at each 200µm interval from 100µm to 900µm along layer V. However, the change did not reach significance in the present study ($p > 0.05$, $n = 5$, Two-way ANOVA, Fig. 6.6).

6.3.3.2 The effect of blockade of the gap junction protein connexin36 on clozapine-induced VFO

Quinine (100µM), which blocks the gap junction protein connexin36, had no significant effect on the median VFO band area power of clozapine-induced fast activity (median control VFO band area power 8.39 (3.94 → 48.00) $10^{-11}V^2$, quinine 7.84 (5.34 → 54.40) $10^{-11}V^2$, $p > 0.05$, $n = 6$, Wilcoxon signed-rank test, Fig. 6.7).

Interestingly, quinine appeared to be associated with a small (2.9 %) but significant reduction in the median peak frequency of clozapine-induced VFO (median control peak frequency 172 (171 → 249) Hz, quinine 167 (166 → 171) Hz, $p > 0.05$, $n = 6$, Wilcoxon signed-rank test, Fig. 6.7). The reduction in peak frequency associated with quinine occurred in each experiment ($n = 6$).

6.3.3.3 The gap junction blocker octanol reversibly abolished clozapine-induced VFO

The gap junction blocker octanol (1mM) significantly attenuated clozapine-induced VFO (median control VFO band area power 9.17 (6.58 → 16.80) $10^{-11}V^2$, octanol 1.7 (1.08 → 3.29) $10^{-11}V^2$, $p < 0.05$, $n = 7$, Wilcoxon signed-rank test, Fig. 6.8). In those experiments where 1mM octanol incompletely reduced VFO, 2mM octanol was sufficient to reach near-total abolition. Following washout of octanol, VFO recovered ($n = 4$).

Octanol (1mM) had no significant effect on the median peak frequency of clozapine-induced VFO (median control peak frequency 232 (172 → 267) Hz, octanol 234 (184 → 256) Hz, $p > 0.05$, $n = 7$, Wilcoxon signed-rank test, Fig. 6.8).

6.3.4 The role of nicotinic receptors in clozapine-induced VFO

In light of the inhibition of neuronal nicotinic receptors by clozapine (Grinevich et al., 2009), and the finding in this thesis that, similar to clozapine, the broad-spectrum nicotinic receptor antagonist d-tubocurarine (d-TC) induced VFO in layer V of 2º somatosensory cortex (section 4.3.9), it was interesting to investigate the effect of the agonist nicotine on clozapine-induced VFO. Three concentrations of nicotine were used: 10nM, 5µM and 10µM.

Nicotine (10nM) had no significant effect on the mean VFO band area power of clozapine-induced fast activity (mean control VFO band area power $7.15 \pm 2.45\ 10^{-11}V^2$, nicotine (10nM) $5.38 \pm 1.95\ 10^{-11}V^2$, $p > 0.05$, $n = 5$, paired t-test, Fig. 6.9). Nicotine (10nM) also had no significant effect on the mean peak frequency of clozapine-induced VFO (mean control peak frequency 216 ± 30 Hz, nicotine (10nM) 216 ± 34 Hz, $p > 0.05$, $n = 5$, paired t-test, Fig. 6.9).

Similarly, nicotine (5µM) had no significant effect on the mean VFO band area power of clozapine-induced fast activity (mean control VFO band area power $7.28 \pm 1.69\ 10^{-11}V^2$, nicotine (5µM) $7.90 \pm 2.01\ 10^{-11}V^2$, $p > 0.05$, $n = 5$, paired t-test, Fig. 6.10). Nicotine (5µM) also had no significant effect on the mean peak frequency of clozapine-induced VFO (mean control peak frequency 212 ± 22 Hz, nicotine (5µM) 220 ± 17 Hz, $p > 0.05$, $n = 5$, paired t-test, Fig. 6.10).

Likewise, nicotine (10µM) had no significant effect on the mean VFO band area power of clozapine-induced fast activity (mean control VFO band area power $7.28 \pm 1.69\ 10^{-11}V^2$, nicotine (10µM) $7.51 \pm 1.97\ 10^{-11}V^2$, $p > 0.05$, $n = 5$, paired t-test, Fig. 6.11). Nicotine (10µM) also had no significant effect on the mean peak frequency of clozapine-induced VFO (mean control peak frequency 212 ± 22 Hz, nicotine (10µM) 214 ± 16 Hz, $p > 0.05$, $n = 5$, paired t-test, Fig. 6.11).

To further investigate a possible role for nicotinic receptors in clozapine-induced VFO, and in light of the finding that d-tubocurarine (10µM) induced VFO in layer V of 2º somatosensory cortex (section 4.3.9), it was interesting to consider the effect of clozapine on d-tubocurarine-induced VFO. Clozapine (20µM) had no significant effect

on the mean VFO band area power of d-tubocurarine-induced fast activity (mean control d-tubocurarine-induced VFO band area power 1.82 ± 0.90 $10^{-10}V^2$, clozapine 1.55 ± 0.79 $10^{-10}V^2$, $p > 0.05$, n = 5, paired t-test, Fig. 6.12). Clozapine also had no significant effect on the mean peak frequency of d-tubocurarine-induced VFO (mean control d-tubocurarine-induced peak frequency 192 ± 5 Hz, clozaine 175 ± 11 Hz, $p > 0.05$, n = 5, paired t-test, Fig. 6.12).

A summary of the pharmacology of clozapine-induced VFO is shown in Fig. 6.13.

6.3.5 The pharmacology of clozapine-induced paroxysmal discharges

Following investigation of the pharmacology of clozapine-induced VFO in layer V of 2º somatosensory cortex *in vitro*, the effect of pharmacological inhibitors on paroxysmal discharges, when present in the traces, was also analysed in an attempt to further elucidate mechanisms.

6.3.5.1 The role of fast glutamatergic synaptic transmission in clozapine-induced paroxysmal discharges

Clozapine-induced paroxysmal discharges were present in 2/5 slices in the data set for the AMPA/kainate glutamate receptor antagonist NBQX. Bath application of NBQX (20µM) appeared to reduce both the frequency (mean control events per minute 1.63 ± 0.97, NBQX 0.97 ± 0.63, n = 2, Fig. 6.14A) and amplitude (mean control event amplitude 324 ± 105 µV, NBQX 234 ± 92.5 µV, n = 2, Fig. 6.14B, C) of paroxysmal events.

Clozapine-induced paroxysmal discharges were not present in the first place in any slices in the data set for the NMDA receptor antagonist D-AP5, so analysis of the effect of antagonism of this receptor was not possible.

6.3.5.2 The role of GABAergic fast synaptic transmission in clozapine-induced paroxysmal discharges

Clozapine-induced paroxysmal discharges were present in 4/5 slices in the data set for the $GABA_A$ receptor antagonist gabazine. Gabazine (500nM) was associated with a non-significant increase in both the frequency (mean control events per minute 2.75 ± 0.60, gabazine 6.67 ± 1.99, $p > 0.05$, n = 4, paired t-test, Fig. 6.15A) and amplitude (mean control event amplitude 189 ± 34 µV, gabazine 995 ± 435 µV, $p > 0.05$, n = 4, paired t-test, Fig. 6.15B, C) of paroxysmal events. Following application of gabazine,

there was an interaction between VFO and paroxysmal discharges in 2/4 (50%) slices whereby VFO were prominent at the start of the event and then temporarily suspended for ~4s during and after the event (Fig. 6.16).

6.3.5.3 The role of gap junctions in clozapine-induced paroxysmal discharges

Clozapine-induced paroxysmal discharges were present in: 2/6 slices in the data set for quinine, which blocks the gap junction protein connexin36; 3/5 slices in the data set for the gap junction blocker octanol; but none of the slices in the data set for the gap junction blocker carbenoxolone.

Quinine (100nM) had no apparent effect on the mean frequency of paroxysmal events (mean control events per minute 2.50 ± 1.50, quinine 2.50 ± 0.83, n = 2, Fig. 6.17A). Quinine also had no apparent effect on the mean amplitude of paroxysmal events (mean control event amplitude 263 ± 4 µV, quinine 245 ± 97 µV, n = 2, Fig. 6.17B, C).

Octanol (1mM) had no significant effect on the mean frequency of paroxysmal events (mean control events per minute 3.00 ± 0.51, octanol 3.44 ± 0.29, $p > 0.05$, n = 3, paired t-test, Fig. 6.18A). Octanol was, however, associated with a non-significant reduction in the amplitude of paroxysmal events (mean control event amplitude 152 ± 23 µV, octanol 68 ± 36 µV, $p > 0.05$, n = 3, paired t-test, Fig. 6.18B, C).

A summary of the pharmacology of clozapine-induced paroxysmal discharges is shown in Fig. 6.19.

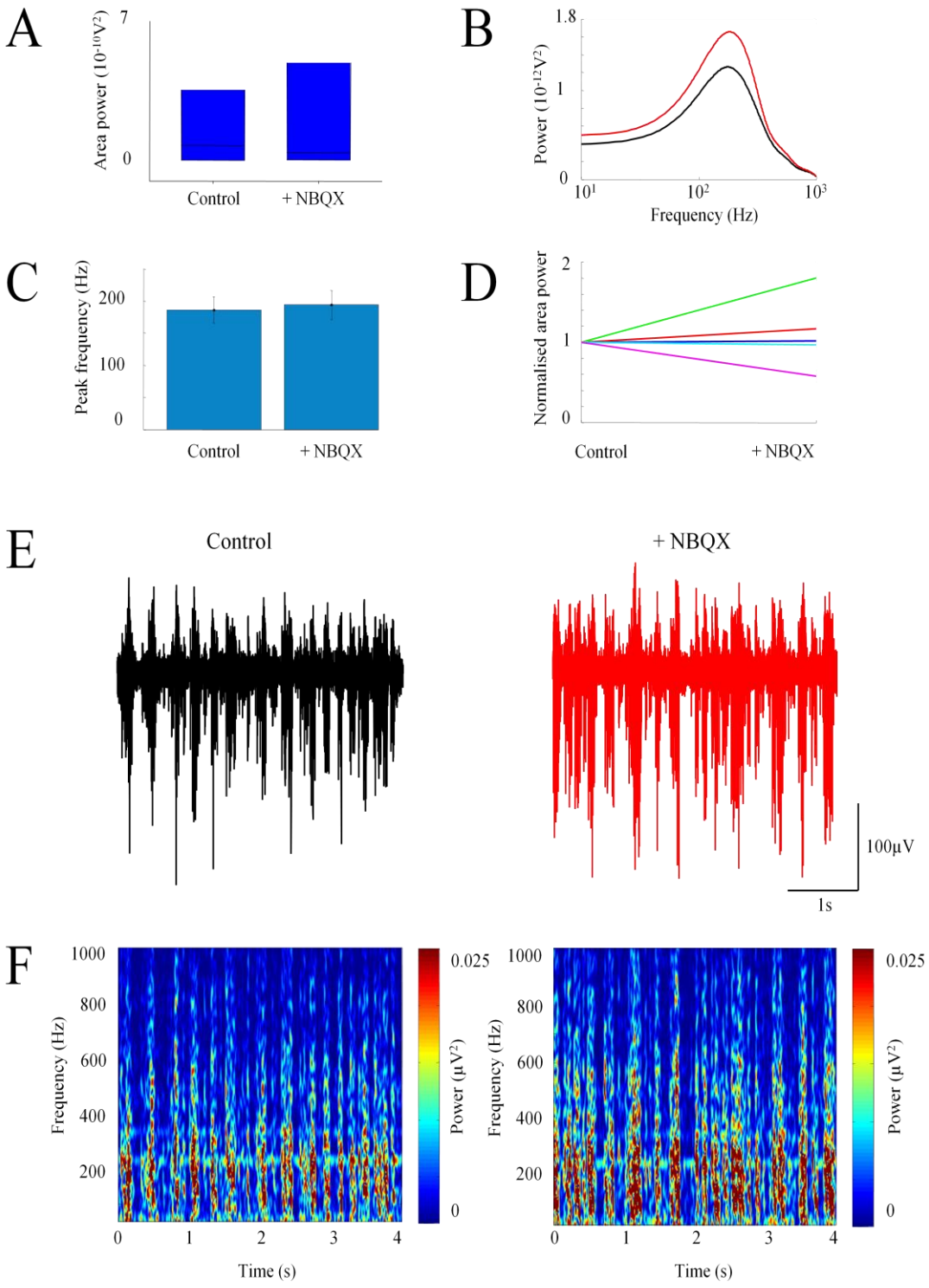

Fig. 6.1. Effect of antagonism of the AMPA/kainate subtypes of glutamate receptor on clozapine-induced VFO (n = 5 slices). (*A*) Box plot showing median VFO band area power (Q1→Q3). (*B*) VFO band pooled power spectra (black line, control; red line, NBQX). (*C*) Bar chart showing VFO band peak frequency (mean ± SEM). (*D*) Line graph illustrating VFO band area power data in individual experiments. Example field traces (*E,* 4s duration, 60-1000Hz band-pass filtered), and corresponding spectrograms (*F*), are shown, before (left) and after (right) bath application of NBQX (20µM).

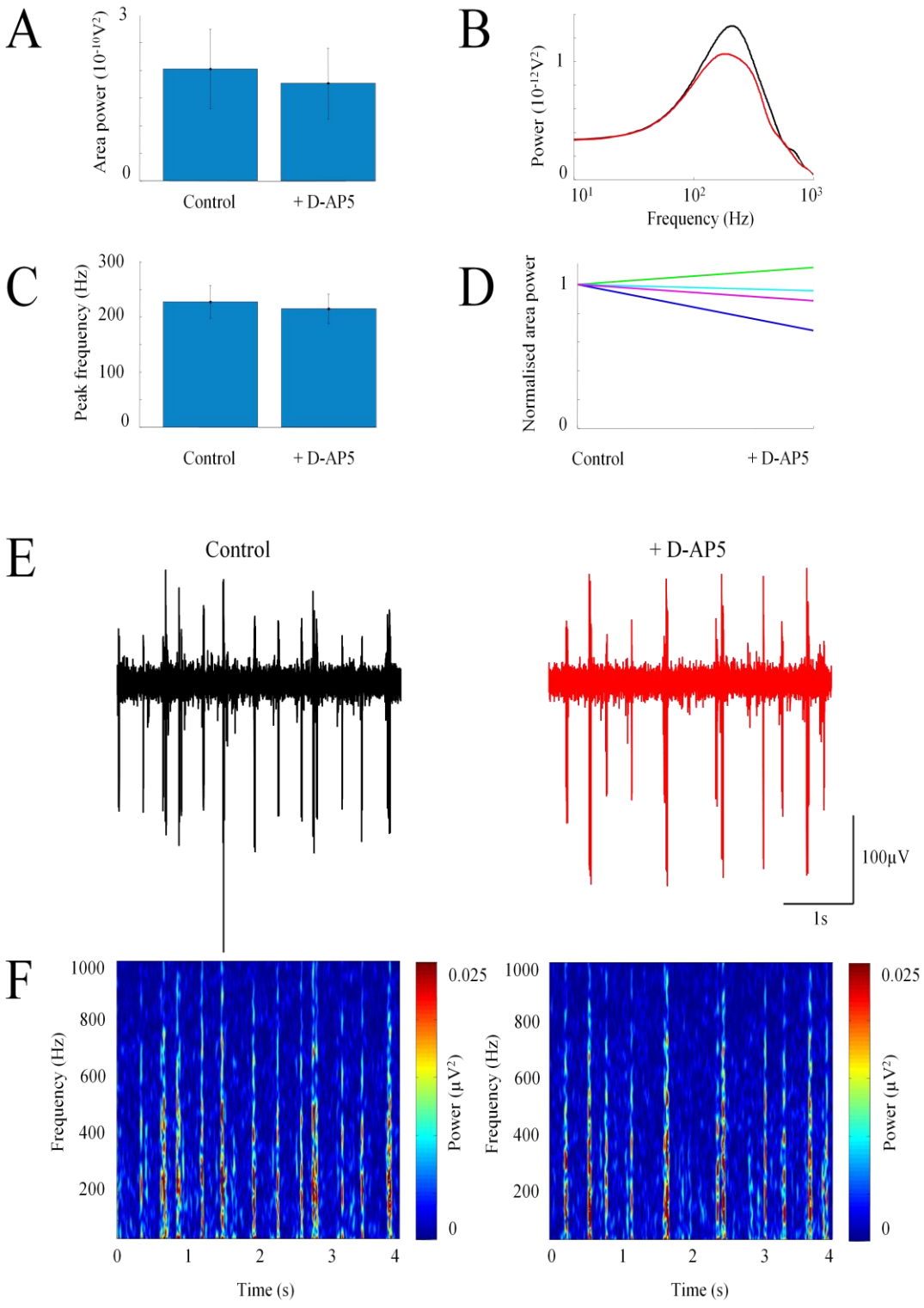

Fig. 6.2. Effect of antagonism of the NMDA subtype of glutamate receptor on clozapine-induced VFO (n = 5 slices). (*A*) Bar chart showing VFO band area power (mean ± SEM). (*B*) VFO band pooled power spectra (black line, control; red line, D-AP5). (*C*) Bar chart showing VFO band peak frequency (mean ± SEM). (*D*) Line graph illustrating VFO band area power data in individual experiments. Example field traces (*E,* 4s duration, 60-1000Hz band-pass filtered), and corresponding spectrograms (*F*), are shown, before (left) and after (right) bath application of D-AP5 (50µM).

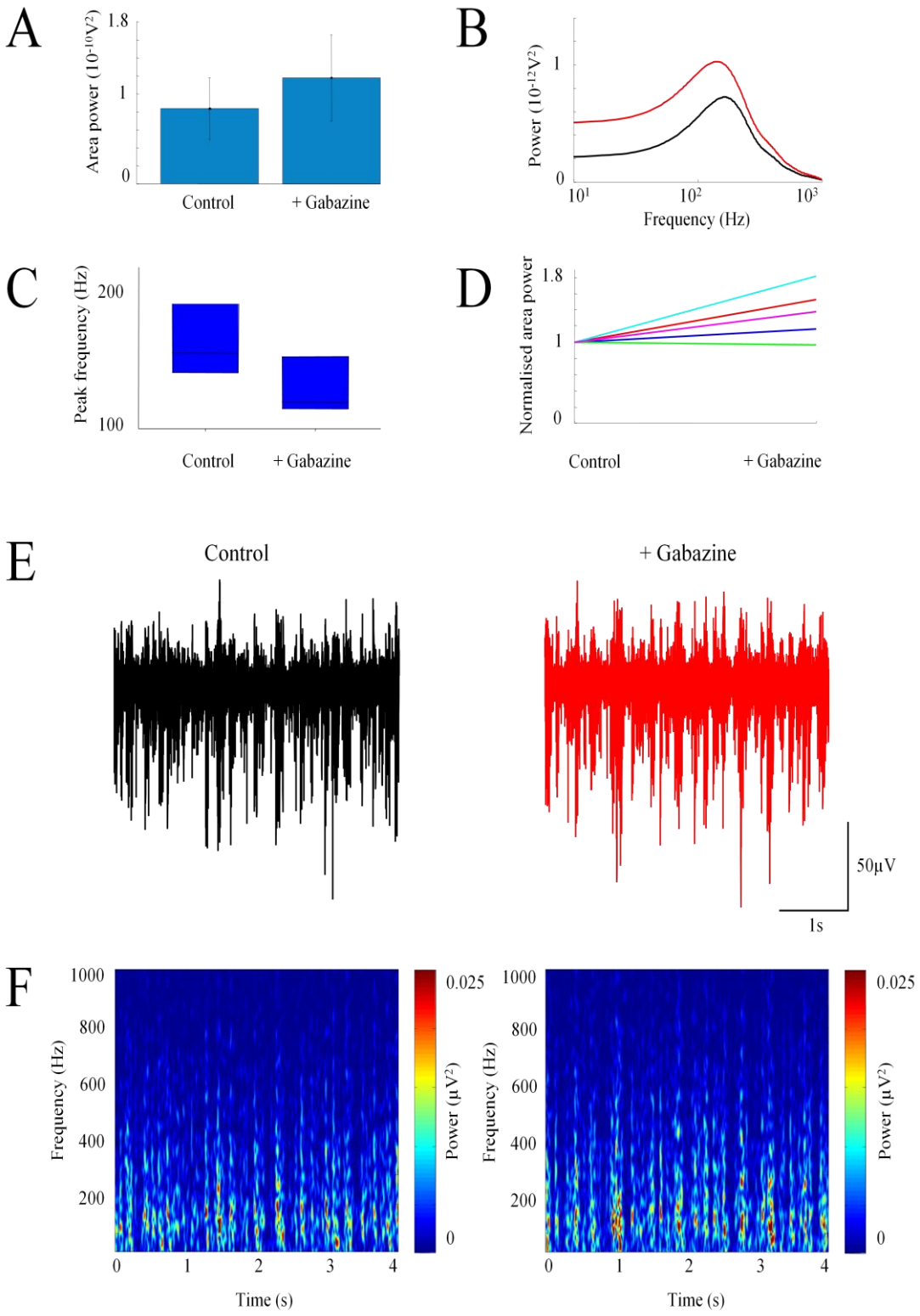

Fig. 6.3. Effect of antagonism of $GABA_A$ receptors on clozapine-induced VFO (n = 5 slices). (*A*) Bar chart showing VFO band area power (mean ± SEM). (*B*) VFO band pooled power spectra (black line, control; red line, gabazine). (*C*) Box plot showing median VFO band peak frequency (Q1 → Q3). (*D*) Line graph illustrating VFO band area power data in individual experiments. Example field traces (*E,* 4s duration, 60-1000Hz band-pass filtered), and corresponding spectrograms (*F*), are shown, before (left) and after (right) bath application of gabazine (500nM).

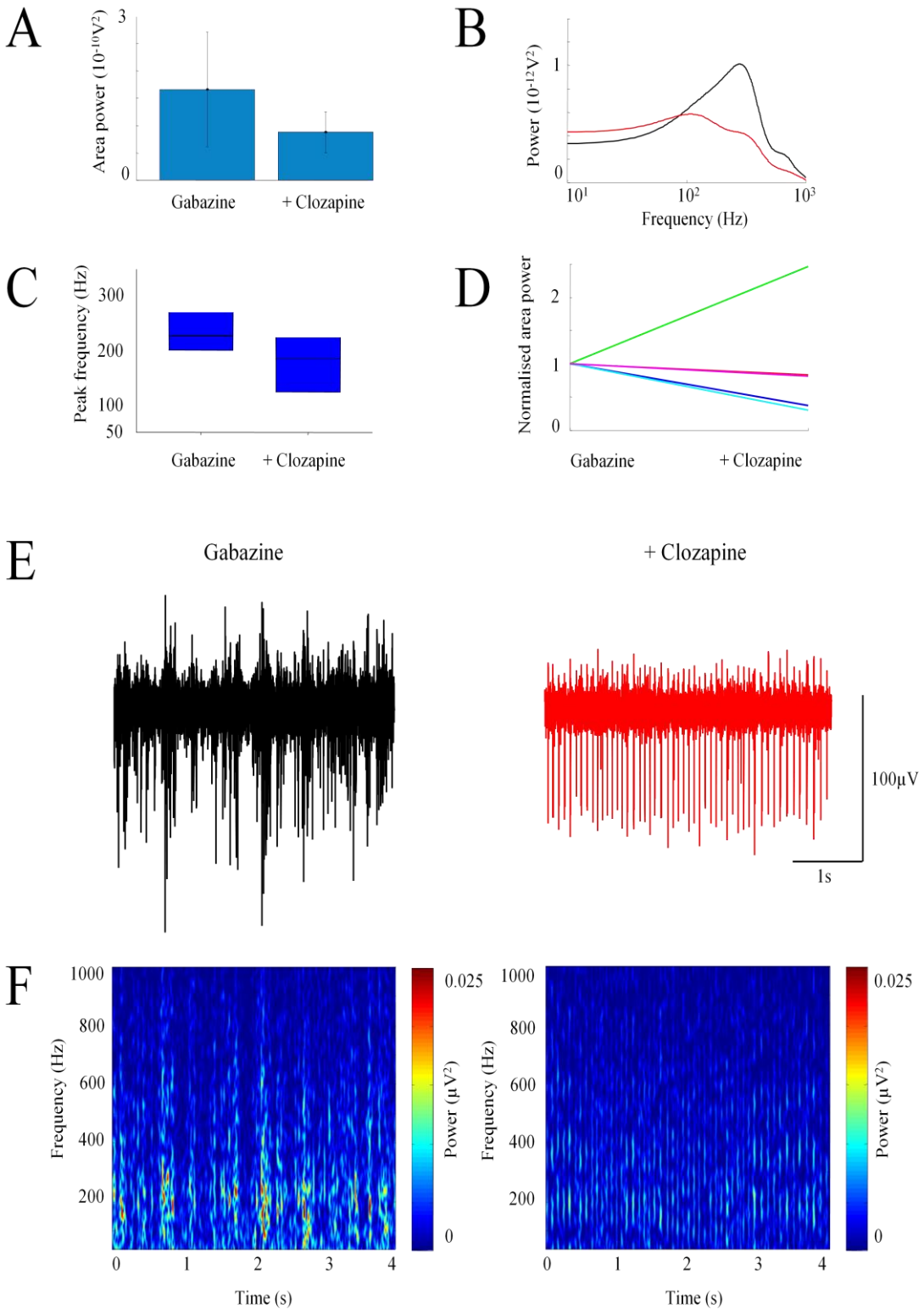

Fig. 6.4. Effect of clozapine (20µM) on gabazine-induced VFO (n = 5 slices). (*A*) Bar chart showing VFO band area power (mean ± SEM). (*B*) VFO band pooled power spectra (black line, gabazine; red line, + clozapine). (*C*) Box plot showing median VFO band peak frequency (Q1→Q3). (*D*) Line graph illustrating VFO band area power data in individual experiments. Example field traces (*E*, 4s duration, 60-1000Hz band-pass filtered), and corresponding spectrograms (*F*), are shown, before (left) and after (right) bath application of clozapine.

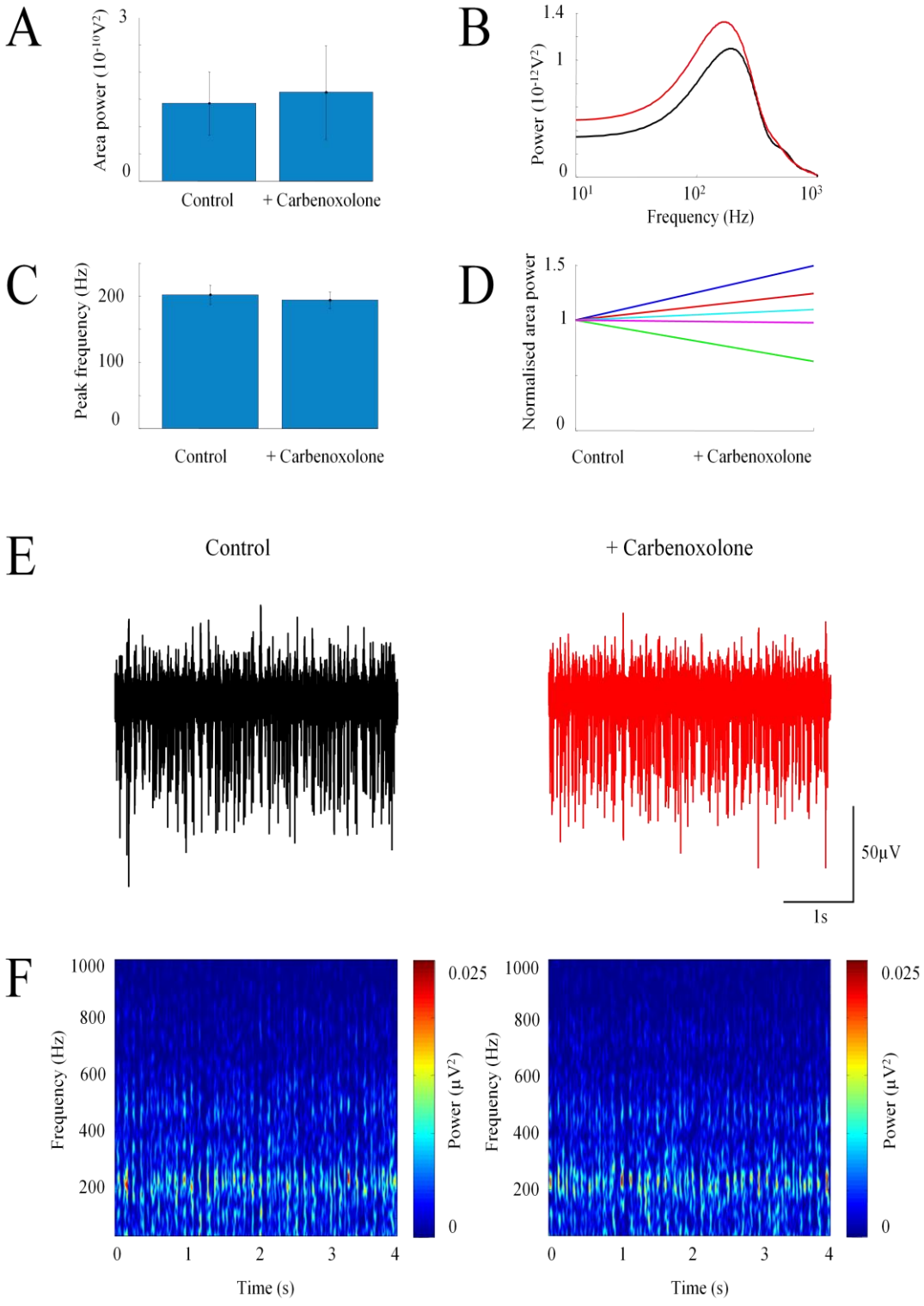

Fig. 6.5. Effect of the gap junction blocker carbenoxolone (200µM) on clozapine-induced VFO (n = 5 slices). (*A*) Bar chart showing VFO band area power (mean ± SEM). (*B*) VFO band pooled power spectra (black line, control; red line, carbenoxolone). (*C*) Bar chart showing VFO band peak frequency (mean ± SEM). (*D*) Line graph illustrating VFO band area power data in individual experiments. Example field traces (*E,* 4s duration, 60-1000Hz band-pass filtered), and corresponding spectrograms (*F*), are shown, before (left) and after (right) bath application of carbenoxolone.

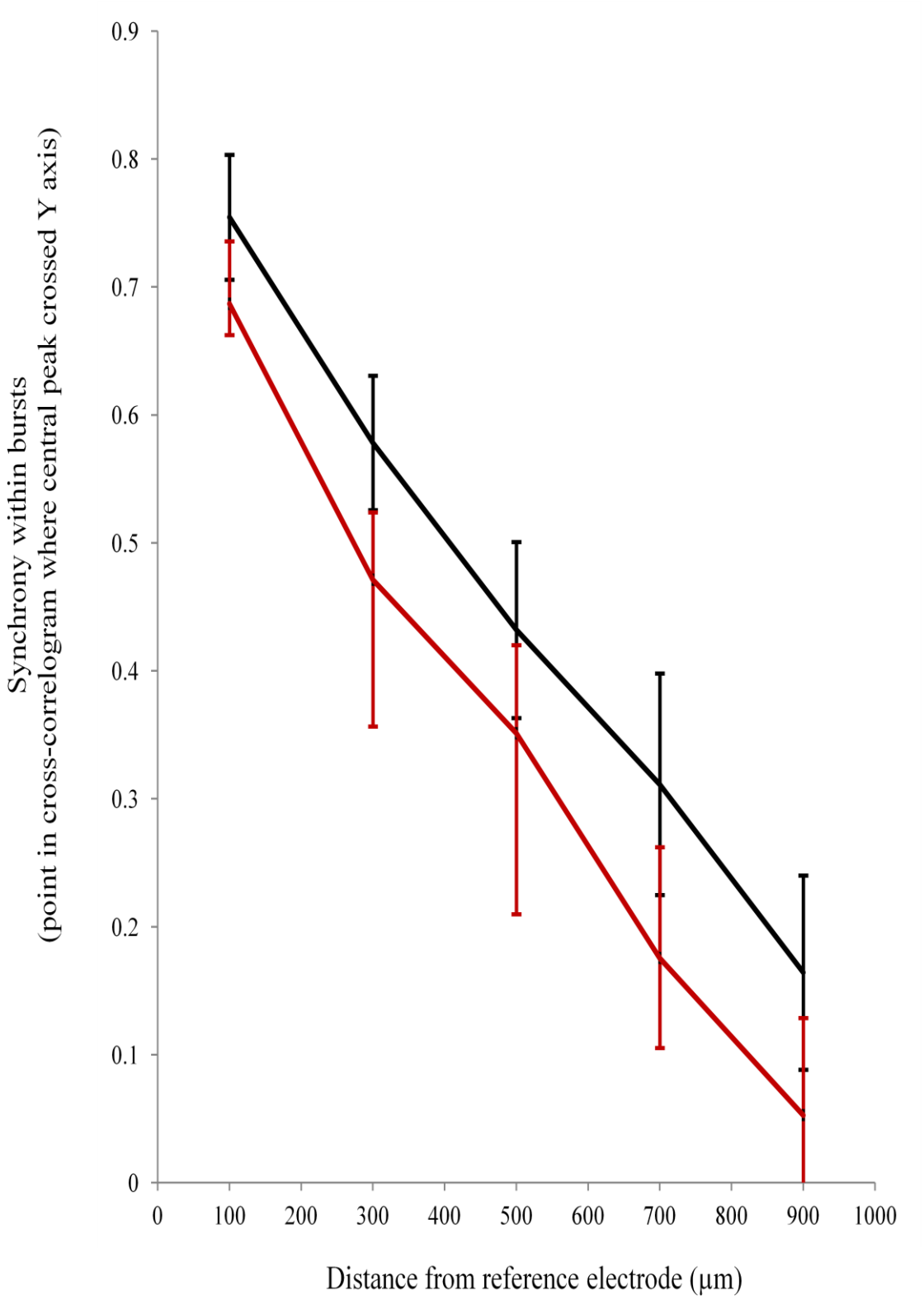

Fig. 6.6 Effect of the gap junction blocker carbenoxolone (100µM carbenoxolone, red; control, black) on synchrony within bursts of VFO in field rhythms from two electrodes at distances from 100 to 900µm apart along layer V of 2° somatosensory cortex (mean ± SEM, n = 5 slices).

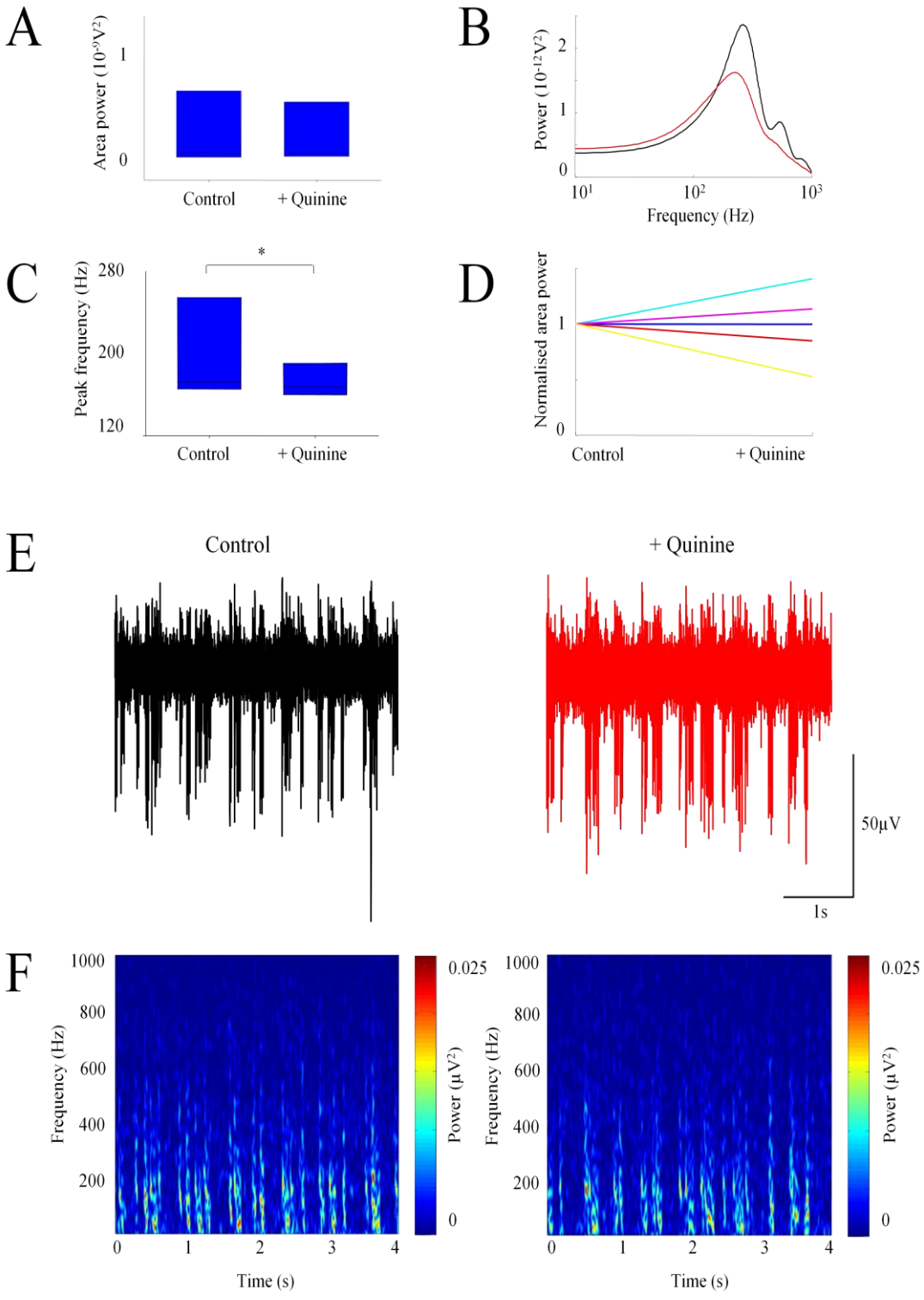

Fig. 6.7. Effect of blockade of the gap junction protein connexin36 with quinine (100µM) on clozapine-induced VFO (n = 6 slices). (*A*) Box plot showing median VFO band area power (Q1→Q3). (*B*) VFO band pooled power spectra (black line, control; red line, quinine). (*C*) Box plot showing median VFO band peak frequency (Q1→Q3). (*D*) Line graph illustrating VFO band area power data in individual experiments. Example field traces (*E,* 4s duration, 60-1000Hz band-pass filtered), and corresponding spectrograms (*F*), are shown, before (left) and after (right) bath application of quinine.

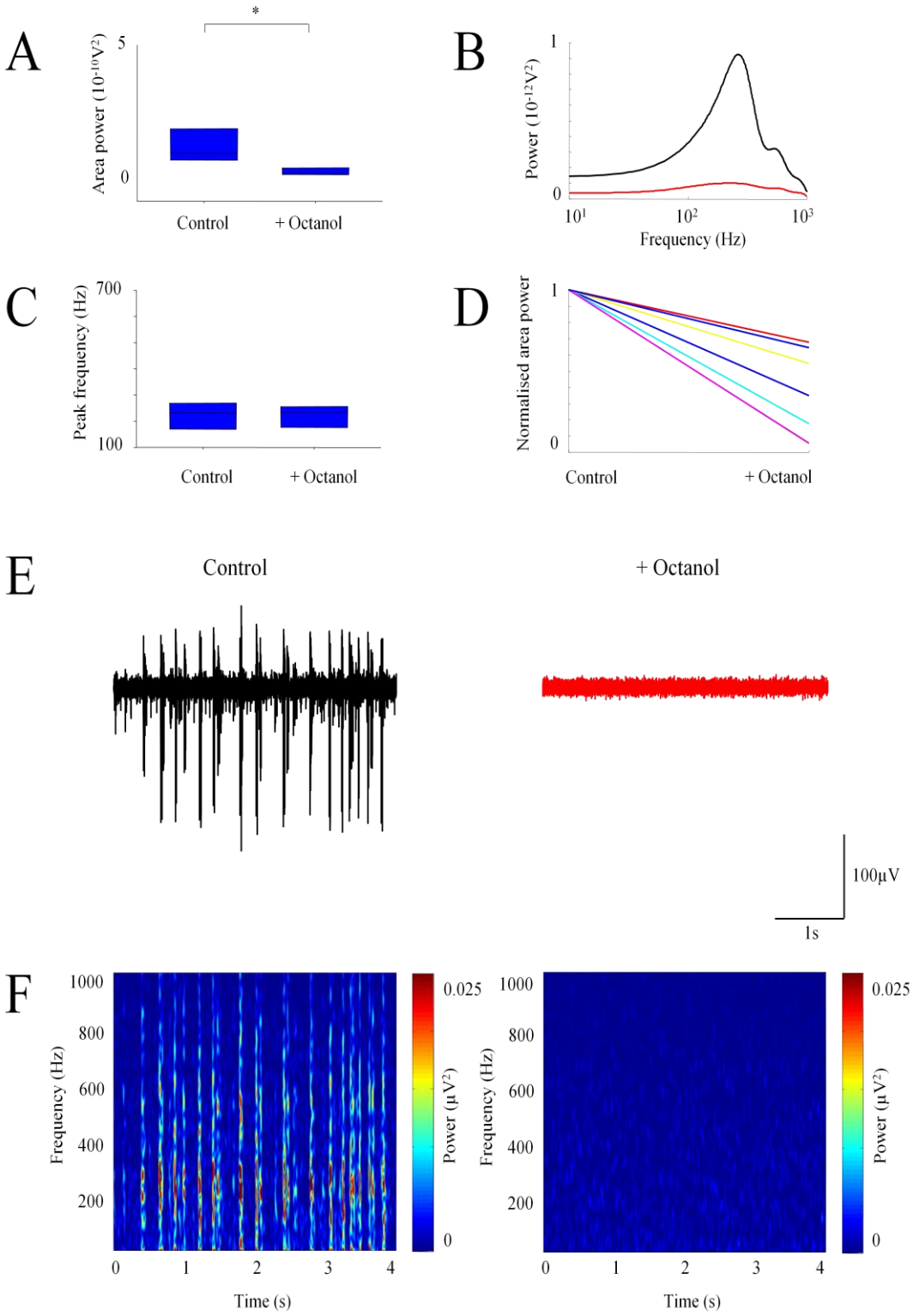

Fig. 6.8. The gap junction blocker octanol (1mM) attenuated clozapine-induced VFO (n = 7 slices). (*A*) Box plot showing median VFO band area power (Q1 → Q3). (*B*) VFO band pooled power spectra (black line, control; red line, octanol). (*C*) Box plot showing median VFO band peak frequency (Q1 → Q3). (*D*) Line graph illustrating VFO band area power data in individual experiments. Example field traces (*E,* 4s duration, 60-1000Hz band-pass filtered), and corresponding spectrograms (*F*), are shown, before (left) and after (right) bath application of octanol.

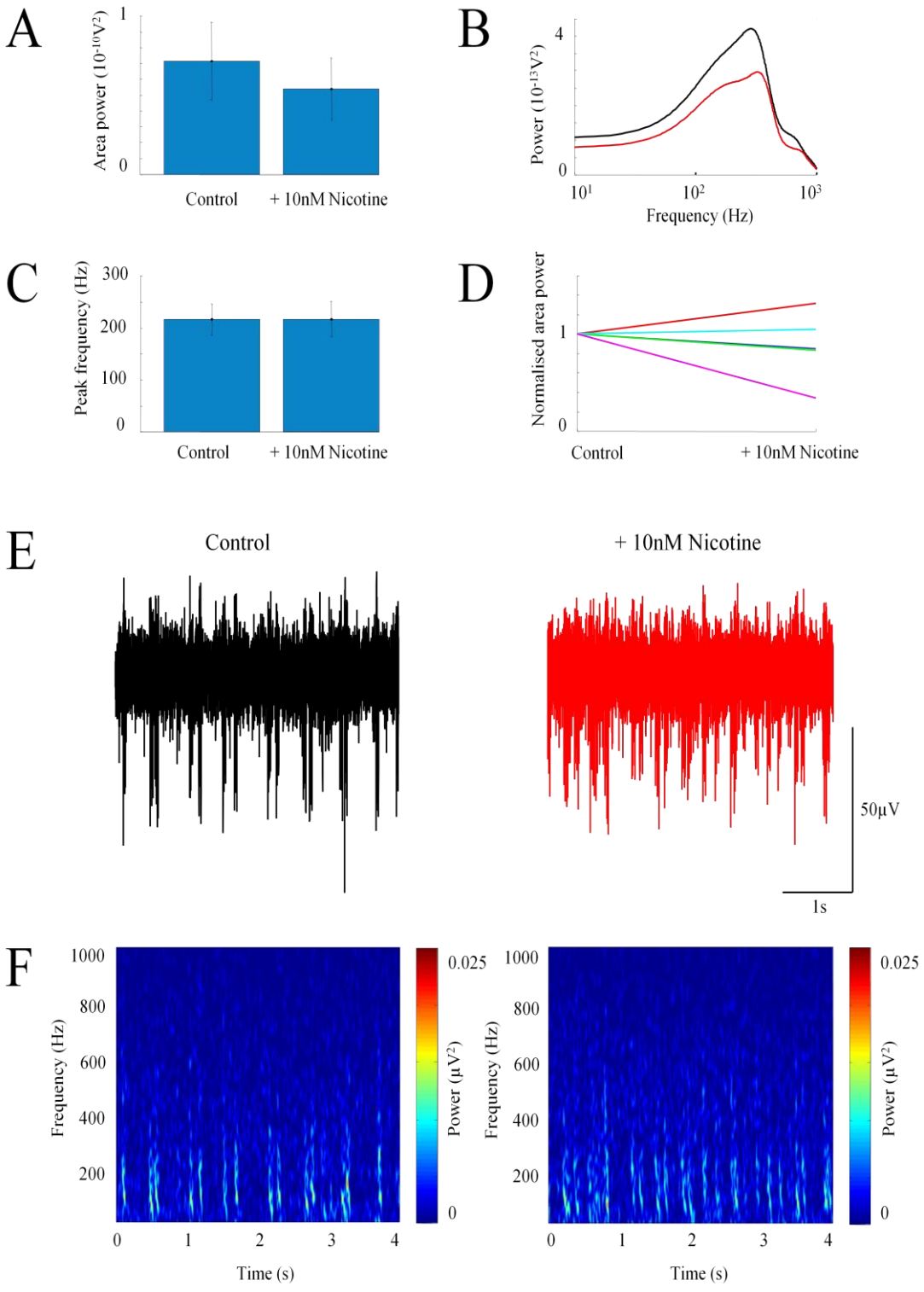

Fig. 6.9. Effect of nicotine (10nM) on clozapine-induced VFO (n = 5 slices). (*A*) Bar chart showing VFO band area power (mean ± SEM). (*B*) VFO band pooled power spectra (black line, control; red line, 10nM nicotine). (*C*) Bar chart showing VFO band peak frequency (mean ± SEM). (*D*) Line graph illustrating VFO band area power data in individual experiments. Example field traces (*E,* 4s duration, 60-1000Hz band-pass filtered), and corresponding spectrograms (*F*), are shown, before (left) and after (right) bath application of nicotine (10nM).

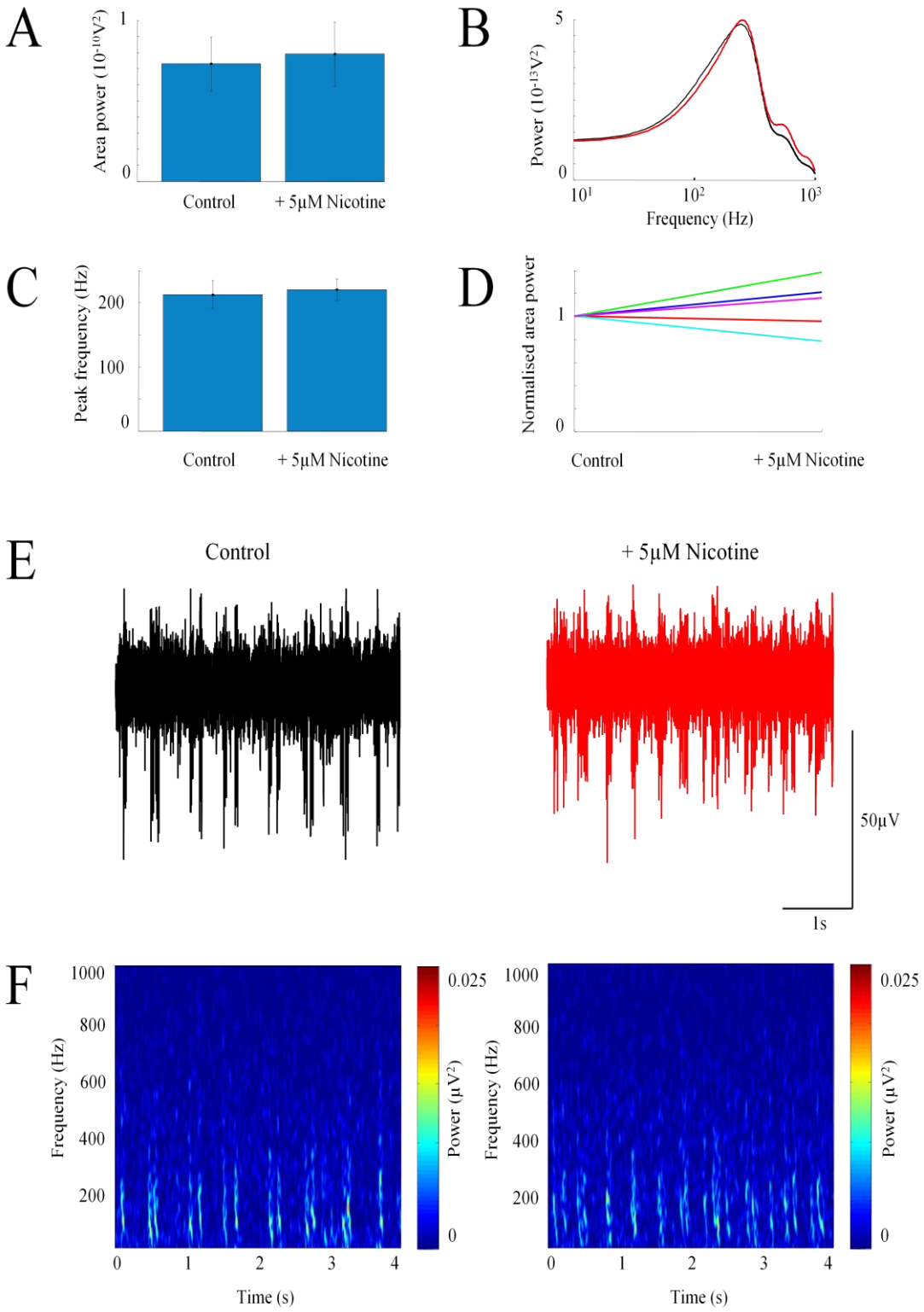

Fig. 6.10. Effect of nicotine (5µM) on clozapine-induced VFO (n = 5 slices). (*A*) Bar chart showing VFO band area power (mean ± SEM). (*B*) VFO band pooled power spectra (black line, control; red line, 5µM nicotine). (*C*) Bar chart showing VFO band peak frequency (mean ± SEM). (*D*) Line graph illustrating VFO band area power data in individual experiments. Example field traces (*E,* 4s duration, 60-1000Hz band-pass filtered), and corresponding spectrograms (*F*), are shown, before (left) and after (right) bath application of nicotine (5µM).

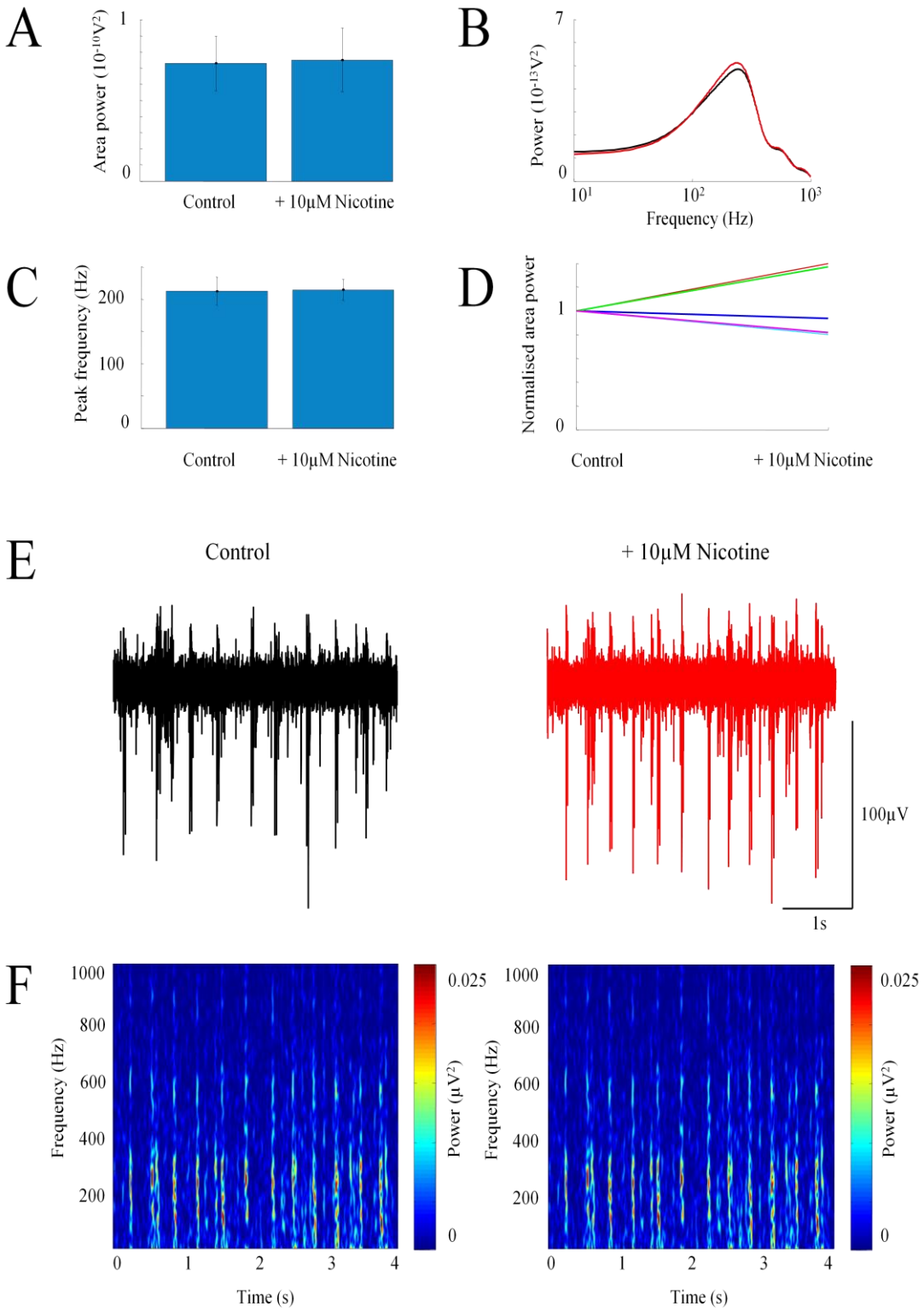

Fig. 6.11. Effect of nicotine (10µM) on clozapine-induced VFO (n = 5 slices). (*A*) Bar chart showing VFO band area power (mean ± SEM). (*B*) VFO band pooled power spectra (black line, control; red line, 10µM nicotine). (*C*) Bar chart showing VFO band peak frequency (mean ± SEM). (*D*) Line graph illustrating VFO band area power data in individual experiments. Example field traces (*E,* 4s duration, 60-1000Hz band-pass filtered), and corresponding spectrograms (*F*), are shown, before (left) and after (right) bath application of nicotine (10µM).

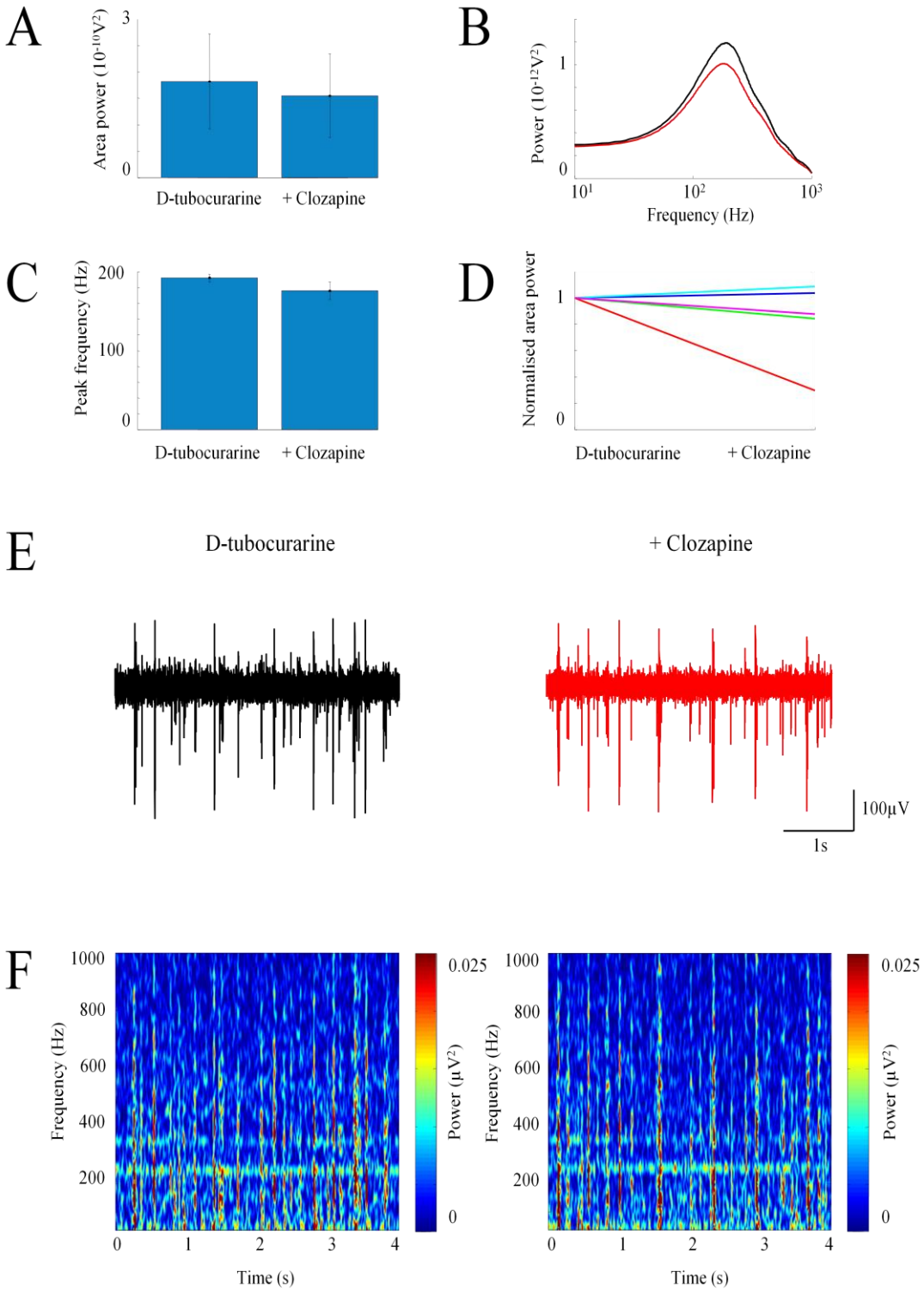

Fig. 6.12. Effect of clozapine (20µM) on d-tubocurarine-induced VFO (n = 5 slices). (*A*) Bar chart showing VFO band area power (mean ± SEM). (*B*) VFO band pooled power spectra (black line, d-tubocurarine; red line, + clozapine). (*C*) Bar chart showing VFO band peak frequency (mean ± SEM). (*D*) Line graph illustrating VFO band area power data in individual experiments. Example field traces (*E,* 4s duration, 60-1000Hz band-pass filtered), and corresponding spectrograms (*F*), are shown, before (left) and after (right) bath application of clozapine.

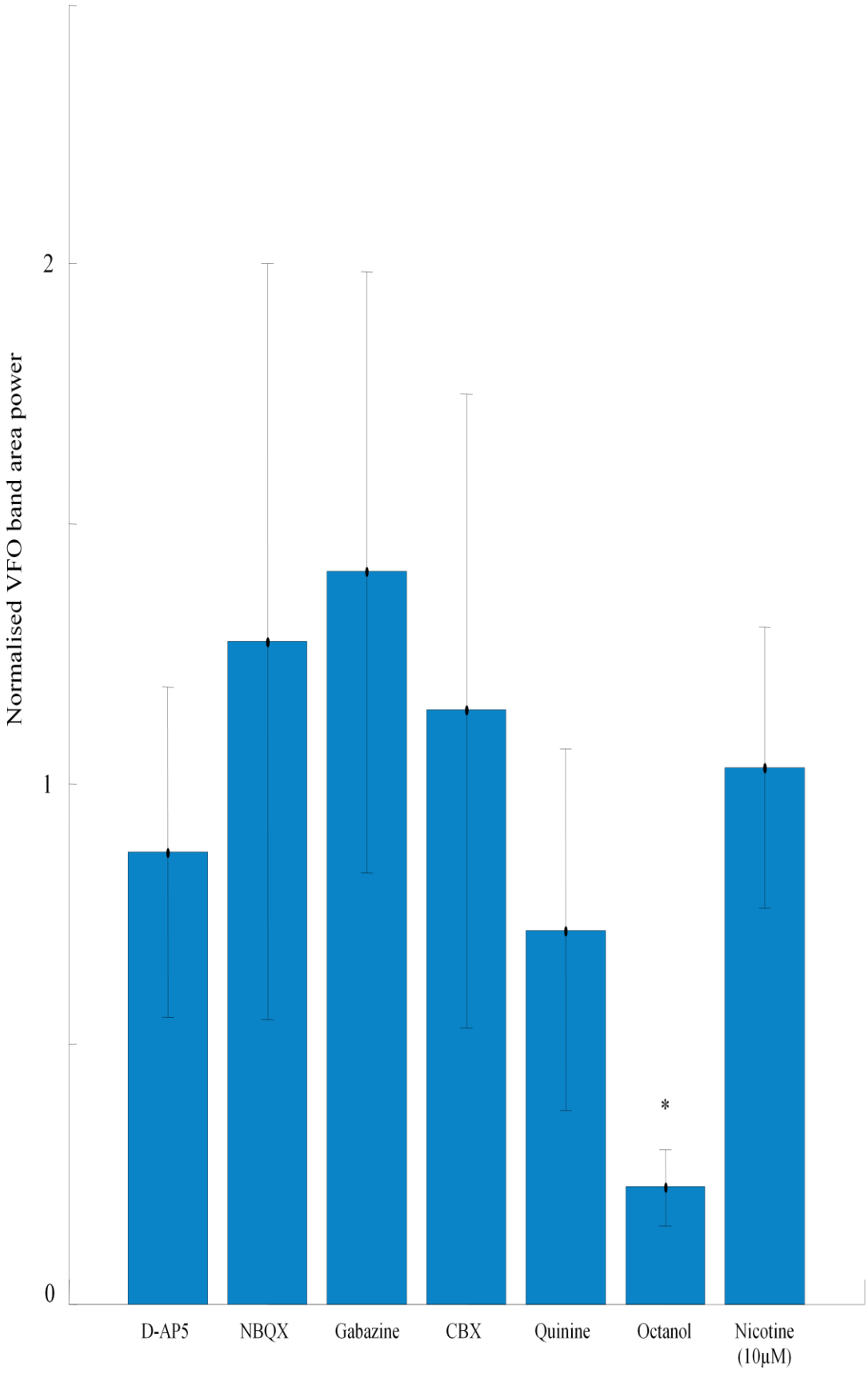

Fig. 6.13. Summary of the effect of pharmacological agents on the normalised VFO band area power of clozapine-induced VFO (mean ± SEM).

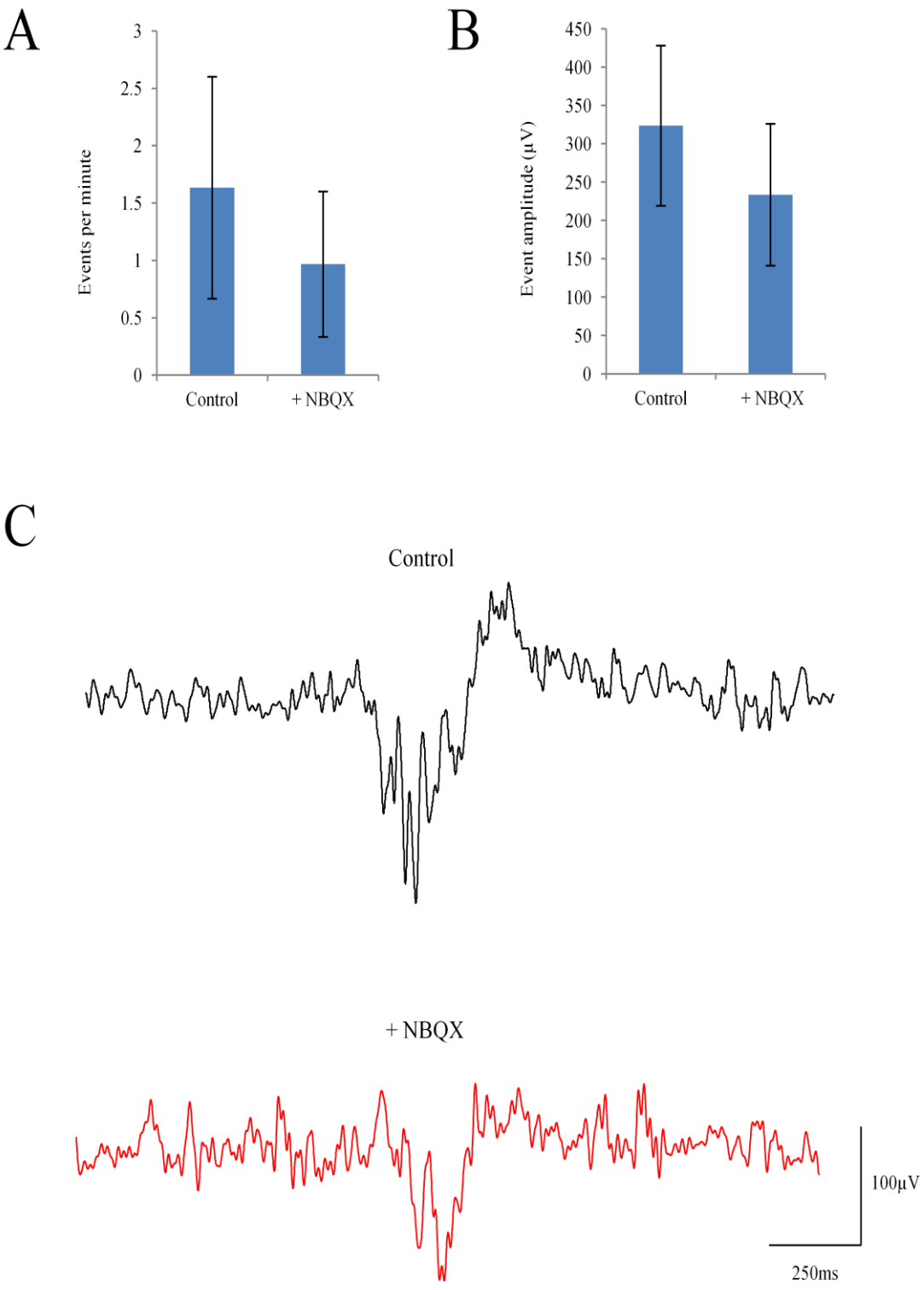

Fig. 6.14. Effect of antagonism of the AMPA/kainate subtypes of glutamate receptor on clozapine-induced paroxysmal discharges (n = 2 slices). (*A*) Frequency of events (mean ± SEM). (*B*) Amplitude of events (mean ± SEM). (*C*) Example field traces (2s duration, 0.5-70Hz band-pass filtered) before (upper, black) and after (lower, red) bath application of NBQX (20µM).

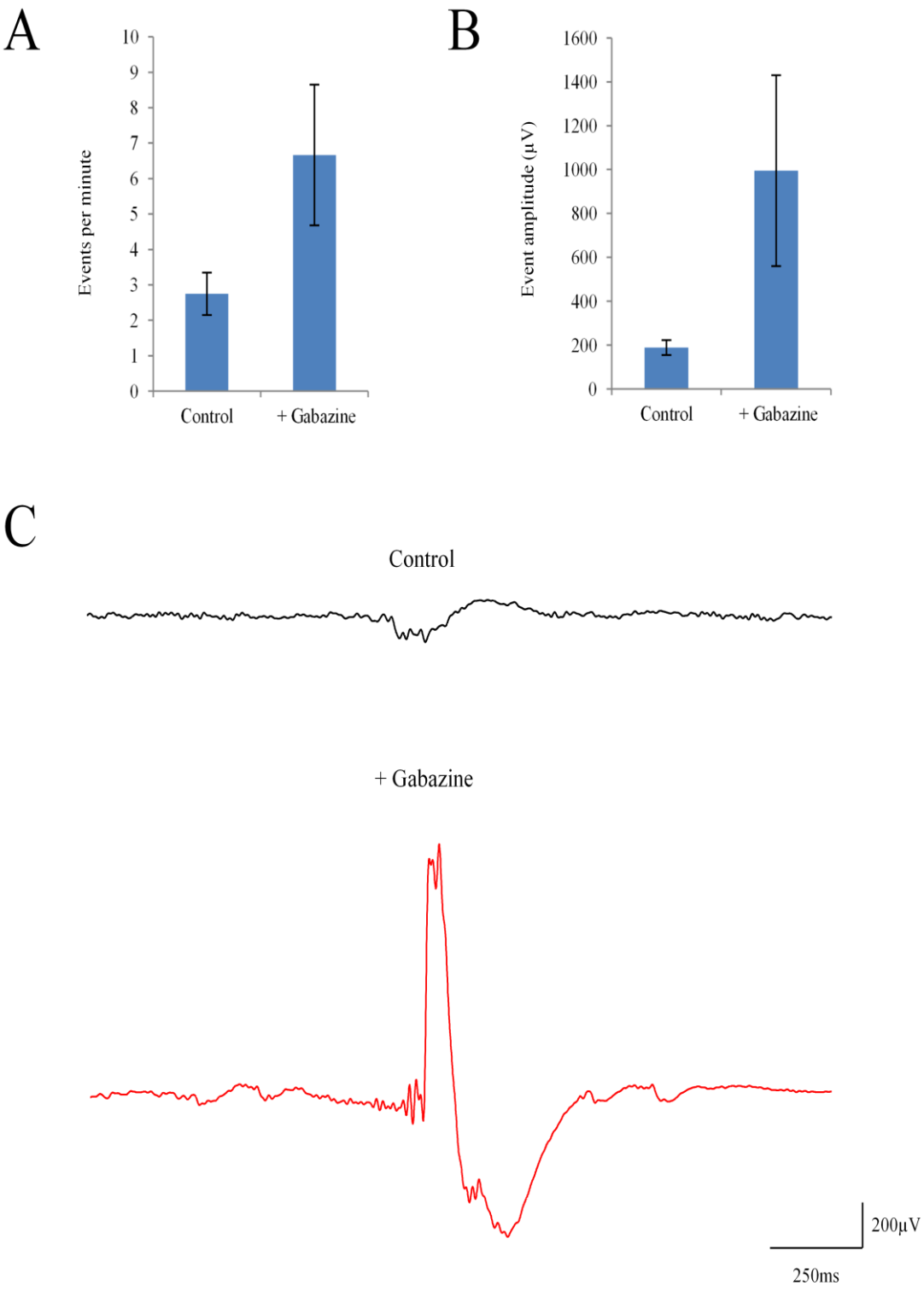

Fig. 6.15. Effect of antagonism of $GABA_A$ receptors on clozapine-induced paroxysmal discharges (n = 4 slices). (*A*) Frequency of events (mean ± SEM). (*B*) Amplitude of events (mean ± SEM). (*C*) Example field traces (2s duration, 0.5-70Hz band-pass filtered) before (upper, black) and after (lower, red) bath application of gabazine (500nM).

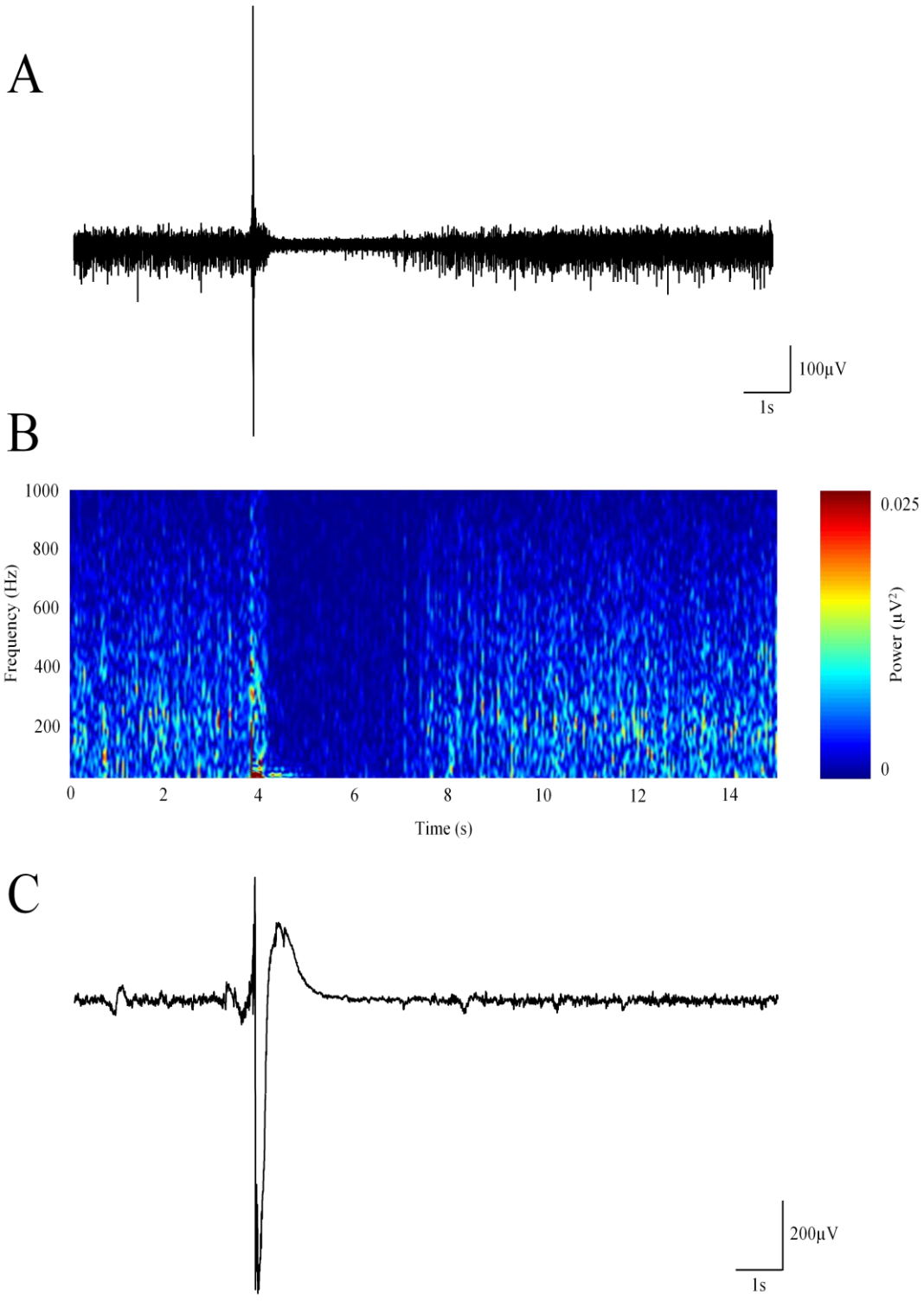

Fig. 6.16. Following application of gabazine (500nM), clozapine-induced VFO could be prominent at the start of, then temporarily suspended during and immediately after, events. (*A*) Example band-pass (60-1000Hz, 15s duration) filtered field trace to illustrate high frequency activity, corresponding spectrogram (*B*), and the same trace with a 0.5-70Hz band-pass filter (*C*) to highlight the paroxysmal event.

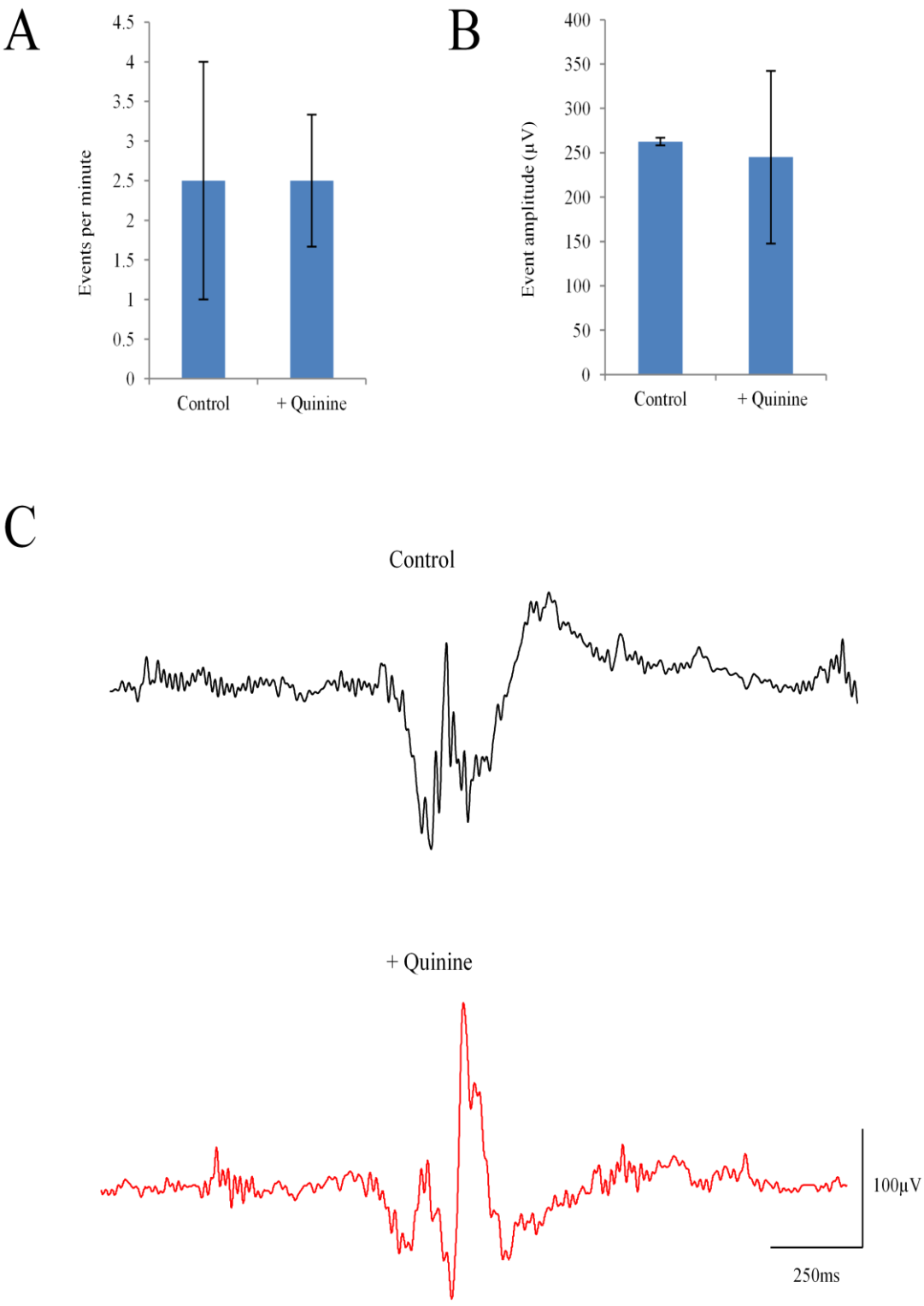

Fig. 6.17. Effect of blockade of the gap junction protein connexin36 with quinine (100µM) on clozapine-induced paroxysmal discharges (n = 2 slices). (*A*) Frequency of events (mean ± SEM). (*B*) Amplitude of events (mean ± SEM). (*C*) Example field traces (2s duration, 0.5-70Hz band-pass filtered) before (upper, black) and after (lower, red) bath application of quinine.

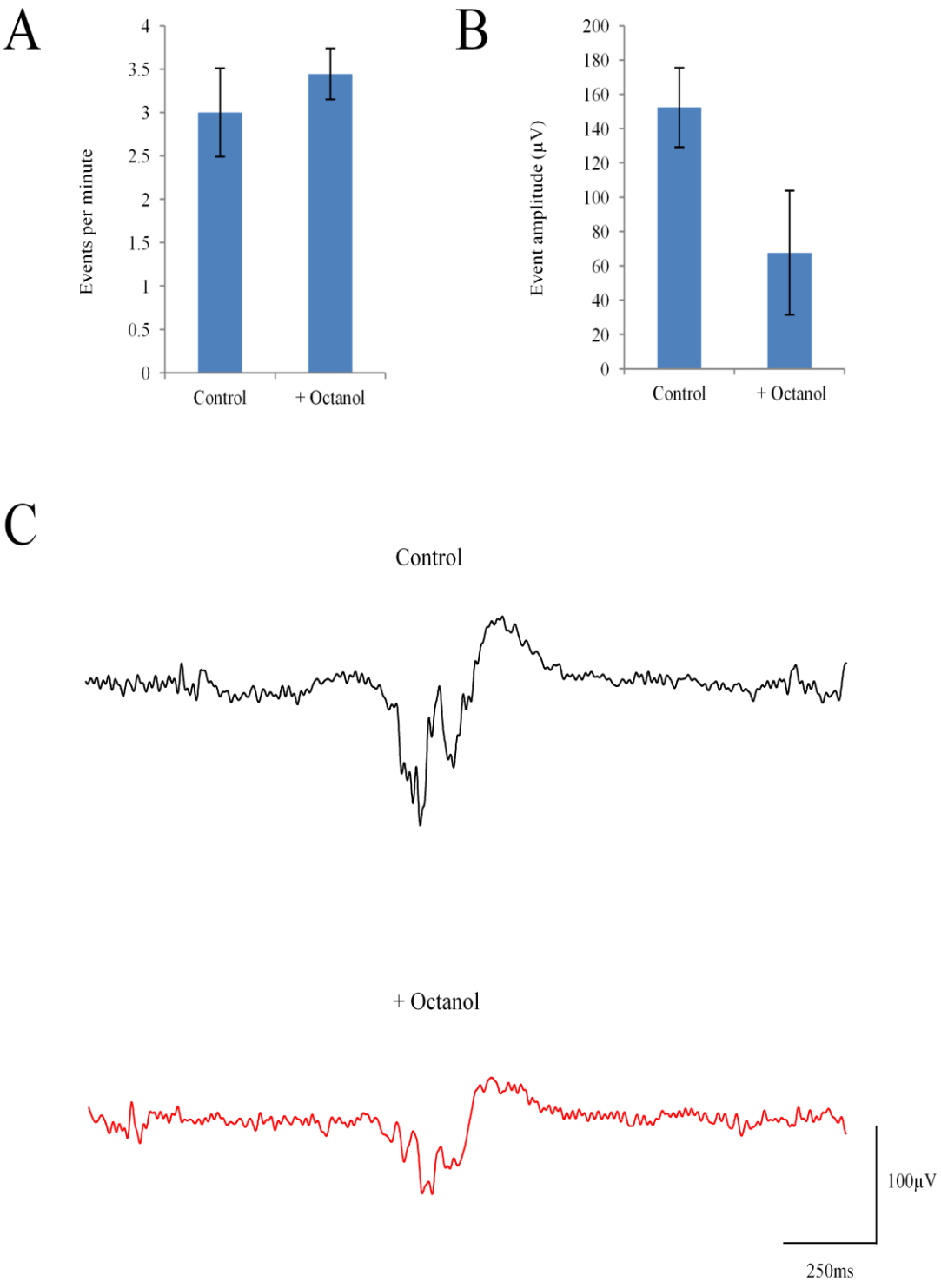

Fig. 6.18. Effect of the gap junction blocker octanol (1mM) on clozapine-induced paroxysmal discharges (n = 3 slices). (*A*) Frequency of events (mean ± SEM). (*B*) Amplitude of events (mean ± SEM). (*C*) Example field traces (2s duration, 0.5-70Hz band-pass filtered) before (upper, black) and after (lower, red) bath application of octanol.

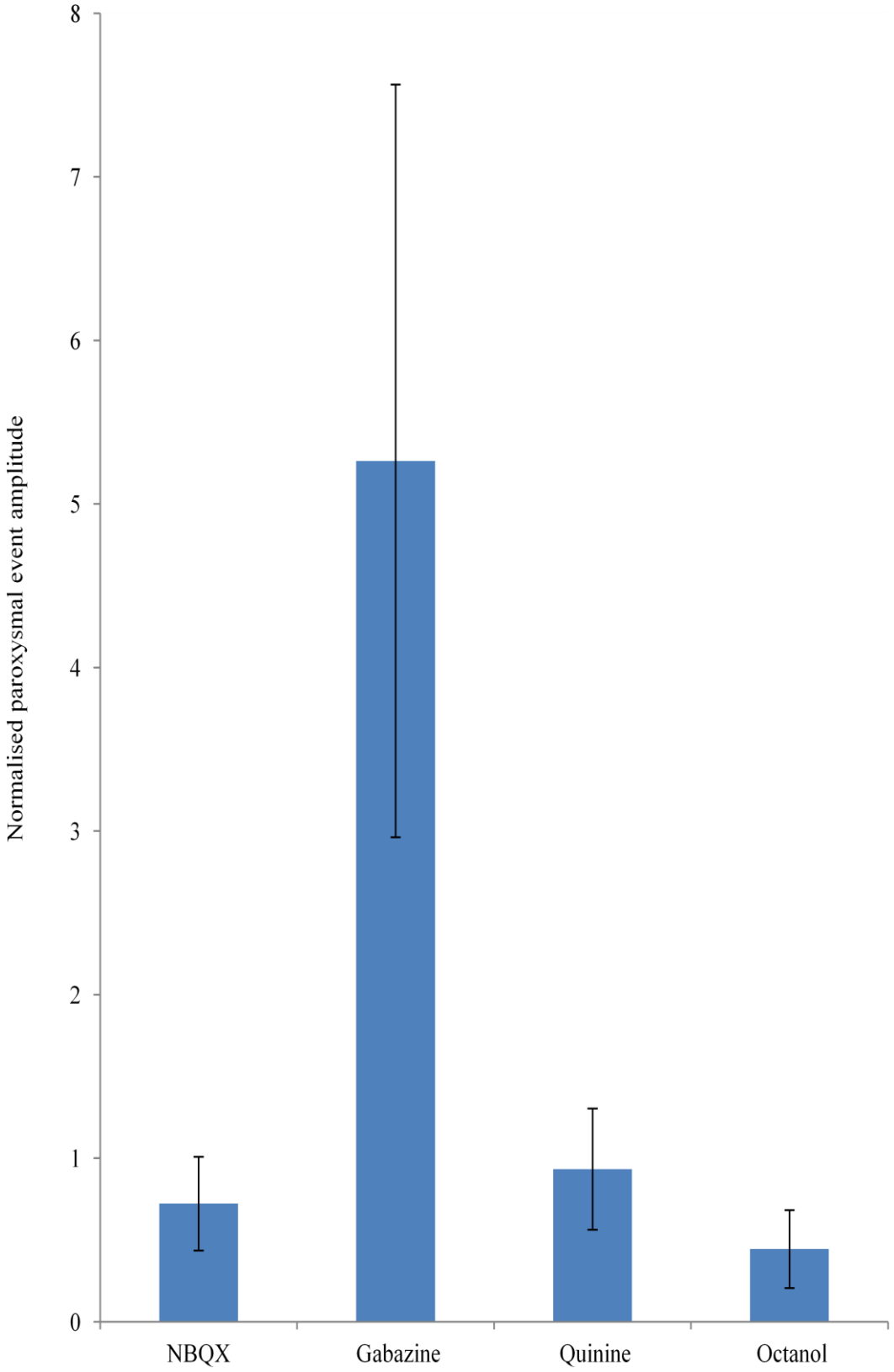

Fig. 6.19. Summary of the effect of pharmacological inhibitors on the normalised amplitude of clozapine-induced paroxysmal events (mean ± SEM).

6.4 Discussion

6.4.1 Pharmacology of clozapine-induced VFO

Possible mechanisms underlying clozapine-induced VFO included fast glutamatergic synaptic transmission, activity of fast-spiking interneurons, suppression of $GABA_A$ receptors, antagonism of neuronal nicotinic receptors, and electrotonic coupling of neurons through gap junctions.

The finding that neither blockade of NMDA nor AMPA receptors had any significant effect to reduce VFO suggests that clozapine-induced VFO is not mediated via fast glutamatergic synaptic transmission.

Similarly, the lack of an attenuating effect of gabazine on clozapine-induced VFO excludes a role for $GABA_A$ receptor-mediated fast inhibition in the mechanism. Thus, clozapine-induced VFO does not appear to arise from the synaptic activity of GABAergic interneurons.

In chapter 4, the finding of IB cell spikelets, which were correlated to some extent with field VFO, suggested the involvement of axonal hyperexcitability in this cell type, with a possible role for the spread of activity through the axonal plexus via electrotonic coupling at gap junctions. In the present chapter, various gap junction blockers were used to investigate a possible role for electrotonic coupling via gap junctions in the mechanism.

Interestingly, however, neither carbenoxolone nor quinine had any significant effect to reduce the power of clozapine-induced VFO. However, quinine did significantly reduce the frequency of clozapine-induced VFO (see below).

The failure of quinine to significantly reduce the power of clozapine-induced VFO does not exclude a role for electrotonic coupling via gap junctions between pyramidal cells in the mechanism because the connexin36-containing gap junctions which quinine blocks are primarily found in gap junctions between interneurons (Hormuzdi et al., 2001;Fukuda et al., 2006;Belluardo et al., 2000;Deans et al., 2001). However, at least some of the gap junctions revealed by freeze fracture of mossy fiber axo-axonic gap junctions were imunopositive for cx36 protein (Hamzei-Sichani et al., 2007).

However, failure of carbenoxolone to significantly reduce either the power or synchrony of clozapine-induced VFO is inconsistent with previous findings in which electrotonic

coupling via gap junctions was implicated in the mechanism underlying VFO (Draguhn et al., 1998;Maier et al., 2003;Jones and Barth, 2002;Nimmrich et al., 2005;Roopun et al., 2010b).

Although the gap junction blocker octanol reversibly abolished clozapine-induced VFO, octanol also potently inhibits voltage-operated Na^+ channels (Hirche, 1985;Horishita and Harris, 2008) and may consequently block action potentials. Indeed, the failure of both carbenoxolone and quinine to significantly reduce clozapine-induced VFO incidence, together with the potent action of octanol on fast sodium conductances suggests that octanol may exert its effect directly on axonal excitability rather than axo-axonic communication. Thus, together these data suggest that clozapine-induced VFO may engender a limited extent of activity spread via gap junctions, and that instead these VFO may arise solely from axonal hyperexcitability. In other words, the fast activity seen was manifest as a collection of multi-unit discharges from local layer V neurons only transiently synchronised by chance.

The possible increase in clozapine-induced VFO associated with gabazine would be consistent with some role for partial disinhibition in clozapine-induced VFO. In the converse experiment, the reduction in gabazine-induced VFO that occurred in some cases after application of clozapine may have resulted from the slices reaching a level of excitability whereby VFO were no longer supported (i.e. slices became 'overcooked' after application of both of these drugs). Alternatively, GABA release has been suggested to be directly excitatory onto pyramidal cell axons (Traub et al., 2003). Thus a reduction in $GABA_A$ receptor function with both gabazine and clozapine may have removed some of the drive to axons possibly underlying the VFO seen.

The small reduction in the peak frequency of clozapine-induced VFO associated with quinine raises the possibility that electrotonic coupling via gap junctions between interneurons has a small modulatory influence on clozapine-induced VFO. Alternatively, the effect may be due to a non-specific effect of quinine on intrinsic membrane conductances. Moreover, in view of the slight nature of the effect (2.9% reduction in median), and the relatively small number of experiments (n = 6), the result may have been a false positive. This subtle effect way also have been due to the non-gap junction-specific effects of quinine on TREK-1 potassium channels partially responsible for control of extracellular potassium ion concentration via astrocytes (Zhou et al., 2009).

The lack of effect of nicotine on clozapine-induced VFO together with the absence of an effect of clozapine on d-tubocurarine-induced VFO suggests that clozapine-induced VFO may not be mediated via antagonism of nicotinic receptors, and that d-tubocurarine-induced VFO may arise from a different mechanism.

6.4.2 Pharmacology of clozapine-induced paroxysmal discharges

The low n number for paroxysmal discharges in pharmacology experiments meant that the statistical analysis was almost certainly underpowered to detect significant changes. Nonetheless, in contrast to clozapine-induced VFO, the possible reduction in the amplitude of clozapine-induced paroxysmal events associated with the AMPA receptor antagonist NBQX is in line with the involvement of fast glutamatergic synaptic transmission in the mechanism underlying these events.

Although gabazine was associated with a non-significant increase in the amplitude of paroxysmal events, evidence considered in the previous chapter suggests partial disinhibition may not be sufficient in itself to precisely mimic clozapine-induced paroxysmal discharges.

As mentioned previously, the potent action of octanol on fast sodium conductances means that it cannot be concluded that the possible reduction in amplitude of clozapine-induced paroxysmal events was specific to the drug's effect on gap junctions.

6.4.3 Selectivity of gap junction blockers, and VFO synchrony

Gap junction blockers have limited selectivity and may have secondary effects on, for example, intrinsic membrane conductances. One example of a non-specific effect is that carbenoxolone may antagonise NMDA receptors (Chepkova et al., 2008), though no effects were seen for NMDA antagonism alone here. Furthermore, as previously mentioned, octanol potently inhibits voltage-operated Na^+ channels (Hirche, 1985;Horishita and Harris, 2008) and consequently blocks action potentials. To investigate the relative effect of octanol on spikes versus gap junctions under the present experimental conditions, it would be interesting to apply this drug to slices during an intracellular recording from a cell with spikelets, and compare its effect on spikes versus spikelets.

The possibility cannot be excluded that there is a role for electrotonic coupling through gap junction proteins not targeted by either carbenoxolone or quinine in the mechanism underlying clozapine-induced VFO (e.g. Kollo et al., 2006).

As mentioned previously, carbenoxolone (100µM) failed significantly to reduce the synchrony of clozapine-induced VFO. However, the possibility that VFO synchrony may have significantly reduced with a higher concentration of this agent could not be excluded. Although 100µM carbenoxolone was sufficient to abolish spontaneous VFO in rat hippocampal slices (Draguhn et al., 1998), 100-200µM was necessary in slices of human epileptic tissue (Roopun et al., 2010b), and even higher concentrations of this agent have been used (e.g. Gigout et al., 2006).

6.4.4 Concluding remarks

In chapter 4, the finding of IB cell spikelets, which were correlated to some extent with field VFO, suggested the involvement of axonal hyperexcitability in this cell type, with a possible role for the spread of activity through the axonal plexus via electrotonic coupling at gap junctions. In the present chapter no chemical synaptic blockers or gap junction conductance-reducing drugs had any significant effect to reduce VFO incidence or power – with the exception of octanol. However, this drug also potently blocks fast sodium conductances so may exert its effect directly on axonal excitability rather than axo-axonic communication, and thus clozapine-induced VFO may arise solely from axonal hyperexcitability in uncoupled local populations of bursting neurons.

Chapter 7

Results – Effect of clozapine on parvalbumin immunoreactivity

7.1 Introduction

In view of parvalbumin (PV) deficits in post-mortem cortical samples from schizophrenic patients (e.g. Hashimoto et al., 2003), it was interesting to investigate the effect of the antipsychotic clozapine on PV immunoreactivity in 'normal' rat brain slices in an attempt to relate clozapine-induced hyperexcitability (see previous chapters) to the drug's antipsychotic efficacy. Examination of the laminar distribution of clozapine's effect on PV interneurons may provide clues with regard to the circuits involved in the mechanism underlying clozapine's therapeutic efficacy.

Aim

Therefore the aim of this chapter is to investigate the effect of clozapine on the number of PV-immunopositive interneurons in 2º somatosensory cortex, and to elucidate the laminar distribution of any such effect.

7.1.1 GABAergic deficits in schizophrenia

A consistent finding in post-mortem studies has been that GAD67, one of the main enzymes that synthesise GABA, is reduced in the dorsolateral prefrontal cortex of patients with schizophrenia (Bird et al., 1978;Hanada et al., 1987), and this occurs selectively in layers III-V (Akbarian et al., 1995), where gamma rhythms are most prominent (Glykos et al., 2012).

Expression of the GABA membrane transporter GAT1 is also reduced suggesting that, in addition to synthesis, re-uptake of GABA is also impaired in schizophrenia (Volk et al., 2001). Given the critical role of GABAergic interneurons in the mechanisms underlying gamma oscillations (Traub et al., 2004;Fries et al., 2007), it is possible that cognitive impairments in schizophrenia arise from reduced gamma synchrony resulting from impaired GABA-mediated inhibition.

7.1.2 Parvalbumin deficits in schizophrenia

Expression of the calcium-binding proteins parvalbumin (PV), calretinin or calbindin, can be used as markers to identify particular morphological and functional subclasses of GABAergic interneurons (Conde et al., 1994;Gabbott and Bacon, 1996;Kawaguchi and Kubota, 1997). Among inhibitory GABAergic interneurons, PV-positive fast spiking interneurons may be especially important in generating synchronous outputs to co-ordinate gamma rhythms (Gloveli et al., 2005;Mann et al., 2005;Klausberger and

Somogyi, 2008;Cardin et al., 2009), and their activity has been shown to have a causal role in generating gamma rhythms in mice *in vivo* (Sohal et al., 2009). PV cells include wide arbour neurons that target cell soma, and chandelier neurons that target axon initial segments (Williams et al., 1992;Lund and Lewis, 1993). PV buffers transient elevations in cytosolic Ca^{2+} (Chard et al., 1993), and so it may influence a range of neuronal properties including excitation and synaptic transmission (Pauls et al., 1996).

PV interneurons appear to have an important role in schizophrenia pathology (Beasley and Reynolds, 1997;Danos et al., 1998;Hashimoto et al., 2003). For example, expression of PV mRNA is reduced in layers III and IV, but not in layers II, V or VI of the dorsolateral prefrontal cortex in post-mortem samples from schizophrenic subjects (Hashimoto et al., 2003). Interestingly, the expression level of PV mRNA per neuron rather than number of neurons with detectable PV mRNA was affected. The PV mRNA expression level per neuron also correlated with reductions in the density of neurons positive for GAD67 mRNA. Thus GAD67 mRNA expression is preferentially reduced in PV-immunopositive interneurons (Hashimoto et al., 2003). Dual label *in situ* hybridisation studies confirmed that in schizophrenic tissue approximately half of the neurons positive for PV mRNA did not have detectable GAD67 mRNA. Therefore it seems that PV interneurons in particular may be functionally impaired in schizophrenia.

PV protein, and PV-immunoreactive axon terminals, are also reduced in prefrontal cortical schizophrenic tissue, again in layer III and IV (Beasley and Reynolds, 1997;Lewis et al., 2001). Furthermore, PV protein is reduced in thalamocortical projection neurons (Danos et al., 1998), and in all hippocampal subfields (Zhang and Reynolds, 2002;Knable et al., 2004) in post-mortem schizophrenic brain.

Chandelier cells are a subclass of PV interneuron which provide strong inhibitory input to pyramidal cell axons via arrays of inhibitory synapses (cartridges) and these cartridges are reduced in post-mortem schizophrenic brain (Woo et al., 1998).

Interestingly, in schizophrenia expression of the $GABA_A$ receptor alpha1 subunit is particularly low in pyramidal cells that receive inhibitory inputs from PV interneurons (Glausier and Lewis, 2011). Thus reduced inhibitory drive from PV cells could be a key aspect of the pathophysiology of schizophrenia and this may have a bearing on the effectiveness of antipsychotic drugs like clozapine.

Consistent with a role in pathological dysfunction in schizophrenia, ultrastructural analysis with electron microscopy revealed that PV neurons are directly innervated by dopaminergic neurons (Sesack et al., 1998).

Incidentally, in humans the locus of the PV gene has been narrowed down to chromosome 22q12-q13.1 (Ritzler et al., 1992), close to the marker D22S278, and this region has been associated with schizophrenia susceptibility (Riley and McGuffin, 2000). However, there may also be environmental influences on PV expression as there is evidence for activity-dependent modulation of the expression of PV and GAD67 (Hendry and Jones, 1988;Benson et al., 1994;Carder et al., 1996;Nie and Wong-Riley, 1996).

7.1.3 Mechanisms underlying parvalbumin deficits in schizophrenia

The mechanisms by which PV cells may become dysfunctional in schizophrenia are not yet clear. Possibilities include reductions in released GABA, lower numbers of postsynaptic $GABA_A$ receptors, alterations in the excitatory drive on to PV neurons, or loss of neurons or inhibitory inputs. A complicating factor is that lowered PV in schizophrenia may be a compensatory change secondary to deficits in GAD67 and reduced GABA. In fact, so many seemingly contrary changes in GABA system function are seen in schizophrenia that it is hard to understand mechanistically what is ‘cause’ and what is ‘compensation’ at all. This has led to other theories linking pathology to modifications in glutamate receptor-mediated excitation.

Indeed, glutamatergic hypofunction and the resulting disruption in GABAergic neurotransmission may be critical to the dysfunction in schizophrenia (Lewis, 2000;Olney et al., 1989;Tamminga, 1998). In line with this idea, there is evidence of pronounced excitatory input from axon collaterals of local pyramidal cells to layer III PV neurons in monkey prefrontal cortex (Melchitzky et al., 2001;Melchitzky and Lewis, 2003).

Furthermore, it has been proposed that NMDA receptor hypofunction may be primary, either directly or indirectly, to changes in PV neurons in schizophrenia (Coyle, 2006;Lisman et al., 2008;Lewis and Gonzalez-Burgos, 2006). PV interneurons receive excitatory inputs via NMDA receptors, especially those containing the NR2A/NR2B subtype associated with changes in glutamatergic drive (Kinney et al., 2006). Interestingly, in most brain regions there is a limited extent of NMDA receptor input into interneurons in the adult. However, in entorhinal cortex, an area implicated in

specific schizophrenia-related pathologies, such NMDA receptor inputs remain substantial in adulthood (Jones and Buhl, 1993).

7.1.4 Parvalbumin deficits in animal models of schizophrenia

PV deficits are also present in animal models of schizophrenia. Administration of methylazoxymethanol acetate reduced PV expression in interneurons throughout the medial prefrontal cortex and ventral subiculum in rats (Lodge et al., 2009). Similarly, LPA1-deficient mice, which show psychomotor-gating deficits and neurochemical changes similar to those in schizophrenia, are associated with a reduction in PV-immunopositive interneuron numbers in layer II of medial entorhinal cortex (Cunningham et al., 2006) – an observation which maps neatly onto deficits in the ability of this layer to generate gamma rhythms .

In line with the proposal that NMDA receptor hypofunction is primary to alterations in PV neurons, NMDA receptor antagonists can induce lowered PV and GAD67 in PV neurons similar to that found in post-mortem schizophrenic tissue (Cochran et al., 2002;Kinney et al., 2006;Behrens et al., 2007b;Amitai et al., 2012). For example, the chronic PCP treatment model of psychosis reduces expression of PV mRNA in rat brain (Cochran et al., 2002;Cochran et al., 2003). Interestingly, co-administration of clozapine, but not haloperidol, reversed the PCP-induced reductions in PV expression in prefrontal cortex (Cochran et al., 2003;Amitai et al., 2012), and it was suggested that recovery of PV expression may be a marker of atypical antipsychotics. (Both antipsychotics reversed PCP-induced reductions in PV expression in the reticular nucleus of the thalamus (Cochran et al., 2003).)

However, although there is a preliminary suggestion in the literature that chronic clozapine administration alone may increase PV expression in rat prefrontal cortex (Scruggs and Deutch, 1999), a different study found no such effect on baseline PV immunoreactivity in either rat hippocampus or frontal cortex (Cahir et al., 2005).

Here, the effect of acute application of clozapine on PV immunoreactivity in slices of 2º somatosensory cortex from untreated, normal rats was investigated *in vitro* and correlated with VFO production.

7.2 Methods

Experiments in this chapter made use of rat brain slice preparations *in vitro*. Slices were 450µm thick sections of 2° somatosensory cortex cut in the horizontal plane from adult male Wistar rats (150-250g). Slices were prepared according to section 2.1-2.3, and the maintenance of slices is described in section 2.4.

PV immunoreactivity was visualised, and quantified in terms of the number of PV-immunopositive cells in microscopic view fields at a magnification of X10, as described in section 2.9. I was aided with the histology in this chapter by A. Simon. The Kruskal-Wallis one way analysis of variance (ANOVA) on ranks test was used for statistical analysis, with the all pairwise multiple comparison procedures test (Dunn's method) for *post-hoc* comparisons.

7.3 Results – Effect of clozapine on parvalbumin immunoreactivity

Before quantification of PV immunoreactivity, 2° somatosensory cortical slices were fixed at three time points: firstly, before application of clozapine (control); secondly, upon first observation of VFO (< 3 hours after application of clozapine); and, thirdly, after VFO had been present for 7 hours. N numbers were as follows: control, n = 50 view fields in 30 sections (40µm thick) re-sectioned from 4 slices (400µm thick); first VFO occurrence, n = 41 view fields in 23 sections (40µm) from 4 slices (400µm); 7h into VFO, n = 56 view fields in 31 sections (40µm) from 4 slices (400µm).

Compared to control, the onset of clozapine-induced VFO in the slice was accompanied by a massive, significant elevation (110% increase in median, $p < 0.05$) in PV immunoreactivity in superficial layers II/III, and, 7 hours later, PV immunoreactivity in these layers remained significantly greater than the control level (median control number of PV-immunopositive cells per view field 42 (22 → 62), 1st VFO 88 (61 → 112), 7h into VFO 91 (54 → 127), Fig. 7.1).

Similarly, in layer IV, VFO onset was associated with a huge, significant increase (168% increase in median, $p < 0.05$) in PV immunoreactivity. 7 hours later, PV immunoreactivity decreased somewhat in this layer (41% reduction in median, $p > 0.05$) but still remained significantly greater than the control level (median control number of PV-immunopositive cells per view field 31 (18 → 53), 1st VFO 83 (60 → 97), 7h into VFO 59 (37 → 99), Fig. 7.1).

In deep layers V/VI, VFO onset was also associated with a significant elevation (50% increase in median, $p < 0.05$) in PV immunoreactivity. 7 hours later, there was a small reduction in PV immunoreactivity in these layers (15% reduction in median, $p > 0.05$) but it remained significantly greater than the control level (median control number of PV-immunopositive cells per view field 40 (23 → 55), 1st VFO 60 (44 → 69), 7h into VFO 51 (35 → 69), Fig. 7.1).

Thus, in terms of laminar effect, the initial increase in PV immunoreactivity was greater in the more superficial laminar groups, layer II/III (110% increase in median) and layer IV (168% increase in median), compared to deeper layers V/VI (50% increase in median). In each laminar group, there was no significant difference in PV immunoreactivity associated with the first occurrence of VFO compared to that 7 hours later ($p > 0.05$).

Overall, when the laminar groups were pooled to give the total for the slice, VFO onset was associated with a large, significant increase (95% increase in median, $p < 0.05$) in PV immunoreactivity, and, 7 hours later, the total PV immunoreactivity remained significantly greater than the control level (median control number of PV-immunopositive cells per view field 117 (84 → 163), 1st VFO 228 (189 → 277), 7h into VFO 216 (120 → 293)).

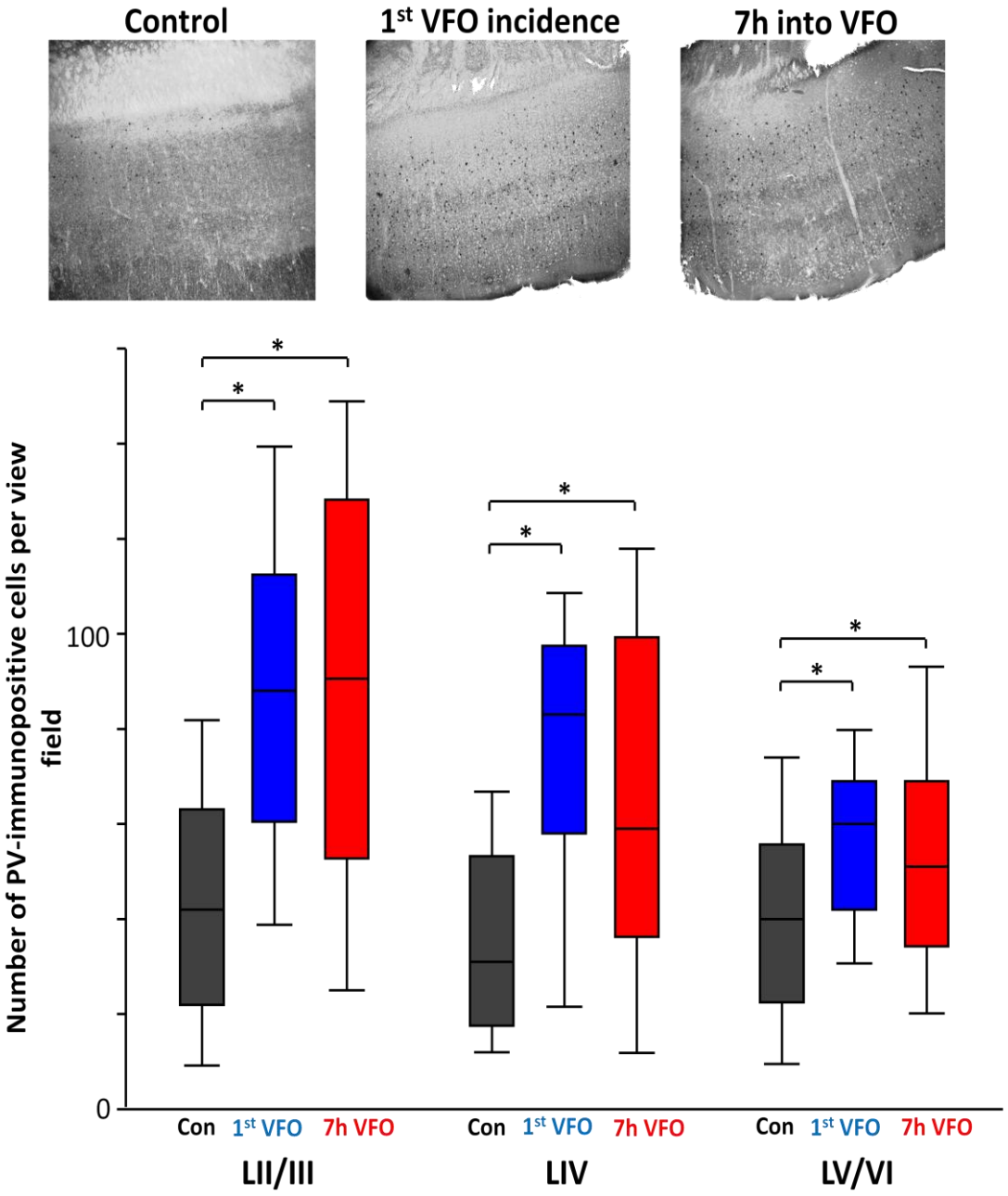

Fig. 7.1. Effect of clozapine (20μM) on the number of parvalbumin-immunopositive interneurons in 2^0 somatosensory cortical laminae. Parvalbumin-immunopositive cells were counted in layer II/III, layer IV, and layer V/VI. Compared to the control, there was a significant increase in the number of parvalbumin-immunopositive cells in each laminar group both when VFO were first observed (< 3 hours after application of clozapine) and after VFO had been present for 7 hours ($p < 0.05$). In the box plot the central line represents the median, the box boundaries represent the interquartile range (Q1 → Q3), and the error bars mark the 10th and 90th percentiles. Example photos are shown at the top with X4 magnification.

7.4 Discussion

PV levels are robustly reduced in post-mortem cortical samples from schizophrenic patients (Beasley and Reynolds, 1997;Danos et al., 1998;Hashimoto et al., 2003). In this thesis, the onset of clozapine-induced VFO was accompanied by a significant elevation in PV immunoreactivity, particularly in layer II-IV, where there was a greater than twofold increase in the signal. It is not clear why clozapine preferentially elevated the PV signal in more superficial layers.

The relatively short timescale of PV upregulation (ca. 3h) suggests that the increase in PV immunoreactivity reflects an increase in PV expression from a level below to a level above the threshold where staining was sufficiently strong to be detected, rather than a change in the phenotype of cells.

It is interesting that the cortical laminae where PV expression is reduced in post-mortem cortical samples from schizophrenic patients, namely layers III and IV (Beasley and Reynolds, 1997;Hashimoto et al., 2003), were among those most affected by the increase in PV immunoreactivity in 2º somatosensory cortex associated with clozapine in this thesis. Furthermore, in LPA1-deficient mice, which model aspects of schizophrenia, the reduction in PV immunopositive interneuron numbers in medial entorhinal cortex is specific to layer II (Cunningham et al., 2006), and clozapine also markedly increased PV immunoreactivity in this layer of 2º somatosensory cortex in this thesis.

The finding that clozapine dramatically increased PV immunoreactivity in layer II-IV in this chapter, together with the finding in chapter 4 of clozapine-induced hyperexcitability in layer V, suggests that clozapine may act to counter PV loss via enhanced excitatory inputs onto superficial interneurons (Watts and Thomson, 2005) from hyperexcitability in layer V. It is also interesting that the pronounced elevation of PV in superficial layers in this chapter corresponds to the superficial origin of clozapine-induced paroxysmal events in chapter 5.

Given that increased PV expression was already present when VFO were first observed, it would appear that altered PV levels are not caused by VFO but instead result from an upstream mechanism.

The finding in this thesis that acute clozapine elevated PV expression in 2º somatosensory cortex *in vitro* is consistent with reports that co-administration of

clozapine reversed PCP-treatment-induced reductions in PV expression in prefrontal cortex (Cochran et al., 2003;Amitai et al., 2012). The finding is also consistent with a preliminary suggestion in a conference abstract that chronic clozapine administration alone may increase PV expression in rat prefrontal cortex (Scruggs and Deutch, 1999). However, the finding is not in agreement with a study in which chronic administration of clozapine had no effect on baseline PV immunoreactivity in either rat hippocampus or frontal cortex (Cahir et al., 2005). Possible reasons for the discrepancy could relate to the method of clozapine delivery (acute application to slices *in vitro* vs intraperitoneal injections *in vivo*) or the different brain regions in question.

7.4.1 Future work

In light of the potential modulation of neuronal excitability and synaptic transmission by PV, it would be interesting to relate intracellular recordings from PV-immunopositive interneurons to changes in PV immunoreactivity.

A green fluorescent protein tag could be used to trace the increase in expression of PV over time.

To elucidate whether upregulation of PV expression may be a marker of atypicality, it would be interesting to compare the effect of clozapine on PV immunoreactivity with that of other antipsychotics, such as the atypical antipsychotic olanzapine, and the classical antipsychotic haloperidol.

To confirm the results, it would be interesting to investigate the effect of clozapine on the neuronal marker NeuN in the present experimental conditions to control for any effect on neuron numbers generally. Similarly, investigation of the effect of clozapine on GAD67, an enzyme that synthesises GABA and a marker for GABAergic inhibitory interneurons, would control for any effects on GABAergic interneurons in general. Indeed, given the reduction in GAD67 in cortical samples from schizophrenic patients (Bird et al., 1978;Hanada et al., 1987;Akbarian et al., 1995) this would be an interesting experiment in itself. It would also be interesting to investigate the effect of clozapine on GABA and calretinin immunoreactivity. Another control would be to ensure that no signal is present upon omission of the primary antibody or each individual step in the immunohistochemistry protocol. Finally, bearing in mind the labile nature of PV, it would be prudent to perform a time-matched control in the absence of clozapine to investigate any changes in PV expression over time.

7.4.2 Concluding remarks

The finding that clozapine increased PV immunoreactivity raises the possibility that clozapine may act to boost GABAergic inhibition in a mechanism involving restoration of PV expression. That is, clozapine may act to counter the reduced inhibitory drive from PV interneurons in schizophrenia (Glausier and Lewis, 2011), possibly via potentiated NMDA receptor-mediated transmission (see section 1.4.2.2-1.4.2.3), and this may be relevant to its therapeutic effect.

Chapter 8

General Discussion

8.1 Summary

The work in this thesis shows an effective *in vitro* animal model of hyperexcitability in cortical tissue associated with the atypical antipsychotic clozapine. Occasional, spontaneous paroxysmal events were seen in association cortex that, when filtered correspondingly to EEG recordings, looked remarkably similar to the clinical presentation. The *in vitro* model data suggested that these synaptic events arose transiently from a background of near-continuous VFO – a situation reported for epileptic human tissue maintained *in vitro* (Roopun et al., 2010b). The mechanism underlying these effects of clozapine was complex: evidence for the involvement of chemical synaptic and gap junctional communication routes was almost completely lacking, but activity in layer V IB neurons correlated well with the local field discharges; both $GABA_A$ receptor blockade and nicotinic acetylcholine receptor blockade failed to completely reproduce the clozapine-related hyperexcitability; parvalbumin levels in cortex were significantly elevated in line with the occurrence and maintenance of clozapine-induced VFO. This final chapter will re-consider these findings in the more general context of clozapine's effectiveness as an antipsychotic and the relationship between excitation and inhibition as relevant to schizophrenia.

8.2 Relation to the clinical presentation

Clozapine-related EEG changes are known to include general slowing of background activity, abnormal theta, abnormal delta, intermittent sharp transients and spike-wave paroxysms – the latter modelled in this thesis (Malow et al., 1994;Welch et al., 1994;Haring et al., 1994;Denney and Stevens, 1995;Freudenreich et al., 1997). With the little data available from clinical collaborators in Newcastle it was clear that, at least in the instances illustrated, the paroxysmal events originated in temporal and parietal regions – hence the choice of analogous brain regions in the *in vitro* model. However, interestingly not all detected events in parietal areas projected to motor regions. This suggests that, as presentation of adverse hyperexcitability with clozapine is usually precipitated by myoclonic jerks, and parietal seizures rarely manifest with motor sequelae, the incidence of clozapine-induce paroxysms may be higher in the medicated population than thought.

When taken together, *in vitro* spatiotemporal progression data for LFPs, spike rates, spike synchrony, and spike-spike correlations, and spike-field correlation data, suggested that clozapine-induced paroxysmal events started superficially in association

cortex, moved deeper and then propagated horizontally along these deep layers. Interestingly, corresponding data suggested that gabazine-induced paroxysmal events also propagated along deep layers and there was some evidence of superficial recruitment. Similarities to some extent in the spatiotemporal progression of events lend some support to the idea that disinhibition may have a role in the mechanism underlying clozapine-induced paroxysmal discharges. However, gabazine-induced paroxysmal events in layer V had a different and more regular shape compared to those induced by clozapine, suggesting that partial disinhibition may not be sufficient *in itself* to precisely mimic clozapine-related hyperexcitability.

8.3 What can we learn from the induction of VFO with clozapine?

The presence of clozapine-induced VFO in wide band recordings *in vitro* in this thesis represented a novel discovery in terms of the effect of clozapine on brain rhythms. Such high frequency activity would not be revealed in scalp EEG recordings in the clinic as a result of the filter settings (0.5 – 70 Hz), which are typical for clinical EEG and prevent contamination of the signal from higher frequency motor unit discharges.

Further to the clinical EEG finding that transient clozapine-related epileptiform activity originated primarily in parietal cortex, the presence of VFO in the isolated microcircuitry of the *in vitro* slice preparation in the functionally equivalent region of brain in the rat, 2º somatosensory cortex, is in line with the particular sensitivity of this region of cortex in the generation of clozapine-related hyperexcitability. This may be at least partially due to the prominence of gap-junctionally connected IB cells in layer V of this region. This particular local circuit has been shown to generate high frequency bursts previously, a property not shared by adjacent primary sensory areas (see Roopun et al., 2010a). Indeed, intracellular studies here showed the closest correlations between IB cell intracellular activity and the field VFO. However, a role for gap junctions is questionable given the results from attempts to pharmacologically block VFO in this thesis. IB cells can burst alone, as a consequence of their intrinsic axonal properties (e.g. Kramer et al., 2008) so it may be that the VFO seen in the field may represent local bursts from functionally unconnected IB neurons – in other words the extracellular VFO potentials may be generated transiently, by partially synchronous multiunit activity. This would also count against the ability of extracranial EEG to detect them as the spatial averaging inherent in such large (1 cm diameter), distally located electrodes may reduce the local VFO field to below background noise levels.

Nevertheless, in line with the idea that VFO may be a biomarker for epilepsy-related cortical pathology (Jacobs et al., 2010), clozapine-induced VFO may represent an early biomarker of clozapine-related hyperexcitability, possibly present before more severe epileptiform activity. Both clozapine and olanzapine induced prominent VFO, but there was only a low extent of VFO associated with haloperidol, consistent with the relative risk of EEG abnormalities associated with these drugs in the clinic (Centorrino et al., 2002). In addition, the presence of relatively strong correlations between IB cell spikelets and field VFO suggested the involvement of axonal hyperexcitability in this cell type in the atypical antipsychotic-specific mechanism.

The presence of spikelets in neuronal subtypes which contribute to the generation of the rhythm may also be a characteristic feature of gap-junction-mediated VFO (Draguhn et al., 1998;Schmitz et al., 2001). An action potential in a pre-junctional neuron can generate a response which is either above or below the threshold required to generate an action potential in the post-junctional neuron, depending on the effectiveness of the coupling at the gap junction. It is thought that spikelets might occur following subthreshold potential changes in postjunctional neurons. However, as mentioned above, no chemical synaptic blockers or gap junction conductance-reducing drugs had any significant effect to reduce VFO incidence or power – with the exception of octanol. But this drug also potently blocks fast sodium conductances so may exert its effect directly on axonal excitability rather than axo-axonic communication. Spikelets are still manifest as partially back-propagated ectopic action potentials even in the presence of gap junction blockers (Roopun et al., 2006), though their incidence is much reduced.

From the data gathered as part of this thesis it is still not clear how the VFO and the, at least casually related, paroxysmal discharges arise. IB cell bursting is dependent on many intrinsic conductances including m-current as well as synaptic inhibition at the axon intial segment and perisomatically. There is no information directly relevant to effects of clozapine on m-current but data here, and in the literature does suggest some effect on the inhibitory system.

8.4 Consequences of raised PV levels

PV levels are robustly reduced in post-mortem cortical samples from schizophrenic patients (Beasley and Reynolds, 1997;Danos et al., 1998;Hashimoto et al., 2003). It has been suggested that this may constitute the primary pathology in schizophrenia (see Introduction). However, PV levels are notoriously labile and are affected by GABA levels and the magnitude and pattern of excitatory input to interneurons – less excitation reduced PV levels. There are clues as to why this may occur in studies showing what PV does functionally at GABAergic terminals: PV is a highly effective sequestering agent for intracellular free calcium. The presence of PV sharply curtails any transient rise in baseline cytosolic calcium from levels above ca. 70 nM. Thus, it has a dramatic effect on excitation/exocytosis coupling, effectively temporally limiting the release of GABA through vesicular fusion on invasion of an action potential at an inhibitory neuronal presynaptic terminal. It has therefore been suggested that reduced PV expression in brain tissue from patients with schizophrenia may be a compensatory mechanism to increase GABAergic inhibition in the light of reduced excitation of interneurons (Javitt, 2010).

Experimentally reducing PV levels by producing knock-out mice with an absence of the PV gene showed the consequences of this 'compensatory' mechanism functionally. Absence of PV was associated with larger, longer stimulated postsynaptic inhibitory events and an elevation in persistent gamma rhythms (Vreugdenhil et al., 2003). Interestingly gamma rhythms are reduced in EEG recordings from patients with schizophrenia, again suggesting a partial compensatory mechanism for this modification in the inhibitory system.

In this thesis, the onset of clozapine-induced VFO was accompanied by a significant elevation in PV immunoreactivity, particularly in layer II-IV, which include the cortical laminae where PV expression is reduced in post-mortem cortical samples from schizophrenic patients, namely layers III and IV (Beasley and Reynolds, 1997;Hashimoto et al., 2003).

The finding that clozapine dramatically increased PV immunoreactivity in layer II-IV, together with the finding of clozapine-induced hyperexcitability in layer V, suggests that clozapine may act primarily to counter schizophrenia-associated PV loss. However, this raises two issues: firstly, if the reduction in PV is to be considered compensatory in schizophrenia then countering this reduction with elevation of PV levels with clozapine

ought to, logically, make the symptoms worse. But the converse is true. This suggests that the reduction in PV expression may indeed be a primary pathology in patients with schizophrenia.

Secondly, the profile of elevated PV expression appeared in layers superficial to the hyperexcitability seen in the model. These layers mapped nicely to the layers where the most overt reduction in PV expression was seen in schizophrenia. As far as the onset of the paroxysmal discharges was concerned (superficial layers first) this raised the suggestion that this facet of clozapine-induced hyperexcitability may be, in part, related to partial disinhibition secondary to reduced GABA release caused by over-sequestration of presynaptic terminal calcium levels. However, as mentioned above, PV expression is highly labile to excitatory inputs and axonal bursting in layer V IB neurons was seen. Layer V excitatory neurons provide inputs onto superficial interneurons (Watts and Thomson, 2005). Thus the hyperexcitability in layer V may boost excitation of superficial interneurons and underlie the elevated PV levels seen in these layers. That is, clozapine may act to counter the reduced inhibitory drive from superficisal PV interneurons in schizophrenia (Glausier and Lewis, 2011), possibly via potentiated NMDA receptor-mediated transmission, and this may be relevant to its therapeutic effect.

8.5 Are we any closer to an underlying mechanism?

None of the above arguments addresses the question of where the layer V hyperexcitability comes from in the first place. PV changes in this layer were modest so unlikely to be directly relevant. Neither can we infer that increased excitation of layer V neurons was via enhanced inputs from superficial layer pyramidal cells (dishinhibited through reduced GABA release caused by the PV changes). While this latter suggestion fits with the timing of the PV elevation and VFO genesis (the PV levels already high when VFO is first seen), very little in the way of synaptic excitation (as EPSPs) was seen accompanying the VFO in layer V. One possibility is that PV-immunopositive interneurons in superficial layers provide some direct inhibition to layer V pyramidal cells via interlaminar axon collaterals. This is not recognised as a major interlaminar pathway from the work of Thomson and colleagues (Watts and Thomson, 2005). However, layer V neurons receive synaptic inhibition precisely timed to superficial layer gamma rhythms (Ainsworth et al., 2011), and a number of more recent exceptions to the proposal for interlaminar communication by Thompson have been discovered (e.g. Lefort et al., 2009).

While the data in this thesis shows a clear correlation between PV levels and hyperexcitability in association cortex, it has proved difficult to separate cause from effect. It may be that arguments such as those above attempting to relate the phenomena to basic excitatory and inhibitory synaptic physiology are flawed. As mentioned in the introduction, the pharmacological profile of atypical antipsychotics is remarkably diverse. To fully understand the processes modelled in this thesis from a mechanistic perspective future work would require a systematic investigation of the effects of each of the receptor systems targeted by clozapine.

Bibliography

Adrian ED (1950) Sensory discrimination with some recent evidence from the olfactory organ. Br Med Bull 6:330-333.

Aghajanian GK, Rasmussen K (1989) Intracellular studies in the facial nucleus illustrating a simple new method for obtaining viable motoneurons in adult rat brain slices. Synapse 3:331-338.

Ainsworth M, Lee S, Cunningham MO, Roopun AK, Traub RD, Kopell NJ, Whittington MA (2011) Dual gamma rhythm generators control interlaminar synchrony in auditory cortex. J Neurosci 31:17040-17051.

Akbarian S, Kim JJ, Potkin SG, Hagman JO, Tafazzoli A, Bunney WE, Jr., Jones EG (1995) Gene expression for glutamic acid decarboxylase is reduced without loss of neurons in prefrontal cortex of schizophrenics. Arch Gen Psychiatry 52:258-266.

Akiyama T, Chan DW, Go CY, Ochi A, Elliott IM, Donner EJ, Weiss SK, Snead OC, III, Rutka JT, Drake JM, Otsubo H (2011) Topographic movie of intracranial ictal high-frequency oscillations with seizure semiology: epileptic network in Jacksonian seizures. Epilepsia 52:75-83.

Akiyama T, Otsubo H, Ochi A, Galicia EZ, Weiss SK, Donner EJ, Rutka JT, Snead OC, III (2006) Topographic movie of ictal high-frequency oscillations on the brain surface using subdural EEG in neocortical epilepsy. Epilepsia 47:1953-1957.

Akiyama T, Otsubo H, Ochi A, Ishiguro T, Kadokura G, Ramachandrannair R, Weiss SK, Rutka JT, Carter SO, III (2005) Focal cortical high-frequency oscillations trigger epileptic spasms: confirmation by digital video subdural EEG. Clin Neurophysiol 116:2819-2825.

Alessandri B, Battig K, Welzl H (1989) Effects of ketamine on tunnel maze and water maze performance in the rat. Behav Neural Biol 52:194-212.

Alldredge BK (1999) Seizure risk associated with psychotropic drugs: clinical and pharmacokinetic considerations. Neurology 53:S68-S75.

Allen PJ, Fish DR, Smith SJ (1992) Very high-frequency rhythmic activity during SEEG suppression in frontal lobe epilepsy. Electroencephalogr Clin Neurophysiol 82:155-159.

Alonso-Solis A, Corripio I, de Castro-Manglano P, Duran-Sindreu S, Garcia-Garcia M, Proal E, Nunez-Marin F, Soutullo C, Alvarez E, Gomez-Anson B, Kelly C, Castellanos FX (2012) Altered default network resting state functional connectivity in patients with a first episode of psychosis. Schizophr Res 139:13-18.

Altar CA, Wasley AM, Neale RF, Stone GA (1986) Typical and atypical antipsychotic occupancy of D2 and S2 receptors: an autoradiographic analysis in rat brain. Brain Res Bull 16:517-525.

Amann BL, Pogarell O, Mergl R, Juckel G, Grunze H, Mulert C, Hegerl U (2003) EEG abnormalities associated with antipsychotics: a comparison of quetiapine, olanzapine, haloperidol and healthy subjects. Hum Psychopharmacol 18:641-646.

Amitai N, Kuczenski R, Behrens MM, Markou A (2012) Repeated phencyclidine administration alters glutamate release and decreases GABA markers in the prefrontal cortex of rats. Neuropharmacology 62:1422-1431.

Antony JT, Elias A, Chacko F, Rajan B (2008) Is clozapine safe in patients with preexisting epilepsy? A report of 2 cases. J Clin Psychiatry 69:328-329.

Arellano JI, DeFelipe J, Munoz A (2002) PSA-NCAM immunoreactivity in chandelier cell axon terminals of the human temporal cortex. Cereb Cortex 12:617-624.

Armstrong-James M, Fox K, Das-Gupta A (1992) Flow of excitation within rat barrel cortex on striking a single vibrissa. J Neurophysiol 68:1345-1358.

Arvanov VL, Liang X, Schwartz J, Grossman S, Wang RY (1997) Clozapine and haloperidol modulate N-methyl-D-aspartate- and non-N-methyl-D-aspartate receptor-mediated neurotransmission in rat prefrontal cortical neurons in vitro. J Pharmacol Exp Ther 283:226-234.

Arvanov VL, Wang RY (1999) Clozapine, but not haloperidol, prevents the functional hyperactivity of N-methyl-D-aspartate receptors in rat cortical neurons induced by subchronic administration of phencyclidine. J Pharmacol Exp Ther 289:1000-1006.

Asano E, Juhasz C, Shah A, Muzik O, Chugani DC, Shah J, Sood S, Chugani HT (2005) Origin and propagation of epileptic spasms delineated on electrocorticography. Epilepsia 46:1086-1097.

Avoli M, Barbarosie M, Lucke A, Nagao T, Lopantsev V, Kohling R (1996a) Synchronous GABA-mediated potentials and epileptiform discharges in the rat limbic system in vitro. J Neurosci 16:3912-3924.

Avoli M, Bernasconi A, Mattia D, Olivier A, Hwa GG (1999) Epileptiform discharges in the human dysplastic neocortex: in vitro physiology and pharmacology. Ann Neurol 46:816-826.

Avoli M, D'Antuono M, Louvel J, Kohling R, Biagini G, Pumain R, D'Arcangelo G, Tancredi V (2002) Network and pharmacological mechanisms leading to epileptiform synchronization in the limbic system in vitro. Prog Neurobiol 68:167-207.

Avoli M, Drapeau C, Louvel J, Pumain R, Olivier A, Villemure JG (1991) Epileptiform activity induced by low extracellular magnesium in the human cortex maintained in vitro. Ann Neurol 30:589-596.

Avoli M, Drapeau C, Perreault P, Louvel J, Pumain R (1990) Epileptiform activity induced by low chloride medium in the CA1 subfield of the hippocampal slice. J Neurophysiol 64:1747-1757.

Avoli M, Gloor P (1982a) Interaction of cortex and thalamus in spike and wave discharges of feline generalized penicillin epilepsy. Exp Neurol 76:196-217.

Avoli M, Gloor P (1982b) Role of the thalamus in generalized penicillin epilepsy: observations on decorticated cats. Exp Neurol 77:386-402.

Avoli M, Louvel J, Kurcewicz I, Pumain R, Barbarosie M (1996b) Extracellular free potassium and calcium during synchronous activity induced by 4-aminopyridine in the juvenile rat hippocampus. J Physiol 493 (Pt 3):707-717.

Avoli M, Nagao T, Kohling R, Lucke A, Mattia D (1996c) Synchronization of rat hippocampal neurons in the absence of excitatory amino acid-mediated transmission. Brain Res 735:188-196.

Avoli M, Olivier A (1989) Electrophysiological properties and synaptic responses in the deep layers of the human epileptogenic neocortex in vitro. J Neurophysiol 61:589-606.

Avoli M, Psarropoulou C, Tancredi V, Fueta Y (1993) On the synchronous activity induced by 4-aminopyridine in the CA3 subfield of juvenile rat hippocampus. J Neurophysiol 70:1018-1029.

Ayala GF, Dichter M, Gumnit RJ, Matsumoto H, Spencer WA (1973) Genesis of epileptic interictal spikes. New knowledge of cortical feedback systems suggests a neurophysiological explanation of brief paroxysms. Brain Res 52:1-17.

Babb TL, Pretorius JK, Kupfer WR, Crandall PH (1989) Glutamate decarboxylase-immunoreactive neurons are preserved in human epileptic hippocampus. J Neurosci 9:2562-2574.

Bak TH, Bauer M, Schaub RT, Hellweg R, Reischies FM (1995) Myoclonus in patients treated with clozapine: a case series. J Clin Psychiatry 56:418-422.

Baker SN, Pinches EM, Lemon RN (2003) Synchronization in monkey motor cortex during a precision grip task. II. effect of oscillatory activity on corticospinal output. J Neurophysiol 89:1941-1953.

Bakshi VP, Swerdlow NR, Geyer MA (1994) Clozapine antagonizes phencyclidine-induced deficits in sensorimotor gating of the startle response. J Pharmacol Exp Ther 271:787-794.

Baldessarini RJ, Centorrino F, Flood JG, Volpicelli SA, Huston-Lyons D, Cohen BM (1993) Tissue concentrations of clozapine and its metabolites in the rat. Neuropsychopharmacology 9:117-124.

Banerjee SP, Zuck LG, Yablonsky-Alter E, Lidsky TI (1995) Glutamate agonist activity: implications for antipsychotic drug action and schizophrenia. Neuroreport 6:2500-2504.

Barch DM, Smith E (2008) The cognitive neuroscience of working memory: relevance to CNTRICS and schizophrenia. Biol Psychiatry 64:11-17.

Barth DS (2003) Submillisecond synchronization of fast electrical oscillations in neocortex. J Neurosci 23:2502-2510.

Baskys A, Wang S, Remington G, Wojtowicz JM (1993) Haloperidol and loxapine but not clozapine increase synaptic responses in the hippocampus. Eur J Pharmacol 235:305-307.

Bear J, Fountain NB, Lothman EW (1996) Responses of the superficial entorhinal cortex in vitro in slices from naive and chronically epileptic rats. J Neurophysiol 76:2928-2940.

Beasley CL, Reynolds GP (1997) Parvalbumin-immunoreactive neurons are reduced in the prefrontal cortex of schizophrenics. Schizophr Res 24:349-355.

Behrens CJ, van den Boom LP, Heinemann U (2007a) Effects of the GABA(A) receptor antagonists bicuculline and gabazine on stimulus-induced sharp wave-ripple complexes in adult rat hippocampus in vitro. Eur J Neurosci 25:2170-2181.

Behrens MM, Ali SS, Dao DN, Lucero J, Shekhtman G, Quick KL, Dugan LL (2007b) Ketamine-induced loss of phenotype of fast-spiking interneurons is mediated by NADPH-oxidase. Science 318:1645-1647.

Belforte JE, Zsiros V, Sklar ER, Jiang Z, Yu G, Li Y, Quinlan EM, Nakazawa K (2010) Postnatal NMDA receptor ablation in corticolimbic interneurons confers schizophrenia-like phenotypes. Nat Neurosci 13:76-83.

Belluardo N, Mudo G, Trovato-Salinaro A, Le GS, Charollais A, Serre-Beinier V, Amato G, Haefliger JA, Meda P, Condorelli DF (2000) Expression of connexin36 in the adult and developing rat brain. Brain Res 865:121-138.

BENASSI P, BERTOLOTTI P (1962) [Experimental research on the anticonvulsant properties of 1-glutamine, 1-asparagine, gamma-aminobutyric acid and gamma-amino-beta-hydroxybutyric acid]. Riv Sper Freniatr Med Leg Alien Ment 86:342-354.

Benneyworth MA, Roseman AS, Basu AC, Coyle JT (2011) Failure of NMDA receptor hypofunction to induce a pathological reduction in PV-positive GABAergic cell markers. Neurosci Lett 488:267-271.

Benson DL, Huntsman MM, Jones EG (1994) Activity-dependent changes in GAD and preprotachykinin mRNAs in visual cortex of adult monkeys. Cereb Cortex 4:40-51.

Bichot NP, Rossi AF, Desimone R (2005) Parallel and serial neural mechanisms for visual search in macaque area V4. Science 308:529-534.

Bird ED, Spokes EG, Barnes J, Mackay AV, Iversen LL, Shepherd M (1978) Glutamic-acid decarboxylase in schizophrenia. Lancet 1:156.

Bliss TV, Collingridge GL (1993) A synaptic model of memory: long-term potentiation in the hippocampus. Nature 361:31-39.

Block Rosen J, Milstein MJ, Haut SR (2012) Olanzapine-associated myoclonus. Epilepsy Res 98:247-250.

Bonelli RM (2003) Olanzapine-associated seizure. Ann Pharmacother 37:149-150.

Bouyer JJ, Montaron MF, Rougeul A (1981) Fast fronto-parietal rhythms during combined focused attentive behaviour and immobility in cat: cortical and thalamic localizations. Electroencephalogr Clin Neurophysiol 51:244-252.

Bouyer JJ, Montaron MF, Vahnee JM, Albert MP, Rougeul A (1987) Anatomical localization of cortical beta rhythms in cat. Neuroscience 22:863-869.

Boyce S, Rupniak NM, Steventon MJ, Cook G, Iversen SD (1991) Psychomotor activity and cognitive disruption attributable to NMDA, but not sigma, interactions in primates. Behav Brain Res 42:115-121.

Bragin A, Azizyan A, Almajano J, Wilson CL, Engel J, Jr. (2005) Analysis of chronic seizure onsets after intrahippocampal kainic acid injection in freely moving rats. Epilepsia 46:1592-1598.

Bragin A, Engel J, Jr., Wilson CL, Fried I, Buzsaki G (1999a) High-frequency oscillations in human brain. Hippocampus 9:137-142.

Bragin A, Engel J, Jr., Wilson CL, Fried I, Mathern GW (1999b) Hippocampal and entorhinal cortex high-frequency oscillations (100--500 Hz) in human epileptic brain and in kainic acid--treated rats with chronic seizures. Epilepsia 40:127-137.

Bragin A, Jando G, Nadasdy Z, Hetke J, Wise K, Buzsaki G (1995) Gamma (40-100 Hz) oscillation in the hippocampus of the behaving rat. J Neurosci 15:47-60.

Bragin A, Mody I, Wilson CL, Engel J, Jr. (2002a) Local generation of fast ripples in epileptic brain. J Neurosci 22:2012-2021.

Bragin A, Wilson CL, Engel J (2003) Spatial stability over time of brain areas generating fast ripples in the epileptic rat. Epilepsia 44:1233-1237.

Bragin A, Wilson CL, Staba RJ, Reddick M, Fried I, Engel J, Jr. (2002b) Interictal high-frequency oscillations (80-500 Hz) in the human epileptic brain: entorhinal cortex. Ann Neurol 52:407-415.

Bredkjaer SR, Mortensen PB, Parnas J (1998) Epilepsy and non-organic non-affective psychosis. National epidemiologic study. Br J Psychiatry 172:235-238.

Bristow LJ, Kramer MS, Kulagowski J, Patel S, Ragan CI, Seabrook GR (1997) Schizophrenia and L-745,870, a novel dopamine D4 receptor antagonist. Trends Pharmacol Sci 18:186-188.

Buzsaki G (1986) Hippocampal sharp waves: their origin and significance. Brain Res 398:242-252.

Buzsaki G, Horvath Z, Urioste R, Hetke J, Wise K (1992) High-frequency network oscillation in the hippocampus. Science 256:1025-1027.

Cahir M, Costello I, King DJ, Reynolds GP (2005) Chronic haloperidol or clozapine treatment does not alter parvalbumin immunoreactivity in the rat frontal cortex or hippocampus. Neurosci Lett 373:57-60.

Camacho A, Garcia-Navarro M, Martinez B, Villarejo A, Pomares E (2005) Olanzapine-induced myoclonic status. Clin Neuropharmacol 28:145-147.

Canuet L, Ishii R, Pascual-Marqui RD, Iwase M, Kurimoto R, Aoki Y, Ikeda S, Takahashi H, Nakahachi T, Takeda M (2011) Resting-state EEG source localization and functional connectivity in schizophrenia-like psychosis of epilepsy. PLoS One 6:e27863.

Carder RK, Leclerc SS, Hendry SH (1996) Regulation of calcium-binding protein immunoreactivity in GABA neurons of macaque primary visual cortex. Cereb Cortex 6:271-287.

Cardin JA, Carlen M, Meletis K, Knoblich U, Zhang F, Deisseroth K, Tsai LH, Moore CI (2009) Driving fast-spiking cells induces gamma rhythm and controls sensory responses. Nature 459:663-667.

Carlen M, Meletis K, Siegle JH, Cardin JA, Futai K, Vierling-Claassen D, Ruhlmann C, Jones SR, Deisseroth K, Sheng M, Moore CI, Tsai LH (2012) A critical role for NMDA receptors in parvalbumin interneurons for gamma rhythm induction and behavior. Mol Psychiatry 17:537-548.

Carlsson M, Carlsson A (1990) Interactions between glutamatergic and monoaminergic systems within the basal ganglia--implications for schizophrenia and Parkinson's disease. Trends Neurosci 13:272-276.

Castner SA, Williams GV, Goldman-Rakic PS (2000) Reversal of antipsychotic-induced working memory deficits by short-term dopamine D1 receptor stimulation. Science 287:2020-2022.

Centorrino F, Price BH, Tuttle M, Bahk WM, Hennen J, Albert MJ, Baldessarini RJ (2002) EEG abnormalities during treatment with typical and atypical antipsychotics. Am J Psychiatry 159:109-115.

Chagnac-Amitai Y, Luhmann HJ, Prince DA (1990) Burst generating and regular spiking layer 5 pyramidal neurons of rat neocortex have different morphological features. J Comp Neurol 296:598-613.

Chard PS, Bleakman D, Christakos S, Fullmer CS, Miller RJ (1993) Calcium buffering properties of calbindin D28k and parvalbumin in rat sensory neurones. J Physiol 472:341-357.

Chepkova AN, Sergeeva OA, Haas HL (2008) Carbenoxolone impairs LTP and blocks NMDA receptors in murine hippocampus. Neuropharmacology 55:139-147.

Chiodo LA, Bunney BS (1983) Typical and atypical neuroleptics: differential effects of chronic administration on the activity of A9 and A10 midbrain dopaminergic neurons. J Neurosci 3:1607-1619.

Chrobak JJ, Buzsaki G (1994) Selective activation of deep layer (V-VI) retrohippocampal cortical neurons during hippocampal sharp waves in the behaving rat. J Neurosci 14:6160-6170.

Chrobak JJ, Buzsaki G (1996) High-frequency oscillations in the output networks of the hippocampal-entorhinal axis of the freely behaving rat. J Neurosci 16:3056-3066.

Cochran SM, Fujimura M, Morris BJ, Pratt JA (2002) Acute and delayed effects of phencyclidine upon mRNA levels of markers of glutamatergic and GABAergic neurotransmitter function in the rat brain. Synapse 46:206-214.

Cochran SM, Kennedy M, McKerchar CE, Steward LJ, Pratt JA, Morris BJ (2003) Induction of metabolic hypofunction and neurochemical deficits after chronic intermittent exposure to phencyclidine: differential modulation by antipsychotic drugs. Neuropsychopharmacology 28:265-275.

Cohen BM, Tsuneizumi T, Baldessarini RJ, Campbell A, Babb SM (1992) Differences between antipsychotic drugs in persistence of brain levels and behavioral effects. Psychopharmacology (Berl) 108:338-344.

Cohen I, Navarro V, Clemenceau S, Baulac M, Miles R (2002) On the origin of interictal activity in human temporal lobe epilepsy in vitro. Science 298:1418-1421.

Cole MW, Anticevic A, Repovs G, Barch D (2011) Variable global dysconnectivity and individual differences in schizophrenia. Biol Psychiatry 70:43-50.

Colpaert FC (2003) Discovering risperidone: the LSD model of psychopathology. Nat Rev Drug Discov 2:315-320.

Conde F, Lund JS, Jacobowitz DM, Baimbridge KG, Lewis DA (1994) Local circuit neurons immunoreactive for calretinin, calbindin D-28k or parvalbumin in monkey prefrontal cortex: distribution and morphology. J Comp Neurol 341:95-116.

Conley RR, Kelly DL (2001) Management of treatment resistance in schizophrenia. Biol Psychiatry 50:898-911.

Connors BW (1984) Initiation of synchronized neuronal bursting in neocortex. Nature 310:685-687.

Cosgrove J, Newell TG (1991) Recovery of neuropsychological functions during reduction in use of phencyclidine. J Clin Psychol 47:159-169.

Cossart R, Bernard C, Ben-Ari Y (2005) Multiple facets of GABAergic neurons and synapses: multiple fates of GABA signalling in epilepsies. Trends Neurosci 28:108-115.

Cossart R, Dinocourt C, Hirsch JC, Merchan-Perez A, De Felipe J, Ben-Ari Y, Esclapez M, Bernard C (2001) Dendritic but not somatic GABAergic inhibition is decreased in experimental epilepsy. Nat Neurosci 4:52-62.

Cosway R, Byrne M, Clafferty R, Hodges A, Grant E, Abukmeil SS, Lawrie SM, Miller P, Johnstone EC (2000) Neuropsychological change in young people at high risk for schizophrenia: results from the first two neuropsychological assessments of the Edinburgh High Risk Study. Psychol Med 30:1111-1121.

COURSIN DB (1954) Convulsive seizures in infants with pyridoxine-deficient diet. J Am Med Assoc 154:406-408.

Coyle JT (2006) Glutamate and schizophrenia: beyond the dopamine hypothesis. Cell Mol Neurobiol 26:365-384.

Creese I, Burt DR, Snyder SH (1976) Dopamine receptor binding predicts clinical and pharmacological potencies of antischizophrenic drugs. Science 192:481-483.

Cunningham MO, Davies CH, Buhl EH, Kopell N, Whittington MA (2003) Gamma oscillations induced by kainate receptor activation in the entorhinal cortex in vitro. J Neurosci 23:9761-9769.

Cunningham MO, Halliday DM, Davies CH, Traub RD, Buhl EH, Whittington MA (2004) Coexistence of gamma and high-frequency oscillations in rat medial entorhinal cortex in vitro. J Physiol 559:347-353.

Cunningham MO, Hunt J, Middleton S, LeBeau FE, Gillies MJ, Davies CH, Maycox PR, Whittington MA, Racca C (2006) Region-specific reduction in entorhinal gamma oscillations and parvalbumin-immunoreactive neurons in animal models of psychiatric illness. J Neurosci 26:2767-2776.

Cunningham MO, Roopun A, Schofield IS, Whittaker RG, Duncan R, Russell A, Jenkins A, Nicholson C, Whittington MA, Traub RD (2012) Glissandi: transient fast electrocorticographic oscillations of steadily increasing frequency, explained by temporally increasing gap junction conductance. Epilepsia 53:1205-1214.

Curio G (2000) Linking 600-Hz "spikelike" EEG/MEG wavelets ("sigma-bursts") to cellular substrates: concepts and caveats. J Clin Neurophysiol 17:377-396.

Curio G, Mackert BM, Burghoff M, Koetitz R, braham-Fuchs K, Harer W (1994) Localization of evoked neuromagnetic 600 Hz activity in the cerebral somatosensory system. Electroencephalogr Clin Neurophysiol 91:483-487.

Daly DA, Moghaddam B (1993) Actions of clozapine and haloperidol on the extracellular levels of excitatory amino acids in the prefrontal cortex and striatum of conscious rats. Neurosci Lett 152:61-64.

Danos P, Baumann B, Bernstein HG, Franz M, Stauch R, Northoff G, Krell D, Falkai P, Bogerts B (1998) Schizophrenia and anteroventral thalamic nucleus: selective decrease of parvalbumin-immunoreactive thalamocortical projection neurons. Psychiatry Res 82:1-10.

Danysz W, Wroblewski JT, Costa E (1988) Learning impairment in rats by N-methyl-D-aspartate receptor antagonists. Neuropharmacology 27:653-656.

Dasheiff RM (1985) d-Tubocurarine causes neuronal death when injected directly into rat brain. Exp Neurol 89:172-188.

Davenport CJ, Brown WJ, Babb TL (1990) Sprouting of GABAergic and mossy fiber axons in dentate gyrus following intrahippocampal kainate in the rat. Exp Neurol 109:180-190.

Davidson M, Reichenberg A, Rabinowitz J, Weiser M, Kaplan Z, Mark M (1999) Behavioral and intellectual markers for schizophrenia in apparently healthy male adolescents. Am J Psychiatry 156:1328-1335.

Davis JM (2006) The choice of drugs for schizophrenia. N Engl J Med 354:518-520.

de Curtis M, Gnatkovsky V (2009) Reevaluating the mechanisms of focal ictogenesis: The role of low-voltage fast activity. Epilepsia 50:2514-2525.

de Guzman P, Inaba Y, Baldelli E, de Curtis M, Biagini G, Avoli M (2008) Network hyperexcitability within the deep layers of the pilocarpine-treated rat entorhinal cortex. J Physiol 586:1867-1883.

de Guzman P, Inaba Y, Biagini G, Baldelli E, Mollinari C, Merlo D, Avoli M (2006) Subiculum network excitability is increased in a rodent model of temporal lobe epilepsy. Hippocampus 16:843-860.

de Paulis T (2001) M-100907 (Aventis). Curr Opin Investig Drugs 2:123-132.

Deans MR, Gibson JR, Sellitto C, Connors BW, Paul DL (2001) Synchronous activity of inhibitory networks in neocortex requires electrical synapses containing connexin36. Neuron 31:477-485.

DeFelipe J (1999) Chandelier cells and epilepsy. Brain 122 (Pt 10):1807-1822.

Degner D, Nitsche MA, Bias F, Ruther E, Reulbach U (2011) EEG alterations during treatment with olanzapine. Eur Arch Psychiatry Clin Neurosci 261:483-488.

Delpire E, Rauchman MI, Beier DR, Hebert SC, Gullans SR (1994) Molecular cloning and chromosome localization of a putative basolateral Na(+)-K(+)-2Cl- cotransporter from mouse inner medullary collecting duct (mIMCD-3) cells. J Biol Chem 269:25677-25683.

Denney D, Stevens JR (1995) Clozapine and seizures. Biol Psychiatry 37:427-433.

Deserno L, Sterzer P, Wustenberg T, Heinz A, Schlagenhauf F (2012) Reduced prefrontal-parietal effective connectivity and working memory deficits in schizophrenia. J Neurosci 32:12-20.

Deshauer D, Albuquerque J, Alda M, Grof P (2000) Seizures caused by possible interaction between olanzapine and clomipramine. J Clin Psychopharmacol 20:283-284.

Devinsky O, Honigfeld G, Patin J (1991) Clozapine-related seizures. Neurology 41:369-371.

Dhillon A, Jones RS (2000) Laminar differences in recurrent excitatory transmission in the rat entorhinal cortex in vitro. Neuroscience 99:413-422.

Di Prisco GV, Freeman WJ (1985) Odor-related bulbar EEG spatial pattern analysis during appetitive conditioning in rabbits. Behav Neurosci 99:964-978.

Dichter M, Spencer WA (1969) Penicillin-induced interictal discharges from the cat hippocampus. I. Characteristics and topographical features. J Neurophysiol 32:649-662.

Draguhn A, Traub RD, Schmitz D, Jefferys JG (1998) Electrical coupling underlies high-frequency oscillations in the hippocampus in vitro. Nature 394:189-192.

Dreier JP, Heinemann U (1991) Regional and time dependent variations of low Mg2+ induced epileptiform activity in rat temporal cortex slices. Exp Brain Res 87:581-596.

Du F, Eid T, Lothman EW, Kohler C, Schwarcz R (1995) Preferential neuronal loss in layer III of the medial entorhinal cortex in rat models of temporal lobe epilepsy. J Neurosci 15:6301-6313.

Du F, Whetsell WO, Jr., bou-Khalil B, Blumenkopf B, Lothman EW, Schwarcz R (1993) Preferential neuronal loss in layer III of the entorhinal cortex in patients with temporal lobe epilepsy. Epilepsy Res 16:223-233.

Duncan GE, Leipzig JN, Mailman RB, Lieberman JA (1998) Differential effects of clozapine and haloperidol on ketamine-induced brain metabolic activation. Brain Res 812:65-75.

Dzhala VI, Staley KJ (2004) Mechanisms of fast ripples in the hippocampus. J Neurosci 24:8896-8906.

Edwards E, Soltani M, Deouell LY, Berger MS, Knight RT (2005) High gamma activity in response to deviant auditory stimuli recorded directly from human cortex. J Neurophysiol 94:4269-4280.

Egan MF, Goldberg TE, Gscheidle T, Weirich M, Rawlings R, Hyde TM, Bigelow L, Weinberger DR (2001) Relative risk for cognitive impairments in siblings of patients with schizophrenia. Biol Psychiatry 50:98-107.

Eid T, Schwarcz R, Ottersen OP (1999) Ultrastructure and immunocytochemical distribution of GABA in layer III of the rat medial entorhinal cortex following aminooxyacetic acid-induced seizures. Exp Brain Res 125:463-475.

Esclapez M, Hirsch JC, Khazipov R, Ben-Ari Y, Bernard C (1997) Operative GABAergic inhibition in hippocampal CA1 pyramidal neurons in experimental epilepsy. Proc Natl Acad Sci U S A 94:12151-12156.

Evins AE, Fitzgerald SM, Wine L, Rosselli R, Goff DC (2000) Placebo-controlled trial of glycine added to clozapine in schizophrenia. Am J Psychiatry 157:826-828.

Ewert TA, Vahle-Hinz C, Engel AK (2008) High-frequency whisker vibration is encoded by phase-locked responses of neurons in the rat's barrel cortex. J Neurosci 28:5359-5368.

Farrant M, Kaila K (2007) The cellular, molecular and ionic basis of GABA(A) receptor signalling. Prog Brain Res 160:59-87.

Fiez JA, Raichle ME, Balota DA, Tallal P, Petersen SE (1996) PET activation of posterior temporal regions during auditory word presentation and verb generation. Cereb Cortex 6:1-10.

Fisher RS, Webber WR, Lesser RP, Arroyo S, Uematsu S (1992) High-frequency EEG activity at the start of seizures. J Clin Neurophysiol 9:441-448.

Foffani G, Uzcategui YG, Gal B, Menendez de la Prida L (2007) Reduced spike-timing reliability correlates with the emergence of fast ripples in the rat epileptic hippocampus. Neuron 55:930-941.

Fogassi L, Luppino G (2005) Motor functions of the parietal lobe. Curr Opin Neurobiol 15:626-631.

Fountain NB, Bear J, Bertram EH 3rd, Lothman EW (1998) Responses of deep entorhinal cortex are epileptiform in an electrogenic rat model of chronic temporal lobe epilepsy. J Neurophysiol 80:230-240.

Freeman WJ, van Dijk BW (1987) Spatial patterns of visual cortical fast EEG during conditioned reflex in a rhesus monkey. Brain Res 422:267-276.

Freudenreich O, Weiner RD, McEvoy JP (1997) Clozapine-induced electroencephalogram changes as a function of clozapine serum levels. Biol Psychiatry 42:132-137.

Fries P (2005) A mechanism for cognitive dynamics: neuronal communication through neuronal coherence. Trends Cogn Sci 9:474-480.

Fries P, Nikolic D, Singer W (2007) The gamma cycle. Trends Neurosci 30:309-316.

Fries P, Reynolds JH, Rorie AE, Desimone R (2001) Modulation of oscillatory neuronal synchronization by selective visual attention. Science 291:1560-1563.

Frohlich F, Bazhenov M, Iragui-Madoz V, Sejnowski TJ (2008) Potassium dynamics in the epileptic cortex: new insights on an old topic. Neuroscientist 14:422-433.

Fujiwara-Tsukamoto Y, Isomura Y, Imanishi M, Fukai T, Takada M (2007) Distinct types of ionic modulation of GABA actions in pyramidal cells and interneurons during electrical induction of hippocampal seizure-like network activity. Eur J Neurosci 25:2713-2725.

Fujiwara-Tsukamoto Y, Isomura Y, Kaneda K, Takada M (2004) Synaptic interactions between pyramidal cells and interneurone subtypes during seizure-like activity in the rat hippocampus. J Physiol 557:961-979.

Fujiwara-Tsukamoto Y, Isomura Y, Takada M (2006) Comparable GABAergic mechanisms of hippocampal seizurelike activity in posttetanic and low-Mg2+ conditions. J Neurophysiol 95:2013-2019.

Fukuda T, Kosaka T, Singer W, Galuske RA (2006) Gap junctions among dendrites of cortical GABAergic neurons establish a dense and widespread intercolumnar network. J Neurosci 26:3434-3443.

Fulton B, Goa KL (1997) Olanzapine. A review of its pharmacological properties and therapeutic efficacy in the management of schizophrenia and related psychoses. Drugs 53:281-298.

Gabbott PL, Bacon SJ (1996) Local circuit neurons in the medial prefrontal cortex (areas 24a,b,c, 25 and 32) in the monkey: I. Cell morphology and morphometrics. J Comp Neurol 364:567-608.

Gaitatzis A, Trimble MR, Sander JW (2004) The psychiatric comorbidity of epilepsy. Acta Neurol Scand 110:207-220.

Gareri P, Condorelli D, Belluardo N, Russo E, Loiacono A, Barresi V, Trovato-Salinaro A, Mirone MB, Ferreri IG, De Sarro G (2004) Anticonvulsant effects of carbenoxolone in genetically epilepsy prone rats (GEPRs). Neuropharmacology 47:1205-1216.

Gemperle AY, Enz A, Pozza MF, Luthi A, Olpe HR (2003) Effects of clozapine, haloperidol and iloperidone on neurotransmission and synaptic plasticity in prefrontal cortex and their accumulation in brain tissue: an in vitro study. Neuroscience 117:681-695.

Giardino L, Bortolotti F, Orazzo C, Pozza M, Monteleone P, Calza L, Maj M (1997) Effect of chronic clozapine administration on [3H]MK801-binding sites in the rat brain: a side-preference action in cortical areas. Brain Res 762:216-218.

Gigout S, Louvel J, Pumain R (2006) Effects in vitro and in vivo of a gap junction blocker on epileptiform activities in a genetic model of absence epilepsy. Epilepsy Res 69:15-29.

Glausier JR, Lewis DA (2011) Selective pyramidal cell reduction of GABA(A) receptor alpha1 subunit messenger RNA expression in schizophrenia. Neuropsychopharmacology 36:2103-2110.

Gloveli T, Dugladze T, Saha S, Monyer H, Heinemann U, Traub RD, Whittington MA, Buhl EH (2005) Differential involvement of oriens/pyramidale interneurones in hippocampal network oscillations in vitro. J Physiol 562:131-147.

Glykos V, Whittington MA, Kaiser M, LeBeau FEN (2012) Catecholamine modulation of network oscillations in the rat medial prefrontal cortex in vitro. Society for Neuroscience conference poster.

Gnatkovsky V, Librizzi L, Trombin F, de Curtis M (2008) Fast activity at seizure onset is mediated by inhibitory circuits in the entorhinal cortex in vitro. Ann Neurol 64:674-686.

Goff DC, Tsai G, Manoach DS, Flood J, Darby DG, Coyle JT (1996) D-cycloserine added to clozapine for patients with schizophrenia. Am J Psychiatry 153:1628-1630.

Gonzalez-Burgos G, Hashimoto T, Lewis DA (2010) Alterations of cortical GABA neurons and network oscillations in schizophrenia. Curr Psychiatry Rep 12:335-344.

Gray CM, Konig P, Engel AK, Singer W (1989) Oscillatory responses in cat visual cortex exhibit inter-columnar synchronization which reflects global stimulus properties. Nature 338:334-337.

Gray CM, Singer W (1989) Stimulus-specific neuronal oscillations in orientation columns of cat visual cortex. Proc Natl Acad Sci U S A 86:1698-1702.

Gray CM, Skinner JE (1988) Centrifugal regulation of neuronal activity in the olfactory bulb of the waking rabbit as revealed by reversible cryogenic blockade. Exp Brain Res 69:378-386.

Green MF (1996) What are the functional consequences of neurocognitive deficits in schizophrenia? Am J Psychiatry 153:321-330.

Grenier F, Timofeev I, Steriade M (2001) Focal synchronization of ripples (80-200 Hz) in neocortex and their neuronal correlates. J Neurophysiol 86:1884-1898.

Grenier F, Timofeev I, Steriade M (2003) Neocortical very fast oscillations (ripples, 80-200 Hz) during seizures: intracellular correlates. J Neurophysiol 89:841-852.

Grinevich VP, Papke RL, Lippiello PM, Bencherif M (2009) Atypical antipsychotics as noncompetitive inhibitors of alpha4beta2 and alpha7 neuronal nicotinic receptors. Neuropharmacology 57:183-191.

Gross J, Schmitz F, Schnitzler I, Kessler K, Shapiro K, Hommel B, Schnitzler A (2004) Modulation of long-range neural synchrony reflects temporal limitations of visual attention in humans. Proc Natl Acad Sci U S A 101:13050-13055.

Haller E, Binder RL (1990) Clozapine and seizures. Am J Psychiatry 147:1069-1071.

Hammer TB, Oranje B, Skimminge A, Aggernaes B, Ebdrup BH, Glenthoj B, Baare W (2013) Structural brain correlates of sensorimotor gating in antipsychotic-naive men with first-episode schizophrenia. J Psychiatry Neurosci 38:34-42.

Hamzei-Sichani F, Davidson KG, Yasumura T, Janssen WG, Wearne SL, Hof PR, Traub RD, Gutierrez R, Ottersen OP, Rash JE (2012) Mixed Electrical-Chemical Synapses in Adult Rat Hippocampus are Primarily Glutamatergic and Coupled by Connexin-36. Front Neuroanat 6:13.

Hamzei-Sichani F, Kamasawa N, Janssen WG, Yasumura T, Davidson KG, Hof PR, Wearne SL, Stewart MG, Young SR, Whittington MA, Rash JE, Traub RD (2007) Gap junctions on hippocampal mossy fiber axons demonstrated by thin-section electron microscopy and freeze fracture replica immunogold labeling. Proc Natl Acad Sci U S A 104:12548-12553.

Hanada S, Mita T, Nishino N, Tanaka C (1987) [3H]muscimol binding sites increased in autopsied brains of chronic schizophrenics. Life Sci 40:259-266.

Hand TH, Hu XT, Wang RY (1987) Differential effects of acute clozapine and haloperidol on the activity of ventral tegmental (A10) and nigrostriatal (A9) dopamine neurons. Brain Res 415:257-269.

Haring C, Fleischhacker WW, Schett P, Humpel C, Barnas C, Saria A (1990) Influence of patient-related variables on clozapine plasma levels. Am J Psychiatry 147:1471-1475.

Haring C, Neudorfer C, Schwitzer J, Hummer M, Saria A, Hinterhuber H, Fleischhacker WW (1994) EEG alterations in patients treated with clozapine in relation to plasma levels. Psychopharmacology (Berl) 114:97-100.

Hashimoto T, Volk DW, Eggan SM, Mirnics K, Pierri JN, Sun Z, Sampson AR, Lewis DA (2003) Gene expression deficits in a subclass of GABA neurons in the prefrontal cortex of subjects with schizophrenia. J Neurosci 23:6315-6326.

HAWKINS JE, Jr., SARETT LH (1957) On the efficacy of asparagine, glutamine, gamma-aminobutyric acid and 1-pyrroiidinone in preventing chemically induced seizures in mice. Clin Chim Acta 2:481-484.

He J, Hsiang HL, Wu C, Mylvagnanam S, Carlen PL, Zhang L (2009) Cellular mechanisms of cobalt-induced hippocampal epileptiform discharges. Epilepsia 50:99-115.

Hedges DW, Jeppson KG (2002) New-onset seizure associated with quetiapine and olanzapine. Ann Pharmacother 36:437-439.

Heinrichs RW, Zakzanis KK (1998) Neurocognitive deficit in schizophrenia: a quantitative review of the evidence. Neuropsychology 12:426-445.

Hendry SH, Jones EG (1988) Activity-dependent regulation of GABA expression in the visual cortex of adult monkeys. Neuron 1:701-712.

Hirai N, Uchida S, Maehara T, Okubo Y, Shimizu H (1999) Enhanced gamma (30-150 Hz) frequency in the human medial temporal lobe. Neuroscience 90:1149-1155.

Hirche G (1985) Blocking and modifying actions of octanol on Na channels in frog myelinated nerve. Pflugers Arch 405:180-187.

Hirota K, Okawa H, Appadu BL, Grandy DK, Devi LA, Lambert DG (1999) Stereoselective interaction of ketamine with recombinant mu, kappa, and delta opioid receptors expressed in Chinese hamster ovary cells. Anesthesiology 90:174-182.

Hoffman RE, Hawkins KA, Gueorguieva R, Boutros NN, Rachid F, Carroll K, Krystal JH (2003) Transcranial magnetic stimulation of left temporoparietal cortex and medication-resistant auditory hallucinations. Arch Gen Psychiatry 60:49-56.

Homayoun H, Moghaddam B (2007) Fine-tuning of awake prefrontal cortex neurons by clozapine: comparison with haloperidol and N-desmethylclozapine. Biol Psychiatry 61:679-687.

Hong LE, Buchanan RW, Thaker GK, Shepard PD, Summerfelt A (2008) Beta (~16 Hz) frequency neural oscillations mediate auditory sensory gating in humans. Psychophysiology 45:197-204.

Horishita T, Harris RA (2008) n-Alcohols inhibit voltage-gated Na+ channels expressed in Xenopus oocytes. J Pharmacol Exp Ther 326:270-277.

Hormuzdi SG, Pais I, LeBeau FE, Towers SK, Rozov A, Buhl EH, Whittington MA, Monyer H (2001) Impaired electrical signaling disrupts gamma frequency oscillations in connexin 36-deficient mice. Neuron 31:487-495.

Hosak L, Libiger J (2002) Antiepileptic drugs in schizophrenia: a review. Eur Psychiatry 17:371-378.

Howard A, Tamas G, Soltesz I (2005) Lighting the chandelier: new vistas for axo-axonic cells. Trends Neurosci 28:310-316.

Huberfeld G, Wittner L, Clemenceau S, Baulac M, Kaila K, Miles R, Rivera C (2007) Perturbed chloride homeostasis and GABAergic signaling in human temporal lobe epilepsy. J Neurosci 27:9866-9873.

Hunt MJ, Raynaud B, Garcia R (2006) Ketamine dose-dependently induces high-frequency oscillations in the nucleus accumbens in freely moving rats. Biol Psychiatry 60:1206-1214.

Ikeda H, Leyba L, Bartolo A, Wang Y, Okada YC (2002) Synchronized spikes of thalamocortical axonal terminals and cortical neurons are detectable outside the pig brain with MEG. J Neurophysiol 87:626-630.

Ikeda H, Wang Y, Okada YC (2005) Origins of the somatic N20 and high-frequency oscillations evoked by trigeminal stimulation in the piglets. Clin Neurophysiol 116:827-841.

Insausti R (1993) Comparative anatomy of the entorhinal cortex and hippocampus in mammals. Hippocampus 3 Spec No:19-26.

Isokawa-Akesson M, Wilson CL, Babb TL (1989) Inhibition in synchronously firing human hippocampal neurons. Epilepsy Res 3:236-247.

Jackson ME, Homayoun H, Moghaddam B (2004) NMDA receptor hypofunction produces concomitant firing rate potentiation and burst activity reduction in the prefrontal cortex. Proc Natl Acad Sci U S A 101:8467-8472.

Jacobs J, LeVan P, Chander R, Hall J, Dubeau F, Gotman J (2008) Interictal high-frequency oscillations (80-500 Hz) are an indicator of seizure onset areas independent of spikes in the human epileptic brain. Epilepsia 49:1893-1907.

Jacobs J, Staba R, Asano E, Otsubo H, Wu JY, Zijlmans M, Mohamed I, Kahane P, Dubeau F, Navarro V, Gotman J (2012) High-frequency oscillations (HFOs) in clinical epilepsy. Prog Neurobiol 98:302-315.

Jacobs J, Zijlmans M, Zelmann R, Chatillon CE, Hall J, Olivier A, Dubeau F, Gotman J (2010) High-frequency electroencephalographic oscillations correlate with outcome of epilepsy surgery. Ann Neurol 67:209-220.

Jahromi SS, Wentlandt K, Piran S, Carlen PL (2002) Anticonvulsant actions of gap junctional blockers in an in vitro seizure model. J Neurophysiol 88:1893-1902.

Jardemark KE, Ai J, Ninan I, Wang RY (2001) Biphasic modulation of NMDA-induced responses in pyramidal cells of the medial prefrontal cortex by Y-931, a potential atypical antipsychotic drug. Synapse 41:294-300.

Javitt DC (2006) Is the glycine site half saturated or half unsaturated? Effects of glutamatergic drugs in schizophrenia patients. Curr Opin Psychiatry 19:151-157.

Javitt DC (2010) Glutamatergic theories of schizophrenia. Isr J Psychiatry Relat Sci 47:4-16.

Javitt DC, Duncan L, Balla A, Sershen H (2005) Inhibition of system A-mediated glycine transport in cortical synaptosomes by therapeutic concentrations of clozapine: implications for mechanisms of action. Mol Psychiatry 10:275-287.

Javitt DC, Zukin SR (1991) Recent advances in the phencyclidine model of schizophrenia. Am J Psychiatry 148:1301-1308.

Jefferys JG (1990) Basic mechanisms of focal epilepsies. Exp Physiol 75:127-162.

Jentsch JD, Redmond DE, Jr., Elsworth JD, Taylor JR, Youngren KD, Roth RH (1997a) Enduring cognitive deficits and cortical dopamine dysfunction in monkeys after long-term administration of phencyclidine. Science 277:953-955.

Jentsch JD, Tran A, Le D, Youngren KD, Roth RH (1997b) Subchronic phencyclidine administration reduces mesoprefrontal dopamine utilization and impairs prefrontal cortical-dependent cognition in the rat. Neuropsychopharmacology 17:92-99.

Jin X, Huguenard JR, Prince DA (2005) Impaired Cl- extrusion in layer V pyramidal neurons of chronically injured epileptogenic neocortex. J Neurophysiol 93:2117-2126.

Jirsch JD, Urrestarazu E, LeVan P, Olivier A, Dubeau F, Gotman J (2006) High-frequency oscillations during human focal seizures. Brain 129:1593-1608.

Jones MS, Barth DS (1999) Spatiotemporal organization of fast (>200 Hz) electrical oscillations in rat Vibrissa/Barrel cortex. J Neurophysiol 82:1599-1609.

Jones MS, Barth DS (2002) Effects of bicuculline methiodide on fast (>200 Hz) electrical oscillations in rat somatosensory cortex. J Neurophysiol 88:1016-1025.

Jones MS, MacDonald KD, Choi B, Dudek FE, Barth DS (2000) Intracellular correlates of fast (>200 Hz) electrical oscillations in rat somatosensory cortex. J Neurophysiol 84:1505-1518.

Jones RS, Buhl EH (1993) Basket-like interneurones in layer II of the entorhinal cortex exhibit a powerful NMDA-mediated synaptic excitation. Neurosci Lett 149:35-39.

Jones RS, Lambert JD (1990a) Synchronous discharges in the rat entorhinal cortex in vitro: site of initiation and the role of excitatory amino acid receptors. Neuroscience 34:657-670.

Jones RS, Lambert JD (1990b) The role of excitatory amino acid receptors in the propagation of epileptiform discharges from the entorhinal cortex to the dentate gyrus in vitro. Exp Brain Res 80:310-322.

Juul PU, Noring U, Fog R, Gerlach J (1985) Tolerability and therapeutic effect of clozapine. A retrospective investigation of 216 patients treated with clozapine for up to 12 years. Acta Psychiatr Scand 71:176-185.

Kalus P, Slotboom J, Gallinat J, Federspiel A, Gralla J, Remonda L, Strik WK, Schroth G, Kiefer C (2005) New evidence for involvement of the entorhinal region in schizophrenia: a combined MRI volumetric and DTI study. Neuroimage 24:1122-1129.

Kananura C, Haug K, Sander T, Runge U, Gu W, Hallmann K, Rebstock J, Heils A, Steinlein OK (2002) A splice-site mutation in GABRG2 associated with childhood absence epilepsy and febrile convulsions. Arch Neurol 59:1137-1141.

Kane J, Honigfeld G, Singer J, Meltzer H (1988) Clozapine for the treatment-resistant schizophrenic. A double-blind comparison with chlorpromazine. Arch Gen Psychiatry 45:789-796.

Kapur S, Seeman P (2002) NMDA receptor antagonists ketamine and PCP have direct effects on the dopamine D(2) and serotonin 5-HT(2)receptors-implications for models of schizophrenia. Mol Psychiatry 7:837-844.

Kasper EM, Lubke J, Larkman AU, Blakemore C (1994) Pyramidal neurons in layer 5 of the rat visual cortex. III. Differential maturation of axon targeting, dendritic morphology, and electrophysiological properties. J Comp Neurol 339:495-518.

Kawaguchi Y, Kubota Y (1997) GABAergic cell subtypes and their synaptic connections in rat frontal cortex. Cereb Cortex 7:476-486.

Keefe RS, Fenton WS (2007) How should DSM-V criteria for schizophrenia include cognitive impairment? Schizophr Bull 33:912-920.

Keefe RS, Silva SG, Perkins DO, Lieberman JA (1999) The effects of atypical antipsychotic drugs on neurocognitive impairment in schizophrenia: a review and meta-analysis. Schizophr Bull 25:201-222.

Kehne JH, Baron BM, Carr AA, Chaney SF, Elands J, Feldman DJ, Frank RA, van Giersbergen PL, McCloskey TC, Johnson MP, McCarty DR, Poirot M, Senyah Y, Siegel BW, Widmaier C (1996) Preclinical characterization of the potential of the putative atypical antipsychotic MDL 100,907 as a potent 5-HT2A antagonist with a favorable CNS safety profile. J Pharmacol Exp Ther 277:968-981.

Keverne EB (1999) GABA-ergic neurons and the neurobiology of schizophrenia and other psychoses. Brain Res Bull 48:467-473.

Khalilov I, Holmes GL, Ben-Ari Y (2003) In vitro formation of a secondary epileptogenic mirror focus by interhippocampal propagation of seizures. Nat Neurosci 6:1079-1085.

Khosravani H, Mehrotra N, Rigby M, Hader WJ, Pinnegar CR, Pillay N, Wiebe S, Federico P (2009) Spatial localization and time-dependant changes of electrographic high frequency oscillations in human temporal lobe epilepsy. Epilepsia 50:605-616.

Khosravani H, Pinnegar CR, Mitchell JR, Bardakjian BL, Federico P, Carlen PL (2005) Increased high-frequency oscillations precede in vitro low-Mg seizures. Epilepsia 46:1188-1197.

Kilner JM, Baker SN, Salenius S, Hari R, Lemon RN (2000) Human cortical muscle coherence is directly related to specific motor parameters. J Neurosci 20:8838-8845.

Kinney JW, Davis CN, Tabarean I, Conti B, Bartfai T, Behrens MM (2006) A specific role for NR2A-containing NMDA receptors in the maintenance of parvalbumin and GAD67 immunoreactivity in cultured interneurons. J Neurosci 26:1604-1615.

Klausberger T, Magill PJ, Marton LF, Roberts JD, Cobden PM, Buzsaki G, Somogyi P (2003) Brain-state- and cell-type-specific firing of hippocampal interneurons in vivo. Nature 421:844-848.

Klausberger T, Marton LF, Baude A, Roberts JD, Magill PJ, Somogyi P (2004) Spike timing of dendrite-targeting bistratified cells during hippocampal network oscillations in vivo. Nat Neurosci 7:41-47.

Klausberger T, Marton LF, O'Neill J, Huck JH, Dalezios Y, Fuentealba P, Suen WY, Papp E, Kaneko T, Watanabe M, Csicsvari J, Somogyi P (2005) Complementary roles of cholecystokinin- and parvalbumin-expressing GABAergic neurons in hippocampal network oscillations. J Neurosci 25:9782-9793.

Klausberger T, Somogyi P (2008) Neuronal diversity and temporal dynamics: the unity of hippocampal circuit operations. Science 321:53-57.

Knable MB, Barci BM, Webster MJ, Meador-Woodruff J, Torrey EF (2004) Molecular abnormalities of the hippocampus in severe psychiatric illness: postmortem findings from the Stanley Neuropathology Consortium. Mol Psychiatry 9:609-20, 544.

Kobayashi K, Oka M, Akiyama T, Inoue T, Abiru K, Ogino T, Yoshinaga H, Ohtsuka Y, Oka E (2004) Very fast rhythmic activity on scalp EEG associated with epileptic spasms. Epilepsia 45:488-496.

Kobayashi M, Wen X, Buckmaster PS (2003) Reduced inhibition and increased output of layer II neurons in the medial entorhinal cortex in a model of temporal lobe epilepsy. J Neurosci 23:8471-8479.

Kohling R, Gladwell SJ, Bracci E, Vreugdenhil M, Jefferys JG (2001) Prolonged epileptiform bursting induced by 0-Mg(2+) in rat hippocampal slices depends on gap junctional coupling. Neuroscience 105:579-587.

Kollo M, Holderith NB, Nusser Z (2006) Novel subcellular distribution pattern of A-type K+ channels on neuronal surface. J Neurosci 26:2684-2691.

Komossa K, Rummel-Kluge C, Hunger H, Schmid F, Schwarz S, Duggan L, Kissling W, Leucht S (2010) Olanzapine versus other atypical antipsychotics for schizophrenia. Cochrane Database Syst RevCD006654.

Kornhuber J, Kornhuber ME (1986) Presynaptic dopaminergic modulation of cortical input to the striatum. Life Sci 39:699-74.

Kornhuber J, Schultz A, Wiltfang J, Meineke I, Gleiter CH, Zochling R, Boissl KW, Leblhuber F, Riederer P (1999) Persistence of haloperidol in human brain tissue. Am J Psychiatry 156:885-890.

Korpi ER, Wong G, Luddens H (1995) Subtype specificity of gamma-aminobutyric acid type A receptor antagonism by clozapine. Naunyn Schmiedebergs Arch Pharmacol 352:365-373.

Koukkou M, Angst J, Zimmer D (1979) Paroxysmal EEG activity and psychopathology during the treatment with clozapine. Pharmakopsychiatr Neuropsychopharmakol 12:173-183.

Kramer MA, Roopun AK, Carracedo LM, Traub RD, Whittington MA, Kopell NJ (2008) Rhythm generation through period concatenation in rat somatosensory cortex. PLoS Comput Biol 4:e1000169.

Krystal JH, Karper LP, Seibyl JP, Freeman GK, Delaney R, Bremner JD, Heninger GR, Bowers MB, Jr., Charney DS (1994) Subanesthetic effects of the noncompetitive NMDA antagonist, ketamine, in humans. Psychotomimetic, perceptual, cognitive, and neuroendocrine responses. Arch Gen Psychiatry 51:199-214.

Kuenzi FM, Fitzjohn SM, Morton RA, Collingridge GL, Seabrook GR (2000) Reduced long-term potentiation in hippocampal slices prepared using sucrose-based artificial cerebrospinal fluid. J Neurosci Methods 100:117-122.

Kumari V, Soni W, Sharma T (1999) Normalization of information processing deficits in schizophrenia with clozapine. Am J Psychiatry 156:1046-1051.

Kumlien E, Lundberg PO (2009) Seizure risk associated with neuroactive drugs: Data from the WHO adverse drug reactions database. Seizure.

Labyt E, Uva L, de Curtis M, Wendling F (2006) Realistic modeling of entorhinal cortex field potentials and interpretation of epileptic activity in the guinea pig isolated brain preparation. J Neurophysiol 96:363-377.

Lahti AC, Koffel B, LaPorte D, Tamminga CA (1995) Subanesthetic doses of ketamine stimulate psychosis in schizophrenia. Neuropsychopharmacology 13:9-19.

Lakatos P, Shah AS, Knuth KH, Ulbert I, Karmos G, Schroeder CE (2005) An oscillatory hierarchy controlling neuronal excitability and stimulus processing in the auditory cortex. J Neurophysiol 94:1904-1911.

Le Van QM, Bragin A, Staba R, Crepon B, Wilson CL, Engel J, Jr. (2008) Cell type-specific firing during ripple oscillations in the hippocampal formation of humans. J Neurosci 28:6104-6110.

Lebeda FJ, Hablitz JJ, Johnston D (1982) Antagonism of GABA-mediated responses by d-tubocurarine in hippocampal neurons. J Neurophysiol 48:622-632.

Lee JW, Crismon ML, Dorson PG (1999a) Seizure associated with olanzapine. Ann Pharmacother 33:554-556.

Lee MA, Jayathilake K, Meltzer HY (1999b) A comparison of the effect of clozapine with typical neuroleptics on cognitive function in neuroleptic-responsive schizophrenia. Schizophr Res 37:1-11.

Lefort S, Tomm C, Floyd Sarria JC, Petersen CC (2009) The excitatory neuronal network of the C2 barrel column in mouse primary somatosensory cortex. Neuron 61:301-316.

Lesh TA, Niendam TA, Minzenberg MJ, Carter CS (2011) Cognitive control deficits in schizophrenia: mechanisms and meaning. Neuropsychopharmacology 36:316-338.

Leucht S, Wahlbeck K, Hamann J, Kissling W (2003) New generation antipsychotics versus low-potency conventional antipsychotics: a systematic review and meta-analysis. Lancet 361:1581-1589.

Levin ED, Perkins A, Brotherton T, Qazi M, Berez C, Montalvo-Ortiz J, Davis K, Williams P, Christopher NC (2009) Chronic underactivity of medial frontal cortical beta2-containing nicotinic receptors increases clozapine-induced working memory impairment in female rats. Prog Neuropsychopharmacol Biol Psychiatry 33:296-302.

Lewis DA (2000) GABAergic local circuit neurons and prefrontal cortical dysfunction in schizophrenia. Brain Res Brain Res Rev 31:270-276.

Lewis DA, Cruz DA, Melchitzky DS, Pierri JN (2001) Lamina-specific deficits in parvalbumin-immunoreactive varicosities in the prefrontal cortex of subjects with schizophrenia: evidence for fewer projections from the thalamus. Am J Psychiatry 158:1411-1422.

Lewis DA, Curley AA, Glausier JR, Volk DW (2012) Cortical parvalbumin interneurons and cognitive dysfunction in schizophrenia. Trends Neurosci 35:57-67.

Lewis DA, Gonzalez-Burgos G (2006) Pathophysiologically based treatment interventions in schizophrenia. Nat Med 12:1016-1022.

Lidsky TI, Yablonsky-Alter E, Zuck L, Banerjee SP (1993) Anti-glutamatergic effects of clozapine. Neurosci Lett 163:155-158.

Lidsky TI, Yablonsky-Alter E, Zuck LG, Banerjee SP (1997) Antipsychotic drug effects on glutamatergic activity. Brain Res 764:46-52.

Lindstrom LH (1988) The effect of long-term treatment with clozapine in schizophrenia: a retrospective study in 96 patients treated with clozapine for up to 13 years. Acta Psychiatr Scand 77:524-529.

Lisman JE, Coyle JT, Green RW, Javitt DC, Benes FM, Heckers S, Grace AA (2008) Circuit-based framework for understanding neurotransmitter and risk gene interactions in schizophrenia. Trends Neurosci 31:234-242.

Liu WP, Xiao B, Li SY, Lu XQ (2008) [Eph in the mechanism of mossy fiber axon sprouting in dentate gyrus in rats with chronic temporal lobe epilepsy]. Zhong Nan Da Xue Xue Bao Yi Xue Ban 33:657-662.

Lodge DJ, Behrens MM, Grace AA (2009) A loss of parvalbumin-containing interneurons is associated with diminished oscillatory activity in an animal model of schizophrenia. J Neurosci 29:2344-2354.

Lopes da Silva FH, van RA, Storm van LW, Tielen AM (1970) Dynamic characteristics of visual evoked potentials in the dog. II. Beta frequency selectivity in evoked potentials and background activity. Electroencephalogr Clin Neurophysiol 29:260-268.

Loscher W, Honack D (1991) Anticonvulsant and behavioral effects of two novel competitive N-methyl-D-aspartic acid receptor antagonists, CGP 37849 and CGP 39551, in the kindling model of epilepsy. Comparison with MK-801 and carbamazepine. J Pharmacol Exp Ther 256:432-440.

Lund JS, Lewis DA (1993) Local circuit neurons of developing and mature macaque prefrontal cortex: Golgi and immunocytochemical characteristics. J Comp Neurol 328:282-312.

Magloczky Z, Freund TF (2005) Impaired and repaired inhibitory circuits in the epileptic human hippocampus. Trends Neurosci 28:334-340.

Maier N, Guldenagel M, Sohl G, Siegmund H, Willecke K, Draguhn A (2002) Reduction of high-frequency network oscillations (ripples) and pathological network discharges in hippocampal slices from connexin 36-deficient mice. J Physiol 541:521-528.

Maier N, Nimmrich V, Draguhn A (2003) Cellular and network mechanisms underlying spontaneous sharp wave-ripple complexes in mouse hippocampal slices. J Physiol 550:873-887.

Malhotra AK, Adler CM, Kennison SD, Elman I, Pickar D, Breier A (1997) Clozapine blunts N-methyl-D-aspartate antagonist-induced psychosis: a study with ketamine. Biol Psychiatry 42:664-668.

Malhotra AK, Pinals DA, Weingartner H, Sirocco K, Missar CD, Pickar D, Breier A (1996) NMDA receptor function and human cognition: the effects of ketamine in healthy volunteers. Neuropsychopharmacology 14:301-307.

Malow BA, Reese KB, Sato S, Bogard PJ, Malhotra AK, Su TP, Pickar D (1994) Spectrum of EEG abnormalities during clozapine treatment. Electroencephalogr Clin Neurophysiol 91:205-211.

Mann EO, Radcliffe CA, Paulsen O (2005) Hippocampal gamma-frequency oscillations: from interneurones to pyramidal cells, and back. J Physiol 562:55-63.

Matsumoto H, MARSAN CA (1964) CORTICAL CELLULAR PHENOMENA IN EXPERIMENTAL EPILEPSY: INTERICTAL MANIFESTATIONS. Exp Neurol 9:286-304.

Maura G, Carbone R, Raiteri M (1989) Aspartate-releasing nerve terminals in rat striatum possess D-2 dopamine receptors mediating inhibition of release. J Pharmacol Exp Ther 251:1142-1146.

Maura G, Giardi A, Raiteri M (1988a) Release-regulating D-2 dopamine receptors are located on striatal glutamatergic nerve terminals. J Pharmacol Exp Ther 247:680-684.

Maura G, Roccatagliata E, Ulivi M, Raiteri M (1988b) Serotonin-glutamate interaction in rat cerebellum: involvement of 5-HT1 and 5-HT2 receptors. Eur J Pharmacol 145:31-38.

McCormick DA, Connors BW, Lighthall JW, Prince DA (1985) Comparative electrophysiology of pyramidal and sparsely spiny stellate neurons of the neocortex. J Neurophysiol 54:782-806.

McCoy L, Richfield EK (1996) Chronic antipsychotic treatment alters glycine-stimulated NMDA receptor binding in rat brain. Neurosci Lett 213:137-141.

McEvoy JP, Lieberman JA, Stroup TS, Davis SM, Meltzer HY, Rosenheck RA, Swartz MS, Perkins DO, Keefe RS, Davis CE, Severe J, Hsiao JK (2006) Effectiveness of clozapine versus olanzapine, quetiapine, and risperidone in patients with chronic schizophrenia who did not respond to prior atypical antipsychotic treatment. Am J Psychiatry 163:600-610.

McGurk SR (1999) The effects of clozapine on cognitive functioning in schizophrenia. J Clin Psychiatry 60 Suppl 12:24-29.

Meduna L, Friedman E (1939) The convulsive-irritative therapy of psychoses. J Am Med Assoc 112:501-509.

Melchitzky DS, Gonzalez-Burgos G, Barrionuevo G, Lewis DA (2001) Synaptic targets of the intrinsic axon collaterals of supragranular pyramidal neurons in monkey prefrontal cortex. J Comp Neurol 430:209-221.

Melchitzky DS, Lewis DA (2003) Pyramidal neuron local axon terminals in monkey prefrontal cortex: differential targeting of subclasses of GABA neurons. Cereb Cortex 13:452-460.

Meldrum B, Garthwaite J (1990) Excitatory amino acid neurotoxicity and neurodegenerative disease. Trends Pharmacol Sci 11:379-387.

Melloni L, Molina C, Pena M, Torres D, Singer W, Rodriguez E (2007) Synchronization of neural activity across cortical areas correlates with conscious perception. J Neurosci 27:2858-2865.

Meltzer HY, Alphs L, Green AI, Altamura AC, Anand R, Bertoldi A, Bourgeois M, Chouinard G, Islam MZ, Kane J, Krishnan R, Lindenmayer JP, Potkin S (2003) Clozapine treatment for suicidality in schizophrenia: International Suicide Prevention Trial (InterSePT). Arch Gen Psychiatry 60:82-91.

Meltzer HY, Matsubara S, Lee JC (1989) Classification of typical and atypical antipsychotic drugs on the basis of dopamine D-1, D-2 and serotonin2 pKi values. J Pharmacol Exp Ther 251:238-246.

Meltzer HY, McGurk SR (1999) The effects of clozapine, risperidone, and olanzapine on cognitive function in schizophrenia. Schizophr Bull 25:233-255.

Mercer A, Bannister AP, Thomson AM (2006) Electrical coupling between pyramidal cells in adult cortical regions. Brain Cell Biol 35:13-27.

Mercer A, Trigg HL, Thomson AM (2007) Characterization of neurons in the CA2 subfield of the adult rat hippocampus. J Neurosci 27:7329-7338.

Michel FJ, Trudeau LE (2000) Clozapine inhibits synaptic transmission at GABAergic synapses established by ventral tegmental area neurones in culture. Neuropharmacology 39:1536-1543.

Middleton SJ, Racca C, Cunningham MO, Traub RD, Monyer H, Knopfel T, Schofield IS, Jenkins A, Whittington MA (2008) High-frequency network oscillations in cerebellar cortex. Neuron 58:763-774.

Mikkonen M, Soininen H, Kalvianen R, Tapiola T, Ylinen A, Vapalahti M, Paljarvi L, Pitkanen A (1998) Remodeling of neuronal circuitries in human temporal lobe epilepsy: increased expression of highly polysialylated neural cell adhesion molecule in the hippocampus and the entorhinal cortex. Ann Neurol 44:923-934.

Miles R, Blaesse P, Huberfeld G, Wittner L, Kaila K (2012) Chloride homeostasis and GABA signaling in temporal lobe epilepsy.

Miles R, Wong RK (1983) Single neurones can initiate synchronized population discharge in the hippocampus. Nature 306:371-373.

Miles R, Wong RK (1987) Inhibitory control of local excitatory circuits in the guinea-pig hippocampus. J Physiol 388:611-629.

Miller EK, Cohen JD (2001) An integrative theory of prefrontal cortex function. Annu Rev Neurosci 24:167-202.

Mody I, Lambert JD, Heinemann U (1987) Low extracellular magnesium induces epileptiform activity and spreading depression in rat hippocampal slices. J Neurophysiol 57:869-888.

MOLONY CJ, PARMELEE AH (1954) Convulsions in young infants as a result of pyridoxine (vitamin B6) deficiency. J Am Med Assoc 154:405-406.

Mouri A, Noda Y, Enomoto T, Nabeshima T (2007) Phencyclidine animal models of schizophrenia: approaches from abnormality of glutamatergic neurotransmission and neurodevelopment. Neurochem Int 51:173-184.

Munoz A, Mendez P, DeFelipe J, varez-Leefmans FJ (2007) Cation-chloride cotransporters and GABA-ergic innervation in the human epileptic hippocampus. Epilepsia 48:663-673.

Naber D, Leppig M, Grohmann R, Hippius H (1989) Efficacy and adverse effects of clozapine in the treatment of schizophrenia and tardive dyskinesia--a retrospective study of 387 patients. Psychopharmacology (Berl) 99 Suppl:S73-S76.

Nie F, Wong-Riley MT (1996) Metabolic and neurochemical plasticity of gamma-aminobutyric acid-immunoreactive neurons in the adult macaque striate cortex following monocular impulse blockade: quantitative electron microscopic analysis. J Comp Neurol 370:350-366.

Nilsen KE, Kelso AR, Cock HR (2006) Antiepileptic effect of gap-junction blockers in a rat model of refractory focal cortical epilepsy. Epilepsia 47:1169-1175.

Nimmrich V, Maier N, Schmitz D, Draguhn A (2005) Induced sharp wave-ripple complexes in the absence of synaptic inhibition in mouse hippocampal slices. J Physiol 563:663-670.

Nishimura M, Sato K (1999) Ketamine stereoselectively inhibits rat dopamine transporter. Neurosci Lett 274:131-134.

Nishimura M, Sato K, Okada T, Yoshiya I, Schloss P, Shimada S, Tohyama M (1998) Ketamine inhibits monoamine transporters expressed in human embryonic kidney 293 cells. Anesthesiology 88:768-774.

Norra C, Waberski TD, Kawohl W, Kunert HJ, Hock D, Gobbele R, Buchner H, Hoff P (2004) High-frequency somatosensory thalamocortical oscillations and psychopathology in schizophrenia. Neuropsychobiology 49:71-80.

Ochi A, Otsubo H, Donner EJ, Elliott I, Iwata R, Funaki T, Akizuki Y, Akiyama T, Imai K, Rutka JT, Snead OC, III (2007) Dynamic changes of ictal high-frequency oscillations in neocortical epilepsy: using multiple band frequency analysis. Epilepsia 48:286-296.

Ohno-Shosaku T, Sugawara Y, Muranishi C, Nagasawa K, Kubono K, Aoki N, Taguchi M, Echigo R, Sugimoto N, Kikuchi Y, Watanabe R, Yoneda M (2011) Effects of clozapine and N-desmethylclozapine on synaptic transmission at hippocampal inhibitory and excitatory synapses. Brain Res 1421:66-77.

Okada Y, Ikeda I, Zhang T, Wang Y (2005) High-frequency signals (> 400 hz): a new window in electrophysiological analysis of the somatosensory system. Clin EEG Neurosci 36:285-292.

Olesen OV (1998) Therapeutic drug monitoring of clozapine treatment. Therapeutic threshold value for serum clozapine concentrations. Clin Pharmacokinet 34:497-502.

Olney JW, Farber NB (1995) Glutamate receptor dysfunction and schizophrenia. Arch Gen Psychiatry 52:998-1007.

Olney JW, Labruyere J, Price MT (1989) Pathological changes induced in cerebrocortical neurons by phencyclidine and related drugs. Science 244:1360-1362.

Otis TS, De Koninck Y, Mody I (1994) Lasting potentiation of inhibition is associated with an increased number of gamma-aminobutyric acid type A receptors activated during miniature inhibitory postsynaptic currents. Proc Natl Acad Sci U S A 91:7698-7702.

Pacia SV, Devinsky O (1994) Clozapine-related seizures: experience with 5,629 patients. Neurology 44:2247-2249.

Pais I, Hormuzdi SG, Monyer H, Traub RD, Wood IC, Buhl EH, Whittington MA, LeBeau FE (2003) Sharp wave-like activity in the hippocampus in vitro in mice lacking the gap junction protein connexin 36. J Neurophysiol 89:2046-2054.

Palma E, Amici M, Sobrero F, Spinelli G, Di AS, Ragozzino D, Mascia A, Scoppetta C, Esposito V, Miledi R, Eusebi F (2006) Anomalous levels of Cl- transporters in the hippocampal subiculum from temporal lobe epilepsy patients make GABA excitatory. Proc Natl Acad Sci U S A 103:8465-8468.

Papatheodoropoulos C (2008) A possible role of ectopic action potentials in the in vitro hippocampal sharp wave-ripple complexes. Neuroscience 157:495-501.

Park S, Holzman PS (1992) Schizophrenics show spatial working memory deficits. Arch Gen Psychiatry 49:975-982.

Pathak HR, Weissinger F, Terunuma M, Carlson GC, Hsu FC, Moss SJ, Coulter DA (2007) Disrupted dentate granule cell chloride regulation enhances synaptic excitability during development of temporal lobe epilepsy. J Neurosci 27:14012-14022.

Pauls TL, Cox JA, Berchtold MW (1996) The Ca2+(-)binding proteins parvalbumin and oncomodulin and their genes: new structural and functional findings. Biochim Biophys Acta 1306:39-54.

Paxinos G, Watson C (1998) The rat brain in stereotaxic coordinates. Academic Press.

Payne JA, Stevenson TJ, Donaldson LF (1996) Molecular characterization of a putative K-Cl cotransporter in rat brain. A neuronal-specific isoform. J Biol Chem 271:16245-16252.

Pearlson GD (1981) Psychiatric and medical syndromes associated with phencyclidine (PCP) abuse. Johns Hopkins Med J 148:25-33.

Perez-Velazquez JL, Valiante TA, Carlen PL (1994) Modulation of gap junctional mechanisms during calcium-free induced field burst activity: a possible role for electrotonic coupling in epileptogenesis. J Neurosci 14:4308-4317.

Peris J, Dwoskin LP, Zahniser NR (1988) Biphasic modulation of evoked [3H]D-aspartate release by D-2 dopamine receptors in rat striatal slices. Synapse 2:450-456.

Pocivavsek A, Icenogle L, Levin ED (2006) Ventral hippocampal alpha7 and alpha4beta2 nicotinic receptor blockade and clozapine effects on memory in female rats. Psychopharmacology (Berl) 188:597-604.

Prasad KM, Patel AR, Muddasani S, Sweeney J, Keshavan MS (2004) The entorhinal cortex in first-episode psychotic disorders: a structural magnetic resonance imaging study. Am J Psychiatry 161:1612-1619.

Prince DA (1968) The depolarization shift in "epileptic" neurons. Exp Neurol 21:467-485.

Prince DA, Jacobs K (1998) Inhibitory function in two models of chronic epileptogenesis. Epilepsy Res 32:83-92.

Prueter C, Waberski TD, Norra C, Podoll K (2002) Palinacousis leading to the diagnosis of temporal lobe seizures in a patient with schizophrenia. Seizure 11:198-200.

Qin P, Xu H, Laursen TM, Vestergaard M, Mortensen PB (2005) Risk for schizophrenia and schizophrenia-like psychosis among patients with epilepsy: population based cohort study. BMJ 331:23.

Quirion R, Hammer RP, Jr., Herkenham M, Pert CB (1981) Phencyclidine (angel dust)/sigma "opiate" receptor: visualization by tritium-sensitive film. Proc Natl Acad Sci U S A 78:5881-5885.

Ribak CE, Bradburne RM, Harris AB (1982) A preferential loss of GABAergic, symmetric synapses in epileptic foci: a quantitative ultrastructural analysis of monkey neocortex. J Neurosci 2:1725-1735.

Riley BP, McGuffin P (2000) Linkage and associated studies of schizophrenia. Am J Med Genet 97:23-44.

Ritzler JM, Sawhney R, Geurts van Kessel AH, Grzeschik KH, Schinzel A, Berchtold MW (1992) The genes for the highly homologous Ca(2+)-binding proteins oncomodulin and parvalbumin are not linked in the human genome. Genomics 12:567-572.

Riva MA, Tascedda F, Lovati E, Racagni G (1997) Regulation of NMDA receptor subunit messenger RNA levels in the rat brain following acute and chronic exposure to antipsychotic drugs. Brain Res Mol Brain Res 50:136-142.

Rodin E (2005) Paper recordings of ultrafast frequencies in experimental epilepsy. Clin EEG Neurosci 36:263-270.

Roopun AK, Cunningham MO, Racca C, Alter K, Traub RD, Whittington MA (2008) Region-specific changes in gamma and beta2 rhythms in NMDA receptor dysfunction models of schizophrenia. Schizophr Bull 34:962-973.

Roopun AK, LeBeau FE, Rammell J, Cunningham MO, Traub RD, Whittington MA (2010a) Cholinergic neuromodulation controls directed temporal communication in neocortex in vitro. Front Neural Circuits 4:8.

Roopun AK, Middleton SJ, Cunningham MO, LeBeau FE, Bibbig A, Whittington MA, Traub RD (2006) A beta2-frequency (20-30 Hz) oscillation in nonsynaptic networks of somatosensory cortex. Proc Natl Acad Sci U S A 103:15646-15650.

Roopun AK, Simonotto JD, Pierce ML, Jenkins A, Nicholson C, Schofield IS, Whittaker RG, Kaiser M, Whittington MA, Traub RD, Cunningham MO (2010b) A nonsynaptic mechanism underlying interictal discharges in human epileptic neocortex. Proc Natl Acad Sci U S A 107:338-343.

Ross FM, Gwyn P, Spanswick D, Davies SN (2000) Carbenoxolone depresses spontaneous epileptiform activity in the CA1 region of rat hippocampal slices. Neuroscience 100:789-796.

Roth BL, Sheffler DJ, Kroeze WK (2004) Magic shotguns versus magic bullets: selectively non-selective drugs for mood disorders and schizophrenia. Nat Rev Drug Discov 3:353-359.

Rougeul A, Bouyer JJ, Dedet L, Debray O (1979) Fast somato-parietal rhythms during combined focal attention and immobility in baboon and squirrel monkey. Electroencephalogr Clin Neurophysiol 46:310-319.

Sachdev P (1998) Schizophrenia-like psychosis and epilepsy: the status of the association. Am J Psychiatry 155:325-336.

Salanova V (2012) Parietal lobe epilepsy. J Clin Neurophysiol 29:392-396.

Sanchez-Vives MV, McCormick DA (2000) Cellular and network mechanisms of rhythmic recurrent activity in neocortex. Nat Neurosci 3:1027-1034.

Schmidt WJ (1994) Behavioural effects of NMDA-receptor antagonists. J Neural Transm Suppl 43:63-69.

Schmitz D, Schuchmann S, Fisahn A, Draguhn A, Buhl EH, Petrasch-Parwez E, Dermietzel R, Heinemann U, Traub RD (2001) Axo-axonal coupling. a novel mechanism for ultrafast neuronal communication. Neuron 31:831-840.

Schwartz JM, Marsh L (2000) The psychiatric perspectives of epilepsy. Psychosomatics 41:31-38.

Schwartzkroin PA, Prince DA (1977) Penicillin-induced epileptiform activity in the hippocampal in vitro prepatation. Ann Neurol 1:463-469.

Schwartzkroin PA, Prince DA (1978) Cellular and field potential properties of epileptogenic hippocampal slices. Brain Res 147:117-130.

Schwartzkroin PA, Prince DA (1980) Changes in excitatory and inhibitory synaptic potentials leading to epileptogenic activity. Brain Res 183:61-76.

Scruggs JL, Deutch AY (1999) Chronic antipsychotic drug administration alters calcium-binding protein levels but not GAD levels in the prefrontal cortex of rat. Schizophr Res 36:119-120.

Sesack SR, Hawrylak VA, Melchitzky DS, Lewis DA (1998) Dopamine innervation of a subclass of local circuit neurons in monkey prefrontal cortex: ultrastructural analysis of tyrosine hydroxylase and parvalbumin immunoreactive structures. Cereb Cortex 8:614-622.

Shim SS, Grant ER, Singh S, Gallagher MJ, Lynch DR (1999) Actions of butyrophenones and other antipsychotic agents at NMDA receptors: relationship with clinical effects and structural considerations. Neurochem Int 34:167-175.

Shimazaki T, Kaku A, Chaki S (2010) D-Serine and a glycine transporter-1 inhibitor enhance social memory in rats. Psychopharmacology (Berl) 209:263-270.

Simmonds MA (1980) Leptazol as a γ-aminobutyric acid antagonist. Br J Pharmacol 70:75P.

Singhal SK, Zhang L, Morales M, Oz M (2007) Antipsychotic clozapine inhibits the function of alpha7-nicotinic acetylcholine receptors. Neuropharmacology 52:387-394.

Slater E, Moran PA (1969) The schizophrenia-like psychoses of epilepsy: relation between ages of onset. Br J Psychiatry 115:599-600.

Sloviter RS (1987) Decreased hippocampal inhibition and a selective loss of interneurons in experimental epilepsy. Science 235:73-76.

Sohal VS, Zhang F, Yizhar O, Deisseroth K (2009) Parvalbumin neurons and gamma rhythms enhance cortical circuit performance. Nature 459:698-702.

Spencer KM, Nestor PG, Niznikiewicz MA, Salisbury DF, Shenton ME, McCarley RW (2003) Abnormal neural synchrony in schizophrenia. J Neurosci 23:7407-7411.

Spencer KM, Nestor PG, Perlmutter R, Niznikiewicz MA, Klump MC, Frumin M, Shenton ME, McCarley RW (2004) Neural synchrony indexes disordered perception and cognition in schizophrenia. Proc Natl Acad Sci U S A 101:17288-17293.

Spivak B, Shabash E, Sheitman B, Weizman A, Mester R (2003) The effects of clozapine versus haloperidol on measures of impulsive aggression and suicidality in chronic schizophrenia patients: an open, nonrandomized, 6-month study. J Clin Psychiatry 64:755-760.

Spray DC, Harris AL, Bennett MV (1981) Gap junctional conductance is a simple and sensitive function of intracellular pH. Science 211:712-715.

Squires RF, Saederup E (1991) A review of evidence for GABergic predominance/glutamatergic deficit as a common etiological factor in both schizophrenia and affective psychoses: more support for a continuum hypothesis of "functional" psychosis. Neurochem Res 16:1099-1111.

Squires RF, Saederup E (1997) Clozapine and some other antipsychotic drugs may preferentially block the same subset of GABA(A) receptors. Neurochem Res 22:151-162.

Squires RF, Saederup E (1998) Clozapine and several other antipsychotic/antidepressant drugs preferentially block the same 'core' fraction of GABA(A) receptors. Neurochem Res 23:1283-1290.

Squires RF, Saederup E, Crawley JN, Skolnick P, Paul SM (1984) Convulsant potencies of tetrazoles are highly correlated with actions on GABA/benzodiazepine/picrotoxin receptor complexes in brain. Life Sci 35:1439-1444.

Staba RJ, Ard TD, Benison AM, Barth DS (2005) Intracortical pathways mediate nonlinear fast oscillation (>200 Hz) interactions within rat barrel cortex. J Neurophysiol 93:2934-2939.

Staba RJ, Brett-Green B, Paulsen M, Barth DS (2003) Effects of ventrobasal lesion and cortical cooling on fast oscillations (>200 Hz) in rat somatosensory cortex. J Neurophysiol 89:2380-2388.

Staba RJ, Wilson CL, Bragin A, Fried I, Engel J, Jr. (2002) Quantitative analysis of high-frequency oscillations (80-500 Hz) recorded in human epileptic hippocampus and entorhinal cortex. J Neurophysiol 88:1743-1752.

Staba RJ, Wilson CL, Bragin A, Jhung D, Fried I, Engel J, Jr. (2004) High-frequency oscillations recorded in human medial temporal lobe during sleep. Ann Neurol 56:108-115.

Stevens JR (1995) Clozapine: the Yin and Yang of seizures and psychosis. Biol Psychiatry 37:425-426.

Stevens JR, Denney D, Szot P (1996) Kindling with clozapine: behavioral and molecular consequences. Epilepsy Res 26:295-304.

Sturgeon RD, Fessler RG, London SF, Meltzer HY (1982) Behavioral effects of chronic phencyclidine administration in rats. Psychopharmacology (Berl) 76:52-56.

Swartz BE, Goldensohn ES (1998) Timeline of the history of EEG and associated fields. Electroencephalogr Clin Neurophysiol 106:173-176.

Symond MP, Harris AW, Gordon E, Williams LM (2005) "Gamma synchrony" in first-episode schizophrenia: a disorder of temporal connectivity? Am J Psychiatry 162:459-465.

Szabadics J, Varga C, Molnar G, Olah S, Barzo P, Tamas G (2006) Excitatory effect of GABAergic axo-axonic cells in cortical microcircuits. Science 311:233-235.

Szente M, Gajda Z, Said AK, Hermesz E (2002) Involvement of electrical coupling in the in vivo ictal epileptiform activity induced by 4-aminopyridine in the neocortex. Neuroscience 115:1067-1078.

Tallon-Baudry C, Bertrand O (1999) Oscillatory gamma activity in humans and its role in object representation. Trends Cogn Sci 3:151-162.

Tamminga CA (1998) Schizophrenia and glutamatergic transmission. Crit Rev Neurobiol 12:21-36.

Tarazi FI, Florijn WJ, Creese I (1996) Regulation of ionotropic glutamate receptors following subchronic and chronic treatment with typical and atypical antipsychotics. Psychopharmacology (Berl) 128:371-379.

Taylor DC (2003) Schizophrenias and epilepsies: why? when? how? Epilepsy Behav 4:474-482.

Thomas RC (1984) Experimental displacement of intracellular pH and the mechanism of its subsequent recovery. J Physiol 354:3P-22P.

Toth P, Frankenburg FR (1994) Clozapine and seizures: a review. Can J Psychiatry 39:236-238.

Towers SK, LeBeau FE, Gloveli T, Traub RD, Whittington MA, Buhl EH (2002) Fast network oscillations in the rat dentate gyrus in vitro. J Neurophysiol 87:1165-1168.

Traub RD, Bibbig A (2000) A model of high-frequency ripples in the hippocampus based on synaptic coupling plus axon-axon gap junctions between pyramidal neurons. J Neurosci 20:2086-2093.

Traub RD, Bibbig A, LeBeau FE, Buhl EH, Whittington MA (2004) Cellular mechanisms of neuronal population oscillations in the hippocampus in vitro. Annu Rev Neurosci 27:247-278.

Traub RD, Contreras D, Cunningham MO, Murray H, LeBeau FE, Roopun A, Bibbig A, Wilent WB, Higley MJ, Whittington MA (2005a) Single-column thalamocortical

network model exhibiting gamma oscillations, sleep spindles, and epileptogenic bursts. J Neurophysiol 93:2194-2232.

Traub RD, Cunningham MO, Gloveli T, LeBeau FE, Bibbig A, Buhl EH, Whittington MA (2003) GABA-enhanced collective behavior in neuronal axons underlies persistent gamma-frequency oscillations. Proc Natl Acad Sci U S A 100:11047-11052.

Traub RD, Pais I, Bibbig A, LeBeau FE, Buhl EH, Garner H, Monyer H, Whittington MA (2005b) Transient depression of excitatory synapses on interneurons contributes to epileptiform bursts during gamma oscillations in the mouse hippocampal slice. J Neurophysiol 94:1225-1235.

Traub RD, Schmitz D, Maier N, Whittington MA, Draguhn A (2012) Axonal properties determine somatic firing in a model of in vitro CA1 hippocampal sharp wave/ripples and persistent gamma oscillations. Eur J Neurosci 36:2650-2660.

Traub RD, Whittington MA, Buhl EH, LeBeau FE, Bibbig A, Boyd S, Cross H, Baldeweg T (2001) A possible role for gap junctions in generation of very fast EEG oscillations preceding the onset of, and perhaps initiating, seizures. Epilepsia 42:153-170.

Traub RD, Whittington MA (2010) Cortical Oscillations in Health and Disease. Oxford University Press.

Traub RD, Whittington MA, Stanford IM, Jefferys JG (1996) A mechanism for generation of long-range synchronous fast oscillations in the cortex. Nature 383:621-624.

Trimble MR (1996) Anticonvulsant-induced psychiatric disorders. The role of forced normalisation. Drug Saf 15:159-166.

Truffinet P, Tamminga CA, Fabre LF, Meltzer HY, Riviere ME, Papillon-Downey C (1999) Placebo-controlled study of the D4/5-HT2A antagonist fananserin in the treatment of schizophrenia. Am J Psychiatry 156:419-425.

Tsai GE, Lin PY (2010) Strategies to enhance N-methyl-D-aspartate receptor-mediated neurotransmission in schizophrenia, a critical review and meta-analysis. Curr Pharm Des 16:522-537.

Tsai GE, Yang P, Chung LC, Tsai IC, Tsai CW, Coyle JT (1999) D-serine added to clozapine for the treatment of schizophrenia. Am J Psychiatry 156:1822-1825.

Tsuneizumi T, Babb SM, Cohen BM (1992) Drug distribution between blood and brain as a determinant of antipsychotic drug effects. Biol Psychiatry 32:817-824.

Tuunainen A, Wahlbeck K, Gilbody S (2002) Newer atypical antipsychotic medication in comparison to clozapine: a systematic review of randomized trials. Schizophr Res 56:1-10.

Uhlhaas PJ, Silverstein SM (2005) Perceptual organization in schizophrenia spectrum disorders: empirical research and theoretical implications. Psychol Bull 131:618-632.

Uhlhaas PJ, Singer W (2010) Abnormal neural oscillations and synchrony in schizophrenia. Nat Rev Neurosci 11:100-113.

Urrestarazu E, Jirsch JD, LeVan P, Hall J, Avoli M, Dubeau F, Gotman J (2006) High-frequency intracerebral EEG activity (100-500 Hz) following interictal spikes. Epilepsia 47:1465-1476.

Van Snellenberg JX, Torres IJ, Thornton AE (2006) Functional neuroimaging of working memory in schizophrenia: task performance as a moderating variable. Neuropsychology 20:497-510.

van Vliet EA, Aronica E, Tolner EA, Lopes da Silva FH, Gorter JA (2004) Progression of temporal lobe epilepsy in the rat is associated with immunocytochemical changes in inhibitory interneurons in specific regions of the hippocampal formation. Exp Neurol 187:367-379.

Vercammen A, Knegtering H, Liemburg EJ, den Boer JA, Aleman A (2010) Functional connectivity of the temporo-parietal region in schizophrenia: effects of rTMS treatment of auditory hallucinations. J Psychiatr Res 44:725-731.

Verma A, Moghaddam B (1996) NMDA receptor antagonists impair prefrontal cortex function as assessed via spatial delayed alternation performance in rats: modulation by dopamine. J Neurosci 16:373-379.

Vierling-Claassen D, Siekmeier P, Stufflebeam S, Kopell N (2008) Modeling GABA alterations in schizophrenia: a link between impaired inhibition and altered gamma and beta range auditory entrainment. J Neurophysiol 99:2656-2671.

Vivar C, Traub RD, Gutierrez R (2012) Mixed electrical-chemical transmission between hippocampal mossy fibers and pyramidal cells. Eur J Neurosci 35:76-82.

Volk D, Austin M, Pierri J, Sampson A, Lewis D (2001) GABA transporter-1 mRNA in the prefrontal cortex in schizophrenia: decreased expression in a subset of neurons. Am J Psychiatry 158:256-265.

von Stein A, Chiang C, Konig P (2000) Top-down processing mediated by interareal synchronization. Proc Natl Acad Sci U S A 97:14748-14753.

Vreugdenhil M, Jefferys JG, Celio MR, Schwaller B (2003) Parvalbumin-deficiency facilitates repetitive IPSCs and gamma oscillations in the hippocampus. J Neurophysiol 89:1414-1422.

Wahlbeck K, Cheine M, Essali MA (2000) Clozapine versus typical neuroleptic medication for schizophrenia. Cochrane Database Syst RevCD000059.

Wallace RH, Marini C, Petrou S, Harkin LA, Bowser DN, Panchal RG, Williams DA, Sutherland GR, Mulley JC, Scheffer IE, Berkovic SF (2001) Mutant GABA(A) receptor gamma2-subunit in childhood absence epilepsy and febrile seizures. Nat Genet 28:49-52.

Walther H, Lambert JD, Jones RS, Heinemann U, Hamon B (1986) Epileptiform activity in combined slices of the hippocampus, subiculum and entorhinal cortex during perfusion with low magnesium medium. Neurosci Lett 69:156-161.

Wang RY, Liang X (1998) M100907 and clozapine, but not haloperidol or raclopride, prevent phencyclidine-induced blockade of NMDA responses in pyramidal neurons of the rat medial prefrontal cortical slice. Neuropsychopharmacology 19:74-85.

Wang Y, Denisova JV, Kang KS, Fontes JD, Zhu BT, Belousov AB (2010) Neuronal gap junctions are required for NMDA receptor-mediated excitotoxicity: implications in ischemic stroke. J Neurophysiol 104:3551-3556.

Watts J, Thomson AM (2005) Excitatory and inhibitory connections show selectivity in the neocortex. J Physiol 562:89-97.

Weigmann H, Hartter S, Fischer V, Dahmen N, Hiemke C (1999) Distribution of clozapine and desmethylclozapine between blood and brain in rats. Eur Neuropsychopharmacol 9:253-256.

Welch J, Manschreck T, Redmond D (1994) Clozapine-induced seizures and EEG changes. J Neuropsychiatry Clin Neurosci 6:250-256.

Welch PD (1967) The Use of Fast Fourier Transform for the Estimation of Power Spectra: A Method Based on Time Averaging Over Short, Modified Periodograms. IEEE Trans Audio Electroacoustics 15:70-73.

Wendling F, Bartolomei F, Bellanger JJ, Chauvel P (2002) Epileptic fast activity can be explained by a model of impaired GABAergic dendritic inhibition. Eur J Neurosci 15:1499-1508.

Wespatat V, Tennigkeit F, Singer W (2004) Phase sensitivity of synaptic modifications in oscillating cells of rat visual cortex. J Neurosci 24:9067-9075.

Whittington MA, Cunningham MO, LeBeau FE, Racca C, Traub RD (2011) Multiple origins of the cortical gamma rhythm. Dev Neurobiol 71:92-106.

Whittington MA, Traub RD (2003) Interneuron diversity series: inhibitory interneurons and network oscillations in vitro. Trends Neurosci 26:676-682.

Williams GV, Rao SG, Goldman-Rakic PS (2002) The physiological role of 5-HT2A receptors in working memory. J Neurosci 22:2843-2854.

Williams SM, Goldman-Rakic PS, Leranth C (1992) The synaptology of parvalbumin-immunoreactive neurons in the primate prefrontal cortex. J Comp Neurol 320:353-369.

Willoughby JO, Fitzgibbon SP, Pope KJ, Mackenzie L, Medvedev AV, Clark CR, Davey MP, Wilcox RA (2003) Persistent abnormality detected in the non-ictal electroencephalogram in primary generalised epilepsy. J Neurol Neurosurg Psychiatry 74:51-55.

Wilson MA, McNaughton BL (1994) Reactivation of hippocampal ensemble memories during sleep. Science 265:676-679.

Wolf P, Trimble MR (1985) Biological antagonism and epileptic psychosis. Br J Psychiatry 146:272-276.

Womelsdorf T, Schoffelen JM, Oostenveld R, Singer W, Desimone R, Engel AK, Fries P (2007) Modulation of neuronal interactions through neuronal synchronization. Science 316:1609-1612.

Wong RK, Traub RD (1983) Synchronized burst discharge in disinhibited hippocampal slice. I. Initiation in CA2-CA3 region. J Neurophysiol 49:442-458.

Woo TU, Whitehead RE, Melchitzky DS, Lewis DA (1998) A subclass of prefrontal gamma-aminobutyric acid axon terminals are selectively altered in schizophrenia. Proc Natl Acad Sci U S A 95:5341-5346.

Woolley J, Smith S (2001) Lowered seizure threshold on olanzapine. Br J Psychiatry 178:85-86.

Woolley ML, Bentley JC, Sleight AJ, Marsden CA, Fone KC (2001) A role for 5-ht6 receptors in retention of spatial learning in the Morris water maze. Neuropharmacology 41:210-219.

Worrell GA, Parish L, Cranstoun SD, Jonas R, Baltuch G, Litt B (2004) High-frequency oscillations and seizure generation in neocortical epilepsy. Brain 127:1496-1506.

Wyderski RJ, Starrett WG, bou-Saif A (1999) Fatal status epilepticus associated with olanzapine therapy. Ann Pharmacother 33:787-789.

Yamaguchi T (1986) Cerebral extracellular potassium concentration change and cerebral impedance change in short-term ischemia in gerbil. Bull Tokyo Med Dent Univ 33:1-8.

Yamamoto BK, Pehek EA, Meltzer HY (1994) Brain region effects of clozapine on amino acid and monoamine transmission. J Clin Psychiatry 55 Suppl B:8-14.

Yang TT, Wang SJ (2005) Effects of haloperidol and clozapine on glutamate release from nerve terminals isolated from rat prefrontal cortex. Synapse 56:12-20.

Ylinen A, Bragin A, Nadasdy Z, Jando G, Szabo I, Sik A, Buzsaki G (1995a) Sharp wave-associated high-frequency oscillation (200 Hz) in the intact hippocampus: network and intracellular mechanisms. J Neurosci 15:30-46.

Ylinen A, Soltesz I, Bragin A, Penttonen M, Sik A, Buzsaki G (1995b) Intracellular correlates of hippocampal theta rhythm in identified pyramidal cells, granule cells, and basket cells. Hippocampus 5:78-90.

Yu S, Ho IK (1990) Effects of GABA antagonists, SR 95531 and bicuculline, on GABAA receptor-regulated chloride flux in rat cortical synaptoneurosomes. Neurochem Res 15:905-910.

Yu YC, He S, Chen S, Fu Y, Brown KN, Yao XH, Ma J, Gao KP, Sosinsky GE, Huang K, Shi SH (2012) Preferential electrical coupling regulates neocortical lineage-dependent microcircuit assembly. Nature 486:113-117.

Zarnowski T, Kleinrok Z, Turski WA, Czuczwar SJ (1994) The competitive NMDA antagonist, D-CPP-ene, potentiates the anticonvulsant activity of conventional antiepileptics against maximal electroshock-induced seizures in mice. Neuropharmacology 33:619-624.

Zhang ET, Hansen AJ, Wieloch T, Lauritzen M (1990) Influence of MK-801 on brain extracellular calcium and potassium activities in severe hypoglycemia. J Cereb Blood Flow Metab 10:136-139.

Zhang Y, Behrens MM, Lisman JE (2008) Prolonged exposure to NMDAR antagonist suppresses inhibitory synaptic transmission in prefrontal cortex. J Neurophysiol 100:959-965.

Zhang ZJ, Reynolds GP (2002) A selective decrease in the relative density of parvalbumin-immunoreactive neurons in the hippocampus in schizophrenia. Schizophr Res 55:1-10.

Zhou M, Xu G, Xie M, Zhang X, Schools GP, Ma L, Kimelberg HK, Chen H (2009) TWIK-1 and TREK-1 are potassium channels contributing significantly to astrocyte passive conductance in rat hippocampal slices. J Neurosci 29:8551-8564.

Zukin SR (1982) Differing stereospecificities distinguish opiate receptor subtypes. Life Sci 31:1307-1310.